

Invasive alien species add to the uncertain future of protected areas

Desika Moodley¹, Llewellyn C. Foxcroft^{2,3}, Ana Novoa¹, Klára Pyšková^{1,4},
Jan Pergl¹, Petr Pyšek^{1,4}

1 Czech Academy of Sciences, Institute of Botany, Department of Invasion Ecology, CZ-252 43, Průhonice, Czech Republic **2** Conservation Services, South African National Parks, Skukuza 1350, South Africa **3** Centre for Invasion Biology, Department of Botany and Zoology, Stellenbosch University, Private Bag X1, Matieland 7602, South Africa **4** Department of Ecology, Faculty of Science, Charles University, Viničná 7, CZ-128 44, Prague, Czech Republic

Corresponding author: Desika Moodley (desikamoodley29@gmail.com)

Academic editor: I. Kühn | Received 19 March 2020 | Accepted 20 March 2020 | Published 18 May 2020

Citation: Moodley D, Foxcroft LC, Novoa A, Pyšková K, Pergl J, Pyšek P (2020) Invasive alien species add to the uncertain future of protected areas. *NeoBiota* 57: 1–5. <https://doi.org/10.3897/neobiota.57.52188>

In a recent article on “The uncertain future of protected lands and waters”, Golden Kroner et al. (2019) suggest that legal changes that temper the regulations in protected areas (PAs) are one of the main threats to biodiversity conservation. By examining Protected Area Downgrading (i.e. relaxing restrictions), Downsizing (i.e. shrinking boundaries) and Degazettement (i.e. complete loss of protection) (in total referred to as PADDD) over the last 126 years, they assessed the factors leading to PADDD events and discuss their consequences for the conservation of PAs in the United States and Amazonian countries. They conclude that most PADDD events were associated with industrial-scale resource extraction and local land pressure and land claims. To mitigate these trends, they recommend increasing research efforts to support evidence-based conservation policies to address the challenges of PADDD. However, they overlook one of the largest threats to conservation and PAs in particular – biological invasions (Foxcroft et al. 2013, 2017). Potentially, invasive alien species (IAS) could be a primary

cause of enacting a PADD event (e.g. relaxing restrictions due to IAS-induced habitat transformation). Additionally, while some of the causes of PADD events stated in the paper centre on conservation planning, forestry, industrial agriculture and mining, IAS can be directly or indirectly associated with all of these. Here, we argue that overlooking the problems associated with IAS in PAs can hinder conservation actions, create biases in the prioritisation of natural resource management and generate false or distorted perceptions for the public.

Globally, the frequency and magnitude of alien species' introductions are changing more rapidly at present than ever before (Seebens et al. 2017) and despite efforts to conserve biodiversity, it is becoming increasingly evident that current approaches and strategies are not sufficient in addressing the scale of biodiversity loss caused by IAS (Le Roux et al. 2019). Consequently, IAS were listed amongst the major drivers of biodiversity loss in the recent Intergovernmental Science-Policy Platform on Biodiversity and Ecosystem Services (IPBES) report (Brondizio et al. 2019); over the last 100 years, an exponential increase in IAS has caused a decrease in the average abundance of native plants, animals and insects by at least one-fifth across many ecosystems. To list some specific examples, a report by the Global Invasive Species Program (De Poorter 2007) identified 487 PAs globally, in which invasive alien plants represented a threat to biodiversity. In Europe, PA managers perceived invasive plants as the second greatest threat to PAs following habitat fragmentation (Pyšek et al. 2013).

In the USA, one of the regions Golden Kroner et al. (2019) used to illustrate their ideas, alien plants were estimated to cover 7.3 million ha across 218 national parks (Allen et al. 2009) and 61% of the 246 park managers indicated that alien plant invasions were of moderate or major concern (Randall 2011). If we compare the numbers of native and alien plant species across 183 PAs in the United States (Figure 1; Suppl. material I: Table S1), there is a large variation in the numbers of alien plants, but they are present in all PAs. Moreover, 87% of these 183 PAs have recently undergone a PADD event (i.e. downgrade and/or downsize; PADDTracker.org, 2019) and most of them contain high numbers of alien plants. For example, the proportion of alien plants in the Hawai'i Volcanoes National Park is as high as 61% of the total flora (Loh et al. 2014). The park also contains 12 alien mammals and 37 alien bird species, of which 13 are common breeders (<https://irma.nps.gov/NPSpecies>, accessed August 2019), including the widespread Japanese white-eye (*Zosterops japonicus*), a vector of introduced avian malaria, a disease widely decimating native bird populations (van Ripper III et al. 1986).

Unfortunately, PADD events are inevitable because they are driven by human development (e.g. mining, forestry, agriculture, urbanisation, oil and gas extraction). The above examples imply that when future PADD events are proposed, the effects of IAS need to be carefully considered. We believe that in PAs containing IAS that are subjected to PADD events, there is a higher probability that IAS will have significant causal environmental and socioeconomic effects (Vilà and Hulme 2017; Mazza and Tricarico 2018), especially after degazettement. Consequently, if it is necessary to enact a PADD, then IAS must be considered in the processes and policies governing these events.

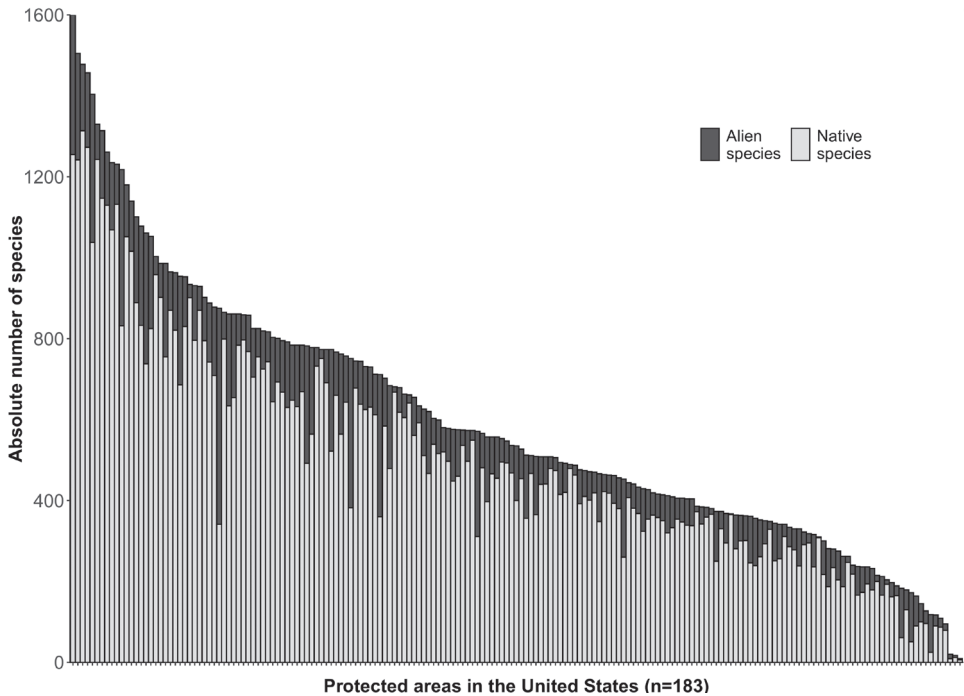


Figure 1. The total number of native and alien plant species recorded across 183 protected areas in the United States (see Suppl. material 1: Table S1 for the park names). Data were derived from the IRMA portal (<https://irma.nps.gov/NPSpecies>, accessed May 2018).

Disregarding IAS when addressing PADD D can compromise the conservation of PAs. For example, in PAs that already comprise alien species, downgrading can increase the probability of their establishment and spread, downsizing exacerbates habitat fragmentation (Golden Kroner et al. 2016) and degazettement can create ideal settings for IAS to spread after conservation measures have ceased. As such, if PAs are to maintain their integrity and efficacy, we need to explicitly consider the multiple interacting drivers (see van Wilgen and Herbst 2017) causing biodiversity loss in these landscapes, particularly if these drivers are exacerbated through regulatory changes (such as PADD D events). We are also fully aware of the knowledge gap that exists regarding PADD D events and their impacts, therefore we emphasise why it is crucial to consider these major drivers. Overlooking the impact of IAS on PAs can misinform stakeholders such as the general public, decision-makers, funding agencies and managers and can affect research needs.

Acknowledgements

The paper was supported by grant no. 18-18495S, EXPRO grant 19-28807X (Czech Science Foundation) and long-term research development project RVO 67985939 (Czech Academy of Sciences).

References

- Allen JA, Brown CS, Stohlgren TJ (2009) Non-native plant invasions of United States national parks. *Biological Invasions* 11: 2195–2207. <https://doi.org/10.1007/s10530-008-9376-1>
- Brondizio ES, Settele J, Díaz S, Ngo HT (2019) Global Assessment Report on Biodiversity and Ecosystem Services (IPBES). IPBES Secretariat.
- De Poorter M (2007) Invasive Alien Species and Protected Areas: A Scoping Report. Part 1. Scoping the Scale and Nature of Invasive Alien Species Threats to Protected Areas, Impediments to IAS Management and Means to Address those Impediments. Global Invasive Species Programme (GISP), 1–94.
- Foxcroft LC, Pyšek P, Richardson DM, Genovesi P [Eds] (2013) *Plant Invasions in Protected Areas: Patterns, Problems and Challenges*. Springer, Dordrecht, 656 pp. <https://doi.org/10.1007/978-94-007-7750-7>
- Foxcroft LC, Pyšek P, Richardson DM, Genovesi P, MacFadyen S (2017) Plant invasion science in protected areas: progress and priorities. *Biological Invasions* 19: 1353–1378. <https://doi.org/10.1007/s10530-016-1367-z>
- Golden Kroner RE, Krithivasan R, Mascia MB (2016) Effects of protected area downsizing on habitat fragmentation in Yosemite National Park (USA), 1864–2014. *Ecology and Society* 21: 1–22. <https://doi.org/10.5751/ES-08679-210322>
- Golden Kroner RE, Qin S, Cook CN, Krithivasan R, Pack SM, Bonilla OD, Cort-Kansinall KA, Coutinho B, Feng M, Martínez Garcia MI, He Y, Kennedy CJ, Lebreton C, Ledezma JC, Lovejoy TE, Luther DA, Parmanand Y, Ruíz-Agudelo CA, Yerena E, Morón Zambrano V, Mascia MB (2019) The uncertain future of protected lands and waters. *Science* 364: 881–886. <https://doi.org/10.1126/science.aau5525>
- Le Roux JJ, Cang H, Castillo ML, Iriondo JM, Jan-Hendrik K, Khapugin AA, Médail F, Rejmánek M, Theron G, Yannelli FA, Hirsch H (2019) Recent anthropogenic plant extinctions differ in biodiversity hotspots and coldspots. *Current Biology* 29: 1–7. <https://doi.org/10.1016/j.cub.2019.07.063>
- Loh RK, Tunison T, Zimmer C, Mattos R, Benitez D (2014) *A Review of Invasive Plant Management in Special Ecological Areas, Hawai'i Volcanoes National Park, 1984–2007*. Technical Report No. 187. Pacific Cooperative Studies Unit, University of Hawai'i, Honolulu, 35 pp.
- Mazza G, Tricarico E (2018) *Invasive Species and Human Health (Vol. 10)*. CAB International, Wallingford, 208 pp. <https://doi.org/10.1079/9781786390981.0000>
- Pyšek P, Genovesi P, Pergl J, Monaco A, Wild J (2013) Plant invasions of protected areas in Europe: An old continent facing new problems. In: Foxcroft LC, Pyšek P, Richardson DM, Genovesi P (Eds) *Plant Invasions in Protected Areas: Patterns, Problems and Challenges*. Springer, Dordrecht, 209–240. https://doi.org/10.1007/978-94-007-7750-7_11
- Randall JM (2011) Protected areas. In: Simberloff D, Rejmánek M (Eds) *Encyclopedia of Biological Invasions*. University of California Press, Berkeley, 563–567.
- Seebens H, Blackburn TM, Dyer EE, Genovesi P, Hulme PE, Jeschke JM, Pagad S, Pyšek P, Winter M, Arianoutsou M, Bacher S, Blasius B, Brundu G, Capinha C, Celesti-Grapo L, Dawson W, Dullinger S, Fuentes N, Jäger H, Kartesz J, Kenis M, Holger K, Kühn I, Lenzner B, Liebhold A, Mosena A, Moser D, Nishino M, Pearman D, Pergl J, Rabitsch

- W, Rojas-Sandoval J, Roques A, Rorke S, Rossinelli S, Roy HE, Scalera R, Schindler S, Štajerová K, Tokarska-Guzik B, van Kleunen M, Walker K, Weigelt P, Yamanaka T, Essl F (2017) No saturation in the accumulation of alien species worldwide. *Nature Communications* 8: 1–9. <https://doi.org/10.1038/ncomms14435>
- van Riper III C, van Riper SG, Goff ML, Laird M (1986) The epizootiology and ecological significance of malaria in Hawaiian land birds. *Ecological Monographs* 56: 327–344. <https://doi.org/10.2307/1942550>
- van Wilgen NJ, Herbst M (2017) Taking Stock of Parks in a Changing World: The SANParks global environmental change assessment. SANParks, Cape Town, 200 pp.
- Vilà M, Hulme PE (2017) *Impact of Biological Invasions on Ecosystem Services*. Springer, Cham, 354 pp. <https://doi.org/10.1007/978-3-319-45121-3>

Supplementary material I

Table S1. A list of protected areas (n = 183) in the United States

Authors: Desika Moodley, Llewellyn C. Foxcroft, Ana Novoa, Klára Pyšková, Jan Pergl, Petr Pyšek

Data type: checklist

Copyright notice: This dataset is made available under the Open Database License (<http://opendatacommons.org/licenses/odbl/1.0/>). The Open Database License (ODbL) is a license agreement intended to allow users to freely share, modify, and use this Dataset while maintaining this same freedom for others, provided that the original source and author(s) are credited.

Link: <https://doi.org/10.3897/neobiota.57.52188.suppl1>

How dense is dense? Toward a harmonized approach to characterizing reefs of non-native Pacific oysters – with consideration of native mussels

Alexandra Markert¹

¹ *Wilhelmshaven, Germany*

Corresponding author: Alexandra Markert (mar-k-art@gmx.de)

Academic editor: S. Gollasch | Received 8 December 2019 | Accepted 3 April 2020 | Published 29 May 2020

Citation: Markert A (2020) How dense is dense? Toward a harmonized approach to characterizing reefs of non-native Pacific oysters – with consideration of native mussels. *NeoBiota* 57: 7–52. <https://doi.org/10.3897/neobiota.57.49196>

Abstract

Pacific oysters *Crassostrea (Magallana) gigas* have been successfully invading ecosystems worldwide. As an ecosystem engineer, they have the potential to substantially impact on other species and on functional processes of invaded ecosystems. Engineering strength depends on oyster density in space and time. Density has not yet been studied on the extent of reef structural dynamics. This study assessed abundance of naturalized Pacific oysters by shell length (SL) of live individuals and post-mortem shells at six sites over six consecutive years during post-establishment. Individual biomass, i.e. live wet mass (LWM), flesh mass (FM) and live shell mass (SM LIVE), were determined from a total of 1.935 live oysters in order to estimate areal biomass. The generic term density attribute was used for SL-related population categories and the biomass variables LWM, FM, SM LIVE and SM. As the oyster invasion modulated resident *Mytilus edulis* beds, the study was supplemented by contemporaneously assessed data of mussels and corresponding analyses.

Interrelations of abundance and areal biomass revealed distinct linkages between specific density attributes. Most importantly, large individuals were identified as intrinsic drivers for the determination of areal biomass. Additionally, allometry of large oysters differed from small oysters by attenuated scaling relations. This effect was enhanced by oyster density as results showed that crowding forced large individuals into an increasing slender shape. The significant relationship between the density attributes large oyster and biomass enabled a classification of reef types by large oyster abundance. Reef type (simple or complex reef) and oyster size (small or large) were considered by implementing a novel concept of weighted twin functions (TF) for the relationship between SL and individual biomass. This study demonstrates that the interplay of scaling parameters (scalar, exponent) is highly sensitive to the estimation of individual biomass (shape) and that putative similar scaling parameters can exceedingly affect the estimation of areal biomass.

For the first time, this study documents the crucial relevance of areal reference, i.e. cluster density (CD) or reef density (RD), when comparing density. RD considers reef areas devoid of oysters and results from CD reduced by reef coverage (RC) as the relative reef area occupied by oysters. A compilation of density attributes at simple and complex reefs shall serve as a density guide. Irrespective of areal reference, oyster structural density attributes were significantly higher at complex than at simple reefs. In contrast, areal reference was of vital importance when evaluating the impact of engineering strength at ecosystem-level. While mussel CD was similar at both reef types, RD at complex reefs supported significantly more large mussels and higher mussel biomass than at simple reefs. Although mussels dominated both reef types by abundance of large individuals, oysters were the keystone engineers by dominating biomass.

The prominent status of large oysters for both allometric scaling and density, presumably characteristic for Pacific oyster populations worldwide, should be considered when conducting future investigations. The effort of monitoring will substantially be reduced as only large oysters have to be counted for an empirical characterization of Pacific oyster reefs. The large oyster concept is independent of sampling season, assessment method or ecosystem, and is also applicable to old data sets. Harmonization on the proposed density attributes with a clear specification of areal reference will allow trans-regional comparisons of Pacific oyster reefs and will facilitate evaluations of engineering strength, reef performance and invasional impacts at ecosystem-level.

Keywords

allometry, biogenic, ecosystem engineering, invasive species, reef complexity, reef density, reef type, reef structure

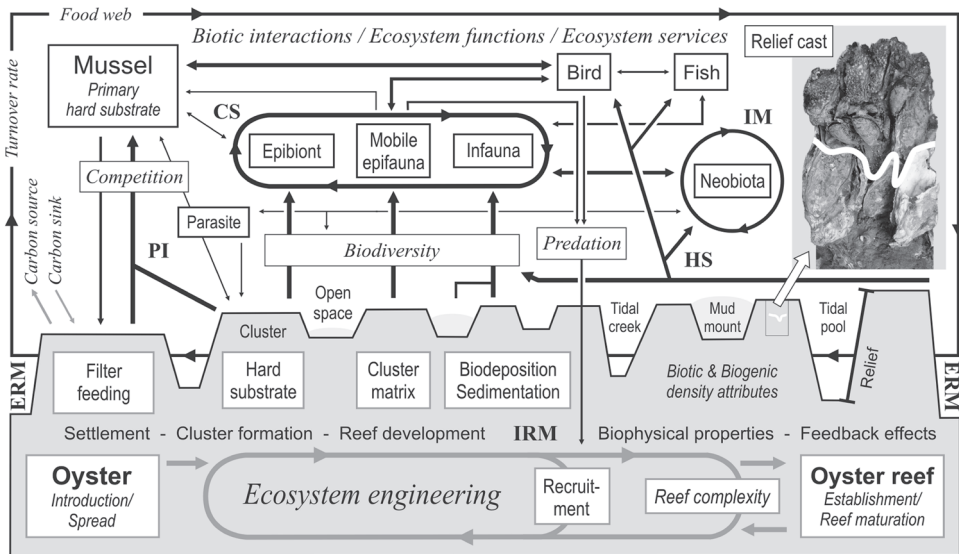
Introduction

The Pacific oyster *Crassostrea (Magallana) gigas* belongs to the most globalized marine invertebrates and is one of the most successful marine invaders worldwide. Oysters are ecosystem engineers as the creation of biogenic structure modulates the availability of resources to other species while biggest effects are attributable to oysters living at high densities, over large areas for a long time (Jones et al. 1994).

To attribute ecological and functional impacts of Pacific oysters to engineering strength in relation to density, space and time, one has to understand underlying processes of the creation of biogenic structures and the development of reef structural components due to increasing density and progressive engineering (Fig. 1). Oyster larva settles on hard substrate where the maturing oyster stays permanently attached. Due to the gregarious nature, clumps of several oysters develop from the process of repetitive settlement. Clumps enlarge by shell accretion and coalesce to oyster clusters. Increasing cluster density due to increasing numbers of live oysters and post-mortem oyster shells force the immobile filter feeder to grow increasingly vertical while a complex three-dimensional cluster matrix develops. A single cluster can cover several to some dozen square meters (Fig. 3A). Several clusters and interspersed oyster unoccupied open spaces perform as a bio-geo-morphological unit, encompassing the total area of an oyster reef. A Pacific oyster reef can reach several to some dozen hectares.

The rough surface structure of the reef reduces hydrodynamic forces which increases sedimentation above the reef and can even affect reef surroundings. High densities of oysters produce high amounts of biodeposit. Fine particles and resuspended material can accumulate in the cluster matrix and in post-mortem articulated oyster shells while individuals on top of the matrix stay clean due to small-scale turbulences at the direct interface. Progressive engineering has strongest effects on intertidal soft substrate environments. The creation of biogenic structure adds hard substrate while sediments increasingly enrich with organic matter. Fine particles and re-suspended material can accumulate in open spaces, i.e. reef areas devoid of oysters, and mud mounts may develop over time. Shells of oysters that died from burial at the bottom of clusters increasingly anchor the biogenic structure as clusters grow in height by vertical shell accretion and by raise of the sediment surface. Increasing rigidity, height and continuity of the system increase small scale tidal flow and intra-reef creeks along clusters or deep tidal pools between clusters can develop over time (Fig. 3A). These reefs harbor submerged sub-habitats even during low tide. The relief of intertidal soft-sediment Pacific oyster reefs can reach several meters (pictured in Folmer et al. 2017, Fig. 2).

Ecosystem engineering effects of introduced Pacific oysters have been discussed by Ruesink et al. (2005) while the authors stressed major gaps in knowledge of the spatial and temporal extent of direct (e.g. habitat use) and indirect (e.g. hydrodynam-



CS Community structure, ERM Extra-reef modification, HS Habitat suitability, IM Invasional meltdown, IRM Intra-reef modification, PI Population interference. Relief cast (18 x 30 cm) Pacific oyster reef *Dornumer Nacken* 2008 (approx. 6 years after initial oyster settlement). White line: Sediment surface. Top: Cluster matrix (live oysters, post-mortem oyster shells and live mussels). Bottom: Cluster anchorage (post-mortem oyster shells). Black arrow width indicates potential relevance of engineering effects on ecosystem-level.

Figure 1. Ecosystem engineering conceptual framework. Effects adapted for non-native Pacific oysters modulating resident intertidal mussel beds in the Wadden Sea of the North Sea.

ics, sediment budgets, nutrient cycling) ecological effects, and pointed out the lack of information especially at ecosystem-level. A lot of studies on engineering effects of non-native Pacific oysters have been performed in North West European Estuaries, and in particular in the UNESCO World Natural Heritage Site Wadden Sea where Pacific oysters have been successfully invading resident intertidal mussel (*Mytilus edulis*) beds (Folmer et al. 2017) (Fig. 1). Although several experimental (laboratory and on site) or in situ studies have been investigating effects of intra-reef modifications on habitat associated macrofauna (i.a. Kochmann et al. 2008, Markert et al. 2010), habitat use by birds (i.a. Markert et al. 2013, Waser et al. 2016), habitat use by fish (Dänhardt et al. in progress), habitat invasion by non-native Asian shore crabs *Hemigrapsus takanoi* (i.a. Markert et al. 2014, Waser et al. in progress), habitat invasion by non-native Japanese seaweed *Sargassum muticum* (i.a. Lang and Buschbaum 2010, Markert and Wehrmann 2013), parasite-host interactions among native and non-native species (i.a. Thieltges et al. 2009, Goedknecht et al. 2017), population dynamics (i.a. Schmidt et al. 2008; Eschweiler and Christensen 2011; Waser et al. 2015; Buschbaum et al. 2016; Reise et al. 2017a, 2017b; Folmer et al. 2017), feedback effects on the oyster itself (i.a. Troost et al. 2008, 2009) or spatially extended extra-reef modifications (i.a. Van der Zee et al. 2012, Walles et al. 2015a, Markert et al. 2016), research is far from estimating the good or the bad about the naturalization of the Pacific oyster in the Wadden Sea ecosystem. “Mussel beds” are still one of the target habitats when evaluating the good ecological status of the Wadden Sea, although most of the beds have been transformed into oyster reefs (Büttger et al. 2010, Folmer et al. 2017). The need for impacts of invasive Pacific oysters to be investigated at a range of invader density has been recognized (Green and Crowe 2014), but uniform measurements or tools that allow for comparison and extrapolation of engineering effects on a spatial scale, i.e. among tidal basins or estuaries and across nations or regions, have not yet been implemented (Folmer et al. 2017). Attempts at reaching trilateral (Netherlands, Germany and Denmark) agreements on monitoring Pacific oysters in the Wadden Sea have been made but national assessment methods had already been established independently and methodological adaption was limited by logistical and, in particular, financial effort. Likewise, the American oyster *Crassostrea virginica* has been studied comprehensively over several decades in restoration projects but universal metrics for evaluating the performance of habitat restoration were only just recently published to fulfill requests from restoration practitioners for a set of specific monitoring guidelines tiered to account for limitations in budgets and expertise (Baggett et al. 2015). Nevertheless, Kellogg et al. (2014) emphasized the need for tools that allow estimations of ecological function and related ecosystem services based on structural parameters of matured *C. virginica* reefs.

Some impacts of naturalizing oysters are considered context-dependent, e.g. provision of primary settling substrate provided at rocky shores or soft-sediments, in salt-marshes or seagrass, by *Sabellaria*-reefs or mussel beds (Padilla 2010, Herbert et al. 2016), but generalities can be deduced only from the physical presence of oysters. Engineering strength may be reflected by oyster density in clusters but the intra-reef pattern, i.e. the variability of oyster density among all intra-reef clusters in relation

to a patchy coverage of the reef area by these clusters, has important implications for a reef's structural dynamics and related biophysical properties. Biophysical interactions, i.e. feedback effects between oyster density, reef coverage, reef relief, reef height, reef areal extent and reef orientation, investigated for *C. virginica* influenced reef performance in terms of population persistence and habitat maintenance (Lenihan 1999, Schulte et al. 2009, Colden et al. 2016, Colden et al. 2017). Live oysters are commonly assessed for population studies but also post-mortem oyster shells enhance habitat heterogeneity, contribute to cluster compaction and provide settling space for spat, and thereby affect reef dynamics and biophysical properties. Mann et al. (2009) and Southworth et al. (2010) comprehensively sampled natural reefs of *C. virginica* with hydraulic patent tongs in order to assess oysters by size class and shell by volume. Shell volume referred to articulated post-mortem oyster shells (boxes), categorized as brown shell (boxes above sediment-water interface) or black shell (boxes exhumed during collection process), and seemed to include shell hash. The relationship between live *C. virginica* shell length and wet shell weight was used to estimate the amount of live shell while shell volume had to be converted to wet shell weight for comparative analyses of live proportions. This displays the complexity of structural attributes of oyster reefs in general and highlights the interplay between methodological approach and data analysis.

The present study provides the first documentation of biogenic density dynamics of Pacific oysters. Monitoring six sites over six consecutive years during post-establishment of the non-native oyster on former intertidal mussel beds in the Central Wadden Sea (Germany) compiled a comprehensive data set on shell length of live oysters and post-mortem oyster shells. Additionally, oyster individual metrics per site and year were measured to determine conversion functions from allometric scaling in order to convert the monitoring data into biomass. The two extensive datasets conditioned on interdependent analyses of the high variable oyster shape in relation to oyster size and oyster density, and interlinked estimations of areal biomass. These analyses coincidentally triggered significant interrelations between size-related population quantities and/or biomass of live oysters and/or post-mortem oyster shells. Results induced the development of a conceptual framework towards a harmonized approach to characterizing Pacific oyster reefs which will facilitate evaluations of Pacific oyster engineering strength at ecosystem-level. Analyses of this study were supplemented by mussel data as the evaluation of dominance, i.e. the determination of the keystone engineer, is one of the basic tasks when oysters invade habitats that are pre-occupied by native ecosystem engineers.

Methods

Study sites

Six sites in the intertidal of the Central Wadden Sea, German Federal State Lower Saxony, southern North Sea (Fig. 2) were monitored between 2008 and 2013 in order

to assess the density of Pacific oysters *Crassostrea (Magallana) gigas* (oyster) and blue mussels *Mytilus edulis* (mussel). The study region is characterized by muddy to sandy tidal flats with a semidiurnal tide cycle, a tidal range from 2.3 m in the west to 3.7 m in the east and a salinity range from 27 to 32. The tidal flats stretch along a 150 km coastline and cover an area of 1,380 km² (Wehrmann 2016). The study sites NL (Nordland 26.1 ha), NOR (Norderney 7.3 ha), DN (Dornumer Nacken 8.3 ha), SP (Swinnplate 9.3 ha), KB (Kaiserbalje 7.0 ha) and RB (Robinsbalje 4.2 ha) are evenly distributed from the most western to the most eastern part of the study region. Tidal elevation with a mean exposure time of about 3.5 hours per tidal cycle was similar at all sites.

The oyster is non-indigenous in the Wadden Sea and has been invading the study region since 1998 (Wehrmann et al. 2000). Settlement occurred predominantly on resident intertidal mussel beds. Oysters spread rapidly (Schmidt et al. 2008) and established self-sustaining populations throughout the study region. By 2006, all of 100 recorded intertidal mussel beds were colonized by oysters (Millat 2008). Since 2008, the oyster has been considered established and all mussel beds have been transformed into oyster reefs. The intra-reef pattern is typically patchy (Fig. 3A). Oyster clusters, i.e. reef areas occupied by oysters, are irregularly interspersed by open spaces, i.e. reef areas devoid of oysters. Clusters consist of clumps of live oysters and post-mortem oyster shells (Fig. 3B). Mussels are present between oysters. Single clusters may cover large reef areas of several dozen square meters. Oyster clumps mainly cover the cluster bottom completely but may also have a scattered distribution. All clusters disconnected by a maximum of 25 m were included when confining the outline of the biogenic structure, thus the reef area (Nehls et al. 2009).



Figure 2. Location of study sites in the intertidal of the Central Wadden Sea, German Federal State Lower Saxony, southern North Sea.

Density metrics

Annual surveys and sample collections took place around low tide mainly during spring. 12 stations per site were randomly selected from a grid superimposed on a diagram of the reef area. Coordinates were recorded and stations in the field were located during each survey by using a handheld GPS. Annual re-location of a given station varied by exact position as GPS accuracy is at best a few meters. At this, re-sampling or sampling in close proximity of beforehand sampled areas was presumed to be excluded. A sample frame of 25 × 25 cm (1/16 m² or 0.0625 m²) was exclusively placed on oyster clusters, i.e. if a station was located in an open space, the closest cluster was sampled. Sample frames typically encompassed surfaces that were completely occupied by oysters. In rare cases, only single clumps, single oysters or mussels were within the frame. All material (excavation depth preferably to a maximum of 10 to 15 cm below sediment surface

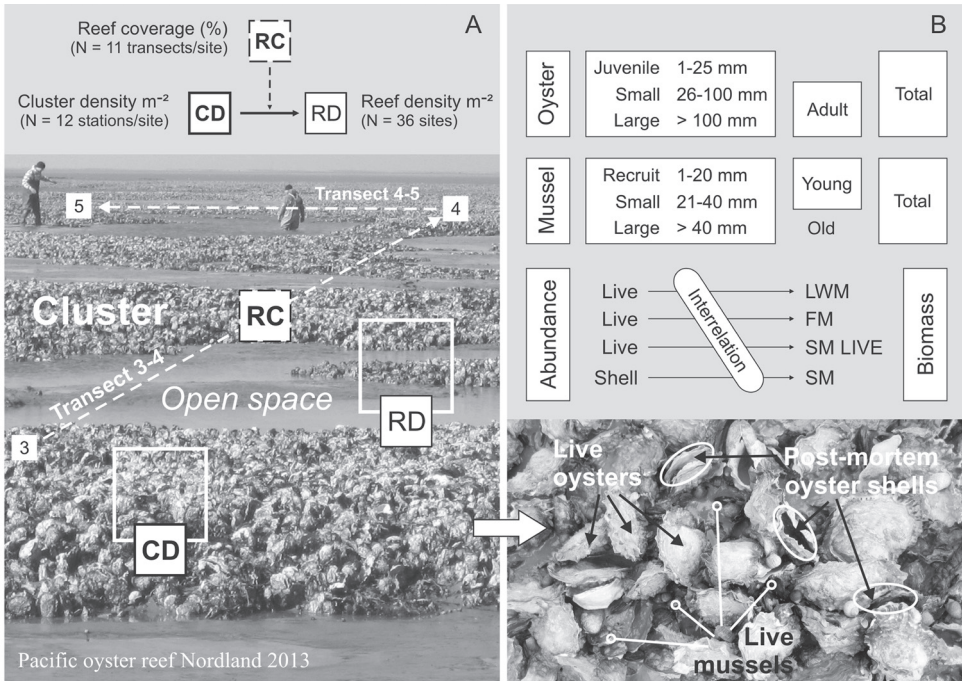


Figure 3. Density conceptual framework. **A** Areal reference. Cluster density (CD) reduced by reef coverage (RC) results in reef density (RD). Depicted are three stations (3/4/5 à 0.0625 m²), two station connecting transects (3-4/4-5) for RC and 1 m² encompassing CD/RD. **B** Density attributes. Abundance was calculated for SL-related population categories of live oysters, oyster shell and live mussels. Areal biomass was calculated from total abundance, respectively. Depicted are oysters and mussels in a cluster (top view). FM = cooked flesh mass, live = abundance of live oysters or mussels, LWM = live wet mass, shell = abundance of live oysters and post-mortem oyster shells, SM = shell mass of live oysters and post-mortem oyster shells, SM LIVE = shell mass of live oysters or mussels. See text for details.

but all live oysters included) was manually collected in buckets and stored in cooling chambers right after returning from the survey. Measurements were carried out after rinsing the samples within the next three days. Shell lengths (SL) of live oysters and post-mortem oyster shells, the latter only intact left valves and no shell fragments, and of live mussels (intact post-mortem mussel shells were extremely scarce due to rapid decay) were measured to the nearest mm. With reference to oysters, SL was recorded as the greatest distance from the hinge to the shell growth margin. This correctly is termed shell height, although commonly used to describe SL (Mann et al. 2009).

Data of each station was standardized to 1 m² cluster density (CD) (N = 432 cluster). CD of the 12 annual stations per site were averaged to CD per site and year (Fig. 3A) (N = 36 reefs). CD of the 12 annual stations per site were reduced by the annual reef coverage (RC) and averaged to reef density (RD) per site and year (N = 36 reefs). RC was assessed contemporaneously to each survey by pacing off all station connecting transects (11). Counts were made using two hand held tally counters, one for foot on cluster and one for foot on open space. RC was the proportion of steps on clusters to total steps of all transects. Total length of all transects per site was assigned to be at least 1 km and subsequently determined the order of the 12 stations. An average 167 ± 50 m per hectare was paced off and 211 ± 57 steps per hectare were made per site and year.

Individual metrics and allometric scaling

The monitoring between 2008 and 2012 was supplemented by a comprehensive biomass determination of in total 1.935 live oysters (SL 26–254 mm) and 1.553 live mussels (SL 11–70 mm). SL, live wet mass (LWM = shell, flesh and retention water), shell mass (SM LIVE) and cooked flesh mass (FM) were assessed from each individual. The determination of oyster individual metrics was based on 8 SL classes: 26–50, 51–75, 76–100, 101–125, 126–150, 151–175, 176–200, > 200 mm. Oysters up to 25 mm were excluded as the complete left valve is calcified to the attachment surface and cannot be removed without damage. The determination of mussel individual metrics was based on 6 SL classes: 11–20, 21–30, 31–40, 41–50, 51–60 and > 60 mm. Mussels up to 10 mm were excluded due to a high risk of damaging and handling efficiency. Immediately after measuring the SL of all individuals collected within the 12 stations, 10 intact and unopened individuals per species and SL class, if available, were randomly selected out of the material pool (Table 1). Fouling organisms were scraped off each shell surface. Specimen-specific SL (mm) and LWM (g), the latter to 0.001 grams accuracy, were recorded. Smaller individuals were placed in numbered tea filter bags and larger individuals numbered with a taped elastic band. Specimens were stored in a freezer and later defrosted before cooking oysters for about 10 minutes and mussels for about 5 minutes. The cooked flesh was separated from each shell, flesh and both valves were placed on paper towels before FM (g) and SM LIVE (g) were recorded to 0.001 grams accuracy.

Table 1. Number of oysters and mussels used to assess individual metrics. SP = Swinnplate, RB = Robinsbalje, NOR = Norderney, NL = Nordland, KB = Kaiserbalje, DN = Dornumer Nacken, LRD = simple reefs with low reef density, HRD = complex reefs with high reef density.

	2008	2009	2010	2011	2012	Total
Oyster						
SP (LRD)	54	57	47	58	60	276
RB (LRD)	43	51	51	62	60	267
NOR (LRD)	57	61	69	74	70	331
NL (HRD)	52	67	69	66	69	323
KB (HRD)	69	75	80	80	77	381
DN (HRD)	68	68	67	74	80	357
LRD	154	169	167	194	190	874
HRD	189	210	216	220	226	1,061
Total	343	379	383	414	416	1,935
Mussel						
SP (LRD)	50	49	60	50	57	266
RB (LRD)	50	49	55	48	55	257
NOR (LRD)	50	50	56	55	50	261
NL (HRD)	50	50	49	49	54	252
KB (HRD)	50	50	50	60	58	268
DN (HRD)	50	50	50	46	53	249
LRD	150	148	171	153	162	784
HRD	150	150	149	155	165	769
Total	300	298	320	308	327	1,553

Analyses of individual metrics were based on means per SL class. Shape was treated as a relative characteristic and was deduced from the relationship between LWM and SL. At a given SL, low LWM was interpreted to represent slender individuals and high LWM was interpreted to represent mighty individuals. The relationship between biomass (LWM, SM LIVE, FM) and SL was described by a power function $y = a(x)^b$, where y = the dependent variable for biomass (g), x = the independent variable for SL (mm), a = scalar and b = exponent (scaling parameters). Conversion functions (CF) describe allometric scaling relations of all SL classes. Oyster shape variability induced a data pooling of oyster individual metrics for allometric scaling. Individual metrics were “weighted” by reef type, i.e. pooling data of all simple reefs with low reef density (LRD) and all complex reefs with high reef density (HRD) (Figs 3, 4). Twin functions (TF) describe separate allometric scaling relations of small (SL 26–100 mm) and large (SL > 100 mm) oysters (Fig. 5). Weighted TF for oyster LWM, FM and SM LIVE and weighted CF for mussel LWM, FM and SM LIVE were determined for a general application (Figs 4, 7; Table 2). Oyster weighted TF and mussel weighted CF were applied to the SL data of the monitoring when estimating density attributes during the study period 2008–2013. SL of post-mortem oyster shells was converted by applying weighted TF for oyster SM LIVE. For additional analyses, allometric scaling relations were also determined after pooling individual metrics by site (local) or by site and year (unique).

Analyses of LWM-conversions were supplemented by the CF SH (Nehls and Büttger 2006) as the regional equation commonly used for Pacific oysters in Schleswig-Holstein (Northern Wadden Sea, Germany) with $a = 0.0032$, $b = 2.2321$, $R^2 = 0.6967$,

$N = 159$ and CF KATS (Walles 2015b) as a local equation determined from Pacific oysters at the reef KATS in the Oosterschelde estuary (The Netherlands) with $a = 0.00224$, $b = 2.13$, $R^2 = 0.97$, $N = 49$.

Density attributes

Density attribute is a generic term for the abundance of SL-related population categories of oysters or mussels, and for oyster or mussel areal biomass (Fig. 3B). Areal biomass in terms of areal LWM, FM and SM LIVE encompassed the total live population, respectively. Oyster areal SM encompassed the shell mass of all live oysters and all post-mortem oyster shells. Abundance of oysters was estimated for total, juvenile, small, large and adult individuals (Fig. 3B). This application-oriented subdivision became evident during data analyses when distinct linkages between individual metrics and oyster density were observed. Oyster spatfalls in the study region took place between late summer and early autumn (unpublished data, in prep.). These oysters had grown up to 25 mm in the following spring and were assigned as juveniles of the respective monitoring year. The remaining adult population (> 25 mm) was reasonably categorized into small (26–100 mm) and large oysters (> 100 mm). This categorization was implemented for live oysters and for oyster shell (live oysters and post-mortem oyster shells). For example, the abundance of large oysters may refer to live oysters only (large live) or to live oysters and post-mortem oyster shells (large shell). Accordingly, the proportion of large live oysters to large oyster shell was expressed as a LIVE-Factor Large. A population categorization by SL was also implemented for mussels, i.e. total, recruits, small, young and old (large) mussels (Fig. 3B). Mussels in the study area reproduced one to several times a year, between early spring and late autumn (unpublished data, in prep.). These mussels had grown up to 20 mm in the following spring and were assigned as recruits of the respective monitoring year. The remaining mature population (> 20 mm) was reasonably categorized into small (21–40 mm) and large mussels (> 40 mm). All large mussels were older than 2 years (unpublished data, in prep.). Recruits and small mussels were reasonably grouped to young mussels (1–40 mm).

Oyster and mussel density attributes were only contrasted within the same areal reference (Fig. 3). The relevance of areal reference in relation to oyster density attributes was exemplarily displayed for two reefs with similar structural density. Intra-reef variation of oyster density attributes was analyzed by determining the coefficient of variation (CV) for all sites and years. Selected CV and density attributes of oysters and mussels were interrelated. Simple linear regression analyses were performed, the coefficients of determination specified and the significance of the slope was tested (t-Test). Proportions of significant interrelations were given when the intercept was negligible, i.e. intercept not significant when $< 5\%$ of y (max). For significant interrelations between areal biomass and the abundance of large individuals, a so-called density scaling was implemented.

Oyster and mussel density attributes of all sites and years were pooled by reef type. Therefore, each site during the study period 2008–2013 was allocated by its abundance of large live oyster RD to one of the defined reef types, i.e. simple reef with low reef density (LRD) or complex reef with high reef density (HRD) (Fig. 4C). Density attributes at simple reefs (all LRD-sites) and at complex reefs (all HRD-sites) ($N = 18$ each) were averaged and the difference between reef types was tested for significance (t-Test). To display the influence of areal reference, significance was also tested between complex reef RD and simple reef CD (Table 3).

Results

Oyster shape and classification of reef types

Oyster shape was highly variable among sites (Fig. 4A). Shape differences between sites became conspicuous in large oysters (> 100 mm) and grew increasingly distinct with increasing SL. Shape of large oysters varied between wide, deep cupped mighty individuals at site SP and narrow, low cupped slender individuals at site DN. Compared to small oysters (26–100 mm), the slope of oyster shape attenuated in large oysters which emphasized a SL-related categorization of oysters into small and large oysters for allometric scaling (Fig. 5).

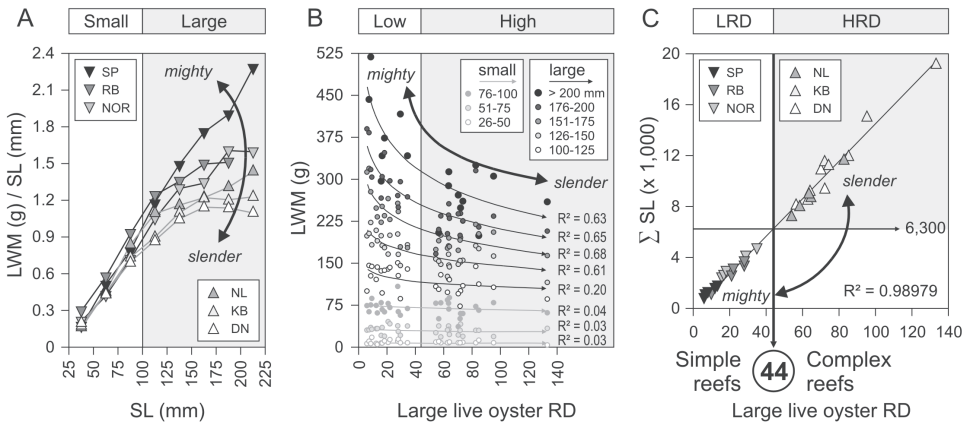


Figure 4. Oyster shape and classification of reef types. **A** Site- (SP-DN) and size-dependent (small/large) oyster shape. Plotted is individual LWM (g) per SL (mm) against SL (mm) of 8 SL classes per site. **B** Density-related (low/high) variation of oyster shape. Plotted is individual LWM (g) of 8 SL classes against large live oyster RD per site and year. Exponential trend of density-related shape difference indicated per SL class. **C** Determination of the threshold density of 44 large live oyster RD to classify sites into simple reefs with low reef density (LRD) and complex reefs with high reef density (HRD). Displayed is the linear relation of large live oyster RD to the sum of their SL. R^2 = coefficient of determination.

Observations in the field indicated that shape differences might be affected by crowding. The most reliable and comparable variable to reflect density was assumed to be biomass but abundance was the available data from monitoring while areal biomass was not yet calculated. The interlinked analyses of individual and areal data of this study eventually detected patterns and the general concept of density attributes (Fig. 3B) was accomplished. At this, large oysters were identified as intrinsic drivers of density (see paragraph on oyster density attributes). However, large oyster individual LWM (g) was exponentially related to oyster density, e.g. large live oyster RD (Fig. 4B). An increasing slender shape of large oysters with increasing RD was apparent. RD had no obvious effect on the shape of small oysters. To meet the distinctiveness of a density-related shape of large oysters for allometric scaling (Fig. 5), a classification into reef types was implemented (Fig. 4C). Therefore, large live oyster RD was related to the sum of their SL values, the latter meant to represent the SL distribution of large live oysters, respectively. A threshold density of 44 large live oyster RD was determined to separate simple reefs with low reef density (LRD) from complex reefs with high reef density (HRD). Throughout the study period of the monitoring between 2008 and 2013, sites SP, RB and NOR were assigned to simple reefs (LRD) and NL, KB and DN to complex reefs (HRD).

Oyster allometric scaling

Oyster individual biomass (LWM, SM LIVE and FM) was highly variable. The range per SL class increased with oyster size and was most considerable in the largest SL class. LWM of oysters larger than 200 mm ranged from 144.7 g (206 mm, KB 2009) to 645.2 g (239 mm, SP 2012) and the same specimens limited the range of SM LIVE (86.4 g to 427.3 g). FM of the SL class > 200 mm ranged from 7.7 g (215 mm, KB 2012) to 65.6 g (211 mm, NOR 2011).

Aiming at the determination of general biomass conversion functions with a universal application, size-dependent and density-related variability of oyster shape was considered for oyster allometric scaling. To mediate between underestimations at reefs with mighty oysters and overestimations at reefs with slender oysters, data of individual metrics was weighted by density. Therefore, individual metrics were grouped to LRD data by pooling individual metrics of all simple reefs (SP, RB, NOR 2008–2012) and to HRD data by pooling individual metrics of all complex reefs (NL, KB, DN 2008–2012) (Fig. 4C). For both reef types, power functions fitted well to the relationship between SL and biomass (LWM_{LRD} : $R^2 = 0.98563$, LWM_{HRD} : $R^2 = 0.97443$, $SM\ LIVE_{LRD}$: $R^2 = 0.98915$, $SM\ LIVE_{HRD}$: $R^2 = 0.97565$, FM_{LRD} : $R^2 = 0.95709$, FM_{HRD} : $R^2 = 0.93187$), but all slopes reflected the above mentioned size-dependent pattern (Fig. 4A). This pattern was also characteristic for all unique relationships, i.e. allometric scaling of individual metrics per site and year. Hence, the conversion of SL would underestimate the biomass of medium sized oysters and largely overestimate the biomass of oysters larger than 175 mm (Fig. 5A). Scaling relations of small oysters

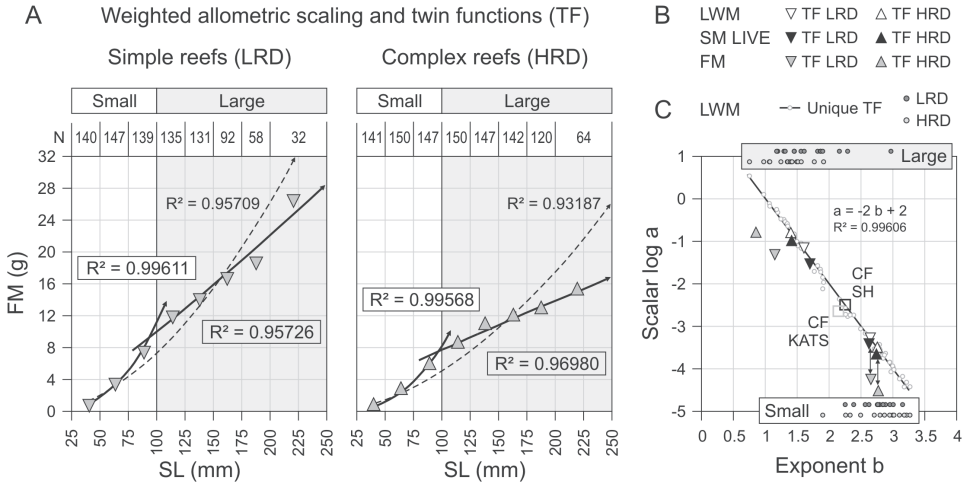


Figure 5. Oyster allometric scaling. **A** Determination of FM weighted TF. Plotted is FM (g) against SL (mm) of 8 SL classes after pooling individual metrics according to reef type (weighted). Displayed are powered relationships of all SL classes (broken line arrows), and of small and large oysters (TF) (black arrows). Given are coefficients of determination (R^2 , FM weighted TF in boxes) and number of oysters per SL class (N). **B** Plotted are scaling parameters of LWM, SM LIVE and FM weighted TF (N = 12 equations, Table 2). Note similar exponents for small oysters (arrows). **C** Plotted are scaling parameters of all LWM TF per site and year (unique) (N = 30 small, N = 30 large). Exponential relationship indicated, equation and coefficient of determination (R^2) given. Distribution of exponents at both reef type is given for small and large oysters (in boxes), respectively. Additionally plotted are scaling parameters of LWM conversion functions of two other studies (CF SH, CF KATS). Large oysters highlighted (gray area). LRD = simple reefs with low reef density, HRD = complex reefs with high reef density, TF = twin function.

attenuated in large oysters and a better fit for the relationship between biomass and SL was achieved by separating scaling relations for small and large oysters (Fig. 5A). These size-dependent power functions were termed twin functions (TF). TF were determined per reef type. The implementation of weighted TF (TF LRD, TF HRD) resulted in four equations (TF LRD/small, TF LRD/large, TF HRD/small and TF HRD/large) for LWM, SM LIVE and FM, respectively (Table 2). Compared to the calculation of oyster areal biomass by using LWM weighted TF, the regional LWM CF, i.e. determined by using the non-weighted and size-independent 5-year data set, underestimated simple reefs and overestimated complex reefs by up to 20 %.

Scaling parameters of all weighted TF (N = 12 equations) were contrasted. Small oysters scaled by similar exponents for LWM, SM LIVE and FM at LRD (b/rounded = 2.63/LWM, 2.61/SM LIVE, 2.63/FM) or at HRD (b/rounded = 2.74/LWM, 2.72/SM LIVE, 2.75/FM) (Fig. 5B). Mass differences primarily resulted from changes of the scalar. In contrast, scaling parameters for large oyster conversion did not show such a regular pattern and especially FM at both reef types scaled under other rules. While LWM and SM LIVE at HRD scaled by similar exponents (b/rounded = 1.40) and mass differences were mainly determined by different scalars, mass differences between

LWM and FM at HRD resulted from different exponents while scalars were similar. Scaling parameters for LWM, SM LIVE and FM appeared to be most heterogenic for large oysters at LRD (Fig. 5B).

Scaling parameters were also determined for small and large oyster LWM per site and year. Scaling parameters of these unique TF (N = 60, 30 small and 30 large) were significantly correlated (Fig. 5C). The scalar exponentially declined with increasing exponent ($\log a = -2.00 b + 1.99$, $R^2 = 0.99606$, $p < 0.001$). Exponential relations were slightly right-displaced for scaling parameters of all simple reefs ($\log a = -2.03 b + 2.09$, $R^2 = 0.99644$, $p < 0.001$) and slightly left-displaced for all complex reefs ($\log a = -1.98 b + 1.94$, $R^2 = 0.99641$, $p < 0.001$). Scaling exponents were high variable and ranged from < 1 to > 3 (Figs 4C, 5). Scaling exponents of large oysters ranged from < 1 to about 2, although one simple reef (SP 2010) had an exponent of 2.95881. Scaling exponents of small oysters ranged from about 2 to > 3 (Figs 4C, 5). Although generated by using all oyster sizes, scaling parameters of LWM conversion functions of two other studies, i.e. CF SH and CF KATS, fitted well to the exponential relationship of all unique TF of this study (Fig. 5C).

Despite the high correlation, small differences between exponents resulted in considerable different LWM (g) while an exponentially lower scalar had a strong additional effect. Considering similar exponents for small oysters ranging from $b = 2.83234$ to $b = 2.87106$ ($d = 0.03872$), the LWM of a 30 mm oyster ranged between 3.1 g and 4.2 g (+ 36 %) and of an 80 mm oyster between 49.4 g and 69.8 g (+ 41 %) (Fig. 6A). Considering small differences between exponents for large oysters ranging from $b = 1.75915$ to $b = 1.90149$ ($d = 0.14234$), the LWM of a 110 mm oyster ranged between 79.6 g and 141.1 g (+ 77 %) and of a 170 mm oyster between 171.2 to 316.6 g (+ 85 %) (Fig. 6A). Similar exponents of CF KATS and CF SH ($d = 0.1021$) resulted in extraordinarily different LWM (Figs 4C, 5A). Although the difference between scalars seemed small ($d = 0.00096$), CF SH estimated between 2 and 2.5-fold more LWM per oyster than CF KATS. The resulting LWM for a 30 mm oyster was 3.1 g and 6.2 g (+ 102 %), for a 80 mm oyster 24.3 g and 56.6 g (+ 123 %), for a 110 mm oyster 50.0 g and 115.3 g (+ 131 %) and for a 170 mm oyster 126.2 g and 304.6 g (+ 141 %) (Fig. 6A). Providing almost equal scalars of large oyster local TF RB ($a = 0.15677$) and large oyster local TF NL ($a = 0.15678$), a slightly higher exponent ($d = 0.03109$) of TF RB resulted in 17 % heavier large individuals, i.e. large oysters at the simple reef RB were mightier than at the complex reef NL (Fig. 6B).

A higher exponent was not generally resulting in more or less LWM, i.e. in mightier or slenderer shaped oysters (Fig. 6). For small oysters, increasing exponents by exponentially declining scalars of unique TF ($R^2 = 0.98539$) (Fig. 6A) and increasing exponents of local TF (Fig. 6B) tended to estimate less LWM of 30 mm oysters ($R^2 = 0.65056$), i.e. trend to a slenderer shape ($R^2 = 0.50646$), and rather more LWM of 80 mm oysters ($R^2 = 0.23768$), i.e. trend to a mightier shape ($R^2 = 0.08260$). These trends were not reflected by weighted TF as the higher exponent of TF HRD generally estimated less LWM, i.e. trend to a more slender shape of small

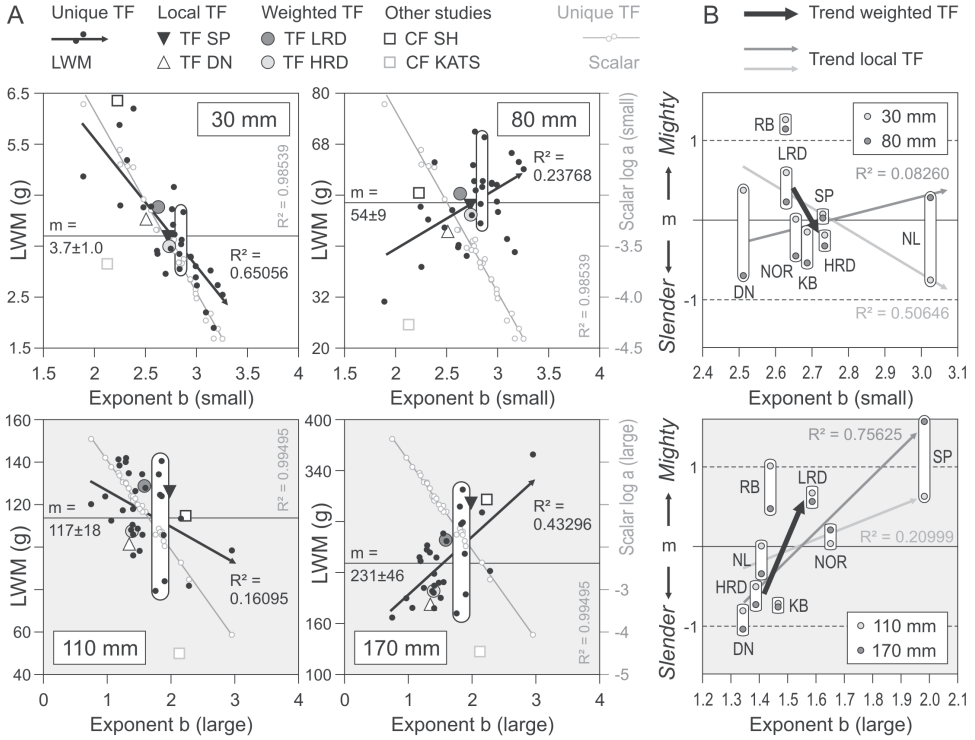


Figure 6. Relationship between scaling exponent and oyster LWM (g) of selected small (SL 30/80 mm, top) and large (SL 110/170 mm, bottom) individuals. **A** Plotted is LWM resulting from unique TF, selected local TF (SP for mighty and DN for slender shaped oysters), weighted TF (LRD, HRD) and CF of two other studies (SH, KATS) against exponent, respectively. Mean LWM (horizontal line, $m \pm SD$) and linear trend of increasing or decreasing LWM with increasing exponent of unique TF indicated (black arrow, R^2). Variability of LWM resulting from similar exponents of unique TF highlighted (rounded boxes). Additionally plotted is the exponential relationship (broken line, R^2 upend) between scalar and exponent of unique TF (gray circles). **B** Plotted is relative shape resulting from local TF (SP, RB, NOR, NL, KB, DN) and weighted TF against exponent. Relative shape = $(LWM - m) / SD$ with 0 = m and 1 = SD . Change of oyster shape with increasing exponent is displayed as a linear trend between sites (gray arrows, R^2). Trend between reef types indicated (black arrow). R^2 = coefficient of determination.

oysters (Figs 5A, B). For large oysters and analogous to small oysters, increasing exponents by exponentially declining scalars of unique TF ($R^2 = 0.99495$) (Fig. 6A) tended to estimate rather less LWM for 110 mm oysters ($R^2 = 0.16095$), i.e. trend to a slenderer shape, and more LWM for 170 mm oysters ($R^2 = 0.43296$), i.e. trend to a mightier shape. These trends were not consistently reflected by local TF or weighted TF (Fig. 6B) as higher exponents tended to or generally (as of TF LRD) estimated more LWM for 110 mm ($R^2 = 0.20999$) and 170 mm ($R^2 = 0.75625$), i.e. trend to a mightier shape of large oysters.

Variability of oyster LWM (kg) RD

The application of unique TF (N = 60, 30 small and 30 large) was expected to result in the most probable LWM (kg) RD per site and year during the study period 2008–2012. Respective RD were the nominal reef density (NRD, N = 30 local, N = 5 regional) when assessing deviations of areal LWM calculated by applying various CF or TF. Dynamic changes of the annual range of deviations per site, i.e. the range of the resulting LWM from the application of TF SP, TF LRD, TF HRD and TF DN, reflected site-specific temporal differences between allometric scaling relations (Fig. 7A). TF DN, representative of the slenderest shaped oysters, underestimated almost all NRD. Areal biomass was on average 23 % lower at simple reefs and 5 % lower at complex reefs which resulted in underestimations of, on average, 9 % in the study region (Fig. 7B). In contrast, TF SP, representative of the mightiest shaped oysters, overestimated most of the NRD (Fig. 7A). Deviations stayed low at the simple reefs SP and RB, but reached already up to 30 % at site NOR. TF SP resulted in distinct overestimations of up to 68 % at complex reefs, leading to an average 37 % higher areal biomass than NRD (Fig. 7A). The application of TF SP resulted in overestimations of on average 30 % in the study region (Fig. 7B). Low deviations were achieved by applying weighted TF, i.e. TF LRD to the monitoring data of simple reefs and TF HRD to the monitoring data of complex reefs. Deviations at the sites ranged from

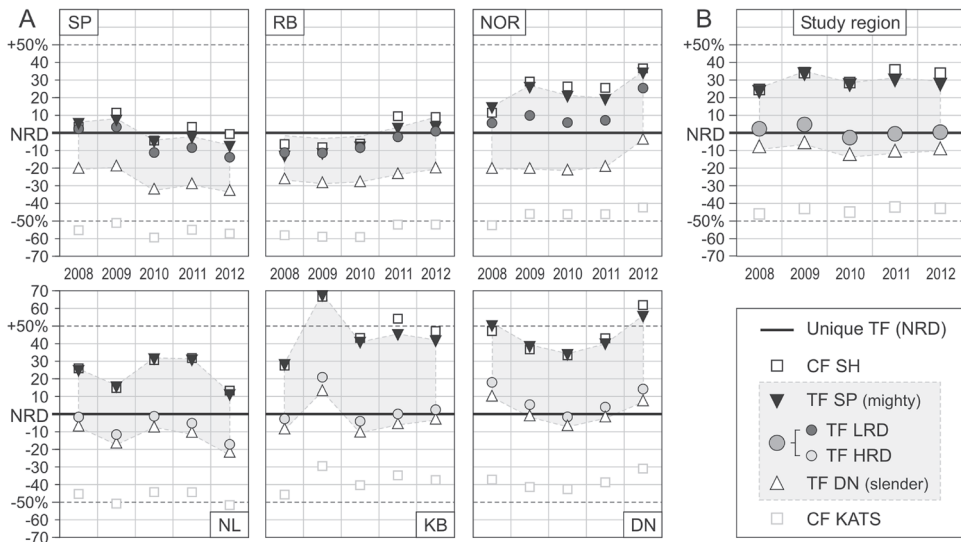


Figure 7. Variability of oyster LWM (kg) RD estimated for the study period 2008–2012. Displayed is the relative deviation (%) from nominal reef density (NRD). NRD was estimated by using unique TF. Deviations were estimated by using weighted TF (LRD, HRD), local TF (SP, DN) or CF of two other studies (SH, KATS). **A** Variability at the study sites. Sites arranged from mighty (SP) to slender (DN) oyster shape, equivalent to increasing reef density at simple (top) and complex reefs (bottom). **B** Variability in the study region. Range of deviation highlighted for TF of this study (gray area).

17 % below to 26 % above NRD, but most of the deviations stayed within $\pm 10\%$. Deviations tended to be lower at simple reefs (mean 0.5 %) and higher at complex reefs (mean 1.4 %). The application of weighted TF resulted in an average 1 % higher biomass in the study region, ranging between 3 % below and 5 % above NRD.

The sensitivity of the interplay of an almost similar exponent and a slightly different scalar (Fig. 6B) was conspicuously reflected by resulting LWM (kg) RD that was calculated from the application of CF SH and CF KATS (Fig. 7). NRD was largely underestimated by the CF KATS (53 % at simple reefs, 41 % at complex reefs) and overestimated by the CF SH (10 % at simple reefs, 39 % at complex reefs). CF SH showed a comparable dynamic as TF SP and its application to the monitoring data resulted in biomass overestimations of on average 32 % in the study region. In contrast, the application of CF KATS resulted in an average 44 % less biomass in the study region.

Mussel allometric scaling

Mussel shape as the proportion of LWM (g) per SL varied between sites (Fig. 8A). Shape differences became obvious in old (large) mussels (> 40 mm) while the relative difference between SL classes did not change with increasing size. Shape differences seemed small but large mussels had a mightier shape (10 % more LWM) at simple reefs than at complex reefs. Thus, individual metrics of mussels from 2008 through 2012 were pooled according to reef type, i.e. weighted to simple (LRD) and complex (HRD) reefs (Fig. 8B,

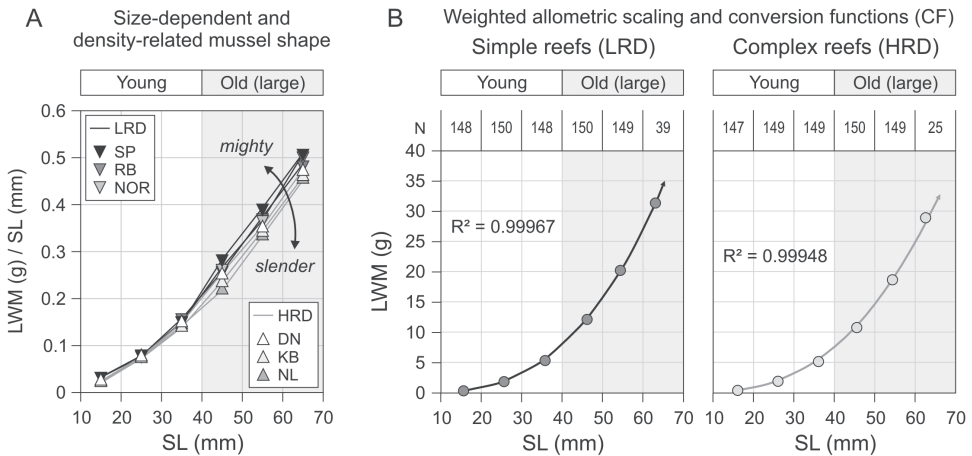


Figure 8. Mussel shape and allometric scaling. **A** Size-dependent (young/old) and density-related (LRD, HRD) mussel shape. Plotted is individual LWM (g) per SL (mm) against SL (mm) of 6 SL classes per site. **B** Determination of LWM weighted CF. Plotted is LWM (g) against SL (mm) of 6 SL classes after pooling individual metrics from 2008 through 2012 according to reef type. Given are powered relationships and coefficients of determination (R^2). Old (large) mussels highlighted (gray area). Number of mussels per SL class is given (N). Scaling parameters of all weighted CF are listed in Table 2.

Table 2). In contrast to size-dependent scaling relations of oysters and the determination of TF, powered CF perfectly described the relationship between mussel biomass and all SL classes (LWM_{LRD} : $R^2 = 0.99967$, LWM_{HRD} : $R^2 = 0.99948$, $SM\ LIVE_{LRD}$: $R^2 = 0.99927$, $SM\ LIVE_{HRD}$: $R^2 = 0.99874$, FM_{LRD} : $R^2 = 0.99845$, FM_{HRD} : $R^2 = 0.99817$).

Areal reference and oyster density attributes

The abundance of live oysters at two reefs (NL 01-04-2008, DN 29-03-2011) with similar areal LWM (kg) was contrasted (Fig. 9A). LWM at both sites was about 25 kg CD and about 12 kg RD as RC (45.9 % at NL in 2008, 46.6 % at DN in 2011) adjusted the density of clusters to the reef area. The difference between density attributes per CD and RD displayed the prominence of areal reference.

At both sites, live oysters were present in all SL classes and reached a maximum length of 230 mm (Fig. 9B). Total live abundance at the reefs differed tremendously (Figs 8A, B). DN had 4,539 total oyster CD and NL only 464. The population at DN consisted of 4,245 juvenile oyster CD and 293 adult oyster CD. Total oyster RD at DN was 2,113 consisting of 1,976 juveniles and 136 adults. Juveniles at DN dominated the total population by 93.5 %. Despite the same season, only 4.2 % were juveniles at NL and the population was dominated by adult oysters. The abundance of 205 adult oyster RD at NL was 50 % higher than at DN. The abundance of small oysters accounted for the difference between the adult populations (Figs 8A, B). A similar density at both reefs was the abundance of large oysters, i.e. 55 RD or 119 CD at NL and 56 RD or 121 CD at DN. The dynamic relation between the density attributes large live oyster and LWM was also reflected by station densities (CD) (Fig. 9C).

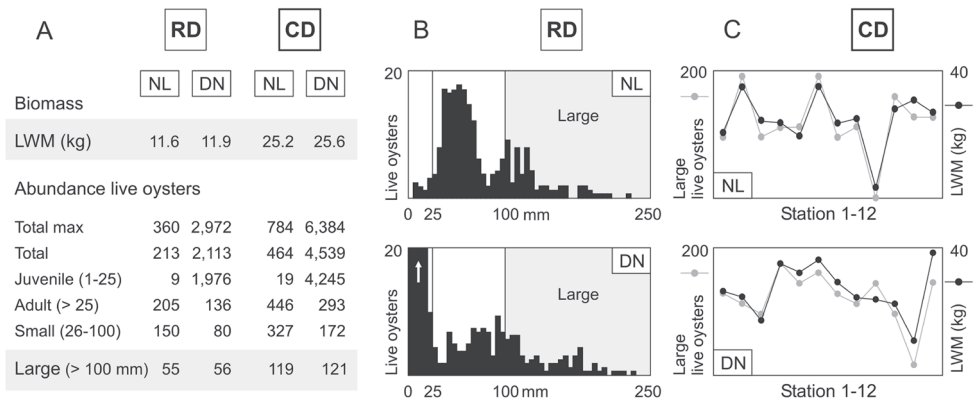


Figure 9. Density of live oysters at site NL on 01-04-2008 and site DN on 29-03-2011. **A** Density attributes LWM (kg) and abundance per areal reference RD and CD. **B** Length frequency distribution of live oyster RD. **C** Density attributes LWM (kg) and large live oyster CD at the 12 monitoring stations. Density metrics and density attributes according to Figure 3.

Intra-reef variation of oyster density attributes

A high spatial variation of oyster density attributes was present at all sites and years ($N = 36$ reefs), and generally resulted in high standard deviations. Coefficients of variation (CV) mainly ranged between 0.2 and 1.0 (Fig. 10). The variability of LWM among the 12 monitoring stations as displayed for the complex reefs NL in 2008 and DN in 2011 (Fig. 9) resulted in CV of about 0.3 which was comparably low compared to other sites (Fig. 10A). Apart from total live oyster abundance, the CV of all density attributes were moderately negative correlated with density (LWM: $R^2 = 0.62635$, $p < 0.001$, Fig. 10A; Large live: $R^2 = 0.60881$, $p < 0.001$; Adult live: $R^2 = 0.41744$, $p < 0.001$; Total live: $R^2 = 0.10091$, $p = 0.06$; SM: $R^2 = 0.58133$, $p < 0.001$, Fig. 10A; Large shell: $R^2 = 0.57057$, $p < 0.001$; Adult shell: $R^2 = 0.63452$, $p < 0.001$; Total shell: $R^2 = 0.28440$, $p < 0.001$).

CV of areal biomass (LWM or SM) and the CV of total or adult abundance (live or shell) were moderately to strongly positive correlated (LWM/total live: $R^2 = 0.51191$, $p < 0.001$; LWM/adult live: $R^2 = 0.54837$, $p < 0.001$, Fig. 10B; SM/total shell: $R^2 = 0.59549$, $p < 0.001$, Fig. 10B; SM/adult shell: $R^2 = 0.74836$, $p < 0.001$), while CV of areal biomass were higher than CV of total or adult oyster abundance (LWM: mean CV = 0.55, SM: mean CV = 0.53, Total live: mean CV = 0.49, Adult live: mean CV =

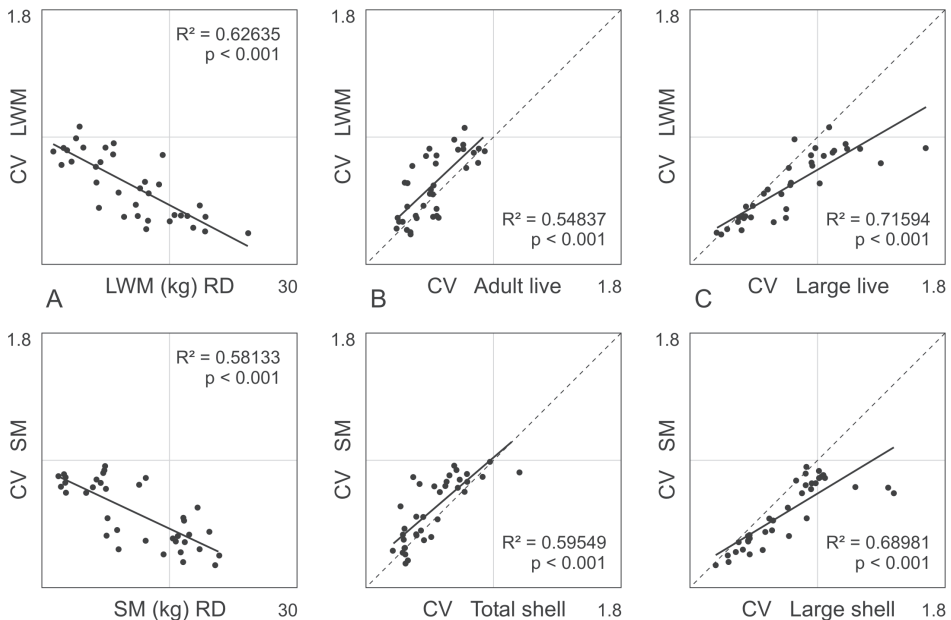


Figure 10. Coefficient of variation (CV) of selected oyster density attributes per site and year ($N = 36$ reefs). **A** Relationship between areal biomass and CV. **B, C** Interrelations between CV of abundance and areal biomass. Given are linear relationship, coefficient of determination (R^2) and significance level (p). Proportional reference line indicated (dotted). See text for all other relationships. Density metrics and density attributes according to Figure 3.

0.47, Total shell: mean CV = 0.46, Adult shell: mean CV = 0.44). CV of areal biomass (LWM or SM) and the CV of large oysters (live or shell) were strongly positive correlated (LWM/large live: $R^2 = 0.71594$, $p < 0.001$; SM/large shell: $R^2 = 0.68981$, $p < 0.001$; Fig. 10C), while CV of large oysters were higher than CV of areal biomass (Large live mean CV = 0.71, Large shell mean CV = 0.68, LWM: mean CV = 0.55, SM: mean CV = 0.53). Correlation between the CV of areal biomass and large oyster abundance was strongest at all complex reefs (LWM/large live: $R^2 = 0.84884$, $p < 0.001$, LWM: mean CV = 0.39, Large live: mean CV = 0.46; SM/large shell: $R^2 = 0.95117$, $p < 0.001$, SM: mean CV = 0.39, Large shell: mean CV = 0.46). As CV of large oysters (live or shell) at some reefs with lowest mean estimates of oyster density reached values well above 1.0, correlation between CV of areal biomass and large oyster abundance was weak at all simple reefs (LWM: $R^2 = 0.26703$, $p < 0.03$, LWM: mean CV = 0.72, Large live: mean CV = 0.95; SM: $R^2 = 0.20197$, $p < 0.06$, SM: mean CV = 0.68, Large shell: mean CV = 0.89).

Interrelations of oyster density attributes

Interrelations between oyster density attributes per site and year ($N = 36$ reefs) revealed distinct linkages, most of them showing strong linear and positive relationships (Figs 11, 12). The abundance of the total live population depended on the abundance of juvenile

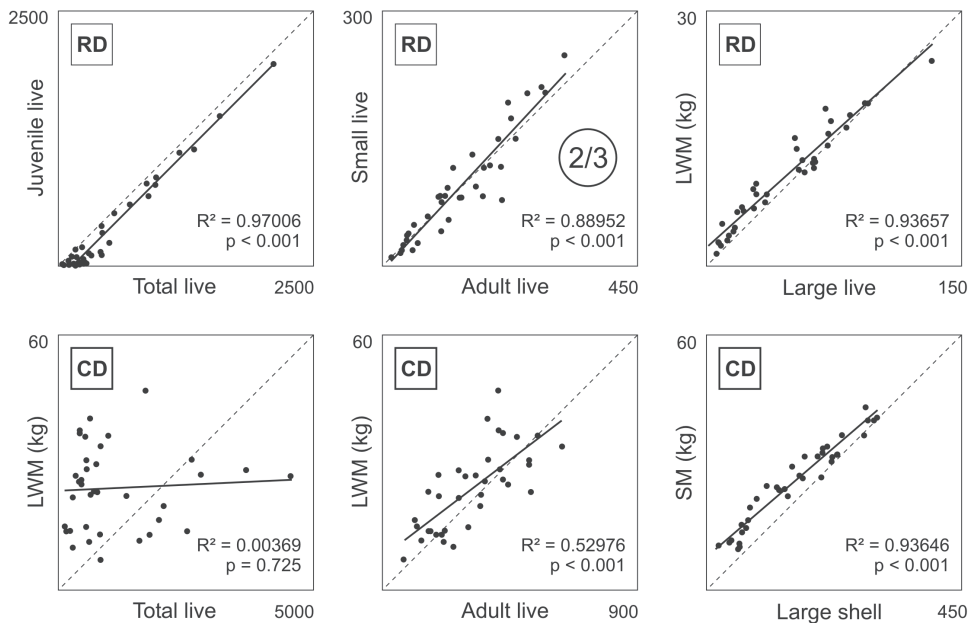


Figure 11. Interrelations between selected oyster density attributes per site and year ($N = 36$ reefs). Given are linear relationship, coefficient of determination (R^2) and significance level (p). Proportional reference line (dotted) and proportions indicated (circles). See text for all other interrelations. Density metrics and density attributes according to Figure 3.

live oysters (RD: $R^2 = 0.97006$, $p < 0.001$, Fig. 11) (CD: $R^2 = 0.98304$, $p < 0.001$). Likewise, the abundance of all shell depended on the abundance of juvenile shell (RD: $R^2 = 0.97673$, $p < 0.001$) (CD: $R^2 = 0.98404$, $p < 0.001$). Abundance of total live oysters was not explaining LWM (RD: $R^2 = 0.04935$, $p = 0.193$) (CD: $R^2 = 0.00369$, $p = 0.725$, Fig. 11). Likewise, the abundance of all shell was not explaining SM (RD: $R^2 = 0.04837$, $p = 0.197$) (CD: $R^2 = 0.00012$, $p = 0.950$). LWM increased with the abundance of adult live oysters (RD: $R^2 = 0.71402$, $p < 0.001$) (CD: $R^2 = 0.52976$, $p < 0.001$, Fig. 11) and SM with the abundance of adult shell (RD: $R^2 = 0.78733$, $p < 0.001$) (CD: $R^2 = 0.59085$, $p < 0.001$), but relationships were relatively low (RD) or even weak (CD) as the abundance of adult oysters largely depended on the abundance of small oysters (live oysters RD: $R^2 = 0.88952$, $p < 0.001$, Fig. 11) (live oysters CD: $R^2 = 0.84851$, $p < 0.001$) (oyster shell RD: $R^2 = 0.95251$, $p < 0.001$) (oyster shell CD: $R^2 = 0.91846$, $p < 0.001$). 2/3 of adult live oysters were small individuals (small adult live = $66.0 \pm 15.4\%$) and 3/4 of adult shell accounted for small shell (small adult shell = $75.3 \pm 11.4\%$). LWM was strongly related to the abundance of large live oysters (RD: $R^2 = 0.93657$, $p < 0.001$, Fig. 11) (CD: $R^2 = 0.90843$, $p < 0.001$) and SM to the abundance of large shell (RD: $R^2 = 0.95113$, $p < 0.001$) (CD: $R^2 = 0.93646$, $p < 0.001$, Fig. 11).

A linear relation existed between the abundance of large live oysters and large shell (RD: $R^2 = 0.84737$, $p < 0.001$, Fig. 12) (CD: $R^2 = 0.78122$, $p < 0.001$). Although a weak negative trend with increasing abundance of large shell was present, the propor-

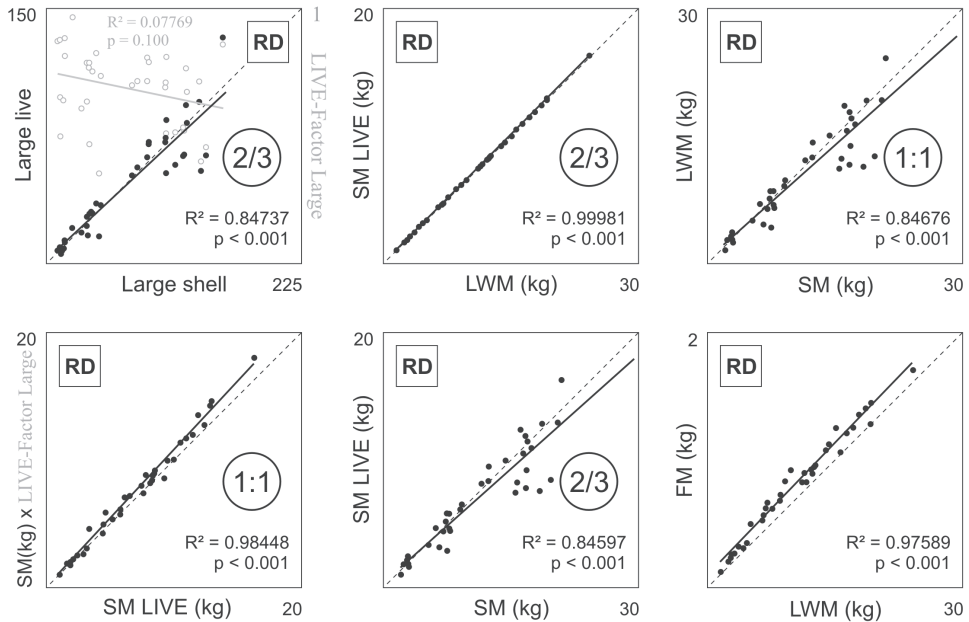


Figure 12. Interrelations between selected oyster density attributes per site and year (N = 36 reefs). Given are linear relationship, coefficient of determination (R^2) and significance level (p). Proportional reference line (dotted) and proportions indicated (circles). See text for all other interrelations. Density metrics and density attributes according to Figure 3.

tion of large live oysters was similar at all sites and years (RD: $R^2 = 0.07769$, $p = 0.100$, Fig. 12) (CD: $R^2 = 0.13573$, $p = 0.027$). 2/3 of all large oysters (LIVE-Factor Large = 69.0 ± 15.0 %) were alive. SM LIVE per site and year was re-calculated by multiplying SM with the respective LIVE-Factor Large. Differences to nominal SM LIVE were negligible (RD: slope = 1.07546, intercept = 0.3 %, $R^2 = 0.98448$, $p < 0.001$, Fig. 12) (CD: slope = 1.06335, intercept = 0.1 %, $R^2 = 0.97377$, $p < 0.001$).

A significant linear relation existed between the density attributes SM LIVE and LWM (RD: $R^2 = 0.99981$, $p < 0.001$, Fig. 12) (CD: $R^2 = 0.99940$, $p < 0.001$). 2/3 of the LWM accounted for SM LIVE (67.6 ± 0.8 %). As a consequence, SM LIVE correlated with the abundance of large live oysters (RD: $R^2 = 0.93833$, $p < 0.001$) (CD: $R^2 = 0.90731$, $p < 0.001$). A linear relation existed between the density attributes SM LIVE and SM (RD: $R^2 = 0.84597$, $p < 0.001$, Fig. 12) (CD: $R^2 = 0.72971$, $p < 0.001$). 2/3 of the SM accounted for SM LIVE (64.4 ± 12.3 %). As a consequence, along with the 2/3 proportions SM LIVE/LWM and SM LIVE/SM, SM equalled LWM (RD: slope = 0.89002, intercept = 2.1 %, $R^2 = 0.84676$, $p < 0.001$, Fig. 12) (CD: slope = 0.84189, intercept = 5.1 %, $R^2 = 0.73000$, $p < 0.001$). Differences between LWM and SM were noteworthy when the proportion of large live oysters was about or below 50 % which was the case in most of the study years at site NL. A strong linear relationship was relating the density attributes FM and LWM (RD: $R^2 = 0.97589$, $p < 0.001$, Fig. 12) (CD: $R^2 = 0.95781$, $p < 0.001$). Approximately 2/30 of the LWM accounted for FM but this was not significant. FM correlated with the abundance of large live oysters (RD: $R^2 = 0.86568$, $p < 0.001$) (CD: $R^2 = 0.79771$, $p < 0.001$).

Interrelations of mussel density attributes

Interrelations between density attributes of live mussels per site and year ($N = 36$ reefs) revealed distinct linkages, some of them showing strong linear and positive relationships (Fig. 13). The abundance of the total population changed in relation to the abundance of recruits (RD: $R^2 = 0.58382$, $p < 0.001$) (CD: $R^2 = 0.86588$, $p < 0.001$), but the influence of young mussels (recruits and small) on total abundance was much stronger (RD: $R^2 = 0.90472$, $p < 0.001$, Fig. 13) (CD: $R^2 = 0.97684$, $p < 0.001$). Total abundance could not explain LWM (RD: $R^2 = 0.24002$, $p = 0.002$) (CD: $R^2 = 0.00620$, $p = 0.648$). In contrast, LWM was strongly related to the abundance of old (large) mussels (RD: $R^2 = 0.93243$, $p < 0.001$, Fig. 13) (CD: $R^2 = 0.79311$, $p < 0.001$). Linear relations, but with distinct lower coefficients of determination, were also present between the abundance of mature mussels (small and large) and LWM (RD: $R^2 = 0.78340$, $p < 0.001$) (CD: $R^2 = 0.53289$, $p < 0.001$). A significant linear relation existed between the density attributes SM LIVE and LWM (RD: $R^2 = 0.98899$, $p < 0.001$, Fig. 13) (CD: $R^2 = 0.97588$, $p < 0.001$). Half of the LWM accounted for SM LIVE (49.9 ± 2.3 %). A strong linear relation existed between the density attributes FM and LWM (RD: $R^2 = 0.99237$, $p < 0.001$, Fig. 13) (CD: $R^2 = 0.97802$, $p < 0.001$). 1/7 of the LWM account-

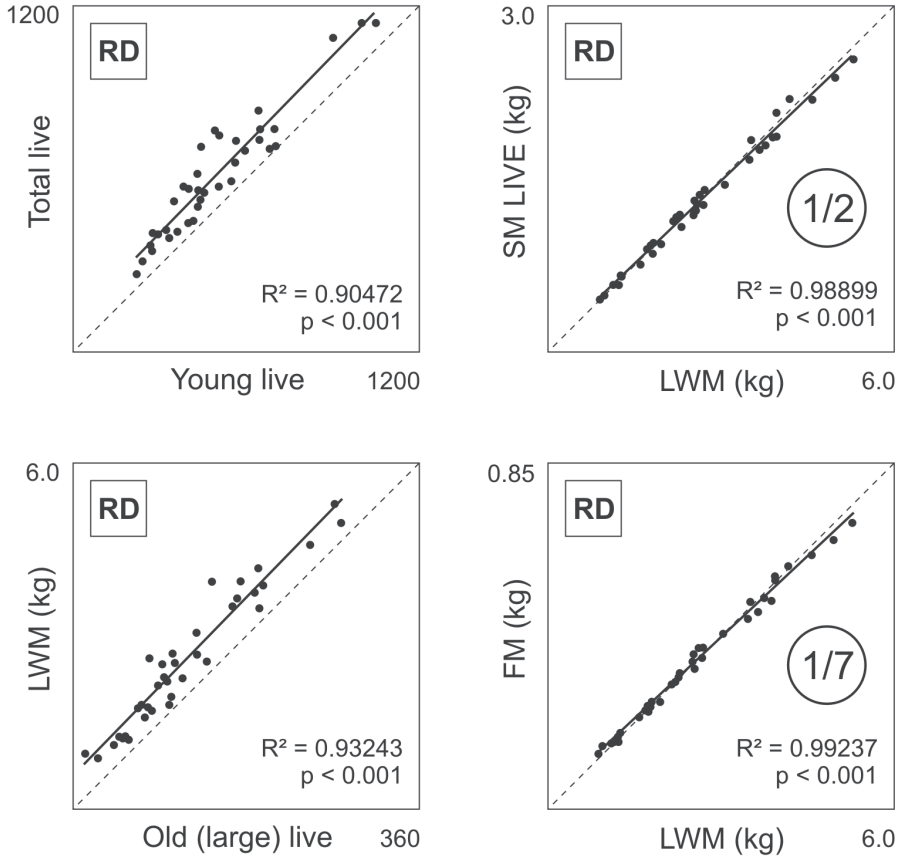


Figure 13. Interrelations between selected mussel density attributes per site and year (N = 36 reefs). Given are linear relationship, coefficient of determination (R^2) and significance level (p). Proportional reference line (dotted) and proportions indicated (circles). See text for all other interrelations. Density metrics and density attributes according to Figure 3.

ed for FM (14.2 ± 0.6 %). SM LIVE and FM were also related to the abundance of large mussels (SM LIVE RD: $R^2 = 0.90923$, $p < 0.001$) (SM LIVE CD: $R^2 = 0.73118$, $p < 0.001$) (FM RD: $R^2 = 0.89214$, $p < 0.001$) (FM CD: $R^2 = 0.67975$, $p < 0.001$).

Density scaling

The significant relationship between areal biomass and large individuals enabled the implementation of a density scaling for oysters and mussels. Oyster and mussel RD-scaling was performed by using RD of large individuals and biomass of all sites and years, respectively (N = 36 reefs). Oyster and mussel CD-scaling was performed by

Table 2. Oyster and mussel scaling parameters (a, b) of powered or linear relationships between individual metrics or density attributes. Allometric scaling (1–4) displayed in Figure 5A and (5, 6) in Figure 8B. Density scaling (7) displayed in Figure 14A and (8) in Figure 14B. R² = coefficient of determination. N = number of basic data points. Reef type determination according to Figure 4C. Density metrics and density attributes according to Figure 3.

A.							
Oyster							
Individual biomass							
Power $y = a(x)^b$	Reef type	y (g)	a	x (mm)	b	R ²	N (individuals)
	LRD	LWM	0.00056	SL Small	2.62918	0.99922	426
	LRD	LWM	0.07430	SL Large	1.58733	0.99339	448
	HRD	LWM	0.00032	SL Small	2.73533	0.99977	438
	HRD	LWM	0.15631	SL Large	1.39051	0.98933	623
	LRD	SM LIVE	0.00041	SL Small	2.60492	0.99932	426
	LRD	SM LIVE	0.03139	SL Large	1.68592	0.99632	448
	HRD	SM LIVE	0.00022	SL Small	2.72139	0.99991	438
	HRD	SM LIVE	0.10021	SL Large	1.40173	0.98607	623
(1)	LRD	FM	0.00006	SL Small	2.63358	0.99611	426
(2)	LRD	FM	0.05292	SL Large	1.13888	0.95726	448
(3)	HRD	FM	0.00003	SL Small	2.75259	0.99568	438
(4)	HRD	FM	0.15576	SL Large	0.84818	0.96980	623
Areal biomass							
Power $y = a(x)^b$	Areal reference	y (kg)	a	x (individuals)	b	R ²	N (reefs/clusters)
	RD	LWM	0.53024	Large live	0.78807	0.94308	36
	RD	SM LIVE	0.36776	Large live	0.78075	0.94425	36
	RD	SM	0.46366	Large shell	0.75970	0.93298	36
	RD	FM	0.05763	Large live	0.70352	0.88740	36
(7)	CD	LWM	0.87434	Large live	0.73150	0.98488	432
	CD	SM LIVE	0.58360	Large live	0.73395	0.98364	432
(8)	CD	SM	0.87596	Large shell	0.68669	0.98203	432
	CD	FM	0.10784	Large live	0.63904	0.95734	432
Linear $y = a(x)+b$							
Areal reference	y (kg)	a	x (kg)	b	R ²	N (reefs/clusters)	
RD	SM LIVE	0.67	LWM		0.99981	36	
RD	FM	0.07	LWM	0.09	0.97589	36	
CD	SM LIVE	0.67	LWM		0.99966	432	
CD	FM	0.07	LWM	0.15	0.98363	432	
B.							
Mussel							
Individual biomass							
Power $y = a(x)^b$	Reef type	y (g)	a	x (mm)	b	R ²	N (individuals)
(5)	LRD	LWM	0.00013	SL	3.00001	0.99967	784
(6)	HRD	LWM	0.00016	SL	2.92377	0.99948	769
	LRD	SM LIVE	0.00005	SL	3.08179	0.99927	784
	HRD	SM LIVE	0.00006	SL	2.98792	0.99874	769
	LRD	FM	0.00006	SL	2.69075	0.99845	784
	HRD	FM	0.00010	SL	2.51770	0.99817	769
Areal biomass							
Linear $y = a(x)+b$	Areal reference	y (kg)	a	x (individuals)	b	R ²	N (reefs/clusters)
	RD	LWM	0.01723	Large	0.54972	0.93423	36
	RD	SM LIVE	0.00819	Large	0.31445	0.90923	36
	RD	FM	0.00225	Large	0.09810	0.89214	36
	CD	LWM	0.01532	Large	2.05974	0.97846	432
	CD	SM LIVE	0.00752	Large	1.07499	0.97139	432
	CD	FM	0.00200	Large	0.33956	0.97029	432
Linear $y = a(x)+b$							
Areal reference	y (kg)	a	x (kg)	b	R ²	N (reefs/clusters)	
RD	FM	0.13	LWM	0.02	0.99237	36	
CD	FM	0.13	LWM	0.07	0.99612	432	

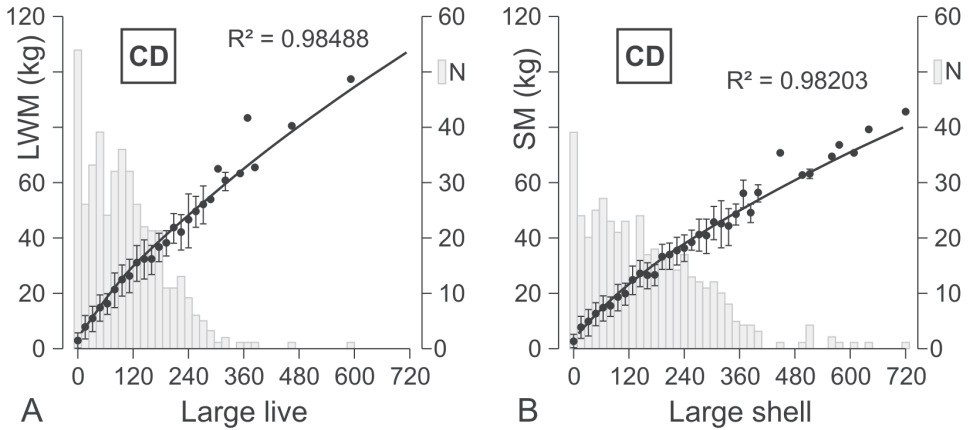


Figure 14. CD-density scaling of large oysters. **A** Plotted is LWM (kg) \pm SD against large live oysters per abundance class. **B** Plotted is SM (kg) \pm SD against large oyster shell per abundance class. Abundance classes derived from pooling 432 stations to intervals of 16 large oyster CD, respectively. N = Number of stations per abundance class (bars). Powered relationship indicated and coefficient of determination (R^2) given. Scaling parameters listed in Table 2 (7, 8). Density metrics and density attributes according to Figure 3.

using the CD of large individuals and biomass at all stations, respectively ($N = 432$ cluster). Therefore, stations were pooled by the abundance of large individuals into abundance classes and mean biomass \pm standard deviation was determined from all stations within each class. As frame size was 1/16 of a square meter, 16 individuals was the minimal interval per abundance class.

37 abundance classes resulted from the maximum abundance of 592 large live oyster CD to scale oyster LWM (Fig. 14A), SM LIVE and FM. 54 of the 432 stations were without large live oysters and had a mean of 3.9 ± 3.4 kg LWM, 2.6 ± 2.2 kg SM LIVE and 421 ± 366 g FM. 45 abundance classes resulted from the maximum abundance of 720 large oyster shell CD to scale oyster SM (Fig. 14B). 39 of the 432 stations were without large oyster shell and had a mean of 3.5 ± 3.2 kg SM. 78 abundance classes resulted from the maximum abundance of 1,248 large live mussel CD to scale mussel LWM, SM LIVE and FM. One of the 432 stations was without large live mussels and had 1.0 kg LWM, 0.5 kg SM LIVE and 187 g FM. Best fit for oyster density scaling per areal reference was a power function $y = a(x)^b$ with $y =$ biomass (kg), $a =$ scalar, $x =$ abundance of large oysters and $b =$ exponent. Best fit for mussel density scaling per areal reference was a linear equation $y = a(x) + b$ with $y =$ biomass (kg), $a =$ scalar, $x =$ abundance of large mussels and $b =$ intercept. Scaling parameters of all equations are given in Table 2.

Simple vs. Complex reefs

Irrespective of areal reference, all oyster density attributes but total or juvenile abundance were significantly different among reef types. Simple reefs with LRD were sig-

Table 3. Oyster and mussel density attributes (mean ± SD) per areal reference (RD, CD) at simple and complex reefs during the study period 2008–2013 (N = 18 reefs per reef type). IND = individuals. Additionally given are proportions of live oysters (LIVE-Factor) and mean oyster SL. Dominance by biomass is given for oysters and dominance by abundance of large individuals is given for mussels. Significant difference between reef types per areal reference and between RD at complex reefs vs. CD at simple reefs is indicated (* p < 0.05, ** p < 0.01, *** p < 0.001). Density metrics and density attributes according to Figure 3.

Areal reference		RD			RD			CD			CD	
Reef type		Simple			Complex			Simple			Complex	
Density attribute	Unit	mean	SD	p	mean	SD	p	mean	SD	p	mean	SD
A.												
Oyster												
Reef coverage	%	33.5	11.9	***	48.9	4.1						
Total live	IND	384.9	368.1		570.5	560.2		1,053.9	844.6		1,183.9	1,217.5
Total shell	IND	1,038.2	1,272.7		1,345.7	798.8	*	2,659.0	2,545.3		2,756.1	1,669.4
Juv live	IND	306.0	358.2		369.6	585.5		827.0	868.0		774.3	1,267.9
Juv shell	IND	870.5	1,213.2		929.8	833.5	*	2,188.0	2,482.7		1,910.7	1,754.5
Adult live	IND	78.9	52.4	***	200.9	59.9		226.9	109.6	***	409.6	109.1
Adult shell	IND	167.7	110.7	***	415.9	98.4		471.0	213.2	***	845.4	170.1
Small live	IND	59.9	48.4	***	128.5	59.4		170.1	107.9	*	261.0	112.5
Small shell	IND	140.5	107.5	***	305.2	92.8		387.3	216.5	**	618.3	166.4
Large live	IND	19.0	9.8	***	72.4	20.0	*	56.8	25.4	***	148.6	39.3
Large shell	IND	27.2	13.5	***	110.7	22.1	*	83.7	40.5	***	227.1	44.4
FM	kg	0.5	0.2	***	1.1	0.2	*	1.4	0.5	***	2.3	0.5
LWM	kg	5.5	2.6	***	15.2	3.6		16.4	5.9	***	31.2	6.8
LWM Small	kg	1.8	1.3	***	3.6	1.5		5.1	2.8	*	7.4	3.1
LWM Large	kg	3.6	1.8	***	11.5	3.5		11.1	5.3	***	23.6	6.7
SM live	kg	3.8	1.7	***	10.2	2.4		11.2	4.0	***	20.9	4.6
SM	kg	5.7	2.5	***	16.5	2.7		17.2	6.0	***	33.7	4.8
LIVE-Factor Total	%	46.1	24.4		37.6	15.8						
LIVE-Factor Juv	%	38.3	31.2		23.3	24.6						
LIVE-Factor Adult	%	50.0	14.2		48.7	9.4						
LIVE-Factor Small	%	44.9	14.6		41.7	11.6						
LIVE-Factor Large	%	71.8	16.2		66.2	13.6						
SL total live	mm	38.3	26.2	*	59.1	26.6						
SL Total shell	mm	27.3	15.6	*	38.0	15.5						
SL Juv live	mm	9.8	4.5		11.1	3.1						
SL Juv shell	mm	10.2	3.5		11.1	2.2						
SL Adult live	mm	82.9	17.6		91.7	13.1						
SL Adult shell	mm	69.5	15.4	*	78.0	7.9						
SL Small live	mm	59.1	9.1		59.6	8.8						
SL Small shell	mm	51.1	7.2		53.9	5.3						
SL Large live	mm	139.9	12.1		143.8	8.2						
SL Large shell	mm	137.3	9.0		142.0	7.4						
B.												
Mussel												
Total	IND	529.7	149.3	*	696.2	243.2	***	1,744.8	825.2		1,434.9	529.4
Recruits	IND	270.9	138.8		316.1	177.7	**	957.1	743.1		660.8	401.6
Small	IND	168.7	80.7	*	234.1	104.0	***	530.6	262.0		479.2	215.7
Young	IND	439.6	156.8		550.2	229.2	***	1,487.7	889.8		1,140.0	510.2
Large/Old	IND	90.0	49.2	**	146.0	71.5	***	257.1	87.7		294.9	137.3
FM	kg	0.3	0.1	*	0.4	0.2	***	0.9	0.2		0.8	0.3
LWM	kg	2.1	1.0	*	3.0	1.2	***	6.3	1.4		6.1	2.4
SM LIVE	kg	1.1	0.5		1.4	0.6	***	3.3	0.7		2.9	1.2
C.												
Dominance												
Oyster	FM	%	59.6	9.0	***	73.9	6.8					
Oyster	LWM	%	70.9	7.8	***	83.8	4.6					
Oyster	SM LIVE	%	75.9	7.0	***	87.9	3.6					
Oyster	SM	%	82.8	5.4	***	92.0	3.0					
Mussel	Large LIVE	%	81.0	7.9	***	64.2	10.0					
Mussel	Large SHELL	%	74.8	10.1	***	54.1	13.0					

nificantly less covered by clusters than complex reefs with HRD (Table 3). The difference of RC did not alter general characteristic differences between reef types but increased the significance level of small oyster occurrence between reef types. Irrespective of areal reference, juvenile oyster abundance (live or shell) was not significantly higher at complex reefs. Likewise, total oyster abundance (live or shell) did not differ between reef types, although slightly higher at complex reefs, but mean oyster size was on average significantly larger at complex reefs than at simple reefs. The size difference resulted from a significantly higher abundance of small and large oysters (live or shell) at complex reefs. The mean size of small or large oysters was similar at both reef types, although slightly larger at complex reefs. The proportion of live oysters per density attribute was similar at both reef types, although slightly lower at complex reefs. Irrespective of areal reference, the structural density attributes large oyster (live or shell) and biomass (FM, LWM, SM LIVE and SM) were significantly higher at complex reefs than at simple reefs. Oyster station density (CD) at simple vs. complex reefs reached maximum values of 17,504 vs. 9,088 juvenile shell, 1,648 vs. 1,776 adult shell, 1,456 vs. 1,536 small shell, 448 vs. 720 large shell or 70 vs. 86 kg SM, 5,104 vs. 6,016 juvenile live oyster, 880 vs. 1,232 adult live oysters, 816 vs. 1,008 small live oysters, 368 vs. 592 large live oysters or 83 vs. 97 kg LWM, respectively. This shows that single clusters at simple reefs can be built by exceptional high oyster density.

CD of mussel abundance and biomass was similar at both reef types, although slightly higher at simple reefs, but the difference of RC altered these relationships. When abundance was calculated across the reef area, mussel recruit RD was still similar between reef types, but significantly more small and especially more large mussels were colonizing complex reefs which also resulted in significantly higher biomass than at simple reefs.

Both reef types were dominated by oyster biomass. Dominance of oyster biomass increased from FM over LWM, SM LIVE to SM but was always significantly higher at complex reefs than at simple reefs. Oyster SM dominated the total SM, i.e. SM of oysters plus SM LIVE of mussels, to 83 % at simple reefs and 92 % at complex reefs. In contrast, both reef types were dominated by mussel abundance when large individuals of both species were taken into account. Dominance of large mussels was significantly higher at simple reefs than at complex reefs but declined from 81 % to 75 % at simple reefs and from 64 % to only 54 % at complex reefs when large post-mortem oyster shells were included in the total abundance of large individuals.

Discussion

Pacific oyster reefs in the study area constitute undisturbed systems without external larval supply from oyster culture, addition of oysters by transplanting or extraction of oysters by harvesting. Results of this study are assumed to comply with naturally matured Pacific oyster reefs worldwide. The prominent status of large oysters for both allometric scaling and density induced the development of a conceptual framework towards a harmonized approach to characterizing Pacific oyster reefs (Box 1). The con-

cept applies to the proposed density attributes of this study (Fig. 3), where biotic density (abundance or biomass of live oysters) is a function of ecological structure and biogenic density (abundance or biomass of oyster shell) is a function of biophysical structure. The concept applies to cluster density (CD) as a function of vertical structure and to reef coverage (RC) as a function of horizontal structure, both resulting in reef density (RD) as a function of reef texture. Reef texture can be equated with reef complexity. Hence, engineering strength as a function of reef complexity or reef performance is assumed to be reflected by RD.

Oyster shape and allometric scaling

Oyster allometric scaling should be rated far more complex than previously considered. Large oysters had an exceptional scaling behavior which considerably affected scaling relations. Length versus weight data indicating a size-dependent scaling behavior was also displayed in earlier studies on Pacific oysters (Nehls and Büttger 2006, Walles et al. 2015b) but was not noticed or not considered relevant. Results of this study conditioned on the implementation of a novel size-dependent concept of twin functions (TF) for the estimation of oyster individual biomass by SL (Fig. 5). This study demonstrated that the interplay of scaling parameters is highly sensitive to the estimation of oyster individual biomass and that conclusions on oyster shape should not be drawn from scaling exponent only (Fig. 6). Shape variability of especially large oysters was remarkably and fundamentally affected the estimation of areal biomass (Fig. 7). Results of this study showed that the shape variation of especially large oysters was related to oyster density which conditioned on the implementation of weighted TF by classifying reefs by oyster density, i.e. the abundance of large live oyster RD. Powell et al. (2016) mentioned that variation in oyster shape has not yet been predictably associated with oyster density. Results of this study imply that this may have been related to the lack of comparable measurements for density.

In accordance with the spatial and temporal variation in the length-biomass relationship for American oysters *C. virginica* (Powell et al. 2016), a negative relationship between scalar and scaling exponent described shape differences of Pacific oysters. Powell et al. (2016) found the scalar of *C. virginica* declining by the cube root. In contrast, the scalar of Pacific oysters declined exponentially. As scaling exponents of both species had the same exceedingly large range from < 1 to > 3 , a higher shape variability of Pacific oysters than of *C. virginica* can be assumed. The variability of Pacific oyster scaling exponents mainly resulted from the separate conversion of small and large oysters but variability per site (spatial) and year (temporal) added to the size-related range (Fig. 5). Powell et al. (2016) suggested that their high variability of scaling exponents was a result of anisodiametric growth and mentioned the contribution of many cohorts over a long period of years. While their analyses were based on individuals representing the size ranges in the samples and size distributions or maximum sizes were not analyzed, the authors discussed the high variability of scaling exponents with respect

to lower condition disproportionately directed at larger *C. virginica*. Given that size-dependent allometric scaling of small and large oysters is characteristic of all oyster species, especially at increasing SL, the maximum shell length class used for allometric scaling, and due to a high variable oyster shape also the number of individuals per SL class, has important implications for the determination of scaling parameters.

Higher scaling exponents of *C. virginica* were characterized by narrower shells (slender shape) and Powell et al. (2016) discussed lower scaling exponents as a mechanism to maximize shell production. As the average value of *C. virginica* scaling exponents was 2, the authors proposed that scaling near the square rather than the cube is a constraint imposed by exigency of carbonate production for reef maintenance and accretion in the face of high rates of taphonomic degradation. In contrast, although this study showed that ad hoc conclusions on oyster shape by scaling exponent only is questionable (Fig. 6), higher scaling exponents of Pacific oysters tended to result in higher biomass, i.e. wider and deeper cupped oysters or a mighty shape (this study, Walles et al. 2015b). Although there was a density-related component, this trend was mainly size-dependent. Small oysters, less space limited at simple reefs and by settling on con-specifics at the upper end of the cluster matrix also at complex reefs, tended to scale near the cube as typically found in other bivalves (Powell et al. 2016). Large oysters, especially when forced by crowding at complex reefs, tended to scale below the square (Fig. 5). The only way to optimize food intake at increasing structural density, i.e. decreasing available space in an increasing 3-dimensional complex matrix, is a high variability of growth form, i.e. oysters are able to grow increasingly slender and long (narrow and low cupped). Density-related shape was also considered for Pacific oysters in the Northern Wadden Sea when determining the CF SH (Nehls and Büttger 2006). To compensate observed shape differences due to crowding, roundish individuals from one low density site, and long and narrow individuals from one high density site were used for allometric scaling, but values for low or high density were not given. Oysters at the reef KATS in the Oosterschelde Estuary were long and narrow (CF KATS) compared to short and wide shaped oysters at other sites in the area (Walles et al. 2015b, 2015c), but densities given in total abundance cannot explain shape differences. CF SH and CF KATS differed by only 0.1 between scaling exponents and 0.001 between scalars, but estimated conspicuous biomass differences, e.g. 230.4 g LWM (CF SH) versus 96.7 g LWM (CF KATS) for a 150 mm oyster. As a consequence, density estimates at complex reefs with high reef density (this study) resulted in about 40 % more (CF SH) versus 40 % less (CF KATS) areal biomass (Fig. 7). Besides examples given for the variability of oyster shape by similar scaling exponents (Fig. 6), this clearly demonstrates that the interplay of the two scaling variables is highly sensitive to the biomass calculation. Underestimating the relevance of the applied conversion function can have fundamental effects on further analyses like potential relationships between abundance and areal biomass. This study considered the observed size-dependent and density-related oyster allometry by implementing weighted TF (Fig. 5, Table 2) which most likely supported the detection of significant interrelations between abundance and areal biomass.

Areal reference and density attributes

Reise et al. (2017a) pointed out that Pacific oyster density comparisons are hampered by different methods of quantification, i.e. coverage, abundance or biomass, and that densities are not convertible. This study is first in documenting the crucial relevance of areal reference, i.e. CD and RD, when comparing densities. Densities per areal reference differed significantly and were clearly not convertible or comparable (Table 3). Naturally matured oyster reefs comprise a multitude of clusters with varying density. Oysters typically cover the occupied bottom of clusters completely. RC results from the patchy distribution of all clusters across the reef area. Such morphology has also been described for reefs of *C. virginica* (i.a. Allen et al. 2011). Coverage was also recognized as an important metric in reef restoration. On the other hand, abundance data of *C. virginica* studies seem to preferably refer to CD. Albeit not always explicitly clarified in the method section, most studies documenting Pacific oyster abundance also seem to refer to CD (i.a. Fey et al. 2010; Büttger et al. 2011; Walles et al. 2015b, 2015c; Holm et al. 2015; Reise et al. 2017a, 2017b). Reise et al. (2017a) stated that abundance of 100 oysters m^{-2} usually amounts to about 25% cover, > 400 m^{-2} to 100 % cover and > 1000 m^{-2} comprise large oysters. Here, cover describes the small-scale distribution within a certain area of a reef but still refers to CD. At this, stations of this study occasionally included only one oyster clump, single oysters or even just mussels and resulted in very low or no oyster CD, i.e. three stations without live oysters, two even without oyster shells, but all three with mussels. A scattered distribution of oysters in certain parts of a reef was reflected by RD, i.e. depending on RC. The method to assess RC that was applied within this monitoring registers steps with “foot on cluster” that may also be only one clump or even a single oyster or mussel, and “foot on open space” that included all unoccupied surfaces of the reef, i.e. also open spaces between scattered distributed oysters. About 1700 steps from pacing off 11 transects between stations determined RC, i.e. the proportion of occupied surface to open space. Transect coverage was highly variable and ranged from 0–78% at simple reefs and from 6–86% at complex reefs. Published data on Pacific oyster RD is scarce (Schmidt et al. 2008) although data potentially exist in all Wadden Sea regions as Folmer et al. (2017) displayed standing stock dynamics between 2000 and 2013 for the regional tidal flat systems (unoccupied areas are included). Uncertainty of areal reference hampers comparability and especially leads to biased interpretation of habitat structure at ecosystem-level. Density attributes per RD or per CD that reflected structure at simple and compact reefs of this study differed significantly, but were similar when areal reference was ignored (Table 3).

Density assessments of introduced Pacific oysters prior to establishment or at low invasive potential mainly focus on maximum abundance of live oysters (i.a. Escapa et al. 2004, Schmidt et al. 2008, Fey et al. 2010, Wrangle et al. 2010). Successful establishment and increasing oyster density disproportionately increase the number of spat and total abundance significantly depends on dynamic changes of spatfall intensity. This study showed that juveniles can account for over 90 % of the total live population

after years of good spatfall (Figs 8, 9). Hence, smallest oysters are often omitted for comparable analyses (Büttger et al. 2011) or are even excluded from assessment due to their difficult detection (Reise et al. 2017a). Inconsistency of the smallest size used to quantify the adult population hamper comparability between studies. Especially the smallest size classes experience exceedingly high fluctuations of oyster occurrence due to sampling season, spatfall intensity or methodological effort. As a consequence, comparison of adult oyster abundance referring to oysters > 20 mm (Reise et al. 2017a), > 25 mm (this study), > 30 mm (Büttger et al. 2011) or even > 58 mm (Holm et al. 2015) is difficult or not even reasonable.

Under the assumption that biomass is an appropriate variable to reflect habitat structure, interrelations presented within this study revealed a rather weak correlation between the abundance of adult oysters and biomass (Fig. 11). Therefore, the adult population category, most likely irrespective of the smallest size class used, does not verifiably qualify for conclusions on habitat structure or cluster matrix which makes comparisons of density by abundance of adult oysters even more questionable. Reise et al. (2017a) investigated the invasion trajectory of Pacific oysters in the northern Wadden Sea and recorded oyster densities by CD. The authors concluded that abundances of about 1,000 adult live oysters (> 20 mm) with a weight of about 30 kg LWM were common features in the Wadden Sea. In contrast, the mean CD of 432 stations over a 6-year period during post-establishment in the Central Wadden Sea (this study) was only 318 adult live oysters (> 25 mm), but this putative low abundance accounted for 24 kg LWM. Only one of the 432 stations of this study consisted of > 1,000 and only 17 % of the stations consisted of > 500 adult live oysters (> 25 mm). In contrast to these comparably low abundances, 33 % of the stations had > 30 kg LWM. The one station with 1,232 adult live oysters (> 25 mm) accounted for 49 kg LWM while the highest biomass of 97 kg LWM corresponded to only 800 adult live oysters (> 25 mm). Fey et al. 2010 reported that “dense reefs” in the western Wadden Sea may contain > 500 adult oysters (CD) and adult was only mentioned in the abstract while not defined or used otherwise throughout the paper), weighing more than 100 kg fresh weight (LWM). Biomass may have been largely overestimated as Fey et al. 2010 applied the CF SH to their high-density reefs. The CF SH estimated about 40 % more biomass at compact reefs of this study. Total abundance assessed at three steady and undisturbed Pacific oyster reefs in the Oosterschelde Estuary was 782, 536 and 396 live oyster CD, accounting for 20, 17 and 11 kg live oyster shell (Walles et al. 2015c). Densities by biomass ranged between characteristic densities at simple and complex reefs of this study (Table 3), but data provided by Walles et al. (2015c) did not allow for comparison of adult live oyster abundance. Nevertheless, this exemplary data compilation displays a high uncertainty when comparing density by total abundance or by abundance of adult oysters especially when conclusions on habitat structure should be drawn.

Increasing oyster density, establishment and maturation of oyster reefs also increase the number of biogenic density variables that can or even should be assessed when population dynamics or especially ecosystem engineering effects are investigated. Additionally to live oysters, also shell of post-mortem oysters contribute to the complexity

of the biogenic structure which influences population dynamics and habitat biophysical properties by feedback effects, especially at ecosystem-level (i.a. Schulte et al. 2009). Besides difficulties of comparing abundance data, also the available biomass data is highly variable. Oyster biomass has been measured as volume in liter (i.a. Mann et al. 2009, Lejart and Hily 2011) or mass/weight in kg of shell, flesh and retention water (LWM, i.a. this study, Büttger et al. 2010, Walles et al. 2015c), shell of live oysters (SM live, i.a. this study, Walles et al. 2015c), wet or dry shell of live and post-mortem oysters (SM, i.a. this study, Walles et al. 2015c), live oysters (LWM) and post-mortem shell (fresh mass, i.a. Lejart and Hily 2011), and also tissue fresh, wet, dry or ash free dry weight (i.a. Mann et al. 2009, Lipcius et al. 2015) was used to describe oyster biomass. Enhanced logistical and especially financial efforts often lead to limited data assessments, e.g. only live oysters, abundance, biomass or simplified biomass assessments due to handling efficiency of clumps that include live oysters with tissue and (at best sediment-free) post-mortem shell (Cognie et al. 2006, Lejart and Hily 2011). Conversions between mass and volume are possible and have been applied in some studies (i.a. Mann et al. 2009). The assessment of LWM for Pacific oysters in the Wadden Sea was adapted to the regional common practice to estimate mussel density and to evaluate the ecological status of mussels (Büttger et al. 2010, Folmer et al. 2017). This study complementarily assessed SM LIVE, SM and FM of live oysters and contemporaneously recorded the density of post-mortem shell. Results revealed significant interrelations which qualified the proposed density attributes for a general application.

The repeated occurrence of 2/3 proportions for a variety of density attributes was striking and may reflect relationships typically found at naturally matured and healthy Pacific oyster reefs. Providing a 2/3 proportion of large live oysters to large shell or SM LIVE to SM, LWM and SM reached the same values because the shell of live oysters (SM LIVE) accounted for 2/3 of the LWM (Fig. 12). A 2:1 relationship between live and post-mortem large oysters was present at almost all reefs investigated. In some years at reef NL, only half of all large oysters were alive. Effects of reef size or reef shape were not investigated within this study but the frequent lower proportion of live oysters at NL may be related to reef density dependent effects with differential feedbacks of ecosystem engineering due to the exceptional size of this reef. NL stretches over 26 ha which is much larger than the average 7 ha of all other reefs investigated. The characteristic 2:1 relationship between live and post-mortem Pacific oysters shell mass was also found at reefs in the Oosterschelde Estuary, The Netherlands (Walles et al. 2015c). In contrast, Mann et al. (2009) stated that good habitats of *C. virginica* are characterized by a 1:2 relationship between live and brown (equivalent to post-mortem shell) shell weight while much lower proportions of live individuals were present in poor habitats.

The use of several population categories to compare oyster density by abundance has also been implemented for *C. virginica*. Similar to juvenile Pacific oysters, *C. virginica* recruits comprise individuals < 25 or < 30 mm (i.a. Peters et al. 2017, Theuerkauf et al. 2017). In contrast, the common practice to subdivide adult *C. virginica* into small and large individuals is not based on demographic or ecological characteristics

but mediated by human interest at the legally harvestable oyster size of ≥ 75 mm (i.a. Chai et al. 1992, Southworth et al. 2004, Peters et al. 2017, Theuerkauf et al. 2017). Interestingly, older studies on the growth rate of small *C. virginica* used size classes < 100 mm (Rothschild et al. 1994). This study found a substantiate subdivision of adult Pacific oysters by the prominent status of large individuals that are > 100 mm. Adult oyster abundance depended on the presence of small oysters, while biomass depended on the number of large oysters (Fig. 11). Large oyster abundance was not subjected to strong short-term fluctuations and reflected areal biomass largely independent of the presence of smaller size classes. The correlation between large oyster abundance and areal biomass was significant for large live oysters and LWM, SM LIVE or FM, respectively, and for large oyster shell and SM. Hence, with respect of areal reference, large oyster abundance can be converted into areal biomass (Figs 9, 11; Table 2).

Reef types

The classification of reef types has also been implemented in other studies to investigate ecosystem engineering impacts of oyster reefs. Different approaches were applied to measure or construct reef types by abundance (i.a. Blomberg et al. 2017), shell layers (i.a. Schulte et al. 2009, Lipcius et al. 2015), cover (i.a. Wagner et al. 2012), weight (i.a. Mann et al. 2009) or liter (i.a. Grabowski 2004, Grabowski and Powers 2004). Two to three reef types were commonly defined. Accordingly, this study classified two reef types, i.e. simple and complex reefs, as more reef types would have led to fuzzy transitions, increasingly unclear delimitations and non-significant differences for the high variability of oyster density at naturally grown reefs. Significant effects of engineering strength may only be detected at significant different structural complexity.

Blomberg et al. (2017) described reef types by abundance of spat (≤ 25 mm) and adult *C. virginica* (> 25 mm) and revealed that differences in oyster reef structure were not affecting the composition of food resources. Providing that representative extracts of the adult *C. virginica* populations were used for their analyses, the size range from 25.4 to 76.8 mm (mean 47 mm) was suitable for comparison with small Pacific oysters (CD) in this study (mean 59 mm) (Table 3). 196 adult (small live) *C. virginica* at natural and 280 at restored reefs were within the range of 170 small live Pacific oysters at simple and 261 at complex reefs. Although small Pacific oyster abundance and their corresponding LWM of 5.1 kg at simple reefs vs. 7.4 kg at complex reefs were significantly different between reef types, the significant structural difference between simple and complex reefs manifested only at 16.4 vs. 31.2 kg LWM. High numbers of small oysters may not have the potential to build high complex 3-dimensional structures. Even the maximum abundance of 1,008 small live Pacific oysters (mean 49 mm) reached only 17.5 kg LWM which would comply with a typical CD at simple reefs. Hence, structural differences revealed by Blomberg et al. (2017) were significant on a local, small-scale consideration but, de facto, most probably too weak to detect ecosystem engineering effects as the described reef types would assign to simple reefs.

Studies investigating *C. virginica* restoration success assessed oyster abundance as a function of reef height (Schulte et al. 2009, Lipcius et al. 2015). Reef height was pre-constructed by placing shell layers at different vertical reliefs. A key mechanism underlying *C. virginica* recovery after 3 years was vertical relief as oyster (total live) abundance was 4-fold higher on high-relief reefs (HRR) than on low-relief reefs (LRR) (Schulte et al. 2009). Abundance comprised mainly small oysters of up to 100 mm while a distinct 3-dimensional matrix built by large individuals was proposed to develop only in the future. This is in contrast to naturally matured Pacific oyster reefs in the Wadden Sea but the approach to define two reef types, beside un-restored bottom (*C. virginica* reefs) vs. open spaces (Pacific oyster reefs), is the same. Complex reefs with high reef density (HRD) and simple reefs with low reef density (LRD) comply with HRR and LRR in terms of differential ecosystem engineering due to vertical structure.

To simulate low or high density, Wagner et al. (2012) constructed reef density on a small-scale pseudo-cluster by spreading clumps of about 10 Pacific oysters between 100 and 150 mm to 2 m² plots of 30 and 70 % cover (number of clumps not given). Although this cover approach is hardly reproducible or comparable to other studies, this investigation (unintentionally?) implemented the prominent status of large oyster abundance by their experimental design. Most likely, this has been supportive in detecting significant differences between target variables meant to reflect engineering strength on a small-scale experimental approach.

Another approach to describe reef types was implemented by Mann et al. 2009. The authors plotted live shell weight against total shell weight and revealed that 92 % of 166 data points were equally distributed between the associations low total shell weight + low live shell weight and high total shell weight + high live shell weight. Although no significant relationship between measurements was found, the observation underpins a classification of two reef types.

Grabowski (2004) and Grabowski and Powers (2004) constructed low habitat complexity or low vertical relief by a layer of unaggregated oyster shell and high habitat complexity or high vertical relief by substituting upward orientated oyster cluster. Comparable liters of shell and cluster were used within studies but varied between studies. Both approaches could detect significant different engineering effects. Grabowski (2004) and Grabowski and Powers (2004) used the terms simple and complex reef for their reef types. The coincidence of terms was only detected at the time of discussing the findings of this study. The intention to express structural differences by the terms simple and complex reef is shared in the two studies but the implementation differs. The terms simple and complex reefs were most suitable for the concept of this study and were retained as the constructed “reefs” rather represented simple or complex clusters and not entire reefs.

This study initially implemented the classification of reef types as a tool for oyster allometric scaling due to the observed density-related variation of oyster shape (see subsection “oyster shape and allometric scaling”). However, pooling the monitoring data by reef type qualified for a delimitation of threshold or target densities to evaluate the status of (naturally matured) Pacific oyster reefs by reef type characteristic density attributes. The need for targeted research of Pacific oyster reefs was emphasized by

Folmer et al. (2017) but the authors stated that natural or targeted levels are hard to answer because these levels are impossible to define for naturally fluctuating populations. Allen et al. (2011) recognized the lack of a clear empirical or theoretical basis for setting operational targets of *C. virginica* population size and structure to evaluate reef-level restoration success. Nevertheless, the authors explicitly recommended a combination of density variables and established threshold and target abundance, biomass and coverage as performance metrics of *C. virginica* restored reefs. This study found a significant relationship between the abundance of large Pacific oysters and areal biomass which enabled the determination of one density variable for the classification of the reef types (Fig. 4C).

The implementation of a threshold density aimed at a general application, i.e. applicable also to data sets of other studies, and the decision was made in favor of large live oyster RD. The areal reference RD considers the variable density of clusters and their spatial distribution across the reef area. At this, RD reflects reef texture or reef complexity. Reef texture or reef complexity has implications for engineering strength at ecosystem-level. High density cluster, i.e. clusters with high vertical structure and a complex matrix, may also develop in restricted parts of simple reefs but on a large-scale perspective, the entity of all clusters and their distribution across the reef area will trigger reef type characteristic engineering effects. RD was also chosen to comply with a variety of monitoring methods, i.e. field studies where coverage was assessed or could possibly be estimated in retrospect, dredging, tong or grab sampling.

By being the counterparts of the areal biomass variables LWM, SM LIVE, FM or SM, the abundance of large live oysters or large oyster shell would have qualified to differentiate simple from complex reefs. The use of abundance over areal biomass as a threshold density was imperative for the interdependent relationship of density-related oyster shape and areal biomass. The threshold density of large live oyster abundance enables its application also to data sets from reduced monitoring effort, e.g. already existing studies where post-mortem shell was not assessed. Irrespective of reef type, the 2:1 relationship between live and post-mortem large oysters resulted in comparable values for areal LWM and SM (Fig. 12). Providing that naturally matured Pacific oyster reefs predominately consist of 2/3 live large oysters, main structural differences between reef types are reflected by the abundance of live large oysters only. Studies that only assessed biomass may use a converted threshold density. For example, using the equation “Oyster/Areal biomass/RD/LWM/Large live” (Table 2), the threshold abundance of 44 large live oyster RD equates to 10.5 kg LWM RD. With respect to areal reference, simple and complex reefs significantly differed by all but juvenile density attributes, including RC (Table 3). Mean oyster size and the proportion of live oysters per density attribute were similar between reef types.

Ruesink et al. (2005) mentioned that *C. virginica* reefs are stronger than those of *C. gigas*. Pacific oyster reefs of this study comprise naturally matured 10 to 15 year old unexploited reefs with live oysters and post-mortem shell up to 268 mm. Vertical structure is built by some large and increasingly slender oysters while small oysters condense the matrix by covering large individuals. Vertical structure at most reefs increased with time by accumulation of sediment, burial of post-mortem oysters and

shell accretion of old and young generations. A similar architecture was described for historic, natural *C. virginica* pre-exploitation reefs (DeAlteris 1988). Irrespective of areal reference, density attributes presented within this study suggest that Pacific oyster reefs in the Central Wadden Sea are stronger in terms of biogenic structure than those of recent *C. virginica*. Biogenic density at natural *C. virginica* reefs in the James River (N = 166) reached 17 kg total shell wet weight m⁻² (live and post-mortem brown shell) while the majority of all “high shell reefs” (N = 76) ranged between 8 and 13 kg (Mann et al. 2009). In comparison, Pacific oyster reefs (N = 36) reached a maximum of 43 kg SM CD (live and post-mortem shell) and complex reefs had on average 34 kg SM CD (N = 18) (Table 3). On the other hand, the assessment of *C. virginica* density by patent tongs may also reflect RD. With a maximum of 21 kg SM RD (N = 36) and an average 16.5 kg SM RD at complex reefs (N = 18) (Table 3), biogenic density at Pacific oyster reefs was still higher than at natural *C. virginica* reefs in the James River. The median of all natural *C. virginica* reefs was 4.8 kg SM which was less than the average 5.7 kg SM RD at simple Pacific oyster reefs. Furthermore, *C. virginica* reefs seem to be characterized by a 1:2 relationship between live and post-mortem brown shell (Mann et al. 2009) while a 2:1 relationship between live and post-mortem shell was characterizing Pacific oyster reefs. Additionally, recruitment of Pacific oysters seems to be more successful than that of *C. virginica*. Irrespective of reef type, juvenile (live or shell) Pacific oysters comprised about 70 % or more of the population (live or shell) (Table 3) while juvenile *C. virginica* seem to hold 30 % or less (Mann et al. 2009, Schulte et al. 2009). Sousa et al. (2009) stated that ecosystem effects of *C. virginica* are similar to Pacific oysters but that *C. virginica*, by forming larger reefs, sustainably affect large-scale hydrodynamics, estuarine water circulation and sedimentation. Reef size of natural *C. virginica* reefs in the James River varied from 1.3 ha to 500 ha subtidal reef area (Mann et al. 2009). The largest reefs, encompassing an immense area of about 2000 ha by bordering on each other, had consistently less than 3 kg total shell wet weight m⁻² (live and post-mortem brown shell). This density was comparable to SM per RD at the simple reef SP of this study. Site SP had the lowest Pacific oyster densities and the lowest coverage throughout the study period. Reef texture had almost no relief and was dominated by strongly scattered distributions of oyster clumps. Ecosystem engineering was observed to be very weak and may not be stronger at potentially larger reef size. In contrast, although density distribution at the complex reef NL was highly variable across the reef area, 35 kg SM CD (870 adult or 240 large shell) covered about 50 % of the reef area. According to its density but also to its exceptional size (26 ha) compared to other study sites (about 8 ha), the complex reef NL experiences accentuated ecosystem engineering and features a pronounced relief with several large tidal pools reaching some dozen square meters which stay inundated to depths of over 1 m during low tide. Independent of reef size, complex reefs are assumed to experience feedback processes that facilitate reef performance, population persistence and reef stability (Markert in prep.).

Population interference and dominance

The distinction of reef types and the implementation of density attributes enabled a first estimate of ecosystem-level impact of oysters on mussels. Analogous to large oysters, oyster density at complex reefs also forced large mussels to grow slenderer than at simple reefs (Fig. 8). Eschweiler and Christensen (2011) found that large mussels tend to move to the bottom of the cluster matrix in the presence of shore crabs. Although large mussels at the bottom are more protected against detrimental barnacle overgrowth (Buschbaum et al. 2016), mussels suffer from reduced food supply and increased sedimentation (Eschweiler and Christensen 2011). A slenderer shape of mussels within densely packed oysters may facilitate a facultative migration to optimize the trade-off by immediate response, e.g. presence/absence of crabs or birds according to inundation or season.

One would expect that the available space is limiting mussel occurrence at complex reefs but mussel CD was not significantly different between reef types (Table 3). This implies that oyster density, i.e. engineering strength, had no effect on mussel density. In contrast, due to a higher RC, RD at complex reefs supported significantly higher mussel biomass, higher abundance of small and especially large mussels. Although proportions of oyster and mussel densities were not affected, this demonstrates the vital importance of areal reference when evaluating engineering effects at ecosystem-level.

Analogous to oysters, abundance of large mussels determined dynamic changes of mussel biomass (Fig. 13). At this, the relationship between large oysters and large mussels was a reliable counterpart of a biomass comparison. At both reef types, more large mussels than large oysters were present but oysters were dominating all biomass variables, i.e. LWM, SM LIVE, SM and FM (pictured in Folmer et al. 2017, Fig. 4). At complex reefs, oyster dominance by biomass was significantly higher and large mussel dominance significantly lower than at simple reefs. Although the proportion of FM to LWM was twice as high in mussels as in oysters, oysters were dominating both reef types by all biomass variables. Considering also the shell of post-mortem oysters to reflect reef biogenic structure, the dominance of large mussels decreased at both reef types and oyster SM largely dominated with over 80 % at simple reefs and over 90 % at complex reefs. This demonstrates the relevance of density attributes that are chosen for the evaluation of dominance.

In the trilateral Wadden Sea, where non-native Pacific oysters have been invading native mussel beds in the intertidal of the Netherlands, Germany and Denmark, a visually appraised “coverage” of the two species, i.e. proportions, is recommended to evaluate dominance (Folmer et al. 2017). To date it is not clear if or under what uniform metrics these oyster/mussel mixed biogenic structures should be called beds or reefs - notwithstanding that these terms relate to differential ecosystem engineering. Most recently, Reise et al. (2017b) suggested the term “oyssel reef” which nicely refers to a coexistence of oysters and mussels but, after all, disrespects the main ecosystem engi-

neering species which is playing the key role in structuring and modulating biophysical properties and habitat characteristics. At this, Reise et al. (2017b) discussed the hostile takeover in terms of ecosystem engineering effects that are characteristic for oysters or complex reefs while mussels were discussed as associated species that live within the cluster matrix. Reise et al. (2017b) contrasted the abundance of adult oysters (> 20 mm) and adult mussels (> 10 mm) at one site in the Northern Wadden Sea but, as adult abundance cannot be reliably compared, data could not reflect the observed oyster dominance in the field. In contrast, the comparison of biomass, abundance of large individuals or the inclusion of post-mortem oyster shell could have led to similar results on dominance that was found within this study. This study will hopefully impel scientists and decision-makers to implement an adapted strategy for the evaluation of the keystone engineering species by uniform metrics, e.g. the proposed density attributes of this study, which will also provide clarification to the denomination of oyster/mussel mixed biogenic structures in the Wadden Sea.

Implications for monitoring

Oyster density assessments are time-consuming and costly. Monitoring reef density dynamics on a large-scale regular basis is a special task that requires even more logistical and financial effort. Monitoring programs implemented after the bioinvasion of Pacific oysters in the trilateral Wadden Sea regions, respectively Western, Central and Northern Wadden Sea, have been reduced or even stopped completely although the need to evaluate long-term ecosystem engineering effects by intensified monitoring was postulated (Folmer et al. 2017). Folmer et al. (2017) also pointed out the lack of systematic measurements and recommended harmonization on density variables and applied method to improve comparability between regions while at the same time maintaining comparability within existing series.

The concept of large oyster abundance as intrinsic drivers of biotic and biogenic Pacific oyster density turned out to be an easy tool that will allow trans-regional comparisons of reef structural complexity independent of methodological approach (hand, dredge, grab, corer or tong), sampling season (spatfall intensity) or ecosystem (rocky shores or soft sediment, different primary settling substrate, intertidal or subtidal, invaded, naturalized or native environment). The concept of large oyster abundance maintains density comparisons within series and also retrospective comparisons of old data sets will be possible. The density attribute large oyster (live or shell) as an equivalent measurement to areal biomass (LWM, SM LIVE, FM or SM), will substantially reduce the logistical and financial effort of future monitoring as only large oysters have to be counted for an empirical characterization of Pacific oyster reefs, i.e. using a 10 cm reference object while exact shell length measurements are not required.

Although this study revealed that the abundance of large oysters (live or shell) can be converted into areal biomass (LWM, SM LIVE, FM or SM), data with different areal references (CD or RD) remain non-convertible and non-comparable. A variety of monitoring methods exist while the nature of the applied method basically determines

areal reference. For example, the deployment of an oyster dredge always results in RD as a haul samples clusters and open spaces between clusters while conclusions on CD cannot be drawn. Field investigations in the intertidal commonly assess oyster density exclusively in clusters (CD) and the coverage of a reef by clusters (RC) has to be assessed separately to estimate RD. This study first displays the crucial relevance of areal reference for comparative analyses of oyster density (see subsection “areal reference and density attributes” and “reef type”) and the respective applied monitoring method should be thoroughly scrutinized with respect to areal reference. Besides raising awareness of the relevance of areal reference, the scope of this study is not to recommend the “best” or “one-fits-all” monitoring method. On the contrary, results of this study indicate that the large oyster concept is independent of monitoring method (if areal reference is considered) and applicable without a significant loss of existing precision levels, especially when the focus of the data analyses concerns the determination of reef type or the empirical characterization of reefs by structural complexity.

The CV is an index of dispersion but also a measure of the SE relative to the mean, i.e. $RSE = CV \times 29 [100/\sqrt{n} (n = 12 \text{ stations of this study})]$. The uncertainty of the mean estimate at the sites of this study mainly ranged between 6 and 29 % for all density attributes while the uncertainty increased with decreasing oyster density. Relative precision of the present monitoring may overall be rated unacceptable and indicate increasing the number of samples, especially at simple reefs. On the other hand, the CV should rather be interpreted as a measure of characteristic intra-reef variability of oyster density distribution than the determination of monitoring precision. Each site of this study has a characteristic intra-reef pattern. Simple reefs can have high oyster densities in some parts of the reef although most parts have very low structural complexity or even a scattered distribution of single oyster clumps. Such a characteristic intra-reef pattern will always lead to high standard deviations and high CV, especially at simple reefs. A higher number of stations would increase the RSE of the mean estimate, but the mean estimate and the natural variability of cluster density distribution across a reef’s area will basically not change. Simple reefs will remain classified as simple reefs no matter whether the number of samples will be increased. At this, the CV at complex reefs with a rather homogenous distribution of oyster density across the reef area was 0.2 which signifies an acceptable “precision level” of 6 %. Nevertheless, the range of CV of all density attributes and CV of all density attributes per site were comparable. In particular, CV of the structural density attributes areal biomass (LWM or SM) and large oyster abundance (live or shell) were strongly correlated and “precision level” of the estimates of mean density at the sites was similar. The similarity between CV of all density attributes, in particular structural, will most likely also apply to other sampling strategies. The reliability of a comparative analysis of large oyster abundance among studies with different sampling designs is presumed to equal otherwise implemented comparisons of areal biomass or adult oysters. At this, the large oyster concept allows monitoring programs/sampling strategies that were established due to local survey resources to be maintained.

Although the choice of monitoring method depends on local logistical and financial feasibility, only RD qualifies for evaluations of the relationship between oyster density and engineering effects on ecosystem-level. Long-term intrinsic processes of a reef (e.g. popu-

lation dynamics, biophysical properties) and direct (e.g. habitat provision) or indirect (e.g. hydrodynamics, sediment budgets, nutrient cycling) engineering effects at ecosystem-level depend on oyster density of the total reef area where the entity of all clusters and their patchy distribution across the reef area perform as a bio-geo-morphological unit.

Conclusion

This study contributes to remedy the state of uncertainties when comparing the density of Pacific oysters and their reefs. The division of oyster populations into size-related abundance categories has been implemented in other studies but interrelations of abundance and biomass have not yet been investigated on an empirical basis. Large Pacific oysters were intrinsic drivers for dynamic changes of density by biomass which offered the opportunity to formulate potential strategies for characterizing Pacific oyster reefs (Box 1). Findings from this study may encourage researchers to detect similar patterns in other oyster species.

Results of this study advocate a harmonization of the developed density attributes with a clear specification of areal reference. This study is the first to provide a comprehensive set of characteristic density attributes per areal references (RD and CD) at two different reef types (simple and complex reefs). The classification of reef types meets the need for targeted research. The compilation of density attributes at simple and complex reefs shall serve as a density guide which enables a context-integrated evaluation of how dense a given reef actually is. By assessing its status, preliminary conclusions on expected low or high impact probability can be drawn.

Focusing on large oyster abundance will reduce monitoring efforts, will enable trans-regional comparisons of reef structure and will facilitate evaluations of engineering strength, reef performance and invasional impacts at ecosystem-level. Complemen-

<p>Box 1. Conceptual framework toward a harmonized approach to characterizing Pacific oyster reefs</p>	<p>4 Abundance of large oysters (live or shell)</p> <ul style="list-style-type: none"> - Intrinsic density attribute of oyster reefs <ul style="list-style-type: none"> • conversion into biotic and biogenic structure (biomass) - Independent of sampling season - Independent of assessment method (e.g. field/dredge) - Independent of (invaded) ecosystem (e.g. rock/soft) - Reduces logistical and financial effort of future monitoring <ul style="list-style-type: none"> • counts of large oysters (SL measurements not necessary) - Applicable to old data sets - Allows trans-regional comparability of oyster density - Allows classification of reef types - Facilitates characterization of oyster reefs - Promotes evaluation of engineering strength <p>5 Classification of reef types (simple or complex reef)</p> <ul style="list-style-type: none"> - Complies with density-related oyster shape <ul style="list-style-type: none"> • improves estimations of individual biomass by SL (application of TF LRD or TF HRD) - Provides reference density attributes <ul style="list-style-type: none"> • characterization of oyster reefs - Promotes evaluation of engineering strength
<p>1 Areal references (cluster density or reef density)</p> <ul style="list-style-type: none"> - CD = function of vertical structure - RC = function of horizontal structure - RD = CD x RC = function of reef texture - RD reflects reef complexity and reef performance <ul style="list-style-type: none"> • RD = function of engineering strength on ecosystem-level <p>2 Density attributes (abundance or biomass)</p> <ul style="list-style-type: none"> - Live oysters or LWM, FM, SM LIVE = biotic density - Shell of live and post-mortem oysters or SM = biogenic density <ul style="list-style-type: none"> • Abundance = juv < 26 mm, small 26-100 mm, large > 100 mm <p>3 Weighted (LRD or HRD) twin functions (small or large)</p> <ul style="list-style-type: none"> - Comply with density-related and size-dependent oyster shape - Improve estimations of individual biomass by SL - Qualify for standard conversion of SL into biomass: <ul style="list-style-type: none"> • TF LRD or TF HRD 	

Box 1.

tary investigations are needed to relate engineering strength in terms of large oyster density to specific ecological effects. Furthermore, the integration of reef areal extent, reef morphology in terms of reef shape or reef orientation, and also a long-term temporal component should be considered.

Acknowledgements

Sincere thanks and great respect to Achim Wehrmann, Abteilung Meeresforschung, Senckenberg am Meer Wilhelmshaven, who managed with utter conviction a continuation of the monitoring over so many years. Appreciation is due to the many people who contributed to the collection of the data. Special thanks to technical assistant Torsten Janßen, Abteilung Meeresforschung, Senckenberg am Meer Wilhelmshaven, who smoothed logistical processes during monitoring. Monitoring was carried out within the framework of the projects (i) “Management der Bioinvasion der Pazifischen Auster”, financially supported from 11/2006 to 12/2008 by the Niedersächsische Wattenmeer Stiftung and the Senckenberg Gesellschaft für Naturforschung, (ii) “SafeGuard. Ausbreitung der Pazifischen Auster”, financially supported from 05/2009 to 10/2012 by the European Regional Development Fund INTERREG IVa and SGN (Senckenberg Gesellschaft für Naturforschung), and (iii) “Klimaveränderung und Bioinvasionen als Steuerungsfaktoren von ecosystem engineering”, financially supported from 05/2012 to 06/2014 by LOEWE (Landes-Offensive zur Entwicklung Wissenschaftlich-ökonomische Exzellenz of the Hessisches Ministerium für Wissenschaft und Kunst), BiK-F (Biodiversität und Klima-Forschungszentrum) and SGN (Senckenberg Gesellschaft für Naturforschung). With kind support from Gabriele Gerlach, IBU (Institut für Biologie und Umweltwissenschaften), Carl von Ossietzky Universität Oldenburg, data was mainly analyzed during a scholarship within the framework of the IBR-project “Interdisciplinary approach to functional biodiversity research”, funded from 08/2015 to 07/2018 by the MWK (Ministerium für Wissenschaft und Kultur) Niedersachsen. Special thanks are due to NLPV (Nationalparkverwaltung Niedersächsisches Wattenmeer) for appropriate authorizations during field work. I am grateful to Ana-Maria Krapal and Philippe Gouletquer for valuable remarks and constructive comments which improved an earlier version of the manuscript.

This article is dedicated to the fond memory of Gerald Millat.

References

- Allen S, Carpenter AC, Luckenbach M, Paynter K, Sowers A, Weissberger E, Wesson J, Westby S (2011) Restoration goals, quantitative metrics and assessment protocols for evaluating success on restored oyster reef sanctuaries. Report of the oyster metrics workgroup Sustainable Fisheries Goal Implementation Team of the Chesapeake Bay Program. <http://www.chesapeakebay.net>

- Baggett LP, Powers SP, Brumbaugh RD, Coen LD, DeAngelis BM, Greene JK, Hancock BT, Morlock SM, Allen BL, Breitburg DL, Bushek D1, Grabowski JH, Grizzle RE, Grosholz ED, La Peyre MK, Luckenbach MW, McGraw KA, Piehler MF, Westby SR, zu Ermgassen PSE (2015) Guidelines for evaluating performance of oyster habitat restoration. *Restoration Ecology* 23: 737–745. <https://doi.org/10.1111/rec.12262>
- Blomberg BN, Lebreton B, Palmer TA, Guillou G, Pollack JB, Montagna PA (2017) Does reef structure affect oyster food resources? A stable isotope assessment. *Marine Environmental Research* 127: 32–40. <https://doi.org/10.1016/j.marenvres.2017.03.003>
- Buschbaum C, Cornelius A, Goedknecht MA (2016) Deeply hidden inside introduced biogenic structures – Pacific oyster reefs reduce detrimental barnacle overgrowth on native blue mussels. *Journal of Sea Research* 117: 20–26. <https://doi.org/10.1016/j.seares.2016.09.002>
- Büttger H, Berg T, Nehls G (2010) Evaluation of mussel beds in the North-Frisian Wadden Sea – according to the EU Water Framework Directive and EU Habitats Directive. In: Marencic et al. (Eds) *Science for Nature Conservation and Management: The Wadden Sea Ecosystem and EU Directives*. Proceedings of the 12th International Scientific Wadden Sea Symposium in Wilhelmshaven, Germany. Waddens Sea Ecosystem No. 26. Common Wadden Sea Secretariat, (Wilhelmshaven). <https://bioconsult-sh.de/de/referenzen/publikationen/>
- Büttger H, Nehls G, Witte S (2011) High mortality of Pacific oysters in a cold winter in the North-Frisian Wadden Sea. *Helgoland Marine Research* 65: 525–532. <https://doi.org/10.1007/s10152-011-0272-1>
- Chai AL, Homer M, Tsai C-F, Gouletquer P (1992) Evaluation of oyster sampling efficiency of patent tongs and an oyster dredge. *North American Journal of Fisheries Management* 12: 825–832. [https://doi.org/10.1577/1548-8675\(1992\)012<0825:EOOSEO>2.3.CO;2](https://doi.org/10.1577/1548-8675(1992)012<0825:EOOSEO>2.3.CO;2)
- Cognie B, Haure J, Barillé L (2006) Spatial distribution in a temperate coastal ecosystem of the wild stock of the farmed oyster *Crassostrea gigas* (Thunberg). *Aquaculture* 259: 249–259. <https://doi.org/10.1016/j.aquaculture.2006.05.037>
- Colden AM, Fall KA, Cartwright GM, Friedrichs CT (2016) Sediment suspension and deposition across restored oyster reefs of varying orientation to flow: implications for restoration. *Estuaries and Coasts* 39: 1435–1448. <https://doi.org/10.1007/s12237-016-0096-y>
- Colden AM, Latour RJ, Lipcius RN (2017) Reef height drives threshold dynamics of restored oyster reefs. *Marine Ecology Progress Series* 582: 1–13. <https://doi.org/10.3354/meps12362>
- DeAlteris JT (1988) The geomorphic development of wreck shoal, a subtidal oyster reef of the James River, Virginia. *Estuaries* 11: 240–249. <https://doi.org/10.2307/1352010>
- Escapa M, Isacch JP, Daleo P, Alberti J, Iribarne O, Borges M, Dos Santos EP, Gagliardini DA, Lasta M (2004) The distribution and ecological effects of the introduced Pacific oyster *Crassostrea gigas* (Thunberg, 1793) in Northern Patagonia. *Journal of Shellfish Research* 23: 765–772.
- Eschweiler N, Christensen HT (2011) Trade-off between increased survival and reduced growth for blue mussels living on Pacific oyster reefs. *Journal of Experimental Marine Biology and Ecology* 403: 90–95. <https://doi.org/10.1016/j.jembe.2011.04.010>
- Fey F, Dankers N, Steenbergen J, Goudswaard K (2010) Development and distribution of the non-indigenous Pacific oyster (*Crassostrea gigas*) in the Dutch Wadden Sea. *Aquaculture* 18: 45–59. <https://doi.org/10.1007/s10499-009-9268-0>

- Folmer E, Büttger H, Herlyn M, Markert A, Millat G, Troost K, Wehrmann A (2017) Beds of blue mussels and Pacific oysters. In: Kloepper S et al. (Eds) Wadden Sea Quality Status Report 2017. Common Wadden Sea Secretariat (Wilhelmshaven). <https://qsr.waddensea-worldheritage.org/reports/beds-blue-mussels-and-pacific-oysters>
- Goedknecht A, Schuster A-K, Buschbaum C, Gergs R, Jung AS, Luttikhuisen PC, van der Meer J, Troost K, Wegner KM, Thielges DW (2017) Spillover but no spillback of two invasive parasitic copepods from invasive Pacific oysters (*Crassostrea gigas*) to native bivalve hosts. *Biological Invasions* 19: 365–379. <https://doi.org/10.1007/s10530-016-1285-0>
- Grabowski JH (2004) Habitat complexity disrupts predator-prey interactions but not the trophic cascade on oyster reefs. *Ecology* 85: 995–1004. <https://doi.org/10.1890/03-0067>
- Grabowski JH, Powers SP (2004) Habitat complexity mitigates trophic transfer on *Crassostrea*-reefs. *Marine Ecology Progress Series* 277: 291–295. <https://doi.org/10.3354/meps277291>
- Green DS, Crowe TP (2014) Context- and density-dependent effects of introduced oysters on biodiversity. *Biological Invasions* 16: 1145–1163. <https://doi.org/10.1007/s10530-013-0569-x>
- Herbert RJH, Humphreys J, Davies CJ, Roberts C, Fletcher S, Crowe TP (2016) Ecological impacts of non-native Pacific oysters (*Crassostrea gigas*) and management measures for protected areas in Europe. *Biodiversity and Conservation* 25: 2835–2865. <https://doi.org/10.1007/s10531-016-1209-4>
- Holm MW, Davids JK, Dolmer P, Vismann B, Hansen BW (2015) Moderate establishment success of Pacific oyster, *Crassostrea gigas*, on a sheltered intertidal mussel bed. *Journal of Sea Research* 104: 1–8. <https://doi.org/10.1016/j.seares.2015.07.009>
- Jones CG, Lawton JH, Shachak M (1994) Organisms as ecosystem engineers. *Oikos* 69: 373–386. <https://doi.org/10.2307/3545850>
- Kellogg LM, Cornwell JC, Owens MS, Luckenbach MW, Ross PG, Leggett TA (2014) Scaling ecosystem services to reef development: effects of oyster density on nitrogen removal and reef community structure. Virginia Institute of Marine Science. College of William and Mary.
- Kochmann J, Buschbaum C, Volkenborn N, Reise K (2008) Shift from native mussels to alien oysters: differential effects of ecosystem engineers. *Journal of Experimental Marine Biology and Ecology* 364: 1–10. <https://doi.org/10.1016/j.jembe.2008.05.015>
- Lang AC, Buschbaum C (2010) Facilitative effects of introduced Pacific oysters on native macroalgae are limited by a secondary invader, the seaweed *Sargassum muticum*. *Journal of Sea Research* 63: 119–128. <https://doi.org/10.1016/j.seares.2009.11.002>
- Lenihan HS (1999) Physical-biological coupling on oyster reefs: habitat structure influences individuals performance. *Ecological Monographs* 69: 251–275. [https://doi.org/10.1890/0012-9615\(1999\)069\[0251:PBCOOR\]2.0.CO;2](https://doi.org/10.1890/0012-9615(1999)069[0251:PBCOOR]2.0.CO;2)
- Lejart M, Hily C (2011) Differential response of benthic macrofauna to the formation of novel oyster reefs (*Crassostrea gigas*, Thunberg) on soft and rocky substrate in the intertidal of the Bay of Brest, France. *Journal of Sea Research* 65: 84–93. <https://doi.org/10.1016/j.seares.2010.07.004>
- Lipcius RN, Burke RP, McCulloch DN, Schreiber SJ, Schulte DM, Seitz RD, Shen J (2015) Overcoming restoration paradigms: value of the historical record and metapopulation

- dynamics in native oyster restoration. *Frontiers in Marine Science* 2: 65. <https://doi.org/10.3389/fmars.2015.00065>
- Mann R, Southworth M, Harding LM, Wesson JA (2009) Population studies of the native Eastern oyster, *Crassostrea virginica*, (Gmelin, 1791) in the James River, Virginia, USA. *Journal of Shellfish Research* 28: 193–220. <https://doi.org/10.2983/035.028.0203>
- Markert A, Wehrmann A, Kroencke I (2010) Recently established *Crassostrea*-reefs versus native *Mytilus*-beds: differences in ecosystem engineering affects the macrofaunal communities (Wadden Sea of Lower Saxony, southern German Bight). *Biological Invasions* 12: 15–32. <https://doi.org/10.1007/s10530-009-9425-4>
- Markert A, Esser W, Frank D, Wehrmann A, Exo KM (2013) Habitat change by the formation of alien *Crassostrea*-reefs in the Wadden Sea and its role as feeding sites for waterbirds. *Estuarine, Coastal and Shelf Science* 131: 41–51. <https://doi.org/10.1016/j.ecss.2013.08.003>
- Markert A, Wehrmann A (2013) Bestandserfassung von *Sargassum muticum* auf dem Nordland im Rahmen einer Bioinvasionsphase. Reports Juni and November 2013. Forschungsauftrag im Rahmen einer Pilotstudie der Nationalparkverwaltung Niedersächsisches Wattenmeer (Wilhelmshaven).
- Markert A, Raupach MJ, Segelken-Voigt A, Wehrmann A (2014) Molecular identification and morphological characteristics of native and invasive Asian brush-clawed crabs from Japanese and German coasts: *Hemigrapsus penicillatus* (De Haan, 1835) versus *Hemigrapsus takanoi* Asakura & Watanabe 2005 (Crustacea: Brachyura). *Organisms, Diversity and Evolution* 14: 369–382. <https://doi.org/10.1007/s13127-014-0176-4>
- Markert A, Matsuyama K, Rohde S, Schupp B, Wehrmann A (2016) First record of the non-native Pacific bryozoan *Smittoidea prolifica* Osburn, 1952 at the German North Sea coast. *Marine Biodiversity* 46: 717–723. <https://doi.org/10.1007/s12526-015-0415-8>
- Millat G (2008) Gesamtbestandserfassung der eulitoralien Miesmuschelbänke bis 2007 im Rahmen des Monitorings zum Miesmuschelbewirtschaftungsplan. Nationalparkverwaltung Niedersächsisches Wattenmeer (Wilhelmshaven).
- Nehls G, Büttger H (2006) Ausbreitung und Nutzung der Pazifischen Auster *Crassostrea gigas* im Nationalpark Schleswig-Holsteinisches Wattenmeer. *Austernbericht 2006*. BioConsult SH (Husum).
- Nehls G, Witte S, Büttger H, Dankers N, Jansen J, Millat G, Herlyn M, Markert A, Kristensen PS, Ruth M, Buschbaum C, Wehrmann A (2009) Beds of blue mussels and Pacific oysters. Thematic Report No. 11. In: Marencic H and de Vlas J (Eds) *Quality Status Report 2009*. Wadden Sea Ecosystem No. 25. Common Wadden Sea Secretariat, Trilateral Monitoring and Assessment Group (Wilhelmshaven). <https://www.waddensea-worldheritage.org/resources/ecosystem-25-wadden-sea-quality-status-report-2009>
- Padilla DK (2010) Context-dependent impacts of a non-native ecosystem engineer, the Pacific oyster *Crassostrea gigas*. *Integrative and Comparative Biology* 50: 213–225. <https://doi.org/10.1093/icb/icq080>
- Peters JW, Eggleston DB, Puckett BJ, Theuerkauf SJ (2017) Oyster demographics in harvested reefs vs. no-take reserves: implications for larval spillover and restoration success. *Frontiers in Marine Science* 4: 326. <https://doi.org/10.3389/fmars.2017.00326>

- Powell EN, Mann R, Ashton-Alcox KA, Kim Y, Bushek D (2016) The allometry of oysters: spatial and temporal variation in the length-biomass relationships for *Crassostrea virginica*. *Journal of the Marine Biological Association of the United Kingdom* 96: 1127–1144. <https://doi.org/10.1017/S0025315415000703>
- Reise K, Buschbaum C, Büttger H, Rick J, Wegner MK (2017a) Invasion trajectory of Pacific oysters in the northern Wadden Sea. *Marine Biology* 164: 68. <https://doi.org/10.1007/s00227-017-3104-2>
- Reise K, Buschbaum C, Büttger H, Wegner MK (2017b) Invading oysters and native mussels: from hostile takeover to compatible bedfellows. *Ecosphere* 8: e01949. <https://doi.org/10.1002/ecs2.1949>
- Rothschild BJ, Ault JS, Gouletquer P, Héral M (1994) Decline of the Chesapeake Bay oyster population: a century of habitat destruction and overfishing. *Marine Ecology Progress Series* 11: 29–39. <https://doi.org/10.3354/meps111029>
- Ruesink JL, Lenihan HS, Trimble AC, Heiman KW, Micheli F, Byers JE, Kay MC (2005) Introduction of non-native oysters. Ecosystem effects and restoration implications. *Annual Review of Ecology, Evolution, and Systematics* 36: 643–689. <https://doi.org/10.1146/annurev.ecolsys.36.102003.152638>
- Schmidt A, Wehrmann A, Dittmann S (2008) Population dynamics of the invasive Pacific oyster *Crassostrea gigas* during the early stages of an outbreak in the Wadden Sea (Germany). *Helgolander Marine Research* 62: 367–376. <https://doi.org/10.1007/s10152-008-0125-8>
- Schulte DM, Burke RP, Lipsius RN (2009) Unprecedented restoration of a native oyster metapopulation. *Science* 325: 1124–1128. <https://doi.org/10.1126/science.1176516>
- Southworth M, Harding J, Mann R (2005) The status of Virginia's Public Oyster Resource 2004. Virginia Institute of Marine Science, College of William and Mary.
- Sousa R, Jorge L, Gutiérrez JL, Aldridge DC (2009) Non-indigenous invasive bivalves as ecosystem engineers. *Biological Invasions* 11: 2367–2385. <https://doi.org/10.1007/s10530-009-9422-7>
- Southworth M, Harding JM, Wesson LA, Mann R (2010) Oyster (*Crassostrea virginica*, Gmelin 1791) population dynamics on public reefs in the Great Wicomico River, Virginia, USA. *Journal of Shellfish Research* 29: 271–290. <https://doi.org/10.2983/035.029.0202>
- Theuerkauf SJ, Eggleston DB, Theuerkauf KW, Puckett BJ (2017) Oyster density and demographic rates on natural intertidal reefs and hardened shoreline structures. *Journal of Shellfish Research* 36: 87–100. <https://doi.org/10.2983/035.036.0111>
- Thieltges DW, Reise K, Prinz K, Jensen KT (2009) Invaders interfere with native parasite-host interactions. *Biological Invasions* 11: 1421–1429. <https://doi.org/10.1007/s10530-008-9350-y>
- Troost K, Kamermans P, Wolff WJ (2008) Larviphagy in native bivalves and an introduced oyster. *Journal of Sea Research* 60: 157–163. <https://doi.org/10.1016/j.seares.2008.04.006>
- Troost K, Gelderman E, Kamermans P, Smaal AC, Wolff WJ (2009) Effects of an increasing filter feeder stock on larval abundance in the Oosterschelde estuary (SW Netherlands). *Journal of Sea Research* 61: 153–164. <https://doi.org/10.1016/j.seares.2008.11.006>
- Van der Zee E, van der Heide T, Donadi S, Eklöf J, Eriksson B, Olf H, van der Veer H, Piersma T (2012) Spatially extended habitat modification by intertidal reef-building bivalves has

- implications for consumer-resource interactions. *Ecosystems* 15: 664–673. <https://doi.org/10.1007/s10021-012-9538-y>
- Wagner E, Dumbauld BR, Hacker SD, Trimble AC, Wisheart LM, Ruesink JL (2012) Density-dependent effects of an introduced oyster, *Crassostrea gigas*, on a native intertidal seagrass, *Zostera marina*. *Marine Ecology Progress Series* 468: 149–160. <https://doi.org/10.3354/meps09952>
- Wallis B (2015a) The ecosystem engineer *Crassostrea gigas* affects tidal flat morphology beyond the boundary of their reef structure. *Estuaries and Coasts* 38: 941–950. <https://doi.org/10.1007/s12237-014-9860-z>
- Wallis B (2015b) The role of ecosystem engineers in the ecomorphological development of intertidal habitats. PhD Thesis. Wageningen University (Wageningen).
- Wallis B, Mann R, Ysebaert T, Troost K, Herman PMJ, Smaal AC (2015c) Demography of the ecosystem engineer *Crassostrea gigas*, related to vertical reef accretion and reef persistence. *Estuarine, Coastal and Shelf Science* 154: 224–233. <https://doi.org/10.1016/j.ecss.2015.01.006>
- Waser AM, Splinter W, van der Meer J (2015) Indirect effects of invasive species affecting the population structure of an ecosystem engineer. *Ecosphere* 6: 109. <https://doi.org/10.1890/ES14-00437.1>
- Waser AM, Deuzeman S, van Kangeri AK, van Winden E, Postma J, de Boer P, van der Meer J, Ens B (2016) Impact on bird fauna of a non-native oyster expanding into blue mussel beds in the Dutch Wadden Sea. *Biological Conservation* 202: 39–49. <https://doi.org/10.1016/j.biocon.2016.08.007>
- Wehrmann A, Herlyn M, Bungenstock F, Hertweck G, Millat G (2000) The distribution gap is closed – first record of naturally settled Pacific oysters *Crassostrea gigas* in the East Frisian Wadden Sea, North Sea. *Senckenbergiana maritima* 30: 153–160. <https://doi.org/10.1007/BF03042964>
- Wehrmann A (2016) Wadden Sea. In: Harff J, Meschede M, Petersen S, Thiede J (Eds) *Encyclopedia of Marine Geosciences*. Springer (Dordrecht). https://doi.org/10.1007/978-94-007-6238-1_143
- Wrange AL, Valero J, Harkestad LS, Strand O, Lindegarth S, Christensen HT, Dolmer P, Kristensen PS, Mortensen S (2010) Massive settlements of the Pacific oyster, *Crassostrea gigas*, in Scandinavia. *Biological Invasions* 12: 1453–1458. <https://doi.org/10.1007/s10530-009-9565-6>

Cryptic diversity and mtDNA phylogeography of the invasive demon shrimp, *Dikerogammarus haemobaphes* (Eichwald, 1841), in Europe

Anna Maria Jazdzewska¹, Tomasz Rewicz^{1,2}, Tomasz Mamos^{1,3}, Remi Wattier⁴,
Karolina Bącela-Spychalska¹, Michał Grabowski¹

1 University of Lodz, Faculty of Biology and Environmental Protection, Department of Invertebrate Zoology and Hydrobiology, Banacha 12/16, 90-237 Lodz, Poland **2** University of Guelph, Centre for Biodiversity Genomics, Guelph, Ontario, Canada **3** University of Basel, Zoological Institute, Vesalasse 1, 4051 Basel, Switzerland **4** Université de Bourgogne Franche Comté, Équipe Écologie Évolutive and SAMBA, UMR CNRS 6282 Biogéosciences, Dijon, France

Corresponding author: Anna Maria Jazdzewska (anna.jazdzewska@biol.uni.lodz.pl)

Academic editor: A. Petrusek | Received 19 September 2019 | Accepted 18 March 2020 | Published 29 May 2020

Citation: Jazdzewska AM, Rewicz T, Mamos T, Wattier R, Bącela-Spychalska K, Grabowski M (2020) Cryptic diversity and mtDNA phylogeography of the invasive demon shrimp, *Dikerogammarus haemobaphes* (Eichwald, 1841), in Europe. NeoBiota 57: 53–86. <https://doi.org/10.3897/neobiota.57.46699>

Abstract

The regions of the Black, Caspian, and Azov seas are known for being both (i) the place of extensive crustacean radiation dated to the times of Paratethys and Sarmatian basins, and (ii) present donors of alien and invasive taxa to many areas worldwide. One amphipod morphospecies, *Dikerogammarus haemobaphes*, is known both as native to rivers draining to the Black and Caspian seas as well as a successful invader (nicknamed demon shrimp) in Central and Western European rivers. Based on mitochondrial (COI and 16S) and nuclear (28S) datasets and 41 sampling sites, representing both the native (19) and the invaded (22) range, we assessed cryptic diversity, phylogeography and population genetics of this taxon. First, we revealed the presence of two divergent lineages supported by all markers and all species delimitation methods. The divergence between the lineages was high (18.3% Kimura 2-parameter distance for COI) and old (ca. 5.1 Ma), suggesting the presence of two cryptic species within *D. haemobaphes*. Lineage A was found only in a few localities in the native range, while lineage B was widespread both in the native and in the invaded range. Although genetic divergence within lineage B was shallow, geographic distribution of 16S and COI haplotypes was highly heterogeneous, leading us to the definition of four Geo-Demographic Units (GDUs). Two GDUs were restricted to the native range: GDU-B1 was endemic for the Durugöl (aka Duruşu) Liman in Turkey, whereas GDU-B2 occurred only in the Dniester River. GDU-B3 was both present in several localities in the native range in the Black Sea drainage area and widespread in Central

and Western Europe. The GDU-B4 was found exclusively in the Moskva River in Russia. Extended Bayesian Skyline Plot indicated steady growth of GDU-B3 population size since 30 ka, pointing to the rather old history of its expansion, first in the late Pleistocene in the native range and nowadays in Central and Western Europe. The analysis of haplotype distribution across the present distribution range clearly showed two invasion routes to Central and Western Europe. The first one, originating from the lower Dnieper, allowed the demon shrimp to colonize Polish rivers and the Mittellandkanal in Germany. The second one, originating from the Danube delta, allowed to colonize the water bodies in the upper Danube basin. The UK population has originated from the Central Corridor, as only a haplotype found exclusively along this route was recorded in the UK. Population genetics analysis showed that the invasion of the demon shrimp along the Central Corridor was not associated with the loss of genetic diversity, which might contribute to the success of this invader in the newly colonized areas.

Keywords

Amphipoda, COI gene, Crustacea, inland waters, invasion routes, non-indigenous species, 16S gene

Introduction

Global climate changes impact the size and extent of areas that may potentially be inhabited by many species (Parmesan 2006). For example, range expansions from the glacial refugia after the last glacial maximum often take several thousands of years (Taberlet et al. 1998; Hewitt 2004). Nowadays, one of the effects of progressive temperature rise over past decades is the range expansion of species into areas where they previously were not present (LeRoux and McGeoch 2008; Ott 2010). This process has accelerated in recent years due to various human activities. For example, many aquatic species benefited from global shipping or interconnection of formerly separated water bodies, allowing spread on a continental scale or even worldwide (e.g., Ricciardi and MacIsaac 2000; Bij de Vaate et al. 2002; Gherardi 2007; Carlton 2011). Many successful invaders belong to crustaceans. Some prominent examples are the spiny-cheek crayfish *Faxonius limosus* (Rafinesque, 1817) and the amphipod *Dikerogammarus villosus* (Sowinsky, 1894) in European fresh waters (Filipová et al. 2011, Rewicz et al. 2015), the cladoceran *Cercopagis pengoi* (Ostroumov, 1891) in the North American Great Lakes (Ricciardi and MacIsaac 2000) or the Chinese mitten crab *Eriocheir sinensis* H. Milne Edwards, 1853 invading brackish and fresh waters globally (Dittel and Epifanio 2009; Hayer et al. 2019). Numerous studies demonstrated well that such invasions may alter, more or less profoundly, the structure and functioning of aquatic ecosystems (DAISIE 2009; Ricciardi and MacIsaac 2011; Strayer 2012).

Molecular methods provide a useful tool for casting light on the processes and pathways of invasions, supplementing observations coming from traditional monitoring (Estoup and Guillemaud 2010). Among others, it enables identification of the source populations and tracking the invasion routes of aquatic organisms (e.g., Cristescu et al. 2004; Audzijonyte et al. 2009; Brown and Stepien 2009, 2010; Cabezas et al. 2014). Some of the studied invasions were associated with a loss of genetic diversity. That is the case of the freshwater amphipod *Crangonyx floridanus* Bousfield, 1963 in

Japan and in the United Kingdom (Nagakubo et al. 2011; Mauvisseau et al. 2019) or the spiny-cheek crayfish *F. limosus* in Europe (Filipová et al. 2011). In contrast, in other aquatic organisms no loss in diversity was observed (Roman and Darling 2007; Wattier et al. 2007; Brown and Stepien 2010; Rewicz et al. 2015). Molecular studies allowed also to reveal multiple invasion events in the case of some species, such as the freshwater amphipod *Gammarus tigrinus* Sexton, 1939 or the marine amphipods *Caprella mutica* Schurin, 1935 and *C. scaura* Templeton, 1836 (Kelly et al. 2006; Ashton et al. 2008; Cabezas et al. 2014). More than one wave of invasion was also suggested for other crustaceans, such as *Limnomysis benedeni* Czerniavsky, 1882 (Audzijonyte et al. 2009) or two European *Carcinus* crab species (Geller et al. 1997). Molecular methods helped to reveal as well the origin of the invasive *Palaemon elegans* Rathke, 1837 population in the Baltic Sea (Reuschel et al. 2010).

Several studies uncovered the presence of substantial cryptic diversity in the invasive aquatic morphospecies with divergent genetic lineages showing different potential to spread and colonize new areas (Kelly et al. 2006; Folino-Remon et al. 2009; Bock et al. 2012). For example, the North-American *G. tigrinus* comprises at least two cryptic species in its native range. However, only one of them was transferred, on several occasions, across the Atlantic Ocean and, in parallel, colonized a wide range of European waters (Rewicz et al. 2019). At the beginning of the 21st century, the same cryptic species has invaded the Laurentian Great Lakes (Kelly et al. 2006). On the other hand, in the case of another well studied invasive amphipod, *Dikerogammarus villosus*, which had widely spread in Central and Western Europe from its native range in the Ponto-Caspian region, there was no evidence for presence of cryptic species and only two weakly divergent genetic lineages were found outside its native range (Wattier et al. 2007; Rewicz et al. 2015).

The area of the Black, Caspian, Azov, and Aral seas is recognized as the region of extensive radiation of crustacean species flocks dated to the times of Parathetys and Sarmatian basins (Cristescu et al. 2003; Cristescu and Hebert 2005). Due to long-term isolation of these water bodies, their fauna consists of many endemic species (Pjatakova and Tarasov 1996; Dumont 2000; Cristescu and Hebert 2005; Nahavandi et al. 2013). In recent years, the area has played an important role as a donor of alien and invasive species for many regions of the world (Ricciardi and MacIsaac 2000; Bij de Vaate et al. 2002; Cristescu et al. 2004; Arbaciauskas et al. 2017; Minchin et al. 2019). The range expansions of the Ponto-Caspian species to other parts of Europe are associated with constructions of canals connecting previously separated river basins. The first connections between the Black Sea and the Baltic Sea drainages date back to the 18th century when the Pripyat-Bug (Royal) and Notecki canals were opened. In later years, canals connected many rivers in Central and Western Europe (Jażdżewski 1980). The history of Ponto-Caspian species invasions let Bij de Vaate et al. (2002) to identify three migration corridors used by aquatic biota to spread all over Europe (Fig. 1). The acceleration of the range expansions was also associated with the intentional transfer of certain crustacean species to artificial reservoirs, especially in the former Soviet Union (Karpevich 1975; Jażdżewski 1980; Arbaciauskas et al. 2017).



Figure 1. European freshwater continental invasion corridors after Bij de Vaate et al. 2002 (orange – Southern, red – Central, blue – Northern corridor) and history of invasion of *D. haemobaphes*. Shading shows the presumed native area, years denote the first reports of *D. haemobaphes* at the respective sites (indicated by arrows). Black dots indicate sampling sites used in this study.

Invasion history of *Dikero gammarus haemobaphes* in Europe

Ponto-Caspian amphipods have high invasion potential, and as many as 13 morphospecies originating from that region have been recorded as alien or invasive elsewhere (Holdich and Pöckl 2007). This number includes three species of the genus *Dikero gammarus* (Ricciardi and MacIsaac 2000; Cristescu et al. 2004; Berezina 2007). One of them, *D. haemobaphes* (nicknamed the demon shrimp), is native to the lower courses of large rivers in the Black and the Caspian drainage areas, to their brackish water lagoons as well as to the Caspian Sea (Sars 1894; Caraușu 1943) (Fig. 1). Already Mordukhai-Boltovskoi (1964) forecasted possible quick range expansion of the demon shrimp in Western Europe, but until 1980 the species was reported only from the lower and middle Dnieper, Dniester, Don, and Volga rivers (Jazdzewski 1980). In 1976, *D. haemobaphes* was found in the upper Danube in Germany (Bij de Vaate et al. 2002). In the 1990s, its rapid expansion in Germany had begun. In 1993, it was observed in the Main-Danube canal (Schleuter et al. 1994) and already in 1994 in the upper Rhine River (Schöll et al. 1995). At the same time, in Russia, it spread up the Volga River until Rybinsky Reservoir and invaded the upper Moskva River (Berezina 2007). *Dikero gammarus haemobaphes* was first recorded in the Vistula River in Poland in 1997, and, during the monitoring of its middle and lower course in 1998 and 1999, it appeared to have established populations there (Konopacka 1998; Bij de Vaate et al. 2002). At the end of the 20th century, the species was commonly found also in the

lower and middle Oder River, Vistula Lagoon, and in the Masurian Lake District in Poland (Jazdzewski 2003; Grabowski et al. 2007b). In 2008, the species was recorded for the first time in the Meuse, Moselle, and Seine rivers in France (Labat et al. 2011). In 2011, it was found in two isolated Alpine lakes in Austria and Germany (present study). In Switzerland the species was reported from the Murtensee in 2011 and from the Neuenburgersee in 2016 (Altermatt et al. 2019). The latest record of this species outside its native range came from 2012 when it was found in the River Severn in Great Britain and, subsequently, it has established sustainable populations in the central part of the country (Aldrige 2013; Etxabe et al. 2015; Constable and Birkby 2016; Johns et al. 2018). As a result, the species is presently distributed in the majority of large European rivers, and the history of its range extension suggests that it has used all three invasion corridors proposed by Bij de Vaate et al. (2002) (Fig. 1).

The demon shrimp has a high potential for invasion (Grabowski et al. 2007a; Bacela et al. 2009; Bacela-Spychalska and Van der Velde 2013). However, another invasive species of the genus *Dikerogammarus*, the so-called killer shrimp *D. villosus*, was often considered a more successful invader (Dick et al. 2002; Rewicz et al. 2015; Kobak et al. 2016), attracting more scientific attention than *D. haemobaphes*. Only two molecular studies on *D. haemobaphes* have been reported so far by Müller et al. (2002) and Cristescu and Hebert (2005). However, the number of localities and individuals sampled in both studies was too low to track the invasion history of the demon shrimp. Recent studies of the congeneric *D. villosus* revealed the absence of cryptic species and no genetic diversity loss along invasion corridors (Wattier et al. 2007; Rewicz et al. 2015).

Based on the thorough sampling across Europe and using two mitochondrial and one nuclear marker, our study aims to reveal the phylogeographic structure and historical population dynamics of *D. haemobaphes* in its native Black Sea basin and in the invaded range. Taking into account what is currently known about the recently studied and closely related killer shrimp, the history of the demon shrimp invasion and the geological history of the native area, we hypothesized that (i) it is plausible that in the native region the demon shrimp encompasses several weakly divergent lineages dating back to Pleistocene, (ii) there are possibly two sources, the Dnieper and the Danube deltas and, hence, two independent routes for the species invasion to Central and Western Europe – the so-called Central Corridor and the Southern Corridor of invasion, respectively, (iii) learning from the invasion history of the closely related killer shrimp, we can expect that the populations of the demon shrimp will also show signs of demographic and spatial expansion and no loss of genetic diversity, except the UK population, in comparison to the source population.

Materials and methods

Sample collection

Dikerogammarus haemobaphes was collected at 55 sites in both its native (23 sites) and invaded (32 sites) ranges between 2000 and 2014 (Table 1). Some localities were geo-

Table 1. Sites where *Dikerogammarus haemobaphes* was collected. N – native range, CC – Central Corridor, SC – Southern Corridor, NC – Northern Corridor; n – number of individuals sequenced for COI and 16S; h – number of haplotypes based on concatenated COI and 16S sequences; A_r and PA_r – allelic and private allelic richness estimates, corrected for sample size through rarefaction; NA – sampling date not available.

Code	Native / invasive	River Basin	River	Country	Latitude / Longitude	Date	n	h	A_r	PA_r
1	N	Durugöl	Durugöl liman	Turkey	41.3163, 28.6205	2007	23	12	4.03	4.03
2	N	Danube	Danube	Romania/Bulgaria	43.7499, 23.8987	2013	1	1	x	x
3	N	Danube	Danube	Romania	45.1595, 28.9089	2013	1	1	x	x
4	N	Dniester	Dniestrovskij Liman	Ukraine	46.3309, 30.0956	2009	8	1	1	0.01
5	N	Dniester	Dniester	Ukraine	46.4127, 30.2585	2009	14	5	3.30	0.79
5A	N	Dniester	Dniester	Ukraine	46.4127, 30.2585	2011				
6	N	Dniester	river near Orhei	Moldova	47.3707, 28.8040	2011	5	1	1	0
7	N	Dniester	Dniester	Ukraine	48.2309, 28.2775	2011	14	4	2.67	0.13
7A	N	Dniester	Dniester	Ukraine	48.2323, 28.2838	2011				
8	N	Akkarzhanka	Akkarzhanka	Ukraine	46.3469, 30.5969	2009	10	4	2.96	1.06
9	N	Akkarzhanka	Dalnik	Ukraine	46.4008, 30.5929	2009	20	4	2.41	0.57
10	N	Bug	Southern Bug	Ukraine	48.169, 30.4512	2009	11	3	1.96	0.01
11	N	Dnieper	Steblevskij Liman	Ukraine	46.614, 32.5159	2009	23	5	1.99	0.09
11A	N	Dnieper	Dnieprovskij Liman	Ukraine	46.5595, 32.3437	2009				
12	N	Dnieper	North Crimean canal	Ukraine	46.1828, 33.5432	2011	10	2	1.52	1
13	N	Dnieper	Kerch peninsula, Frontove	Ukraine	45.1865, 35.4718	2011	21	4	3.27	0.52
14	N	Dnieper	Dnieper	Ukraine	47.7918, 35.1255	2009	6	3	2.74	0.77
15	N	Dnieper	Saksahan	Ukraine	48.3533, 33.8621	2009	9	2	1.57	0
16	N	Dnieper	Dnieper	Ukraine	48.4658, 35.0648	2006	5	3	2.73	0.87
16A	N	Dnieper	Dnieper	Ukraine	48.4646, 35.1322	2006				
17	N	Dnieper	Dnieper-Donbas channel	Ukraine	49.0342, 36.1045	2011	6	2	1.97	0
18	N	Don	Krasnopavlivski zaliv	Ukraine	49.0971, 36.4267	2011	11	3	2.44	0.48
19	N	Don	Doniec	Ukraine	48.8915, 37.8011	2011	17	3	2.50	0
20	CC	Dnieper	Kievski Reservoir	Ukraine	51.0675, 30.3907	2009	4	1	1	0
20A	CC	Dnieper	Desna	Ukraine	51.4848, 31.3308	NA				
21	CC	Dnieper	channel in Dubay village	Belarus	52.03, 26.8504	2010	10	3	2.31	0.52
22	CC	Vistula	Bug	Poland	52.1748, 23.4342	2004	5	3	2.86	0
22A	CC	Vistula	Bug	Poland	52.1748, 23.4342	2003				
23	CC	Vistula	Bug	Poland	52.4141, 22.5612	2004	10	3	2.49	0.11
24	CC	Vistula	Bug	Poland	52.5333, 21.259	2003	7	4	3.31	0.22
25	CC	Vistula	Vistula	Poland	50.5194, 21.5965	2002	17	3	1.65	0.05
25A	CC	Vistula	Vistula	Poland	50.4224, 21.3104	2002				
26	CC	Vistula	Vistula	Poland	51.661, 21.483	2002	10	3	2.04	0.59
27	CC	Vistula	Vistula	Poland	52.6945, 19.0212	2000	5	3	2.86	0.06
28	CC	Vistula	Vistula lagoon	Poland	54.2729, 19.4134	2000	14	3	2.29	0
28A	CC	Vistula	Vistula lagoon	Poland	54.3243, 19.5194	2000				
28B	CC	Vistula	Vistula lagoon	Poland	54.3381, 19.2322	2002				
29	CC	Vistula	canal between Luknajno and Śniardwy lakes	Poland	53.7991, 21.6355	2002	7	2	1.99	0
30	CC	Oder	Warta	Poland	52.6505, 14.9999	2001	9	3	2.78	0
31	CC	Oder	Oder	Poland	52.7332, 14.3785	2001	19	6	2.85	0.52
31A	CC	Oder	Oder	Poland	52.6697, 14.461	2001				
32	CC	Oder	Oder	Poland	52.4396, 14.5779	2001	12	2	1.45	0
32A	CC	Oder	Oder	Poland	52.4396, 14.5772	2001				
33	CC	Elbe	Mittellandkanal	Germany	52.3016, 11.3711	2010	2	2	x	x
34	CC	Ems	Mittellandkanal	Germany	52.3082, 7.6272	2010	2	1	x	x
35	SC	Danube	Starnbergersee	Germany	47.9734, 11.3518	2011	20	1	1	0
36	SC	Danube	Traunsee	Austria	47.9008, 13.7686	2011	21	1	1	0
37	SC	Danube	Danube	Austria	48.1625, 16.5165	2005	3	2	2	0
37A	SC	Danube	Danube	Austria	48.2991, 16.3469	2005				
38	SC	Danube	Danube	Hungary	47.7856, 18.96	2011	4	2	1.96	0
38A	SC	Danube	Danube	Hungary	47.8149, 18.864	2013				
39	SC	Danube	Balaton	Hungary	46.9139, 17.8935	2006	19	2	1.29	0
40	NC	Volga	Moskva	Russia	55.5969, 37.1223	NA	9	3	2.41	2.41
40A	NC	Volga	Moskva	Russia	55.5969, 37.1223	NA				
41	UK	Great Ouse	Great Ouse	United Kingdom	52.1344, -0.4662	2014	9	1	1	0

graphically very close (ca. 20 km distance) to each other (same site number in Table 1, but one of the two or three indicated with letter A or B), so we decided to combine them with the closest sampling site to simplify further analysis (Table 1). As a result, our dataset comprises 41 localities, of which 19 belonged to the native and 22 to the invaded range (Fig. 2). All the sampling sites were located in public and non-protected areas. In the native area, sampling was done along the western and northern coast of the Black Sea either in limans of large coastal rivers or lower courses of large rivers (e.g., Danube, Dniester, Dnieper). The area around the Azov Sea was included in the sampling campaign, but the demon shrimp was not found in any of the 15 sampling sites visited. The Caspian Sea was not included in our study. The sampling in the invaded areas covered all three invasion corridors used by aquatic species to spread in Central, Western, and Northern Europe (see Bij de Vaate et al. 2002) including the recently colonized waters in the UK.

Molecular analysis

The total DNA was extracted from 434 individuals according to the standard phenol-chloroform method (for details see Hillis et al. 1996). Air-dried DNA pellets were eluted in 100 μ l of TE buffer, pH 8.0, stored at 4 °C until amplification, and subsequently at -20 °C for long-term storage. Two mtDNA markers: a gene for the 16S ribosomal RNA (16S rRNA; ca. 320 bp fragment) and the standard barcoding fragment of the cytochrome c oxidase subunit I gene (COI; 658 bp fragment) were amplified. LR-J-GAM/LR-N-GAM primers (Müller et al. 2002) and reaction conditions after Grabowski et al. (2012) were used for 16S rRNA amplification. COI gene was amplified using LCO1490/HCO2198 (Folmer et al. 1994) and UCOIR/UCOIF (Costa et al. 2009) primers and reaction conditions following Hou et al. (2007). Sequences were obtained using BigDye sequencing protocol on the Applied Biosystems 3730x1 capillary sequencer by Macrogen Inc., Korea. Sequencing of the COI gene was performed unidirectionally (with the forward primer). In cases when the quality of the obtained sequence was not sufficient, a reverse sequencing was applied as well. Sequencing of the 16S gene was bidirectional. Sequences were edited, aligned with the ClustalW algorithm (Chenna et al. 2003) using BioEdit 7.2.5, and trimmed to the length of the shortest one. The resulting 433 sequences of 16S (302 bp) and COI (598 bp) were subsequently concatenated for the purpose of the analyses.

Haplotypes were retrieved using DNA SP v5 both for individual markers and for the concatenated sequences (Librado and Rozas 2009). Then, at least two individuals of lineage A as well as each detected geo-demographic unit (GDU, defined based on the spatial distribution of well-supported lineages on the chronogram, see Results for details) were amplified for the additional nuclear marker, 28S rRNA, for phylogeny reconstruction. The nuclear marker was amplified with 28F and 28R primers and reaction conditions published by Hou et al. (2007).

Relevant voucher information, taxonomic classifications, and the COI barcode sequences are publicly accessible through the public data set “DHAEMOBA”

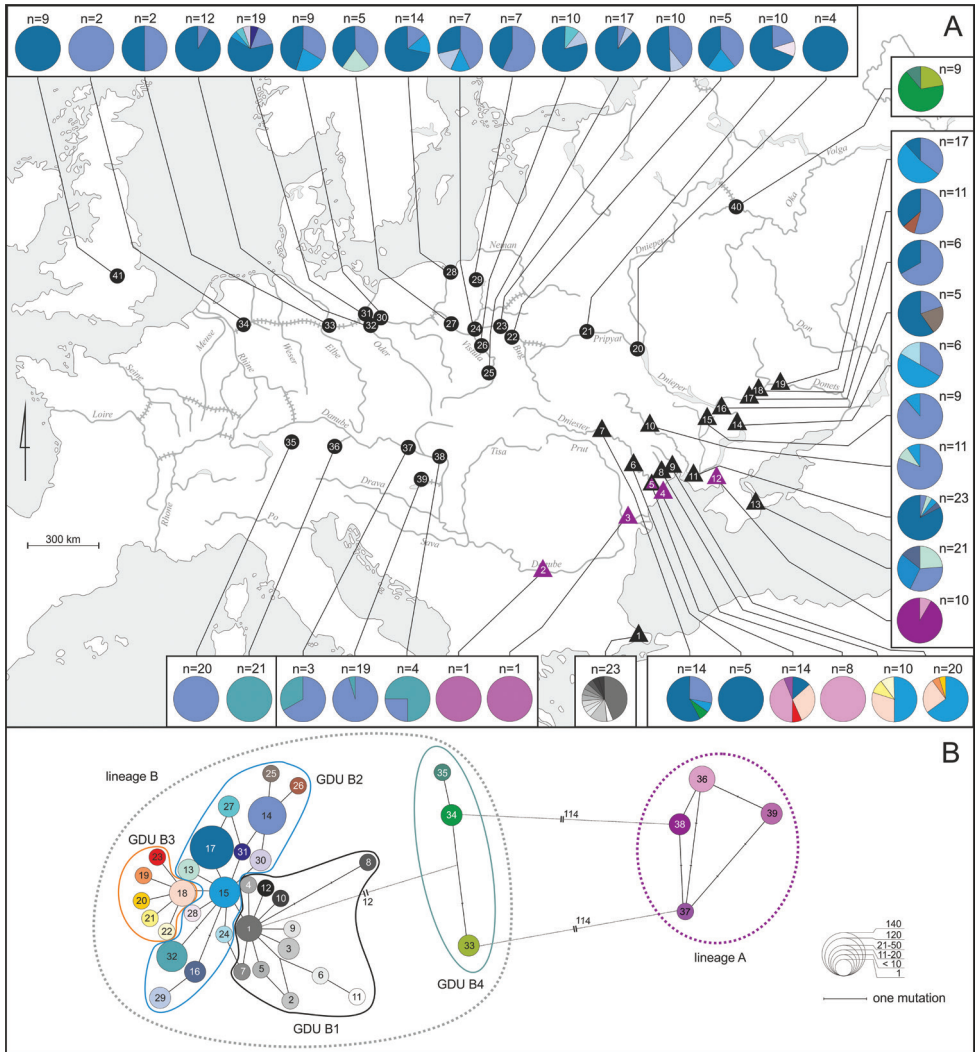


Figure 2. A geographic distribution of *D. haemobaphes* haplotypes in the native and invaded area. Numbers in triangles (native range) or circles (invaded range) represent sampling localities coded as in Table 1. Sites with lineage A indicated with purple. n = number of sequences analyzed in the site **B** the minimum spanning network of mtDNA haplotypes identified in *D. haemobaphes*. The size of circle denotes the frequency of each haplotype. The numbers correspond to the haplotype numbers. GDU – geo-demographic unit.

(<https://doi.org/10.5883/DS-DHAEMOBA>) on the Barcode of Life Data Systems (BOLD; www.boldsystems.org) (Ratnasingham and Hebert 2007). Newly generated sequences were also deposited in GenBank: COI: MN342874–MN343144, MN343146–MN343307; 16S: MN343308–MN343578, MN343580–MN343741; 28S: MN343743–MN343753.

Time calibrated reconstruction of phylogeny

Bayesian time-calibrated phylogeny was reconstructed in BEAST, version 2.5.2 (Bouckaert et al. 2014) to infer the time frame of the *D. haemobaphes* diversification. The COI and 16S mitochondrial markers were used as separate partitions in the Bayesian inference analysis (BI). The priors to evolutionary models were set using bModelTest (Bouckaert and Drummond 2017). The strict clock was calibrated with the COI mutation rate set at 0.01773 substitutions/site/Ma as proposed for amphipods by Copilaș-Ciocianu et al. (2019), given that very similar rates were reported for the family Gammaridae in other studies (Mamos et al. 2016; Grabowski et al. 2017). Four runs of Markov chain Monte Carlo (MCMC), each 20 million iterations long and sampled every 1000 iterations, were performed. Runs were examined using Tracer v 1.6, and all the sampled parameters achieved a sufficient sample size (ESS > 200). Tree files were combined using Log-Combiner 1.8.1 (Drummond et al. 2012), with the removal of the non-stationary 25% burn-in phase. The maximum clade credibility chronogram was generated using TreeAnnotator 2.5.2 (Bouckaert et al. 2014). For additional support of tree topology, the concatenated COI + 16S dataset was analyzed with the Maximum Likelihood (ML) method, using the Tamura 3-parameter model (Tamura 1992) selected through the Bayesian Information Criterion (BIC) with 10000 bootstrap replicates. ML analysis was performed in MEGA X (Kumar et al. 2018).

Tests for cryptic diversity

To visualize molecular divergence of mtDNA haplotypes, a Minimum Spanning Network was generated using Arlequin 3.5.1.2 (Excoffier and Lischer 2010). Pairwise Kimura 2-parameter (K2P) distances were estimated using MEGA X (Kumar et al. 2018).

Four molecular species delimitation methods were applied to reveal the potential Molecular Operational Taxonomic Units (MOTUs) that could represent putative cryptic species within the studied demon shrimp populations. Two methods were distance-based: Barcode Index Number (BIN) System (Ratnasingham and Hebert 2013), and the barcode-gap approach using the Automatic Barcode Gap Discovery (ABGD) (Puillandre et al. 2012). The following two were tree-based, a phylogenetic approach using Generalized Mixed Yule Coalescent (GMYC) model-based method (Pons et al. 2006), according to Monaghan et al. (2009) and the Bayesian implementation of the Poisson Tree Processes (bPTP) (Zhang et al. 2013). For both tree-based methods, we have used the already generated Bayesian time-calibrated phylogeny.

The BIN method is implemented as part of the Barcode of Life Data system (BOLD; Ratnasingham and Hebert 2007). Newly submitted sequences are compared together with sequences already available in BOLD. Sequences are clustered according to their molecular divergence using algorithms that aim at finding discontinuities between clusters. Each cluster is ascribed a globally unique and specific identifier (aka

Barcode Index Number or BIN), already available or newly created if the submitted sequences do not cluster with previously known BINs. Each BIN is registered in BOLD.

The ABGD method is based upon pairwise distance measures. With this method, the sequences are partitioned into groups (MOTUs), such that the distance between two sequences from two different groups will always be larger than a given threshold distance (i.e., barcode gap). We used primary partitions as a principle for group definition, as they are typically stable on a broader range of prior values, minimize the number of false-positives (over-split species), and are usually close to the number of taxa described by taxonomists (Puillandre et al. 2012). The default value of 0.001 was used as the minimum intraspecific distance. As there is currently no consensus about which maximum intraspecific distance is reflecting delimitation of species, neither based on morphology (Costa et al. 2007; Weiss et al. 2014; Katouzian et al. 2016) nor on reproductive barrier (Laguerre et al. 2014) we explored a set of values up to 0.1. The standard Kimura 2-parameter (K2P) model correction was applied (Hebert et al. 2003).

The GMYC method defines MOTUs through identification of the switch from intraspecific branching patterns (coalescent) to interspecific species branching patterns (Yule process) on a phylogenetic tree. First, a log-likelihood ratio test is performed to assess if the GMYC model fits the observed data significantly better than the null model of a single coalescent species. If there is evidence for overlooked species inside the phylogenetic tree, the threshold model is tested for the observed data to estimate the boundary between intra- and interspecific branching patterns. The Bayesian tree was uploaded into the R (R Core Team, 2013) software package ‘SPLITS’ (Species Limits by Threshold Statistics) (Ezard et al. 2009) and analyzed using the single threshold model.

The bPTP is another phylogeny-based method. The bPTP incorporates the number of substitutions in the model of speciation and assumes that the probability that a substitution gives rise to a speciation event follows a Poisson distribution. The branch lengths of the input tree are supposed to be generated by two independent classes of the Poisson events, one corresponding to speciation and the other to coalescence. Additionally, the bPTP adds Bayesian support values (BS) for the delimited species (Zhang et al. 2013). The analysis was performed on the bPTP webserver (available at <http://www.species.h-its.org/ptp/>) with 500 000 iterations of MCMC and 10% burn-in.

The 28S rRNA nuclear phylogeny was reconstructed for *Dikerogammarus haemobaphes*, *D. bispinosus* Martynov, 1925, and *D. villosus* using the Maximum Likelihood method and the Tamura 3-parameter model selected through BIC as a best fitting model (Tamura 1992). All positions with less than 95% site coverage were eliminated. The bootstrap test was done with 500 replicates (Saitou and Nei 1987). These analyses were done in MEGA X (Kumar et al. 2018). Sequences of *D. villosus* (KF478495, KF478496) and *Pontogammarus robustoides* (Sars, 1894) (KF478447) used as an outgroup were retrieved from GenBank.

Demography

To reveal the historical demography of *D. haemobaphes*, we used the Extended Bayesian Skyline Plot (eBSP) (Heled and Drummond 2008) constructed in BEAST, version 2.5.2 (Bouckaert et al. 2014), using COI and 16S as separate partitions. The eBSP was performed for the lineage A and three out of four geo-demographic units (GDUs) identified in the lineage B (see results). Due to a small number of individuals representing the clade from the Moskva River in Russia (GDU B4), this unit was not explored. The clock rate and model selection were performed the same way as in the case of time-calibrated phylogeny reconstruction. The population scaling factor was set to 0.5. To ensure convergence, four runs of MCMC, each 100 million iterations long and sampled every 5000 iterations, were performed. Runs were examined using Tracer v 1.6; all the sampled parameters achieved sufficient sample sizes ($ESS > 200$) and presented congruent results. The final figures were generated in R (R Core Team, 2013).

We have also examined the current demographic status of the lineage A and three GDUs of lineage B of *D. haemobaphes* in Arlequin 3.5 (Excoffier and Lischer 2010) with mismatch distribution, supplemented by the selective neutrality tests, i.e., Tajima's D (Tajima 1989) and Fu's F_s (Fu 1997) as indicators of population expansion. We verified the validity of both models (sudden demographic and spatial expansion) with the sum of squared deviations (SSD) between observed and expected mismatches and by the Harpending's Raggedness statistics (Harp).

Diversity and differentiation along Central Corridor

The haplotype diversity was assessed by calculating the allelic richness (A_p), and the private allelic richness (PA_p), where haplotypes equaled to alleles, corrected for a common sampling size using a rarefaction approach (Leberg 2002) in case of localities with at least three individuals. Calculations were done using Hp-Rare 1.1 (Kalinowski 2005).

We used 19 sites along the Central Corridor to test for a positive correlation between genetic differentiation and the distance between sites (isolation-by-distance, IBD). Besides, the data from these sites were used to check whether diversity (haplotype diversity, nucleotide diversity, A_p , PA_p , see Table 1, Suppl. material 1: Table S1) was associated with geographical distance from the source area (Dnieprovski Liman). We evaluated the trend in haplotype diversity, nucleotide diversity, allelic richness, and private allelic richness along the Central Corridor of the invasion by calculating Pearson Correlation Coefficient. The distances (Suppl. material 1: Table S1) were estimated using Google Earth v.7.1.2 as a measurement of shortest distance along the waterway (Google Earth, option path, zoomed enough to fit the line in the riverbed) of Central Corridor starting from our sampling locality 11A (Dnieprovski Liman) to locality 32 (Oder). IBD was tested using the Mantel test between $F_{st}/(1-F_{st})$ and geographic dis-

tance as recommended by Rousset (1997) for testing IBD in one-dimensional linear systems, with 100000 permutations, using the ISOLDE software embedded in the GenePop on the Web 4.2 package (Raymond and Rousset 1995).

Results

Cryptic diversity within *Dikerogammarus haemobaphes*

In the dataset composed of 433 sequences, we identified 15 haplotypes of 16S (302 bp) and 27 haplotypes of COI (598 bp). The concatenation of both fragments (900 bp) resulted in the recognition of 39 mtDNA haplotypes derived from different combinations of the 16S and COI haplotypes (Suppl. material 2: Table S2, Suppl. material 3: Table S3). The pairwise K2P distance between the haplotypes ranged from 0.002 to 0.183 for COI and from 0.003 to 0.099 for 16S; the highest values suggesting the presence of cryptic diversity within the studied morpho-species.

All the COI sequences, represented by 27 haplotypes, were uploaded into the Barcode of Life Data System (BOLD), resulting in two Barcode Index Numbers (BINs) obtained (Fig. 3). The BIN AAX9262 was attributed to 406 sequences (23 COI haplotypes) and was already reported in BOLD and GenBank associated with *D. haemobaphes*. The mean K2P distance within this BIN was 0.0023, and the maximal K2P distance was 0.0263. The BIN ADB9467, associated with 27 sequences (four COI haplotypes), has not been reported before. The mean K2P distance within this BIN is 0.0013, and the maximal K2P distance is 0.0051. The closest BIN to ADB9467 is the AAX9262, with an average K2P distance of 0.176.

Automatic Barcode Gap Discovery (ABGD) was performed on two data sets (i) 27 sequences, each representing one of the 27 COI haplotypes and (ii) 433 sequences, representing all individuals sequenced. The first analysis indicated the existence of two MOTUs (lineages A, B), divergent by the 0.183 maximum K2P distance, that may be interpreted as two potential cryptic species (Fig. 3). The individuals belonging to the lineage A included only four haplotypes (27 sequences) and were found in five localities, exclusively in the native range of *Dikerogammarus* species (two sites in the lower Danube, two in the lower Dniester and one on the Kerch Peninsula). The lineage B consisted of 23 haplotypes (406 sequences) widely distributed both in the native and the invaded range of *D. haemobaphes*. The second analysis resulted in partitioning all COI sequences into three groups. One corresponded to the lineage A, while within the lineage B, the sequences from individuals found in the River Moskva in Russia were separated as yet another MOTU.

The GMYC analysis also rejected the null model of the *D. haemobaphes* sequences representing a single species. The single threshold method of lineage identification allowed to recognize five entities: lineage A and lineage B, the latter further divided into four sub-lineages (Fig. 3). The estimated number of species in bPTP ranged from three to five, the best Bayesian support (>0.987) being for three (Fig. 3).

All the five methods used for species delimitation are congruent at recognizing the lineage A as distinct from any other MOTU. Given the extremely high K2P-distance

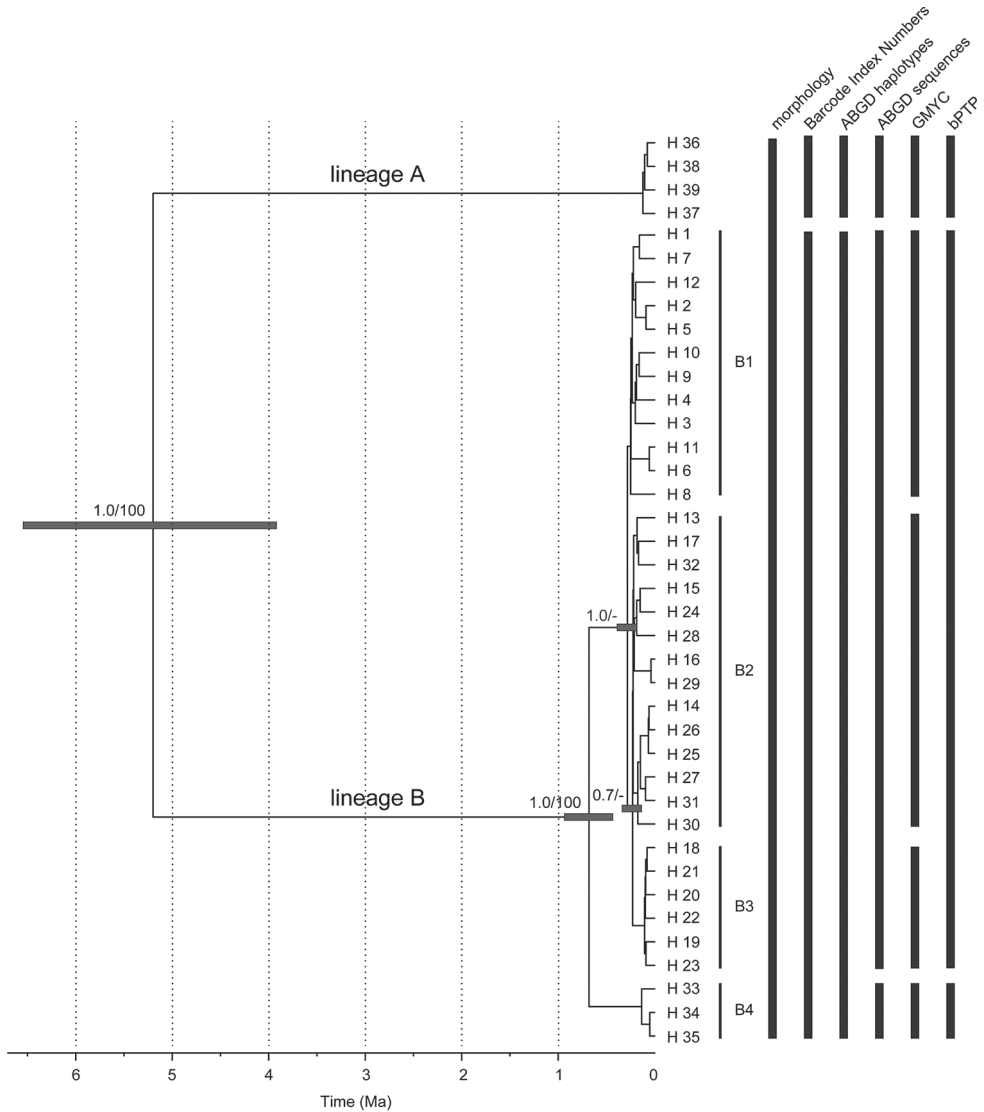


Figure 3. Time-calibrated phylogeny of *Dikerogammarus haemobaphes* and the results of different species delimitation methods. Maximum clade credibility chronogram was inferred from a strict molecular clock model based on the COI + 16S data set of *D. haemobaphes*. The numbers given next to the respective main nodes indicate Bayesian posterior probabilities (> 0.5) and ML bootstrap values (> 50%). B1-4 represent the geo-demographic units within the lineage B. BIN – Barcode Index Number (BIN) System, ABGD haplotypes – Automatic Barcode Gap Discovery based on haplotypes, ABGD sequences – Automatic Barcode Gap Discovery based on all sequences, GMYC – Generalized Mixed Yule Coalescent, bPTP – Bayesian Poisson Tree Processes.

(max 0.183) between lineage A and all the others, we can conclude the presence of cryptic diversity within *D. haemobaphes*. In addition, since this lineage is restricted only to the native range, we do not use it in tracking the demon shrimp invasion in

Europe. Lineage B was recognized by BINs and, partially, by ABGD as one MOTU, while other methods subdivided it into smaller groups. Given the weak phylogenetic support for these sublineages and lack of congruent delimitation results (Fig. 3) we decided not to treat them as cryptic species, yet taking into account their allopatry (see below), we refer to them further as geo-demographic units (GDU B1–4).

The phylogeny reconstruction based on the 28S rRNA confirmed the separation of *D. villosus* and *D. bispinosus* from *D. haemobaphes*, as well as the clear separation of lineages A and B, further supporting the presence of two cryptic species within *D. haemobaphes* (Fig. 4). Within the morphospecies *D. haemobaphes*, the lineage A considerably differed from lineage B and, although with quite a low bootstrap support, showed more affinities to *D. bispinosus* than to lineage B.

Time-calibrated reconstruction of phylogeny

The Bayesian phylogenetic reconstruction indicated the existence of two main lineages, A and B (Fig. 3). Lineage A is constituted by four haplotypes (36–39). These haplotypes were found in the Dniester river and its liman, the lower course of the Danube river, and in one locality at the Crimean peninsula. Lineage B can be, taking into account the results of MOTU delimitation together with the allopatric distribution of delimited entities, further divided into four geo-demographic units. The geo-demographic unit B1 (GDU B1) includes 12 haplotypes (haplotype numbers 1–12) endemic to Durugöl (Duruşu) liman in Turkey; GDU B2 includes 14 haplotypes (haplotype numbers 13–17 and 24–32) found both in native as well as recently invaded range. GDU B3 is represented by six haplotypes (haplotype numbers 18–23) found only in the Dniester river. The remaining three haplotypes (haplotype numbers 33–35) made up GDU B4 and were found exclusively in the Moskva River in Russia. The Bayesian chronogram showed that lineage A diverged from the rest ca. 5.1 Ma, whereas GDU B4 diverged from GDU B1–3 ca. 750 ka, GDU B1 diverged from GDU B2–3 ca. 300 ka, while the split between GDU B2 and GDU B3 was ca. 250 ka.

Historical and contemporary expansion, colonization routes and source population for the UK, Balaton Lake and Alpine lakes

The results of eBSP analysis indicated that the size of populations within the lineage A remained stable between 80 and 20 ka, followed by a slight decrease from 20 to 15 ka and a large decrease during the last 10 ka (Fig. 5).

Within the lineage B, the GDU B1 from the Durugöl (Duruşu) liman in Turkey experienced slight growth from 80 ka till 50 ka. Later, the population remained stable. On the contrary, the widespread and invasive clade GDU B2 retained stable size till ca. 2.5 ka, and after that experienced accelerated growth. The Dniester population (GDU B3) was stable until ca. 10 ka; later steady but slow growth can be observed. There were not enough sequences of GDU B4 to perform the eBSP analysis.

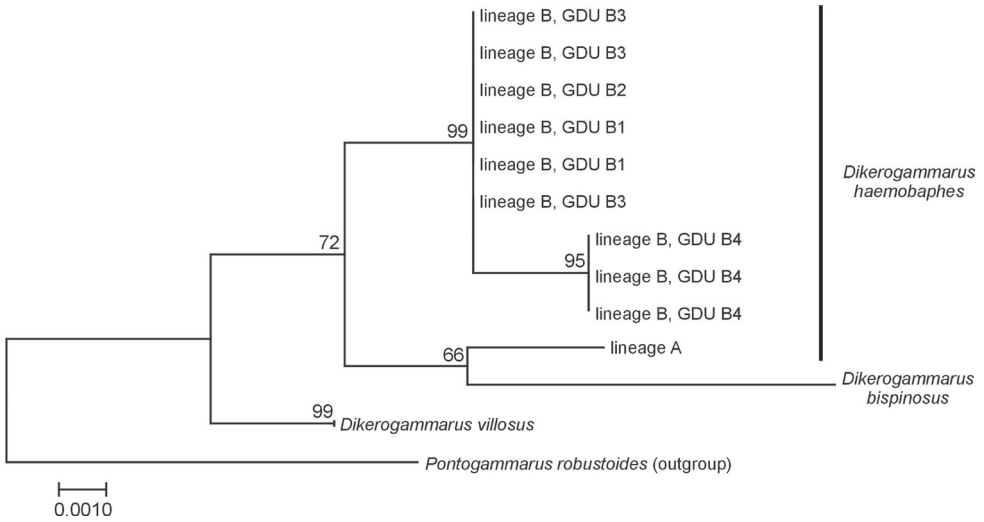


Figure 4. Maximum Likelihood tree of *Dikerogammarus* spp. based on the 28S rRNA gene. Sequences representing *D. haemobaphes* lineage A, each of the geo-demographic units (GDU B1-4) within *D. haemobaphes* lineage B as well as *D. bispinosus* and *D. villosus* were used. The evolutionary history was inferred by using the Maximum Likelihood method and the Tamura 3-parameter model. All positions with less than 95% site coverage were eliminated. Bootstrap test was applied with 500 replicates. Information about the *D. bispinosus* sequence may be found in public BOLD dataset: DHAEMOBA. *Dikerogammarus villosus* and *Pontogammarus robustoides* sequences were retrieved from GenBank.

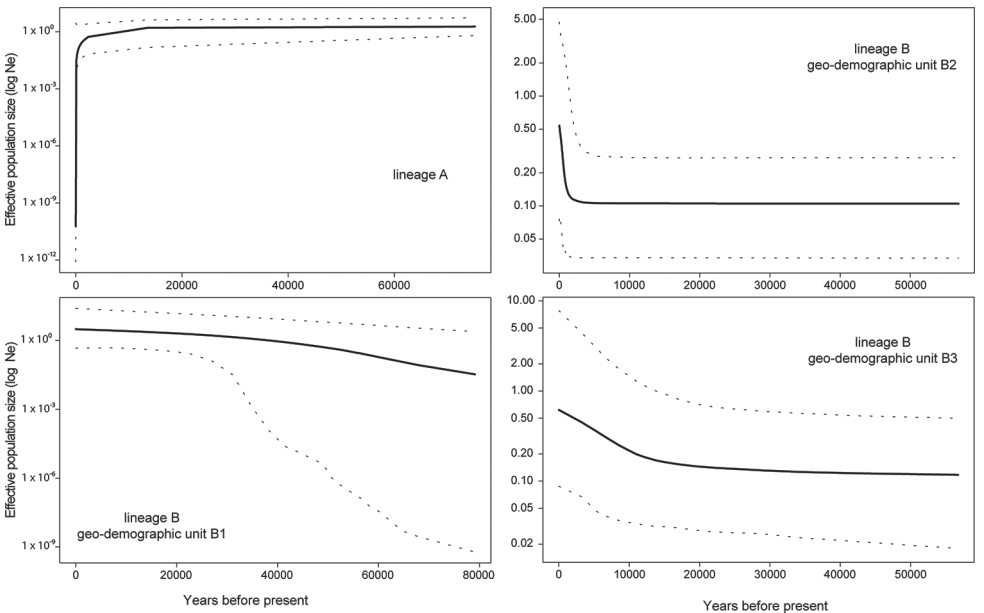


Figure 5. Multilocus extended Bayesian Skyline Plots for four lineages / geo-demographic units (GDU) of *Dikerogammarus haemobaphes*. Solid lines indicate the median posterior effective populations size through time; dotted lines indicate the 95% highest posterior density interval for each estimate.

Table 2. Historical demography based on concatenated mtDNA sequences (COI and 16S) from the lineage A and the Geo-Demographic Units (GDU) within the lineage B in the native region of *Dikerogammarus haemobaphes*. For details about locations, see Table 1 and Fig. 2. Demography: Harp, Harpending's raggedness index; SSD, sum of squared deviations; D, Tajima's D; F_s , Fu's F_s tests; p, p value. The statistically significant p values (below 0.05) are marked in bold.

Lineage/area	Locations	Spatial			Demographic				D	p	F_s	p	
		Harp	p	SSD	p	Harp	p	SSD					p
<i>Dikerogammarus haemobaphes</i> Lineage A (BIN ADB9467)													
Lineage A	2, 3, 4, 5/5A, 12	0.113	0.342	0.007	0.207	0.113	0.340	0.007	0.333	-0.597	0.337	-0.218	0.405
<i>Dikerogammarus haemobaphes</i> Lineage B (BIN AAX9262)													
GDU-B3	5/5A, 6, 7/7A, 8, 9	0.069	0.265	0.002	0.283	0.069	0.269	0.002	0.448	-0.887	0.242	-3.621	0.041
GDU-B2	11/11A, 13, 14	0.076	0.431	0.019	0.204	0.076	0.343	0.023	0.155	0.215	0.618	0.572	0.647
GDU-B1	1	0.067	0.475	0.004	0.497	0.067	0.429	0.004	0.586	-1.923	0.013	-8.472	0.000

Mismatch analysis showed that neither demographic nor spatial expansion model could be rejected for the lineage A or for any GDU of the lineage B (Table 2). Both neutrality tests suggested the recent expansion only in the case of the GDU B1 from the Durugöl (Duruşu) liman, while the Fu's F_s suggests a recent expansion of the GDU B3 from the Dniester. Interestingly, neither of the neutrality tests indicated recent population size expansion for the widespread and invasive GDU B2.

The analysis of mtDNA haplotype distribution across the distribution range of the demon shrimp clearly showed the two invasion routes to Central and Western Europe (Fig. 2). The most frequently observed in the invaded area were haplotypes 14 and 17. However, while haplotype 14 was found in several localities both along the Central and Southern Corridor, haplotype 17 and haplotype 15 were present only in the North-Western Black Sea drainage (excluding the Danube and its delta) and in the Central Corridor. Only the mtDNA haplotype 17 was found in the UK, suggesting that the local population derives from the Central Corridor. We found four private haplotypes (haplotypes 28–31) in the invaded range in Belarus and Poland. They were not encountered in the native area, probably due to their generally very low frequency. Additionally, it is worth noting that haplotype 32 was found exclusively along the Southern Corridor (Danube drainage). Single haplotypes were recorded in the two Alpine lakes. In the case of Starnbergersee in Germany (site 35), it was haplotype 14, while in the Traunsee in Austria (site 36), only haplotype 32 was found. The population of Balaton lake consisted predominantly of individuals bearing haplotype 14 with a small share of individuals with haplotype 32.

Molecular diversity patterns

The highest diversity within the *D. haemobaphes* lineage B expressed by the number of mtDNA haplotypes (12) as well as by the highest private allelic richness was observed in the Durugöl (Duruşu) liman ($A_r = 4.03$ and $PA_r = 4.03$, respectively) (Table 1). In all the other localities within the native range of the species, the number of detected haplotypes did not exceed five. The allelic richness was higher than three in two cases, in

the Dniester (station 5/5A) and in the Dnieper at Kerch Peninsula (station 13) with the values 3.30 and 3.27, respectively. The private allelic richness was high in the Akkarzhanka River (station 8, $PA_r = 1.06$) and in the Dnieper at station 16/16A ($PA_r = 0.87$).

In the invaded range, the number of haplotypes was the highest in the Oder River (station 31/31A, six haplotypes) followed by the station 24 in the Bug River with four haplotypes recorded (Table 1). In all the other stations, the number of detected haplotypes did not exceed three. Allelic richness ranged from one to 3.31, with the highest values observed in the Bug River at station 24 ($A_r = 3.31$) followed by the station 22/22A in the same river and by the station 27 in the Vistula River (in both cases A_r equaled 2.86). The highest private allelic richness was observed in the Vistula River at station 26 ($PA_r = 0.59$). Slightly lower values ($PA_r = 0.52$) characterized the channel in Dubay village (Dnieper River system, station 21) and in the Oder River at the station 31/31A.

No loss of allelic richness was observed along the Central Corridor, ca. 2500 km from the source population to the furthest locality studied, as the highest value of this parameter was observed in the Bug River (station 24, $A_r = 3.31$) in Poland, ca. 1960 km from the source area (Table 1, Suppl. material 1: Table S1). We observed a weak isolation-by-distance (IBD) effect (Mantel test, $R^2 = 0.0369$, $p = 0.037$) (Fig. 6A).

A slight decrease, although not statistically significant, in haplotype diversity ($R^2 = 0.006$, $r(17) = -0.07$; $p = 0.76$), nucleotide diversity ($R^2 = 0.018$, $r(17) = -0.13$; $p = 0.59$), allelic richness ($R^2 = 0.001$, $r(17) = -0.02$; $p = 0.92$), private allelic richness ($R^2 = 0.131$, $r(17) = -0.36$; $p = 0.13$) were observed along the Central Corridor of invasion (starting in the source of the corridor at the Dnieprovski Liman locality 11A, belonging to the native range of the species) (Fig. 6B–E, Suppl. material 1: Table S1).

Discussion

The Ponto-Caspian region appears to be one of the main donors of alien aquatic species invading Central and Western Europe as well as North America (Bij de Vaate et al. 2002; Audzijonyte et al. 2006, 2008; Neilson and Stepien 2011; Snyder et al. 2014). Some of them are now recognized as a serious threat to the invaded ecosystems (DAISIE 2009). *Dikerogammarus haemobaphes* is one of the three *Dikerogammarus* species that have colonized vast areas of Europe during recent decades, and even recently it has gained new territories outside continental Europe, i.e., in the UK (Labat et al. 2011; Aldridge 2013; Etxabe et al. 2015; Constable and Birkby 2016).

Phylogeography and demography in the native region

We observed the presence of two highly divergent lineages among the individuals of the demon shrimp (Fig. 3). The COI K2P distance between these two lineages was 0.183, which exceeded the threshold limit widely used for amphipod species delineation and observed even between many morphologically well-defined species (Costa et al. 2009; Raupach et al. 2015; Lobo et al. 2017). The distinctness of these two di-

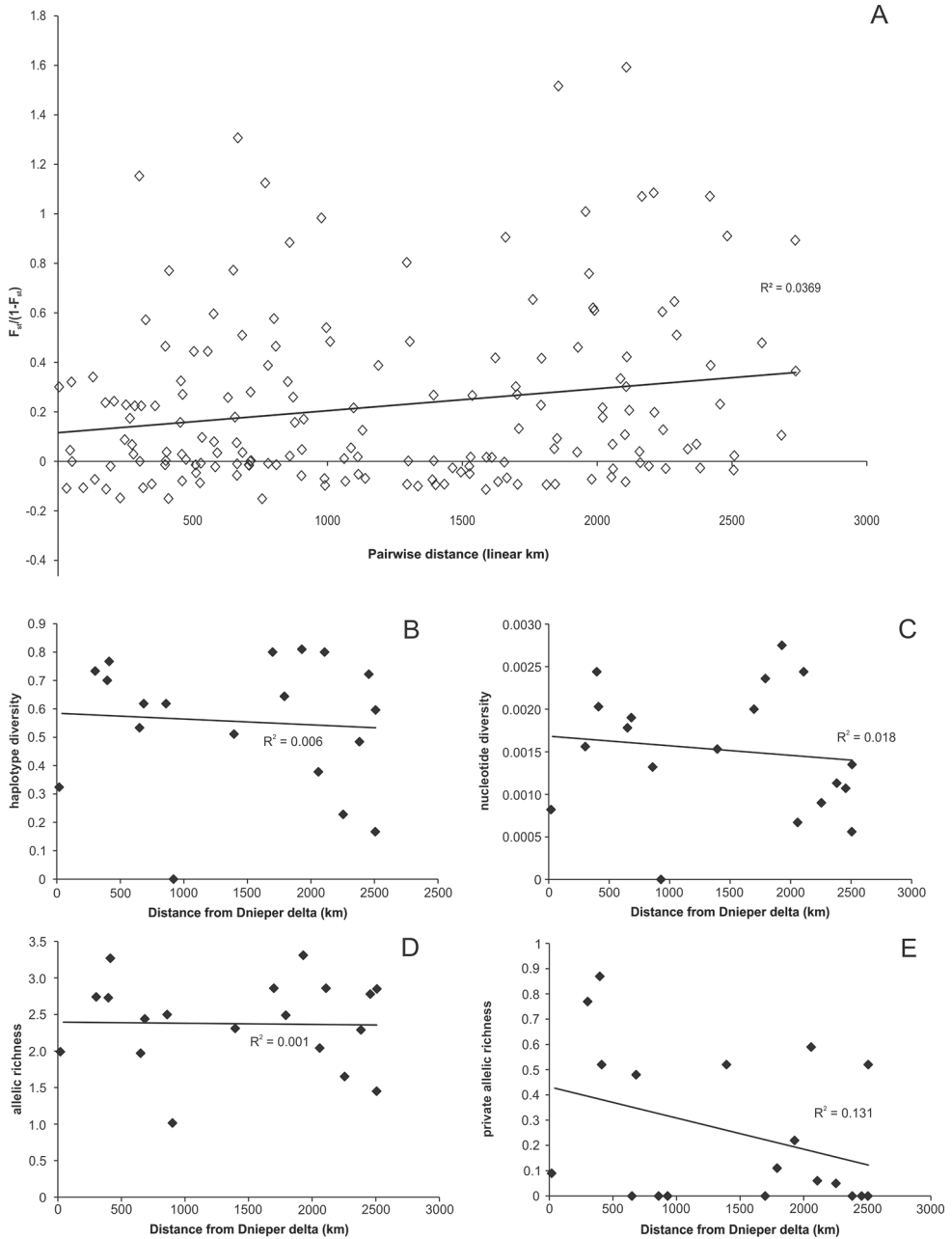


Figure 6. A plot of pairwise $F_{st}/(1-F_{st})$ versus pairwise linear distance of 19 populations of *D. haemobaphes* encompassing source populations for the Central Corridor and Central Corridor itself. Plot of: Haplotype diversity (B), nucleotide diversity (C), allelic richness (D) and private allelic richness (E) within 19 populations of *D. haemobaphes* along source populations for the Central Corridor and Central Corridor itself (see Suppl. material 1: Table S1 for details).

vergent lineages was also supported by the nuclear (28S) gene (Fig. 4). The divergence between these two lineages possibly dates back to 5.1 Ma (Fig. 3). This coincides with the eustatic marine regression and the formation of separate Dacian and Kimmerian basins in the present Ponto-Caspian area (Cristescu et al. 2003; Stoica et al. 2013). The considerable extension of freshwater habitats in this area during the Pliocene may have induced the evolution of species with freshwater preferences. Among them could be the lineage A, as our findings suggest that it occurs in fresh and not in brackish waters of the north-west Black Sea basin.

Dikerogammarus haemobaphes was originally described from the brackish waters of the Caspian Sea, while Martynov (1919), based on the material from the lower Don River, described the riverine form *Dikerogammarus haemobaphes* morpho *fluviatilis* to distinguish it from the brackish water population. Some authors followed this separation (e.g., Căraușu 1943; Căraușu et al. 1955) and since then the above-mentioned form has often been treated as a valid species (Straškraba 1962; Barnard and Barnard 1983; Jażdżewski and Konopacka 1988; Özbek and Özkan 2011). However, the morphological features separating *D. haemobaphes* and *Dikerogammarus fluviatilis* were extremely poorly defined by Martynov (1919), so the existence of the latter species remains unclear, and a thorough taxonomic revision was recommended (Jażdżewski and Konopacka 1988). Our study of the material molecularly assigned to the lineage A did not reveal any morphological evidence that would allow to classify it as *D. fluviatilis* or as any other species than *D. haemobaphes*. Given the wide distribution of the lineage B in the native region and taking into account that it includes the presumably Caspian lineage from the Moskva River, we believe that this lineage most probably represents the “real” *D. haemobaphes*. Thus the lineage A is an undescribed cryptic lineage known so far only from the lower Danube and other rivers in the north-western Black Sea region.

The results of eBSP analyses indicate a recent (less than 20 ka) substantial decrease in the effective population size within the lineage A that may explain its rarity and lack of invasion potential. Such demographic decline is hard to explain, but it may be associated with the late Pleistocene/early Holocene marine transgression and subsequent salinity rise in consequence of reconnection of the former Pontic Lake to the Mediterranean Sea that made up the present Black Sea (Svitoch et al. 2000; Badertscher et al. 2011). This might have forced the numerous freshwater species to move up the rivers emptying to the Black Sea, disconnecting their populations and causing demographic declines.

The divergence pattern within the *D. haemobaphes* lineage B in its native range is shallow but reflected, to some extent, by the geographic distribution of GDUs. For example, GDU B4 found exclusively in the Moskva River (Caspian Basin) apparently diverged from the others at about 750 ka (Fig. 3), already after the Black and Caspian basins disconnected (Cristescu et al. 2003). A similar separation of genetic lineages was observed for several other local crustacean taxa, including amphipods, mysids, and some cladocerans (Cristescu et al. 2003, 2004; Cristescu and Hebert 2005; Audzijonyte et al. 2009). Geo-demographic unit B1, represented by 12 haplotypes that emerged ca.

200–300 ka was, in our study, restricted to a single locality in the Durugöl (Duruşu) liman in Turkey. A similar pattern was observed for *D. villosus* (Rewicz et al. 2015), and our findings support the hypothesis that the populations of freshwater and oligohaline crustaceans inhabiting the Ponto-Caspian region have started to diverge during the significant salinity rise that caused a barrier for gene flow between biota “imprisoned” in the nearly freshwater lagoons and limans (Badertscher et al. 2011; Rewicz et al. 2015).

The eBSP analysis showed different historical demographic patterns in the remaining geo-demographic units. In the case of GDU B1, restricted to the Durugöl Liman, the effective population size remained relatively stable. The two GDUs found in the North Black Sea basin (B2 and B3) seem to experience demographic growth in the last couple of thousands of years. These results stay in contrast with the ones obtained for *D. villosus*; in this case, the post-Pleistocene demographic boost was observed in all the studied lineages of the species (Rewicz et al. 2015).

Invasion routes

The distribution of mtDNA haplotypes along the expansion routes clearly points out to the Dnieper River as a donor of invaders for the Central Corridor and, subsequently, for Western Europe. It is supported by the haplotype composition of the studied populations, with haplotypes, such as the most common haplotype 17, unique for the Dniester, Dnieper, Bug, Vistula, Oder and all along the Mittellandkanal in Germany but absent from the Danube and from the Alpine lakes. In the UK we found only haplotype 17, which suggests that the Central Corridor was also the most probable source for the introduction of *D. haemobaphes* to the UK.

In contrast, the Danubian expansion route is characterized by only two haplotypes, haplotype 14 that is shared with the Central Corridor and the private haplotype 32. Such poor haplotype diversity in the Southern Corridor is hard to explain. Already in the 1950s, the demon shrimp was reported from the middle Danube above Győr in Hungary, and in 1994, it was found as high as the Danube-Main canal in Germany (Straškraba 1962; Schleuter et al. 1994; Borza et al. 2015). In the early 1990s it was abundant in the German part of the Danube, but soon after the appearance of the killer shrimp, the population of demon shrimp in that area declined (Weinzierl et al. 1996; Kley and Maier 2006; Borza et al. 2018). Similar observations were made in other rivers: Rhine, Lahn, Drava, Oder, and Vistula (Weinzierl et al. 1996; Bernauer and Jansen 2006; Kley and Maier 2006; Grabowski et al. 2007b; Chen et al. 2012; Čuk et al. 2019; own unpublished data), suggesting effective replacement of this species by *D. villosus*, even if in some conditions co-existence of *D. haemobaphes* and *D. villosus* was observed (Borza et al. 2017; Hellmann et al. 2017). Taking into account all the above, we cannot exclude a possibility that the haplotype diversity in the Southern Corridor had once been richer but pauperized after the populations of the demon shrimp declined following lengthy interaction with the killer shrimp.

Interestingly, while the demon shrimp was a successful invader reaching Western Europe via the Central Corridor, the killer shrimp expanded to this area via the Southern Corridor. The population of *D. villosus* from the lower Dnieper expanded its range along the Central Corridor only to central Poland (Rewicz et al. 2015). The interspecific competition between both congeneric invasive species may be the reason for these differences. The killer shrimp is known to be a very active and robust competitor, which may force less competitive species (such as *D. haemobaphes*) to leave their optimal ecological niches and extend their ranges into habitats yet unoccupied by competitors (Kobak et al. 2016 and references therein). Additionally, the presence of stronger competitors may lead to niche partitioning as it was observed for *Dikerogammarus* spp. in the Danube (Borza et al. 2017). Such factors have possibly promoted range extension of the less competitive species and may help to explain why *D. haemobaphes* conquered rivers along the Central Corridor (Kobak et al. 2016).

The Southern Corridor seems to be the most probable source from which demon shrimp colonized the three studied lakes: the large lowland Balaton Lake in Hungary, as well as the two submontane Alpine lakes – the Traunsee in Austria and the Starnbergersee in Germany. The lake Balaton is connected to the Danube by the Sió canal, allowing different organisms to spread, and the presence of alien species was reported from the lake already since the 1930s (Muskó et al. 2007). The spontaneous range extension through the Danube-Balaton waterway is most probable, but an unintentional introduction of *D. haemobaphes* together with another crustacean species, *Limnomysis benedeni*, used as a food source for fish, could also be possible (Muskó 1992; Muskó et al. 2007). The two submontane Alpine lakes also belong to the Danube drainage area, but they are connected to the Danube by relatively small tributaries, namely fast-flowing submontane rivers. The presence of the demon shrimp was not confirmed from these watercourses (Altermatt et al. 2019). Thus, the most probable invasion vector, in this case, is an unintentional introduction associated with recreational activities such as sailing or diving, as it was reported for *D. villosus* by Baćela-Spychalska et al. (2013). High potential for such dispersal was experimentally evidenced also for the demon shrimp (Baćela-Spychalska 2016).

The small sample of *D. haemobaphes* from the Moskva River in Russia, also situated outside the native range of studied species (ca. 3000 km up from the Volga delta), seems to be a sister group to all the other GDUs within lineage B found in the Black Sea as well as in Central and Western Europe (Fig. 3). A single available COI sequence mined from GenBank (GenBank accession number: AY529049) and labelled as coming from the Caspian Sea (Cristescu and Hebert 2005) represented the same haplotype as eight out of ten sequences from the site in the Moskva River. This suggests that the Caspian Sea served as a donor for this population, which most likely arrived there via the Volga River belonging to the Northern Corridor of invasion. This scenario may be supported by the fact that *D. haemobaphes* has been recorded all along the Volga River as well as in its tributary Oka (Zadin 1964) and finally from the Moskva river (Lvova et al. 1996). Intentional introductions and extensive shipping accelerated its invasion process to a large number of water reservoirs built on the Volga River (Karpevich 1975; Slynko et al. 2002). The lack of other molecular data from the Caspian and Azov

seas does not allow to track the invasion process in the Northern Corridor in detail. However, it has to be underlined that the shores of the Azov Sea were covered by our sampling and no demon shrimp were found there.

The divergence of the Black and the Caspian Sea populations was observed in the cases of several Ponto-Caspian crustaceans (Cristescu et al. 2003, 2004) and similar situations may be expected for the presently studied species. Although we have found some private haplotypes occurring only in the invaded range of *D. haemobaphes*, they are all closely linked with the most common haplotypes found in the Dnieper River and its liman. No haplotypes of unknown origin were recorded in Western Europe, so the Caspian Sea may be excluded as a likely source of invading population along the Central and Southern invasion corridors.

Although a weak signal of IBD was recorded, all other measures expressing changes in the level of genetic diversity along the Central Corridor of the invasion were not significant, showing no bottleneck effect associated with the invasion of *D. haemobaphes* along the invasion corridor. The detected isolation by distance may come from the fact that a relatively high number (four) of private haplotypes existed at some sites in the invaded area (Fig. 6). It could lead falsely to suggest isolation of the invading population from the source one. Generally, it is expected that the molecular diversity in the invaded range might be reduced due to a relatively small number of newcomers. However, recent studies show that such a phenomenon does not have to be as common as previously predicted (Roman and Darling 2007). No genetic diversity loss was observed either during the invasion of *D. villosus* invasion in Europe (Wattier et al. 2007; Rewicz et al. 2015) or in case of dreissenid mussels and fish in the North American Great Lakes area (Stepien et al. 2005). The phenomena that can explain the lack of genetic diversity loss may be associated with rapid colonization by a large population of invaders or subsequent multiple invasion waves (Stepien et al. 2005; Roman and Darling 2007). In the present case, historical data suggest that the first alternative is more likely.

In conclusion, our results further confirm that the geological history of the Ponto-Caspian region stimulated divergence and speciation in the local freshwater and oligohaline organisms. Some of the resulting closely related lineages cannot be separated morphologically and, at the present stage, have to be treated as cryptic ones. Some of them, such as the lineage A of *D. haemobaphes*, remained in the area of origin, while others, such as the lineage B, successfully conquered new areas. The colonization of Western Europe by the demon shrimp followed mainly the Central Corridor, while another successful invader, the killer shrimp, used the Southern Corridor predominantly. These differences may be explained by interspecific competition with the killer shrimp (Kobak et al. 2016) that could force *D. haemobaphes* to leave the native range to reduce the competitive pressure. Another reason may be competitive niche partitioning, as observed by Borza et al. (2017) and perhaps different habitat characteristics of the rivers making up the two invasion corridors. Finally, we conclude the demon shrimp extended its range rapidly and that the expanding population was large as evidenced by the lack of loss of genetic diversity in the populations studied along the Central Corridor.

Acknowledgments

The study was partially funded by the Committee on Scientific Research (3P04F01322), Polish Ministry for Science and Higher Education grants: sampling (NN304081535, NN304350139, NN303579439), molecular analysis (NN304350139) and partially by the statutory funds of the Department of Invertebrate Zoology and Hydrobiology of University of Lodz. Tomasz Rewicz and Tomasz Mamos were supported by the Scholarship of the Polish National Agency for Academic Exchange (NAWA) at Bekker Programme (TR project nb. PPN/BEK/2018/1/00162, TM project nb. PPN/BEK/2018/1/00225). The authors thank Peter Borza, Bartosz Janic, Ewa Janowska, Radomir Jaskuła, Krzysztof Jazdzewski, Alicja Konopacka, Sergiy Kudrenko, Marek Michalski, Mykola Ovcharenko, Maciej Podsiadło, Alexander Prokin, Agnieszka Rewicz, Mikhail Son and Oleksandr Usov for their help in collecting the material for this study. Alicja Konopacka is acknowledged for identifying some material for this study. Drew Constable (National Hydroecology Team, Environment Agency UK) is greatly appreciated for providing the demon shrimp sample from the UK. We express our gratitude to the two anonymous reviewers and the editor, Adam Petrussek, for providing useful comments that allowed us to improve our work.

References

- Aldridge D (2013) GB non-native organism rapid risk assessment for *Dikerogammarus haemobaphes* (Eichwald, 1841). <http://www.nonnativespecies.org/downloadDocument.cfm?id=870> [accessed 05 September 2019]
- Altermatt F, Alther R, Fišer C, Švara V (2019) Amphipoda (Flohkrebse) der Schweiz: Checkliste, Bestimmung und Atlas. Fauna Helvetica 32. Info fauna CSCF (Neuchâtel): 1–389.
- Arbačiauskas K, Šidagytė E, Šniaukštaitė V, Lesutienė J (2017) Range expansion of Ponto-Caspian peracaridan Crustaceans in the Baltic Sea basin and its aftermath: Lessons from Lithuania. Aquatic Ecosystem Health & Management 20: 393–401.
- Ashton GV, Stevens MI, Hart MC, Green DH, Burrows MT, Cook EJ, Willis KJ (2008) Mitochondrial DNA reveals multiple Northern Hemisphere introductions of *Caprella mutica* (Crustacea, Amphipoda). Molecular Ecology 17: 1293–1303. <https://doi.org/10.1111/j.1365-294X.2007.03668.x>
- Audzijonyte A, Daneliya ME, Vainola R (2006) Comparative phylogeography of Ponto-Caspian mysid crustaceans: isolation and exchange among dynamic inland sea basins. Molecular Ecology 15: 2969–2984. <https://doi.org/10.1111/j.1365-294X.2006.03018.x>
- Audzijonyte A, Wittmann KJ, Ovcarenko I, Vainola R (2009) Invasion phylogeography of the Ponto-Caspian crustacean *Limnomysis benedeni* dispersing across Europe. Diversity and Distributions 15: 346–355. <https://doi.org/10.1111/j.1472-4642.2008.00541.x>
- Audzijonyte A, Wittmann KJ, Vainola R (2008) Tracing recent invasions of the Ponto-Caspian mysid shrimp *Hemimysis anomala* across Europe and to North America with mitochon-

- drial DNA. *Diversity and Distributions* 14: 179–186. <https://doi.org/10.1111/j.1472-4642.2007.00434.x>
- Bacela K, Konopacka A, Grabowski M (2009) Reproductive biology of *Dikerogammarus haemobaphes* – an invasive gammarid (Crustacea: Amphipoda) colonizing running waters in Central Europe. *Biological Invasions* 11: 2055–2066. <https://doi.org/10.1007/s10530-009-9496-2>
- Bacela-Spychalska K (2016) Attachment ability of two Ponto-Caspian amphipod species may promote their overland transport. *Aquatic Conservation: Marine & Freshwater Ecosystems* 26: 196–201. <https://doi.org/10.1002/aqc.2565>
- Bacela-Spychalska K, Grabowski M, Rewicz T, Konopacka A, Wattier R (2013) The ‘killer shrimp’ *Dikerogammarus villosus* (Crustacea, Amphipoda) invading Alpine lakes: overland transport by recreational boats and scuba-diving gear as potential entry vectors? *Aquatic Conservation: Marine and Freshwater Ecosystems* 23: 606–618. <https://doi.org/10.1002/aqc.2329>
- Bacela-Spychalska K, Van der Velde G (2013) There is more than one ‘killer shrimp’: trophic positions and predatory abilities of invasive amphipods of Ponto-Caspian origin. *Freshwater Biology* 58: 730–741. <https://doi.org/10.1111/fwb.12078>
- Badertscher S, Fleitmann D, Cheng H, Edwards RL, Göktürk OM, Zumbüh A, Leuenberger M, Tüysüz O (2011) Pleistocene water intrusions from the Mediterranean and Caspian seas into the Black Sea. *Nature Geoscience* 4: 236–239. <https://doi.org/10.1038/ngeo1106>
- Barnard JL, Barnard CM (1983) *Freshwater Amphipoda of the world*. Hayfield Association, Mt. Vernon, Virginia, 830 pp.
- Berezina N (2007) Invasions of alien amphipods (Amphipoda: Gammaridea) in aquatic ecosystems of North-Western Russia: pathways and consequences. *Hydrobiologia* 590: 15–29. <https://doi.org/10.1007/s10750-007-0753-z>
- Bernauer D, Jansen W (2006) Recent invasions of alien macroinvertebrates and loss of native species in the upper Rhine River, Germany. *Aquatic Invasions* 1: 55–71. <https://doi.org/10.3391/ai.2006.1.2.2>
- Bij de Vaate A, Jazdzewska K, Ketelaars HAM, Gollasch S, Van der Velde G (2002) Geographical patterns in range extension of Ponto-Caspian macroinvertebrate species in Europe. *Canadian Journal of Fisheries and Aquatic Sciences* 59: 1159–1174. <https://doi.org/10.1139/f02-098>
- Bock DG, MacIsaac HJ, Cristescu ME (2012) Multilocus genetic analyses differentiate between widespread and spatially restricted cryptic species in a model ascidian. *Proceedings of the Royal Society B* 279: 2377–2385. <https://doi.org/10.1098/rspb.2011.2610>
- Borza P, Csányi B, Huber T, Leitner P, Paunović M, Remund N, Graf W (2015) Longitudinal distributional patterns of Peracarida (Crustacea, Malacostraca) in the River Danube. *Fundamental and Applied Limnology* 187: 113–126. <https://doi.org/10.1127/fal/2015/0769>
- Borza P, Huber T, Leitner P, Remund N, Graf W (2017) Current velocity shapes co-existence patterns among invasive *Dikerogammarus* species. *Freshwater Biology* 62: 317–328. <https://doi.org/10.1111/fwb.12869>
- Borza P, Huber T, Leitner P, Remund N, Graf W (2018) How to coexist with the ‘killer shrimp’ *Dikerogammarus villosus*? Lessons from other invasive Ponto-Caspian peracarids. *Aquatic Conservation: Marine and Freshwater Ecosystems* 28(6): 1441–1450. <https://doi.org/10.1002/aqc.2985>

- Bouckaert R, Heled J, Kühnert D, Vaughan T, Wu CH, Xie D, Suchard MA, Rambaut A, Drummond AJ (2014) BEAST 2: a software platform for Bayesian evolutionary analysis. *PLoS Computational Biology* 10(4): e1003537. <https://doi.org/10.1371/journal.pcbi.1003537>
- Bouckaert RR, Drummond AJ (2017) bModelTest: Bayesian phylogenetic site model averaging and model comparison. *BMC Evolutionary Biology* 17(1): 1–42. <https://doi.org/10.1186/s12862-017-0890-6>
- Brown JE, Stepien CA (2009) Invasion genetics of the Eurasian round goby in North America: tracing sources and spread patterns. *Molecular Ecology* 18: 64–79. <https://doi.org/10.1111/j.1365-294X.2008.04014.x>
- Brown JE, Stepien CA (2010) Population genetic history of the dreissenid mussel invasions: expansion patterns across North America. *Biological Invasions* 12: 3687–3710. <https://doi.org/10.1007/s10530-010-9763-2>
- Cabezas MP, Xavier R, Branco M, Santos AM, Guerra-García JM (2014) Invasion history of *Caprella scaura* Templeton, 1836 (Amphipoda: Caprellidae) in the Iberian Peninsula: multiple introductions revealed by mitochondrial sequence data. *Biological Invasions* 16: 2221–2245. <https://doi.org/10.1007/s10530-014-0660-y>
- Caraușu S (1943) Amphipodes de Roumanie. I. Gammaridés de type Caspien. *Insstitutul de Cercetari Piscicole al Romaniei, Bucuresti*, 293 pp.
- Caraușu S, Dobreanu E, Manolache C (1955) Amphipoda Forme Salmastre si de Apa Dulce. *Fauna Republicii Populare Romine, Bucuresti*, 409 pp. [in Romanian]
- Carlton JT (2011) The global dispersal of marine and estuarine crustaceans. In: Galil BS, Clark PF, Carlton JT (Eds) *In the wrong place – alien marine crustaceans: distribution, biology and impacts*. Springer, Dordrecht, Heidelberg, London, New York, 3–23. https://doi.org/10.1007/978-94-007-0591-3_1
- Chen W, Bierbach D, Plath M, Streit B, Klaus S (2012) Distribution of amphipod communities in the Middle to Upper Rhine and five of its tributaries. *BioInvasions Records* 1: 263–271. <https://doi.org/10.3391/bir.2012.1.4.04>
- Chenna R, Sugawara H, Koike T, Lopez R, Gibson TJ, Higgins DG, Thompson JD (2003) Multiple sequence alignment with the Clustal series of programs. *Nucleic Acids Research* 31: 3497–3500. <https://doi.org/10.1093/nar/gkg500>
- Constable D, Birkby NJ (2016) The impact of the invasive amphipod *Dikerogammarus haemobaphes* on leaf litter processing in UK rivers. *Aquatic Ecology* 50: 273–281. <https://doi.org/10.1007/s10452-016-9574-3>
- Copilaș-Ciocianu D, Sidorov D, Gontcharov A (2019) Adrift across tectonic plates: molecular phylogenetics supports the ancient Laurasian origin of old limnic crangonyctid amphipods. *Organisms Diversity & Evolution* 19: 191–207. <https://doi.org/10.1007/s13127-019-00401-7>
- Costa FO, DeWaard JR, Boutillier J, Ratnasingham S, Dooh RT, Hajibabaei M, Hebert PDN (2007) Biological identifications through DNA barcodes: the case of the Crustacea. *Canadian Journal of Fisheries and Aquatic Sciences* 64: 272–295. <https://doi.org/10.1139/f07-008>
- Costa FO, Henzler CM, Lunt DH, Whiteley NM, Rock J (2009) Probing marine *Gammarus* (Amphipoda) taxonomy with DNA barcodes. *Systematics and Biodiversity* 7: 365–379. <https://doi.org/10.1017/S1477200009990120>

- Cristescu MEA, Hebert PDN (2005) The “Crustacean Seas” – an evolutionary perspective on the Ponto-Caspian peracarids. *Canadian Journal of Fisheries and Aquatic Sciences* 62: 505–517. <https://doi.org/10.1139/f04-210>
- Cristescu MEA, Hebert PDN, Onciu TM (2003) Phylogeography of Ponto-Caspian crustaceans: a benthic-planktonic comparison. *Molecular Ecology* 12: 985–996. <https://doi.org/10.1046/j.1365-294X.2003.01801.x>
- Cristescu MEA, Witt JDS, Grigorovich IA, Hebert PDN, MacIsaac HJ (2004) Dispersal of the Ponto-Caspian amphipod *Echinogammarus ischnus*: invasion waves from the Pleistocene to the present. *Heredity* 92: 197–203. <https://doi.org/10.1038/sj.hdy.6800395>
- Ćuk R, Milisa M, Atanacković A, Dekić S, Blažeković L, Žganec K (2019) Biocontamination of benthic macroinvertebrate assemblages in Croatian major rivers and effects on ecological quality assessment. *Knowledge and Management of Aquatic Ecosystems* 420: 1–11. <https://doi.org/10.1051/kmae/2019003>
- DAISIE (2009) *Handbook of Alien Species in Europe*. Springer, Dordrecht, 399 pp.
- Dick JTA, Platvoet D, Kelly DW (2002) Predatory impact of the freshwater invader *Dikergammarus villosus* (Crustacea: Amphipoda). *Canadian Journal of Fisheries and Aquatic Sciences* 59: 1078–1084. <https://doi.org/10.1139/f02-074>
- Dittell AI, Epifanio CE (2009) Invasion biology of the Chinese mitten crab *Eriocheir sinensis*: A brief review. *Journal of Experimental Marine Biology and Ecology* 374: 79–92. <https://doi.org/10.1016/j.jembe.2009.04.012>
- Drummond AJ, Suchard MA, Xie D, Rambaut A (2012) Bayesian Phylogenetics with BEAUti and the BEAST 1.7. *Molecular Biology and Evolution* 29: 1969–1973. <https://doi.org/10.1093/molbev/mss075>
- Dumont HJ (2000) Endemism in the Ponto-Caspian fauna, with special emphasis on the Onychopoda (Crustacea). *Advances in Ecological Research* 31: 181–196. [https://doi.org/10.1016/S0065-2504\(00\)31012-1](https://doi.org/10.1016/S0065-2504(00)31012-1)
- Estoup A, Guillemaud T (2010) Reconstructing routes of invasion using genetic data: why, how and so what? *Molecular Ecology* 19: 4113–4130. <https://doi.org/10.1111/j.1365-294X.2010.04773.x>
- Etxabe AG, Short S, Flood T, Johns T, Ford AT (2015) Pronounced and prevalent intersexuality does not impede the “Demon Shrimp” invasion. *PeerJ* 3: e757. <https://doi.org/10.7717/peerj.757>
- Excoffier L, Lischer HEL (2010) Arlequin suite ver 3.5: a new series of programs to perform population genetics analyses under Linux and Windows. *Molecular Ecology Resources* 10: 564–567. <https://doi.org/10.1111/j.1755-0998.2010.02847.x>
- Ezard T, Fujisawa T, Barraclough TG (2009) Splits: species’ limits by threshold statistics. R package version, 1(11): r29.
- Filipová L, Lieb DA, Grandjean F, Petrusek A (2011) Haplotype variation in the spiny-cheek crayfish *Orconectes limosus*: colonization of Europe and genetic diversity of native stocks. *Journal of the North American Benthological Society* 30: 871–881. <https://doi.org/10.1899/10-130.1>
- Folino-Rorem NC, Darling JA, D’Ausilio CA (2009) Genetic analysis reveals multiple cryptic invasive species of the hydrozoan genus *Cordylophora*. *Biological Invasions* 11: 1869–1882. <https://doi.org/10.1007/s10530-008-9365-4>

- Folmer OM, Black WH, Lutz R, Vrijenhoek R (1994) DNA primers for amplification of mitochondrial cytochrome *c* oxidase subunit I from metazoan invertebrates. *Molecular Marine Biology and Biotechnology* 3: 294–299.
- Fu Y-X (1997) Statistical tests of neutrality of mutations against population growth, hitchhiking, and background selection. *Genetics* 147: 915–925. <https://www.genetics.org/content/147/2/915.short>
- Geller JB, Walton ED, Grosholz ED, Ruiz GM (1997) Cryptic invasions of the crab *Carcinus* detected by molecular phylogeography. *Molecular Ecology* 6(10): 901–906. <https://doi.org/10.1046/j.1365-294X.1997.00256.x>
- Gherardi F (2007) Biological invasions in inland waters: an overview. In: Gherardi F (Ed.) *Biological Invaders in Inland Waters: Profiles, Distribution, and Threats*. Springer, Dordrecht, 3–25. https://doi.org/10.1007/978-1-4020-6029-8_1
- Grabowski M, Bącela K, Konopacka A (2007a) How to be an invasive gammarid (Amphipoda: Gammaroidea) – comparison of life history traits. *Hydrobiologia* 590: 75–84. <https://doi.org/10.1007/s10750-007-0759-6>
- Grabowski M, Jazdzewski K, Konopacka A (2007b) Alien Crustacea in Polish waters – Amphipoda. *Aquatic Invasions* 2: 25–38. <https://doi.org/10.3391/ai.2007.2.1.3>
- Grabowski M, Mamos T, Bącela-Spychalska K, Rewicz T, Wattier RA (2017) Neogene paleogeography provides context for understanding the origin and spatial distribution of cryptic diversity in a widespread Balkan freshwater amphipod. *PeerJ* 5: e3016. <https://doi.org/10.7717/peerj.3016>
- Grabowski M, Rewicz T, Bacela-Spychalska K, Konopacka A, Mamos T, Jazdzewski K (2012) Cryptic invasion of Baltic lowlands by freshwater amphipod of Pontic origin. *Aquatic Invasions* 7: 337–346. <https://doi.org/10.3391/ai.2012.7.3.005>
- Hayer S, Brandis D, Hartl GB, Ewers-Saucedo C (2019) First indication of Japanese mitten crabs in Europe and cryptic genetic diversity of invasive Chinese mitten crabs. *Neobiota* 50: 1–29. <https://doi.org/10.3897/neobiota.50.34881>
- Hebert PDN, Cywinska A, Ball SL, deWaard JR (2003) Biological identifications through DNA barcodes. *Proceedings of the Royal Society B-Biological Sciences* 270: 313–321. <https://doi.org/10.1098/rspb.2002.2218>
- Heled J, Drummond AJ (2008) Bayesian inference of population size history from multiple loci. *BMC Evolutionary Biology* 8: 1–289. <https://doi.org/10.1186/1471-2148-8-345>
- Hellmann C, Schöll F, Worischka S, Becker J, Winkelmann C (2017) River-specific effects of the invasive amphipod *Dikerogammarus villosus* (Crustacea: Amphipoda) on benthic communities. *Biological Invasions* 19: 381–398. <https://doi.org/10.1007/s10530-016-1286-z>
- Hewitt GM (2004) Genetic consequences of climatic changes in the Quaternary. *Philosophical Transactions of the Royal Society B* 359: 183–195. <https://doi.org/10.1098/rstb.2003.1388>
- Hillis DM, Mable BK, Moritz C (1996) Applications of molecular systematics. In: Hillis DM, Moritz C, Mable B (Eds) *Molecular Systematics*. Sunderland: Sinauer Associates, Massachusetts, 515–543. <https://doi.org/10.2307/1447682>
- Holdich DM, Pöckl M (2007) Invasive crustaceans in European inland waters. In: Gherardi F (Ed.) *Biological Invaders in Inland Waters: Profiles, Distribution, and Threats*. Springer, Dordrecht, 29–75. https://doi.org/10.1007/978-1-4020-6029-8_2

- Hou ZG, Fu JH, Li SQ (2007) A molecular phylogeny of the genus *Gammarus* (Crustacea: Amphipoda) based on mitochondrial and nuclear gene sequences. *Molecular Phylogenetics and Evolution* 45: 596–611. <https://doi.org/10.1016/j.ympev.2007.06.006>
- Jazdzewski K (1980) Range extensions of some gammaridean species in European inland waters caused by human activity. *Crustaceana Supplement* 6: 84–107. <https://www.jstor.org/stable/25027516>
- Jazdzewski K (2003) An invasive Ponto-Caspian amphipod – *Dikerogammarus haemobaphes* (Eichwald, 1841) – conquers Great Masurian Lakes, north-eastern Poland. *Fragmenta Faunistica* 46: 19–25. <https://doi.org/10.3161/00159301FF2003.46.1.019>
- Jazdzewski K, Konopacka A (1988) Notes on the gammaridean Amphipoda of the Dniester River basin and Eastern Carpathians. *Crustaceana Supplement* 13: 72–89. <https://www.jstor.org/stable/25027753>
- Johns T, Smith DC, Homann S, England JA (2018) Time-series analysis of a native and a non-native amphipod shrimp in two English rivers. *BioInvasions Record* 7: 101–110. <https://doi.org/10.3391/bir.2018.7.2.01>
- Kalinowski ST (2005) HP-RARE 1.0: a computer program for performing rarefaction on measures of allelic richness. *Molecular Ecology Notes* 5: 187–189. <https://doi.org/10.1111/j.1471-8286.2004.00845.x>
- Karpevich AF (1975) *Theory and Practice of Acclimatization of Aquatic Organisms*. Pishchevaya Promyshlennost, Moscow. [In Russian]
- Katouzian AR, Macher JN, Weiss M, Saboori A, Leese F, Weigand AM (2016) Drastic underestimation of amphipod biodiversity in the endangered Irano-Anatolian and Caucasus biodiversity hotspots. *Scientific Reports* 6: e22507. <https://doi.org/10.1038/srep22507>
- Kelly DW, Muirhead JR, Heath DD, MacIsaac HJ (2006) Contrasting patterns in genetic diversity following multiple invasions of fresh and brackish waters. *Molecular Ecology* 15: 3641–3655. <https://doi.org/10.1111/j.1365-294X.2006.03012.x>
- Kimura M (1980) A simple method for estimating evolutionary rates of base substitutions through comparative studies of nucleotide sequences. *Journal of Molecular Evolution* 16: 111–120. <https://doi.org/10.1007/BF01731581>
- Kley A, Maier G (2006) Reproductive characteristics of invasive gammarids in the Rhine-Main-Danube catchment, South Germany. *Limnologica* 36(2): 79–90. <https://doi.org/10.1016/j.limno.2006.01.002>
- Kobak J, Rachalewski M, Baćela-Spychalska K (2016) Conquerors or exiles? Impact of interference competition among invasive Ponto-Caspian gammarideans on their dispersal rates. *Biological Invasions* 18: 1953–1965. <https://doi.org/10.1007/s10530-016-1140-3>
- Konopacka A (1998) Nowy dla Polski gatunek kielża, *Dikerogammarus haemobaphes* (Eichwald, 1841) (Crustacea, Amphipoda), oraz dwa inne rzadkie gatunki skorupiaków obunogich w Wiśle. *Przegląd Zoologiczny* 42(3–4): 211–218. [In Polish]
- Kumar S, Stecher G, Li M, Knyaz C, Tamura K (2018) MEGA X: Molecular Evolutionary Genetics Analysis across computing platforms. *Molecular Biology and Evolution* 35: 1547–1549. <https://doi.org/10.1093/molbev/msy096>
- Labat F, Piscart C, Fontan B (2011) First records, pathways and distributions of four new Ponto-Caspian amphipods in France. *Limnologica* 41: 290–295. <https://doi.org/10.1016/j.limno.2010.12.004>

- Lagrué C, Wattier R, Galipaud M, Gauthey Z, Rullmann J-P, Dubreuil C, Rigaud T, Bollache L (2014) Confrontation of cryptic diversity and mate discrimination within *Gammarus pulex* and *Gammarus fossarum* species complexes. *Freshwater Biology* 59: 2555–2570. <https://doi.org/10.1111/fwb.12453>
- Leberg PL (2002) Estimating allelic richness: Effects of sample size and bottlenecks. *Molecular Ecology* 11: 2445–2449. <https://doi.org/10.1046/j.1365-294X.2002.01612.x>
- LeRoux PC, McGeoch MA (2008) Rapid range expansion and community reorganization in response to warming. *Global Change Biology* 14: 2950–2962. <https://doi.org/10.1111/j.1365-2486.2008.01687.x>
- Librado P, Rozas J (2009) DnaSP v5: a software for comprehensive analysis of DNA polymorphism data. *Bioinformatics* 25: 1451–1452. <https://doi.org/10.1093/bioinformatics/btp187>
- Lobo J, Ferreira MS, Antunes IC, Teixeira MAL, Borges LMS, Sousa R, Gomes PA, Costa MH, Cunha MR, Costa FO (2017) Contrasting morphological and DNA barcode-suggested species boundaries among shallow-water amphipod fauna from the southern European Atlantic coast. *Genome* 60: 147–157. <https://doi.org/10.1139/gen-2016-0009>
- Lvova AA, Paliy AV, Sokolova NY (1996) Ponto-Caspian immigrants in the Moscow River within Moscow City. *Zoologicheskii Zhurnal* 75: 1273–1274.
- Mamos T, Wattier R, Burzyński A, Grabowski M (2016) The legacy of a vanished sea: a high level of diversification within a European freshwater amphipod species complex driven by 15 My of Paratethys regression. *Molecular Ecology* 3: 795–810. <https://doi.org/10.1111/mec.13499>
- Martynov AM (1919) About Malacostraca on the vicinity of the Rostov-on-Don. *Protocol zasedania Obschestva Estestvoznania Donskogo Universiteta, Rostov-on-Don*, 41–47. [in Russian]
- Mauvisseau Q, Davy-Bowker J, Bryson D, Souch GR, Burian A, Sweet M (2019) First detection of a highly invasive freshwater amphipod *Crangonyx floridanus* (Bousfield, 1963) in the United Kingdom. *BioInvasions Records* 8: 1–7. <https://doi.org/10.3391/bir.2019.8.1.01>
- Minchin D, Arbačiauskas K, Daunys D, Ezhova E, Grudule N, Kotta J, Molchanova N, Olenin S, Višinskienė G, Strake S (2019) Rapid expansion and facilitating factors of the Ponto-Caspian invader *Dikerogammarus villosus* within the eastern Baltic Sea. *Aquatic Invasions* 14: 165–181. <https://doi.org/10.3391/ai.2019.14.2.02>
- Monaghan MT, Wild R, Elliot M, Fujisawa T, Balke M, Inward DJ, Lees DC, Ranaivosolo R, Eggleton P, Barraclough TG, Vogler AP (2009) Accelerated species inventory on Madagascar using coalescent-based models of species delineation. *Systematic Biology* 58: 298–311. <https://doi.org/10.1093/sysbio/syp027>
- Mordukhai-Boltovskoi FD (1964) Caspian fauna beyond the Caspian Sea. *International Review of Hydrobiology and Hydrography* 49: 139–176. <https://doi.org/10.1002/iroh.19640490105>
- Müller JC, Schramm S, Seitz A (2002) Genetic and morphological differentiation of *Dikerogammarus* invaders and their invasion history in Central Europe. *Freshwater Biology* 47: 2039–2048. <https://doi.org/10.1046/j.1365-2427.2002.00944.x>
- Muskó IB (1992) Amphipoda species found in Lake Balaton since 1987. *Miscellanea Zoologica Hungarica* 7: 59–64.

- Muskó IB, Balogh CS, Tóth ÁP, Varga É, Lakatos GV (2007) Differential response of invasive malacostracan species to lake level fluctuations. *Hydrobiologia* 590: 65–74. <https://doi.org/10.1007/s10750-007-0758-7>
- Nagakubo A, Sekine K, Tanaka Y, Kuranishi RB, Kanada S, Tojo K (2011) Rapid expansion of the distributional range and the population genetic structure of the freshwater amphipod *Crangonyx floridanus* in Japan. *Limnology* 12: 75–82. <https://doi.org/10.1007/s10201-010-0323-3>
- Nahavandi N, Ketmaier V, Plath M, Tiedemann R (2013) Diversification of Ponto-Caspian aquatic fauna: Morphology and molecules retrieve congruent evolutionary relationships in *Pontogammarus maeoticus* (Amphipoda: Pontogammaridae). *Molecular Phylogenetics and Evolution* 69: 1063–1076. <https://doi.org/10.1016/j.ympev.2013.05.021>
- Neilson ME, Stepien CA (2011) Historic speciation and recent colonization of Eurasian monkey gobies (*Neogobius fluviatilis* and *N. pallasii*) revealed by DNA sequences, microsatellites, and morphology. *Diversity and Distributions* 17: 688–702. <https://doi.org/10.1111/j.1472-4642.2011.00762.x>
- Ott J (2010) Dragonflies and climatic changes - recent trends in Germany and Europe. In: Ott J (Ed.) *Monitoring Climatic Change With Dragonflies*. *BioRisk* 5: 253–286. <https://doi.org/10.3897/biorisk.5.857>
- Özbek M, Özkan N (2011) *Dikerogammarus istanbulensis* sp. n., a new amphipod species (Amphipoda: Gammaridae) from Turkey with a key for the genus. *Zootaxa* 2813: 55–64. <https://doi.org/10.11646/zootaxa.2813.1.2>
- Parmesan C (2006) Ecological and evolutionary responses to recent climate change. *Annual Review of Ecology, Evolution, and Systematics* 37: 637–669. <https://doi.org/10.1146/annurev.ecolsys.37.091305.110100>
- Pjatakova GM, Tarasov AG (1996) Caspian Sea amphipods: biodiversity, systematic position and ecological peculiarities of some species. *Journal of Salt Lake Research* 5: 63–79. <https://doi.org/10.1007/BF01996036>
- Pons J, Barraclough TG, Gomez-Zurita J, Cardoso A, Duran DP, Hazell S, Kamoun S, Sumlin WD, Vogler AP (2006) Sequence-based species delimitation for the DNA taxonomy of undescribed insects. *Systematic Biology* 55: 595–609. <https://doi.org/10.1080/10635150600852011>
- Puillandre N, Lambert A, Brouillet S, Achaz G (2012) ABGD, Automatic Barcode Gap Discovery for primary species delimitation. *Molecular Ecology* 21: 1864–1877. <https://doi.org/10.1111/j.1365-294X.2011.05239.x>
- Ratnasingham S, Hebert PDN (2007) The Barcode of Life Data System. (<http://www.barcodinglife.org>). *Molecular Ecology Resources* 7: 355–364. <https://doi.org/10.1111/j.1471-8286.2007.01678.x>
- Ratnasingham S, Hebert PDN (2013) A DNA-Based Registry for All Animal Species: The Barcode Index Number (BIN) System. *PLoS ONE* 8: e66213. <https://doi.org/10.1371/journal.pone.0066213>
- Raupach MJ, Barco A, Steinke D, Beermann J, Laakmann S, Mohrbeck I, Neumann H, Kihara TC, Pointner K, Radulovici A, Segelken-Voigt A, Wesse C, Knebelberger T (2015) The application of DNA barcodes for the identification of marine crustaceans from the North Sea and adjacent regions. *PLoS ONE* 10: 1–23. <https://doi.org/10.1371/journal.pone.0139421>

- Raymond M, Rousset F (1995) Genepop (Version-1.2) – Population-Genetics Software for Exact Tests and Ecumenicism. *Journal of Heredity* 86: 248–249. <https://doi.org/10.1093/oxfordjournals.jhered.a111573>
- R Core Team (2013) R: A language and environment for statistical computing. R Foundation for Statistical Computing, Vienna. <http://www.R-project.org>
- Reuschel S, Cuesta JA, Schubart CD (2010) Marine biogeographic boundaries and human introduction along the European coast revealed by phylogeography of the prawn *Palaemon elegans*. *Molecular Phylogenetics and Evolution* 55(3): 765–775. <https://doi.org/10.1016/j.ympev.2010.03.021>
- Rewicz T, Grabowski M, Tończyk G, Konopacka A, Bącela-Spychalska K (2019) *Gammarus tigrinus* Sexton, 1939 continues its invasion in the Baltic Sea: first record from Bornholm (Denmark). *BioInvasions Records* 8: 862–870. <https://doi.org/10.3391/bir.2019.8.4.14>
- Rewicz T, Wattier R, Grabowski M, Rigaud T, Bącela-Spychalska K (2015) Out of the Black Sea: Phylogeography of the Invasive Killer Shrimp *Dikerogammarus villosus* across Europe. *PLoS ONE* 10(2): e0118121. <https://doi.org/10.1371/journal.pone.0118121>
- Ricciardi A, MacIsaac HJ (2000) Recent mass invasion of the North American Great Lakes by Ponto-Caspian species. *Trends in Ecology and Evolution* 15(2): 62–65. [https://doi.org/10.1016/S0169-5347\(99\)01745-0](https://doi.org/10.1016/S0169-5347(99)01745-0)
- Ricciardi A, MacIsaac HJ (2011) Impacts of biological invasions on freshwater ecosystems. In: Richardson DM (Ed.) *Fifty Years of Invasion Ecology: The Legacy of Charles Elton*. Wiley-Blackwell: 211–224. <https://doi.org/10.1002/9781444329988.ch16>
- Roman J, Darling JA (2007) Paradox lost: genetic diversity and the success of aquatic invasions. *Trends in Ecology and Evolution* 22: 455–464. <https://doi.org/10.1016/j.tree.2007.07.002>
- Rousset F (1997) Genetic differentiation and estimation of gene flow from F-statistics under isolation by distance. *Genetics* 145: 1219–1228.
- Saitou N, Nei M (1987) The neighbour-joining method: A new method for constructing phylogenetic trees. *Molecular Biology and Evolution* 4: 406–425. <https://doi.org/10.1093/oxfordjournals.molbev.a040454>
- Sars GO (1894) Crustacea caspia. Contributions to the knowledge of the Carcinological Fauna of the Caspian Sea. Part III. Amphipoda. Gammarida. *Bulletin de l'Academie Imperiale des Sciences de St.-Petersbourg* 5(1): 179–223. [343–378] <https://doi.org/10.5962/bhl.title.10631>
- Schleuter M, Schleuter A, Potel S, Banning M (1994) *Dikerogammarus haemobaphes* (Eichwald 1841) (Gammaridae) aus der Donau erreicht über den Main-Donau-Kanal den Main. *Lauterbornia* 19: 155–159.
- Schöll F, Becker C, Tittizer T (1995) Das Makrozoobenthos des schiffbaren Rheins von Basel bis Emmerich 1986–1995. *Lauterbornia* 21: 115–137.
- Slynko YuV, Korneva LG, Rivier IK, Shcherbina KH, Papchenkov VG, Orlova MI, Therriault TW (2002) Caspian-Volga-Baltic invasion corridor. In: Leppäkoski E, Gollasch S, Olenin S (Eds) *Invasive Aquatic Species of Europe. Distribution, Impacts and Management*. Kluwer Academic Publishers, Dordrecht, 399–411. https://doi.org/10.1007/978-94-015-9956-6_40
- Snyder RJ, Burlakova LE, Karatayev AY, MacNeill DB (2014) Updated invasion risk assessment for Ponto-Caspian fishes to the Great Lakes. *Journal of the Great Lakes Research* 40: 360–369. <https://doi.org/10.1016/j.jglr.2014.03.009>

- Stepien CA, Brown JE, Neilson ME, Tumeo MA (2005) Genetic diversity of invasive species in the Great Lakes versus their Eurasian source populations: Insights for risk analysis. *Risk Analysis* 25: 1043–1060. <https://doi.org/10.1111/j.1539-6924.2005.00655.x>
- Stoica M, Lazăr I, Krijgsman W, Vasiliev I, Jipa D, Floroiu A (2013) Paleoenvironmental evolution of the East Carpathian foredeep during the late Miocene-early Pliocene (Dacian Basin; Romania). *Global and Planetary Change* 103: 135–148. <https://doi.org/10.1016/j.gloplacha.2012.04.004>
- Straškraba M (1962) Amphipoden der Tschechoslowakei nach den Sammlungen von Prof. Hrabě. *Acta Societatis Zoologicae Bohemoslovenicae* 26: 117–145.
- Strayer DL (2012) Eight questions about invasions and ecosystem functioning. *Ecology Letters* 15: 1199–1210. <https://doi.org/10.1111/j.1461-0248.2012.01817.x>
- Svitoch AA, Selivanov AO, Yanina TA (2000) Paleohydrology of the Black Sea Pleistocene Basins. *Water Resources* 27: 594–603. <https://doi.org/10.1023/A:1026661801941>
- Taberlet P, Fumagalli L, Wust-Saucy AG, Cossons J-F (1998) Comparative phylogeography and postglacial colonization routes in Europe. *Molecular Ecology* 7: 453–464. <https://doi.org/10.1046/j.1365-294x.1998.00289.x>
- Tajima F (1989) Statistical method for testing the neutral mutation hypothesis by DNA polymorphism. *Genetics* 123: 585–595. <https://www.ncbi.nlm.nih.gov/pmc/articles/PMC1203831/>
- Tamura K (1992) Estimation of the number of nucleotide substitutions when there are strong transition-transversion and G + C-content biases. *Molecular Biology and Evolution* 9: 678–687. <https://doi.org/10.1093/oxfordjournals.molbev.a040752>
- Wattier RA, Haine ER, Beguet J, Martin G, Bollache L, Musko IB, Platvoet D, Rigaud T (2007) No genetic bottleneck or associated microparasite loss in invasive populations of freshwater amphipod. *Oikos* 116: 1941–1953. <https://doi.org/10.1111/j.0030-1299.2007.15921.x>
- Weinzierl A, Potel S, Banning M (1996) *Obesogammarus obesus* (SARS 1894) in der oberen Donau (Amphipoda, Gammaridae). *Lauterbornia* 26: 87–91.
- Weiss M, Macher JN, Seefeldt MA, Leese F (2014) Molecular evidence for further overlooked species within the *Gammarus fossarum* complex (Crustacea: Amphipoda). *Hydrobiologia* 721: 165–184. <https://doi.org/10.1007/s10750-013-1658-7>
- Zhadin VI (1964) Higher crustaceans of the Oka River collected in 1959. *Trudy Zoologicheskogo Instituta* 32: 149–154. [in Russian]
- Zhang J, Kapli P, Pavlidis P, Stamatakis A (2013) A general species delimitation method with applications to phylogenetic placements. *Bioinformatics* 29: 2869–2876. <https://doi.org/10.1093/bioinformatics/btt499>

Supplementary material 1

Table S1

Authors: Anna Maria Jążdżewska, Tomasz Rewicz, Tomasz Mamos, Remi Wattier, Karolina Bącela-Spychalska, Michał Grabowski

Data type: calculations

Explanation note: Molecular diversity measures calculated for the populations in the native range (mostly Dnieper River) (N) and along the invasion corridor (I, Central Corridor) of *Dikerogammarus haemobaphes*.

Copyright notice: This dataset is made available under the Open Database License (<http://opendatacommons.org/licenses/odbl/1.0/>). The Open Database License (ODbL) is a license agreement intended to allow users to freely share, modify, and use this Dataset while maintaining this same freedom for others, provided that the original source and author(s) are credited.

Link: <https://doi.org/10.3897/neobiota.57.46699.suppl1>

Supplementary material 2

Table S2

Authors: Anna Maria Jążdżewska, Tomasz Rewicz, Tomasz Mamos, Remi Wattier, Karolina Bącela-Spychalska, Michał Grabowski

Data type: GenBank data

Explanation note: GenBank accession numbers for all three studied genes and the presentation of haplotypes recognized for 16S, COI and concatenated data.

Copyright notice: This dataset is made available under the Open Database License (<http://opendatacommons.org/licenses/odbl/1.0/>). The Open Database License (ODbL) is a license agreement intended to allow users to freely share, modify, and use this Dataset while maintaining this same freedom for others, provided that the original source and author(s) are credited.

Link: <https://doi.org/10.3897/neobiota.57.46699.suppl2>

Supplementary material 3**Table S3**

Authors: Anna Maria Jażdżewska, Tomasz Rewicz, Tomasz Mamos, Remi Wattier, Karolina Bącela-Spychalska, Michał Grabowski

Data type: distribution

Explanation note: The distribution of recognized haplotypes (concatenated 16S and COI sequences).

Copyright notice: This dataset is made available under the Open Database License (<http://opendatacommons.org/licenses/odbl/1.0/>). The Open Database License (ODbL) is a license agreement intended to allow users to freely share, modify, and use this Dataset while maintaining this same freedom for others, provided that the original source and author(s) are credited.

Link: <https://doi.org/10.3897/neobiota.57.46699.suppl3>

First insights into the molecular population structure and origins of the invasive Chinese sleeper, *Percottus glenii*, in Europe

Joanna Grabowska¹, Yuriy Kvach^{2,3}, Tomasz Rewicz^{4,5}, Mihails Pupins⁶,
Iuliia Kutsokon⁷, Ihor Dykyy⁸, Laszlo Antal⁹, Grzegorz Zięba¹,
Vytautas Rakauskas¹⁰, Teodora Trichkova¹¹, Andris Čeirāns⁶, Michał Grabowski⁴

1 University of Lodz, Faculty of Biology and Environmental Protection, Department of Ecology and Vertebrate Zoology, Łódź, Poland **2** Institute of Marine Biology of the NAS of Ukraine, Odessa, Ukraine **3** Institute of Vertebrate Biology of the CAS, Brno, Czech Republic **4** University of Lodz, Faculty of Biology and Environmental Protection, Department of Invertebrate Zoology and Hydrobiology, Łódź, Poland **5** University of Guelph, Centre for Biodiversity Genomics, Guelph, Ontario, Canada **6** Daugavpils University, Institute of Life Sciences and Technologies, Department of Ecology, Daugavpils, Latvia **7** National Academy of Science of Ukraine, Schmalhausen Institute of Zoology, Kyiv, Ukraine **8** Ivan Franko National University of Lviv, Department of Zoology, Lviv, Ukraine **9** University of Debrecen, Department of Hydrobiology, Debrecen, Hungary **10** Nature Research Centre, Laboratory of Fish Ecology, Vilnius, Lithuania **11** Institute of Biodiversity and Ecosystem Research of the BAS, Sofia, Bulgaria

Corresponding author: Joanna Grabowska (joanna.grabowska@biol.uni.lodz.pl)

Academic editor: A. Petrussek | Received 30 November 2019 | Accepted 16 April 2020 | Published 1 June 2020

Citation: Grabowska J, Kvach Yu, Rewicz T, Pupins M, Kutsokon I, Dykyy I, Antal L, Zięba G, Rakauskas V, Trichkova T, Čeirāns A, Grabowski M (2020) First insights into the molecular population structure and origins of the invasive Chinese sleeper, *Percottus glenii*, in Europe. NeoBiota 57: 87–107. <https://doi.org/10.3897/neobiota.57.48958>

Abstract

The aim of our study was to provide a first overview of the population genetic structure of the invasive Chinese sleeper, *Percottus glenii*, (Actinopterygii: Odontobutidae) in European water bodies. This species originates from inland waters of north-eastern China, northern North Korea and the Russian Far East. The 1172 bp long portion of the cytochrome b gene was sequenced from Chinese sleeper specimens collected from a variety of water bodies in Belarus, Bulgaria, Hungary, Germany, Latvia, Lithuania, Poland, Russia (European part) and Ukraine. Our study revealed that the invasive Chinese sleeper in Europe consists of at least three distinct haplogroups that may represent independent introduction events from different parts of its native area; i.e. three founding populations: (1) Baltic haplogroup that may originate either from fish introduced inadvertently from Russia or from some unidentified source (release by aquarists). So far, this haplogroup has been found only in the Daugava basin in Latvia. (2) East-European haplogroup that may

originate from an unintentional introduction to the Volga basin in Russia and has expanded westward. So far, this group was recorded in the Volga, Upper Dnieper and Neman drainages in Belarus, Lithuania, and Russia. (3) Carpathian haplogroup, that originated from individuals unintentionally introduced with Asian cyprinid fishes to Lviv region in Ukraine and are now widely distributed in Central Europe.

Keywords

Amur sleeper, exotic fish, invasion pathways, phylogeography

Introduction

Inland fisheries and fish farming are commercially important activities in many countries, but the associated risk management (such as quarantine control) is usually less rigid than is the case with other taxa (Copp et al. 2005). With increasing globalisation, the number of fish introductions has increased in recent decades, posing ecological and evolutionary threats to biodiversity (Hulme 2009; Vitule et al. 2009; Gozlan et al. 2010; Cucherousset and Olden 2011). The negative influence of alien species on endemic fauna includes predation, food and spatial competition, hybridization, the spread of parasites and pathogens, and modification of food chains (Leunda 2010; Cucherousset and Olden 2011).

The Chinese sleeper, *Percottus glenii* Dybowski, 1877, formerly known as the Amur sleeper, is a successful alien freshwater fish species in European waters, with a high invasive potential (Negring and Steinhof 2015; European Commission 2016). Since its introduction at the beginning of the 20th century, the species has continuously expanded its invasive range in Eurasia (Reshetnikov 2010, 2013; Reshetnikov and Ficetola 2011). The native range of the Chinese sleeper encompasses inland waters of north-eastern China, northern North Korea and the Russian Far East, including the middle and lower stretches of the River Amur with the tributaries Zeya, Sungari, Ussuri as well as the Lake Khanka basin and drainages of the rivers Gou, Liaohe, Never, and Yalu (China, North Korea) (Mori 1936; Bogutskaya and Naseka 2002; Miller and Vasil'eva 2003; Kottelat and Freyhof 2007; Bogutskaya et al. 2008; Reshetnikov 2010). Some introduction events appear noteworthy in the history of the Chinese sleeper invasion in Europe. Specimens were first transported to Saint Petersburg from the River Zeya (Russian Far East) in 1912 (Kuderskiy 1982) by a scientific expedition as ornamental fish and subsequently kept in an aquarium (Nabatov 1914). In 1916 four individuals were released into a garden pond (Fig. 1A), where they founded a population that was reported to eradicate the entire local fish fauna (Dmitriev 1971). During the 1920s, the Chinese sleeper invaded many water bodies around Saint Petersburg (Kuderskiy 1982) and in the 1950s it was recorded in the shallow waters of the Gulf of Finland in the Baltic Sea (Dmitriev 1971).

Another introduction took place in 1950, when ichthyologists from Moscow State University and the Polar Institute of Marine Fisheries and Oceanography (PINRO) transported fish from the Amur River and released them into the Tarakanov and Ostankino ponds in Moscow (Reshetnikov 2004; Reshetnikov and Ficetola 2011) (Fig.

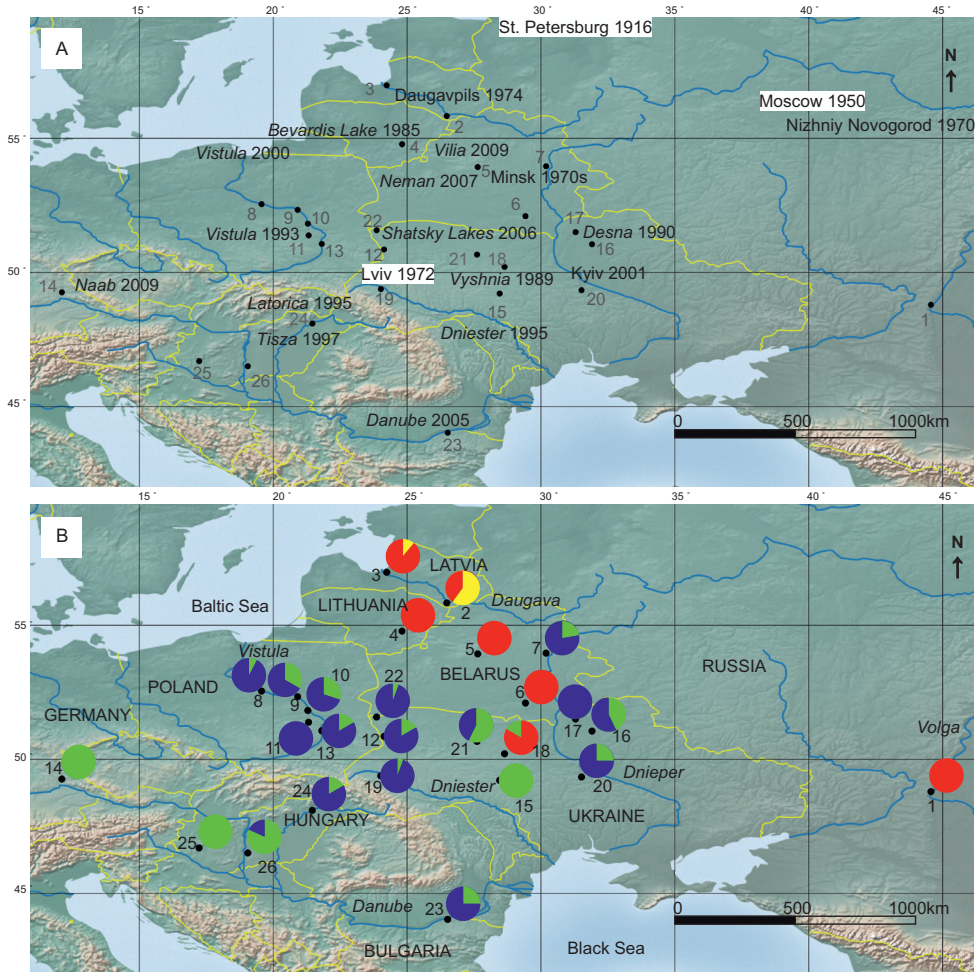


Figure 1. **A** history of the expansion of the Chinese sleeper in Europe (the earliest introduction is indicated and highlighted in white) in relation to the location of sampling sites (sites in close geographic proximity pooled for demographic analyses and assigned the same number) **B** distribution and proportional abundance of Chinese sleeper cytochrome b haplogroups in the study area. Haplogroup I (yellow), haplogroup II (red), haplogroup III (subgroup IIIa – green; subgroup IIIb – blue).

1A). A further invasion of Chinese sleeper is associated with the increasing popularity of Asian cyprinid cultivation in the former Soviet Union from the 1950s to the 1970s. During that time, Chinese sleepers were reported several times from fish ponds after inadvertent introduction with commercial cyprinids. The introductions have facilitated further invasion by active and passive dispersal (Reshetnikov 2010; Reshetnikov and Ficetola 2011).

The history of the Central European population of Chinese sleeper started in 1972, when it was found in the Velykyi Lubin fish farm (River Dniester basin) near Lviv, Ukraine (Fedoniuk 2005; Reshetnikov 2013; Kutsokon 2017) (Fig. 1A). Ac-

According to Reshetnikov (2013), this was the most probable secondary source of the invasion to several other countries in Central Europe, given that it was subsequently reported from Poland in 1993 (Antychowicz 1994), Hungary in 1997 (Harka 1998), Slovakia in 1998 (Koščo et al. 1999), Bulgaria in 2003 (Jurajda et al. 2006), Romania in 2005 (Popa et al. 2006), and Germany in 2009 (Reshetnikov and Schliewen 2013; Nehring and Steinhof 2015).

In the invaded areas, Chinese sleepers are locally abundant, especially in small, stagnant and eutrophic water bodies that are overgrown with vegetation, such as oxbow lakes, floodplain pools, bogs and ponds, both natural and artificial (Koščo et al. 2003; Grabowska et al. 2011; Reshetnikov 2013; Rechulicz et al. 2015). They appear to avoid running waters, though they may temporally occur in flowing water or occupy habitats that provide shelter from the current. Their invasion of new localities still continues, via both active and passive dispersal (Reshetnikov 2013). Human activity, such as fish cultivation, is considered one of the primary reasons for accidental introduction of the Chinese sleeper to geographically distant locations (Reshetnikov 2013). Given that the species is still treated as both an ornamental and baitfish, another suspected human-mediated explanation for its dispersal is a release by aquarists and anglers (Reshetnikov 2013; Rakauskas et al. 2016b). Anthropogenic introductions have facilitated further expansion via natural mechanisms, particularly through drainage ditches, streams and rivers that seem to serve as invasion highways at river drainage scale (Reshetnikov 2013). The Chinese sleeper is capable of depleting the diversity of macroinvertebrates, amphibians, reptiles, and fishes (Koščo et al. 2008; Grabowska et al. 2009, 2019; Pupins and Pupina 2012, 2018; Reshetnikov, 2013; Rakauskas et al. 2016a), making it a serious threat to European freshwater ecosystems. In consequence, it was included in the invasive alien species list of European Union concern (European Commission 2016).

The genetic diversity and population structure of the Chinese sleeper are poorly known, though data were recently collected for part of its native range in China in the River Amur and Liaohe basins (Xu et al. 2013, 2014). These data showed the presence of three Chinese sleeper lineages that supposedly diverged during the Pleistocene; two of them were sympatric in both basins, while the third was restricted to the Amur basin. In its native range, the Chinese sleeper was characterised by a high degree of genetic structure among populations, which can be attributed to its limited dispersal (Xu et al. 2014). So far, with the exception of a single ambiguous study on a population from the River Siret in Romania (Luca et al. 2014), there have been no attempts to reveal the genetic structure and possible origins of the Chinese sleeper populations in its invasive range.

Our study is the first to address this gap in understanding about such a widespread and important invasive species, and is based on samples collected from almost all European countries that currently support populations of the Chinese sleeper. Our aim is to provide a better understanding of the dynamics, pathways, and vectors of the expansion of the Chinese sleeper in Europe. In particular we aimed to: 1) test whether the invasive population of the Chinese Sleeper in Central Europe comes from one or

several introduction events and their sources; 2) detect, on the basis of already published data, the source of European populations in its native range; 3) verify whether, as suggested by the literature, Ukraine is the location of the initial introduction and a donor for subsequent expansion into Central Europe; 4) discuss the pathways and vectors that could play a role in driving the expansion of the Chinese sleeper in Europe and shaping its genetic structure.

Materials and methods

DNA extraction, amplification, sequencing, and dataset assemblage

Total DNA was extracted from 261 individuals collected on 26 sampling sites in Central (Germany, Poland, Hungary) and Eastern Europe (Latvia, Lithuania, Belarus, Ukraine, Russia and Bulgaria) (Fig. 1A, B, Table 1), from a piece of a fin tissue, with the Chelex (Casquet et al. 2012) or standard phenol-chloroform (Hillis et al. 1996) procedures. The ca. 1200 bp long fragment of cytochrome b (cyt b) gene was amplified using the primer pair Glu-2 and Pro-R1 and reaction conditions of Hardman and Page (2003). The PCR products (5 µl) were cleaned with Exonuclease I (2 U, EURx Ltd., Gdańsk, Poland) and alkaline phosphatase Fast Polar-BAP (1 U, EURx Ltd., Gdańsk, Poland) treatment, according to the manufacturer's guidelines, and sent for sequencing in both directions to Macrogen Europe (Amsterdam, the Netherlands). The identity of the obtained sequences was verified using BLAST (Altschul et al. 1990). Sequences were edited, aligned and trimmed to 1172 bp using Geneious 10.2.6 (Kearse et al. 2012). In the case of six individuals, the chromatograms contained double peaks. These double peaks were confirmed by sequencing both DNA strands (5' to 3' and 3' to 5'). Un-phasing of such sites in order to define the actual haplotypes was completed in DnaSP v5 (Librado and Rozas 2009). The sequences of the resulting haplotypes were translated into amino acid sequences using Geneious 10.2.6 to check for the presence of stop codons that could identify them as NUMT-pseudogenes. No such cases were found and we assumed that they represented fully functional versions of the mitochondrial COI genes. All the sequences were deposited in GenBank under accession numbers (MN555819–MN556085). The DNA sequences containing relevant voucher information were deposited in the online database of the Barcode of Life Data Systems (BOLD) (Ratnasingham and Hebert 2007) accessible through the public data set "PEGLE" (dx.doi.org/10.5883/DS-PERCCOTT). All specimens were deposited in the permanent collection of the Department of Invertebrate Zoology and Hydrobiology, University of Lodz, Poland. Having no possibility to validate the tentative heteroplasmy by repeating DNA extractions from the samples in question, we have excluded the sequences MN555836, MN555846, MN555858, MN555862, MN555864, MN555959, MN556020, MN556038, MN556052, MN556058, MN556059, MN556064 from subsequent analyses. Hence, the final dataset was composed of 255 cytochrome b sequences.

Table 1. Sampling sites of Chinese sleeper. Localities geographically very close (ca. 20 km distance) to each other were pooled to simplify the demographic analyses. They were given the same site number.

Site	Code	Country	Latitude / Longitude	Date	Drainage	Locality	No. of individuals	No. of sequences
1	RUS1	Russia	48.7953, 44.5641	2018	Volga	Volgograd	10	10
2	LAT1	Latvia	55.8348, 26.4843	2017	Daugava	Daugavpils city	10	10
3	LAT2	Latvia	56.9772, 24.2409	2017	Daugava	Riga city	9	9
4A	LT1	Lithuania	54.7835, 24.8125	2019	Nemunas	Neris River drainage	9	9
4B	LT2	Lithuania	54.8430, 25.3406	2019	Nemunas	Neris River drainage	4	4
5	BLR1	Belarus	53.9329, 27.6398	2017	Dnieper	Minsk	10	10
6	BLR2	Belarus	52.0994, 29.4222	2017	Dnieper	Syrod – Gomel oblast	12	12
7	BLR3	Belarus	53.9621, 30.1924	2017	Dnieper	Mogilev oblast	9	9
8	PL1	Poland	52.5459, 19.5659	2018	Vistula	Włocławski Reservoir	13	13
9	PL2	Poland	52.3356, 20.9142	2018	Vistula	Łomianki	12	12
10	PL3	Poland	51.8206, 21.2942	2018	Vistula	Pilica River, Zagroby	11	12
11	PL4	Poland	51.3843, 21.3227	2018	Vistula	Niemianowice	11	11
12	PL5	Poland	50.8569, 24.1415	2018	Vistula	Western Bug Zosin	3	3
12	PL6	Poland	50.5376, 23.7342	2018	Vistula	Western Bug Nadolce	3	3
13	PL7	Poland	51.0663, 21.8140	2018	Vistula	Łopoczno	10	10
14	GER1	Germany	49.2630, 12.1096	2015	Danube	Kranzloh fish pond	7	7
14	GER2	Germany	49.2647, 12.1298	2015	Danube	Torngrube	7	7
15	UA1	Ukraine	49.2158, 28.4578	2016	Southern Bug	Vinnitsia	1	1
15	UA3	Ukraine	49.2158, 28.4578	2018	Southern Bug	Vinnitsia region	3	3
16	UA2	Ukraine	51.0528, 31.9069	2018	Dnieper	Desna River Nizhyn	7	7
17	UA4	Ukraine	51.5041, 31.2943	2016	Dnieper	Desna River Chernihiv	2	2
18	UA5	Ukraine	50.2070, 28.6420	2016	Dnieper	Teteriv River, Huiva	1	1
18	UA11	Ukraine	50.5103, 29.3078	2018	Dnieper	Berezsi	6	7
19	UA6	Ukraine	49.3827, 24.0204	2017	Dniester	River Kuna basin, Lviv oblast	3	3
19	UA7	Ukraine	49.8483, 24.0521	2017	Dniester	Lviv oblast	4	4
19	UA18	Ukraine	49.8001, 24.0164	2018	Dniester	Stryiska Pond, Lviv	11	11
20	UA8	Ukraine	49.3395, 31.5156	2016	Dnieper	Dnipro, Mliiv	1	1
20	UA9	Ukraine	50.3511, 30.4557	2018	Dnieper	Novosilky – pond	3	3
21	UA10	Ukraine	50.6673, 27.6121	2018	Dnieper	Chyzhivka	11	15
22	UA12	Ukraine	51.5774, 23.8628	2018	Vistula/Dnieper	Shatsk Lakes, Canal in Zatyshshia	6	6
22	UA13	Ukraine	51.5543, 23.9179	2018	Vistula/Dnieper	Shatsk Lakes, Canal in Melnyky	4	4
22	UA14	Ukraine	51.5488, 23.9221	2018	Vistula/Dnieper	Shatsk Lakes, Melnyky Pond	1	1
22	UA15	Ukraine	51.5270, 23.8527	2018	Vistula/Dnieper	Shatsk Lakes, Canal in Illichivka,	2	2
22	UA17	Ukraine	51.5774, 23.8628	2018	Vistula/Dnieper	Shatsk Lakes, Canal in Zatyshshia	5	5
23	BUL1	Bulgaria	44.0267, 26.5170	2015	Danube	Kalimok	8	8
24	H1	Hungary	48.0953, 21.4629	2018	Danube	Rakamaz oxbow lake, Tiszanagyfalu	12	12
25	H2	Hungary	46.6939, 17.2373	2018	Danube	Canal in Kis-Balaton reservoir, Fenékpuszta	9	9
26	H3	Hungary	46.5063, 19.0531	2018	Danube	Maloméri main canal, Homokmégy	11	11

Analysis of molecular data

Haplotypes within the cytochrome b dataset as well diversity statistics; i.e. the number of haplotypes (k), haplotypic diversity (h) and nucleotide diversity (π) (Nei 1987), were obtained using the DnaSP v5 software (Librado and Rozas 2009).

The demographic status of European populations of Chinese sleeper was examined in Arlequin 3.5 (Excoffier and Lischer 2010). We assessed current demographic status with mismatch distribution, supplemented with selective neutrality tests; i.e. Tajima's D (Tajima 1989) and Fu's FS (Fu 1997) as indicators of population expansion. The genetic connectivity between different sampling sites was tested with the F_{ST} estimator (Weir and Hill 2002) in Arlequin 3.5, using default software set-ups. Analysis of molecular variance (AMOVA; Excoffier et al. 1992), with two schemes, was applied to reveal whether and how the European population of Chinese sleeper is spatially structured. In the first scheme, countries were used as the basic grouping factor for sampling sites, assuming that they may represent different and independent introduction events. In the second scheme, sampling sites were grouped according to river drainages (Table 1). As some localities were geographically close (ca. 20 km distance), we pooled them with the closest sampling site to increase the number of individuals per site and to simplify the analysis.

The relationships among the Chinese sleeper haplotypes identified during this study were analysed and graphically presented as a median-joining network with the aid of PopART 1.7 (Bandelt et al. 1999). Additionally, the phylogenetic position of these haplotypes in regards to the clades found within the native population of Chinese sleeper from China in the study by Xu et al. (2013, 2014) was reconstructed using the Maximum Likelihood approach (ML), with 1,000 bootstrap replicates, in MEGA X (Kumar et al. 2018). The HKY+G (Hasegawa-Kishino-Yano, Gamma distribution) (Hasegawa et al. 1985) was chosen, in the same software, as the best fitting substitution model. The cytochrome b sequences of *Odontobutis obscura* (AB021243), *Odontobutis potamophila* (AY722247) and *Odontobutis platycephala* (DQ010651) from GenBank (Benson et al. 2005), were used as an outgroup.

Results

The 1172 bp long portion of cytochrome b gene was sequenced from 261 Chinese sleeper individuals collected from a variety of water bodies in Belarus, Bulgaria, Hungary, Germany, Latvia, Lithuania, Poland, Russia (European part) and Ukraine (Table 1, Suppl. material 1: Table S1). We obtained 267 sequences, since six of the sequenced fish revealed double cytochrome b sequences. The latter included five individuals from Ukraine (4 ind. from site 19, 1 ind. from site 20), as well as one individual from Poland (site 10), but were excluded from our dataset. As a result, the dataset contained 255 sequences with 45 variable sites and no indels. The nucleotide diversity per site (Π) was 0.007 (SD: 0.001), while the average number of nucleotide differences (k) was 7.9. The number of haplotypes (h) defined in our dataset equalled 22 with the haplotype diversity (H_d) of 0.685 (SD: 0.018).

A Median-Joining network revealed that the haplotypes identified in our dataset formed three major groups, with partially disjunct geographic distributions (Figs 1B, 2). Haplogroup I consisted of three haplotypes only and was found exclusively in Latvia. Haplogroup II consisted of five haplotypes. Its topology was star-like

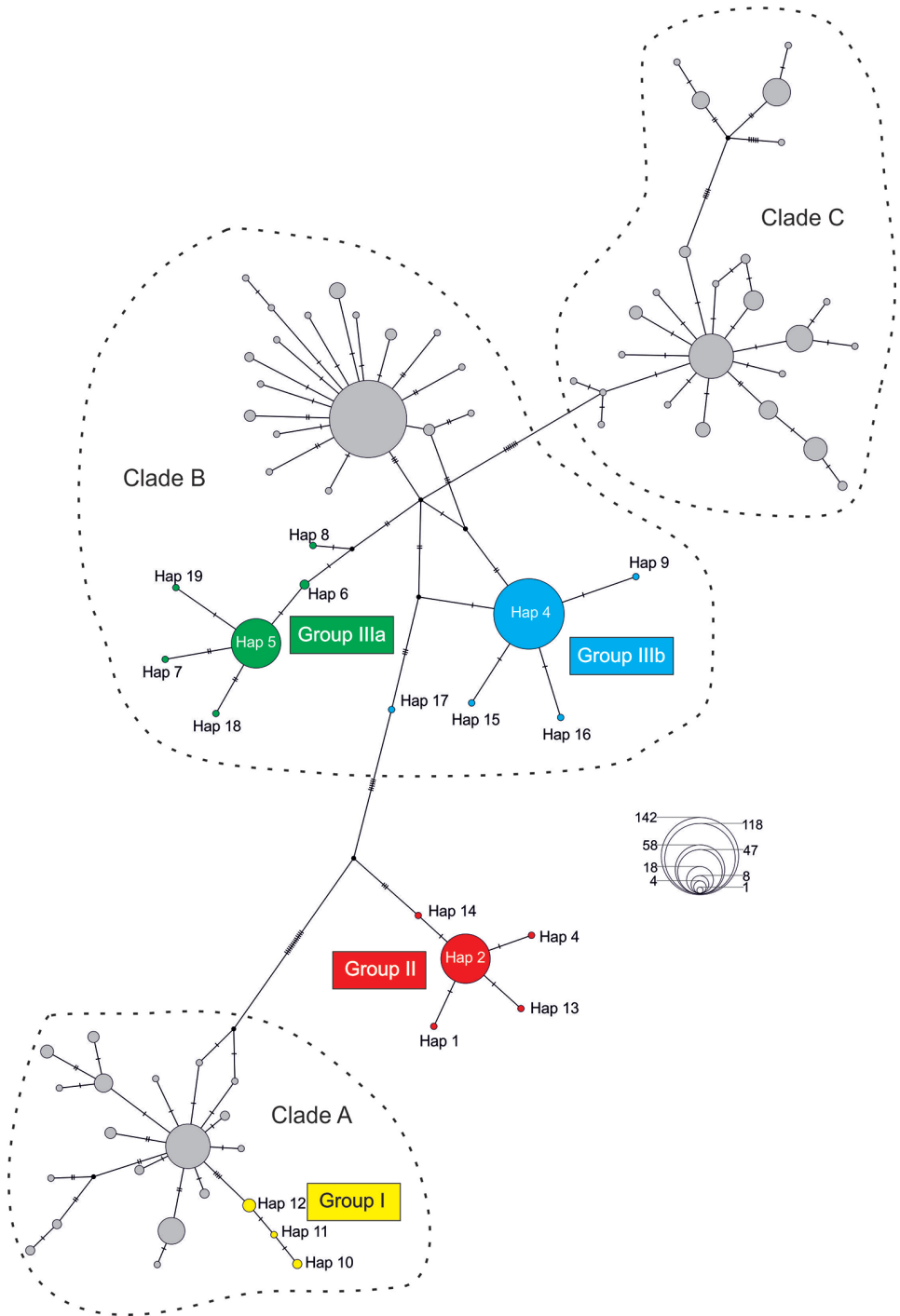


Figure 2. Median-Joining network showing phylogenetic relationships among Chinese sleeper cytochrome b haplotypes identified in our study and those (in grey) reported by Xu et al. (2014) from the native range in China. Circle size is proportional to the number of individuals with a given haplotype (see open circles with numbers).

with the central, most abundant, haplotype 2. This haplogroup was found only in the eastern part of the studied region, namely in eastern Lithuania, Latvia and Belarus as well as in northern Ukraine. Haplogroup III included as many as eleven haplotypes and had a more complex, partially star-like and partially reticulate topology. Haplotypes 4 and 5 were the most abundant. This haplogroup might be further divided into two subgroups; i.e. subgroup IIIa centred around haplotype 5, and subgroup IIIb centred around haplotype 4. Subgroup IIIa was present in southern Ukraine and, together with subgroup IIIb, at one site in Belarus. Subgroup IIIb prevailed in western Ukraine. Both subgroups were found in Poland, Bulgaria and Hungary, while only subgroup IIIa was found in the sampled sites in Germany.

Mismatch distribution analysis, accompanied by Tajima's D and Fu's FS neutrality tests (Table 2), rejected a model of recent demographic expansion for the European population of Chinese sleeper. However, the spatial expansion model could not be dismissed.

Analysis of Molecular Variance (Table 3) showed that 44.9% of the observed genetic variation may be explained by partitioning the dataset according to country of sample origin. The remaining 55.1% of variation in our dataset can be attributed to differences between the sampling sites (30.8%) and the variation within them (24.3%). Partitioning the dataset by river basin explained only 39.5% of the observed variation, while 36.1% of the variation could be accounted for by differentiation among sites.

The F_{ST} coefficient values (0.00–0.99) suggested extremely varied levels of genetic connectivity among sampling sites (Fig. 3, Suppl. material 2: Table S2). All sampled populations from Russia (site 1), Latvia (sites 2 and 3), Lithuania (site 4), two from

Table 2. Results of mismatch distribution analysis and Tajima's D and Fu's FS neutrality tests for Chinese sleeper.

	Demographic expansion	Spatial expansion
SSD*	0.5771	0.0844
SSD P -value	0.0000	0.2300
Raggedness index	0.2354	0.2354
Raggedness P-value	1.0000	0.4300
Tajima's D	0.2036	
Tajima's D P -value	0.6710	
Fu's FS	4.4171	
Fu's FS P -value	0.8810	

*SSD – the sum of squared deviations.

Table 3. Results of AMOVA for Chinese sleeper.

Source of variation	d.f.	Sum of squares	Variance components	Variance [%]	Fixation Indices
Sampling sites grouped according to countries					
Among groups	8	534.85	1.94 Va	44.87	F_{SC} : 0.56
Among populations within groups	17	225.37	1.33 Vb	30.84	F_{ST} : 0.76
Within populations	229	240.03	1.05 Vc	24.29	F_{CT} : 0.45
Total	254	1000.24	4.31		
Sampling sites grouped according to river basins					
Among groups	8	506.99	1.69 Va	39.46	F_{SC} : 0.60
Among populations within groups	17	253.23	1.55 Vb	36.10	F_{ST} : 0.76
Within populations	229	240.03	1.05 Vc	24.44	F_{CT} : 0.40
Total	254	1000.24	4.29		

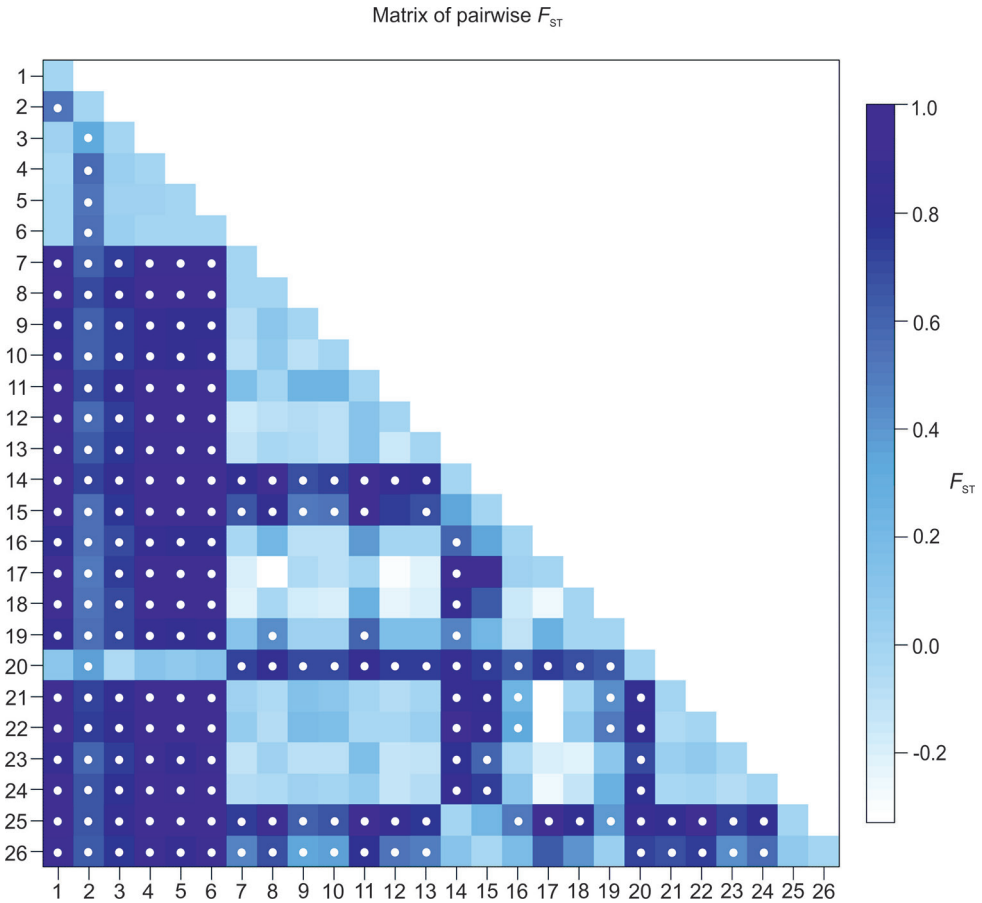


Figure 3. Population connectivity illustrated by a matrix of pairwise F_{ST} values (see also Table S2). White dots indicate F_{ST} P values significantly different from zero ($P < 0.05$). Sites in close geographic proximity pooled for demographic analyses and assigned the same number.

Belarus (sites 5 and 6) and one from Ukraine (site 20) formed a group that was relatively isolated from all other populations, while a high level of genetic connectivity is retained within this group. A population from Germany (site 14), one from Ukraine (site 15), and two from Hungary (site 25 and 26) appeared to have no connectivity with populations from other areas. However, this finding may be related to a highly uneven sample size between some of these localities. In contrast, the remaining populations can be characterized by relatively high or moderate levels of genetic connectivity.

Phylogenetic reconstruction of relationships among the haplotypes observed in our dataset and those defined by Xu et al. (2014) in populations of Chinese sleeper from the Liaohe and Amur River basins in north-eastern China revealed that our haplogroups I and III can be attributed to Xu et al. (2014) clades A and B, respectively (Fig. 4). However, none of the haplotypes in our dataset is identical to any haplotype from Xu et al. (2014). Haplogroup II formed a separate clade, more closely related to clades B and C than to clade A (as defined by Xu et al. 2014).

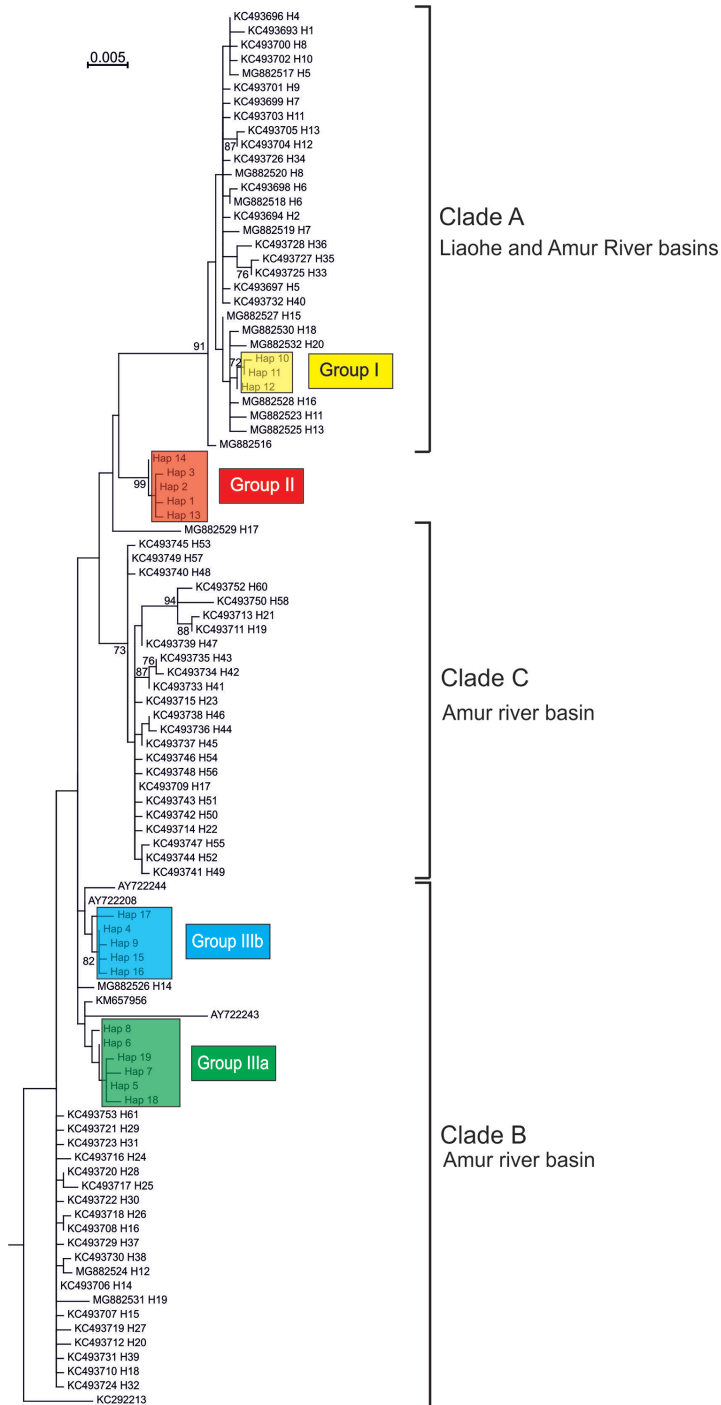


Figure 4. Maximum Likelihood tree showing the relationships of cytochrome b haplotypes identified in our study with the haplotypes from the native area in China (Xu et al. 2013, 2014). Numbers at each node are bootstrap probabilities based on 1000 replications; shown only when they are 70% or higher. Outgroup not shown.

Discussion

Our study revealed that the invasive Chinese sleeper in Europe consists of at least three distinct haplogroups that may represent independent introduction events from different parts of its native range. Haplogroup I, henceforth termed “Baltic”, was found only in Latvia (Fig. 1B) in natural stagnant waters in the River Daugava drainage (Baltic Sea basin). In the native range of the Chinese sleeper, this haplogroup occurs in China in the Liaohe drainage and in the River Argun (left tributary of the River Amur) (Xu et al. 2014).

The first records of the Chinese sleeper in Latvia come from small natural ponds in the city centre of Daugavpils (Fig. 1A), that are not connected with any river system (Pupina et al. 2015). It was unknown how the species was introduced there but the population may have arisen from releases by local aquarists or fishermen (Plikšs and Aleksejevs 1998). Further investigation confirmed several sources of anthropogenic introductions in Latvia, including releases by aquarists and by anglers using them as a live bait, as well as through intentional stocking to control the density of *Carassius* sp. or as a prey for northern pike, *Esox lucius*, Linnaeus, 1758 (Pupiņš and Čeirāns, unpublished data). In addition, several Latvian websites currently offer sexually mature Chinese sleeper for purchase to stock ponds (Pupina et al. 2015; Pupiņš and Čeirāns, unpublished data). This information, combined with an absence of local haplotypes in any other population from the invasive range, strongly suggest that aquarist and angler releases of specimens translocated directly from China is possible, particularly when taking into account that China is a known exporter of ornamental pet species collected in the wild (Nijman 2010).

Another possibility is that the Chinese sleeper population in Latvia derives from a much earlier release by aquarists in Saint Petersburg in 1916 (Kuderskiy 1982), which would explain the coexistence of haplogroup I with haplogroup II that is distributed primarily in northern Europe (Fig. 1B). Unfortunately, we have no access to comparative material from that location to verify this scenario.

Haplogroup II was recorded in Lithuania (the River Neman drainage), Latvia (the River Daugava drainage), Belarus and northern Ukraine (the River Dnieper drainage) (Fig. 1B). It has not been found in any of the earlier studied Chinese populations (Xu et al. 2014). Considering the distribution of this group of haplotypes, mainly in the northern, and possibly eastern, part of its invasive range, we cannot discount the possibility that it may also be associated with the first introduction to Saint Petersburg at the beginning of the 20th century (Fig. 1A). These first individuals came from the River Zeya that is a left tributary of the River Amur and runs through the Russian Far East, but not through China (Kuderskiy 1982). Unfortunately, there is no information about the genetic structure of the Chinese sleeper from that part of its native range to indicate it as a possible source for haplotype group II.

According to the literature, after rapidly spreading in the vicinity of Saint Petersburg, most probably due to active dispersal, the species was soon found in several new locations (Kuderskiy 1982). In Lithuania, the Chinese sleeper was first recorded in

Lake Bevardis in 1985 (Virbickas 2000) (Fig. 1A). Its occurrence in coastal waters of the Gulf of Finland of the Baltic Sea (Dmitriev 1971) could allow migration in the oligohaline waters along the south-eastern Baltic coast, entering other river systems and forming secondary sources for the invasion in inland waters. However, during its initial phase of expansion in Lithuania, the Chinese sleeper was only recorded in small ponds and oxbows and not in the River Neman, so an inland expansion along the Baltic coast was probably through human releases. Only later did it spread inland via the basins of the Rivers Neman and Daugava. This scenario could explain the co-occurrence of the haplogroup II with haplogroup I in the two sampling sites in Latvia, which are located in the Daugava basin. The Chinese sleeper has been reported from the River Neman in Belarus since 2007 (Semenchenko et al. 2009) (Fig. 1A), and in 2009 it was found in the Belarusian part of the River Daugava (Lukina 2011). The spread of the Chinese sleeper in this north-eastern part of its invasive range is consistent with the distribution of haplogroup II (Fig. 1B).

Moreover, the population from the lower River Volga drainage, the only sample we obtained from Russia, also belongs to haplogroup II (Fig. 1B). The first reports of Chinese sleeper from this part of Russia come from 1970–1971, when the Chinese sleeper was accidentally inadvertently introduced with common carp, *Cyprinus carpio* Linnaeus, 1758, from the River Amur basin to the Ilev fish farm in Nizhniy Novgorod province (Fig. 1A), Volga basin, Russia (Kuderskiy 1980).

Haplogroup III was common in Ukraine and the only haplogroup found in Poland, Hungary, Bulgaria and Germany (Fig. 1B). It was also found in one locality in Belarus (the River Dnieper) (Fig. 1B). The distribution of this haplogroup strictly overlaps with the distribution of the so-called “Carpathian population” as defined by Kvach et al. (2016b), with which it is apparently identical. Thus, we retain the designation “Carpathian” for this haplogroup. It supports the proposition that the fish farm near Lviv in Ukraine, where the Chinese sleeper was first recorded in 1972 (Fedoniuk 2005) (Fig. 1B), could be the source population for many further introductions and subsequent dispersal through Central Europe (Reshetnikov 2013; Kutsokon 2017). The Chinese sleeper was introduced unintentionally to the Lviv region, Western Ukraine, during stocking of commercial fish, juvenile silver carp, *Hypophthalmichthys molitrix* (Valenciennes, 1844), at the end of the 1960s (Reshetnikov 2013). The source of this introduction is unknown, but it could have been translocated directly from China or from other fish farms where Asian cyprinids were cultivated, such as those in Uzbekistan or Kazakhstan.

This scenario is not unlikely, as in 1958, the Chinese sleeper was introduced together with juvenile silver carp and grass carp, *Ctenopharyngodon idella* (Valenciennes, 1844), from Harbin (China) to the Almaty fish farm in Kazakhstan (Seleznev 1974). In 1961 it was probably transported from China to Akkurgan fish farm (River Syr Darya basin) in Uzbekistan (Borisova 1972). Haplogroup III is widely distributed in the native range of the Chinese sleeper in the northern China (Xu et al. 2014). It occurs in the River Hun (a tributary of the Liaohe) and in rivers of the River Amur system; i.e. Songhua, Argun, Nenjiang and Middle Amur, bordering Russia. It is also present in an

area close to Harbin (China), mentioned as a source from which the Chinese sleeper was collected for stocking in Kazakhstan in the 1960s. Thus, although these historical explanations for the Chinese sleeper in Uzbekistan and Kazakhstan have recently been questioned by Reshetnikov (2010), the results of our molecular studies do not exclude such a scenario for the origin of the population in Ukraine.

The later expansion of the species from Ukraine was both passive as an outcome of stocking cultivated Asian cyprinids in ponds, as well as active dispersal through aquatic networks. The Chinese sleeper was transported with silver carp to Transcarpathia, where it was first reported in the River Latorica in 1995 (Syvokhop 1998). Another route was along the River Tisza basin where it was reported in Hungary in 1997 (Harka 1998) (Fig. 1A) and in Slovakia in 1998 (Koščo et al. 1999). It expanded down the River Danube, facilitated by flooding, and was first observed in both the Bulgarian (Jurajda et al. 2006) (Fig. 1A) and Romanian section of the Danube in 2005 (Popa et al. 2006). The westernmost population of the Chinese sleeper in the Danube basin was recorded in 2009 in extensive enclosed fish ponds located in the River Naab basin, Bavaria, Germany (Reshetnikov and Schliewen 2013; Nehring and Steinhof 2015) (Fig. 1A). For decades, these ponds have been used extensively for fish production (Reshetnikov and Schliewen 2013). Reshetnikov and Schliewen (2013) assumed that the Chinese sleeper was accidentally introduced into these fish ponds with commercial fish transportation. We found only one haplotype (H5) in this population, which is the second most common and widespread in Central Europe, including Ukraine and Hungary.

In Ukraine the Carpathian population of the Chinese sleeper has spread through the Dniester basin since 1995 (Korte et al. 1999; Fedoniuk 2005; Moshu and Kiriyak 2011). In the Southern Bug (Boh) basin it has been known since 2009 from Vinnytsia (Kutsokon et al. 2014; Kutsokon 2017). In the Vistula basin, the Chinese sleeper was first reported in 1988, from the River Vyshnia in Ukraine (Movchan 1989) (Fig. 1A). In 1993 it extended its range to the Middle Vistula in Poland (Antychowicz 1994) and reached the Vistula delta in 2000 (Kostrzewa et al. 2004) (Fig. 1A). In 2006 it was found in the Shatsky Lakes in Ukraine, which connect the Vistula and Dnieper basins (Liesnik 2008) (Fig. 1A). The haplotypic composition of the Chinese sleeper population in Poland is the most similar to that in western Ukraine i.e. in the Shatsky Lakes (Fig. 1B). The route and vector of the Chinese sleeper introduction to Poland are unknown but, considering our results, unintended translocation with aquaculture stocking from Ukraine is the most probable, with commercial websites in Poland offering stocking material of carp and other species from Ukraine.

The origin of the Chinese sleeper in the River Dnieper is controversial. It was first reported from the city of Minsk in Belarus in the 1970s (Rizevski et al. 1999) (Fig. 1A). In the River Desna (left Dnieper tributary), in Russia, it was recorded in 1990 (Reshetnikov 2010) (Fig. 1A). In Ukraine (Middle Dnieper basin) it was first reported in 2001 from the vicinity of Kyiv (Sabodash et al. 2002) (Fig. 1A). It subsequently spread south, where it was found in the Dnieper tributaries (Kutsokon 2017). In the Middle Dnieper, only haplogroup IIIa was recorded, the same as in the Southern Bug (Boh) basin (Fig. 1B). This finding corroborates that Chinese sleepers from

the Dnieper and Southern Bug form one population with those from the Carpathian region, as previously hypothesized by Kvach et al. (2016b) based on the parasitological studies. We observed a decrease of genetic diversity in the Carpathian population from its presumed source (Lviv region), from where it subsequently colonised other regions (Upper Danube, Middle Vistula, Middle Dnieper, Southern Bug) (Fig. 1B).

Based on demographic analyses, such as the F_{ST} and AMOVA, we estimate the genetic connectivity between most of the Chinese sleeper populations to be high, and the molecular diversity in Central Europe showing no clear spatial structure, neither following river basins nor grouping by country. This finding suggests a rather multidirectional spread of the species in Central Europe. Interestingly, we observed a cessation of gene flow among populations from Latvia and elsewhere. This outcome suggests an independent introduction of the Chinese sleeper in Latvia and possible isolation of this population. However, more studies involving nuclear markers are needed to fully resolve this question.

In conclusion, based on the spatial distribution of mitochondrial cytochrome b diversity, we can distinguish three Chinese sleeper haplogroups in Europe, that may represent three discrete introduced populations: (1) A Baltic haplogroup that may originate from fish introduced unintentionally from Russia or from some unidentified vectors, probably releases by aquarists. To date this population was found only in the Daugava basin in Latvia. (2) East-European haplogroup, which possibly originates from an unintentional introduction to the Volga basin in Russia and with subsequent westward expansion. This group has been recorded in the Volga, Upper Dnieper and Neman drainages in Belarus, Lithuania, and Russia. (3) Carpathian haplogroup, originating from individuals inadvertently introduced with Asian cyprinid fishes to the Lviv region in Ukraine, which occurs in the basins of the Rivers Danube, Dnieper and Vistula in Belarus (eastern part), and also in Bulgaria, Germany, Hungary, Poland, and Ukraine.

Acknowledgements

The work conducted by YK, MP, IK and AC was partly supported by the Joint Ukrainian-Latvian R&D project “The ecological and biological triggers of expansion of the invasive fish, Chinese sleeper (*Percottus glenii*), in Eastern Europe”. The work performed by LA was partly supported by the Higher Education Institutional Excellence Programme (NKFIH-1150-6/2019) of the Ministry of Innovation and Technology in Hungary, within the framework of the 4th thematic programme of the University of Debrecen. Laboratory work and molecular analysis was supported by internal funds of the University of Lodz and also partly funded by the National Science Centre, Poland (grant no. 2014/15/B/NZ8/00266). We thank Vasilij Boldyrev (Volgograd Division of the State Institute of Lake and River Fisheries, Volgograd, Russia) for his help in sampling in the River Volga, Dr Anatolij Roman (National Museum of Natural History at the National Academy of Sciences of Ukraine, Kyiv, Ukraine) for providing samples from Northern Ukraine, Dr Markéta Ondračková (Institute of Vertebrate Bi-

ology of the Czech Academy of Sciences, Brno, Czech Republic) for providing samples from the Upper Danube basin, Dr hab. Jacek Rechulicz for providing samples from Western Bug, and Krisztián Nyeste (University of Debrecen, Department of Hydrobiology, Debrecen, Hungary) for his help with sampling in Hungary. We are grateful to prof. Carl Smith (Faculty of Biology & Environmental Protection, University of Lodz) for language editing of our manuscript.

References

- Altschul SF, Gish W, Miller W, Myers EW, Lipman DJ (1990) Basic local alignment search tool. *Journal of Molecular Biology* 215: 403–410. [https://doi.org/10.1016/S0022-2836\(05\)80360-2](https://doi.org/10.1016/S0022-2836(05)80360-2)
- Antychowicz J (1994) *Percottus glehni* w naszych wodach. *Komunikaty Rybackie* 2: 21–22. [in Polish]
- Bandelt H, Forster P, Röhl A (1999) Median-joining networks for inferring intraspecific phylogenies. *Molecular Biology and Evolution* 16(1): 37–48. <https://doi.org/10.1093/oxford-journals.molbev.a026036>
- Benson DA, Karsch-Mizrachi I, Lipman DJ, Ostell J, Wheeler DL (2005) GenBank: update. *Nucleic Acids Research* 33: D34–D38. <https://doi.org/10.1093/nar/gkh045>
- Bogutskaya NG, Naseka AM (2002) *Percottus glenii* Dybowski, 1877. *Freshwater Fishes of Russia*. Zoological Institute RAS. Saint Petersburg, Russia. http://www.zin.ru/Animalia/Pisces/eng/taxbase_e/species_e/perccottuss_el.htm
- Bogutskaya NG, Naseka AM, Shedko SV, Vasil'eva ED, Chereshev IA (2008) The fishes of the Amur River: updated check-list and zoogeography. *Ichthyological Exploration in Freshwaters* 19: 301–366.
- Borisova AT (1972) Sluchaynye vselentsy v vodoemakh Uzbekistana. *Voprosy Ikhtiologii* 12(1): 49–53. [in Russian]
- Copp GH, Bianco PG, Bogutskaya NG, Erős T, Falka I, Ferreira MT, Fox MG, Freyhof J, Gozlan RE, Grabowska J, Kováč V, Moreno-Amich R, Naseka AM, Peñáz M, Povž M, Przybylski M, Robillard M, Russell IC, Stakėnas S, Šumer S, Vila-Gispert A, Wiesner C (2005) To be, or not to be, a non-native freshwater fish? *Journal of Applied Ichthyology* 21: 242–262. <https://doi.org/10.1111/j.1439-0426.2005.00690.x>
- Cucherousset J, Olden JD (2011) Ecological impacts of non-native freshwater fishes. *Fisheries* 36: 215–230. <https://doi.org/10.1080/03632415.2011.574578>
- Dmitriev MA (1971) Ostorozhno, rotan. *Rybovodstvo i rybolovstvo* 1: 26–27. [in Russian]
- European Commission (2016) Commission Implementing Regulation (EU) 2016/1141 of 13 July 2016 adopting a list of invasive alien species of Union concern pursuant to Regulation (EU) No 1143/2014 of the European Parliament and of the Council. *Official Journal of the European Union* (L189): 4–8.
- Excoffier L, Lischer HEL (2010) Arlequin suite ver 3.5: A new series of programs to perform population genetics analyses under Linux and Windows. *Molecular Ecology Resources* 10: 564–567. <https://doi.org/10.1111/j.1755-0998.2010.02847.x>

- Excoffier L, Smouse PE, Quattro JM (1992) Analysis of molecular variance inferred from metric distances among DNA haplotypes: Application to human mitochondrial DNA restriction data. *Genetics* 131: 479–491. <https://doi.org/10.1007/s00424-009-0730-7>
- Fedoniuk OV (2005) Holoveshka amurska (*Percottus glenii*) v umovakh vodoym Lvivshchyny. In: Bioriznomanittia ta rol zootsenozu v prirodnykh i antropogennykh ekosystemakh: Materialy III Mizhnarodnoy naukovoyi konferentsii, Dnipropetrovsk, 4–6 zhovtnia 2005 r. Vydavnytsvo DNU (Dnipropetrovsk): 102–104. [in Ukrainian]
- Fu YX (1997) Statistical tests of neutrality of mutations against population growth, hitchhiking and background selection. *Genetics* 147(2): 915–925
- Gozlan RE, Britton JR, Cowx I, Copp GH (2010) Current knowledge on non-native freshwater fish introductions. *Journal of Fish Biology* 76: 751–786. <https://doi.org/10.1111/j.1095-8649.2010.02566.x>
- Grabowska J, Błońska D, Kati S, Nagy SA, Kakareko T, Kobak J, Antal L (2019) Competitive interactions for food resources between the invasive Amur sleeper (*Percottus glenii*) and threatened European mudminnow (*Umbra krameri*). *Aquatic Conservation: Marine and Freshwater Ecosystems* 29: 2231–2239. <https://doi.org/10.1002/aqc.3219>
- Grabowska J, Grabowski M, Pietraszewski D, Gmur J (2009) Non-selective predator – the versatile diet of Amur sleeper (*Percottus glenii* Dybowski, 1877) in Vistula River (Poland), a newly invaded ecosystem. *Journal of Applied Ichthyology* 25: 451–459. <https://doi.org/10.1111/j.1439-0426.2009.01240.x>
- Grabowska J, Pietraszewski D, Przybylski M, Tarkan AS, Marszał L, Lampart-Kałużniacka M (2011) Life-history traits of Amur sleeper, *Percottus glenii*, in the invaded Vistula River: early investment in reproduction but reduced growth rate. *Hydrobiologia* 661: 197–210. <https://doi.org/10.1007/s10750-010-0524-0>
- Harka Á (1998) Magyarország faunájának új halfaja: az amurgéb (*Percottus glehni* Dybowski, 1877). *Halászat* 91(1): 32–33. [in Hungarian]
- Hasegawa M, Kishino H, Yano T (1985) Dating the human-ape split by a molecular clock of mitochondrial DNA. *Journal of Molecular Evolution* 22: 160–174. <https://doi.org/10.1007/BF02101694>
- Hillis DM, Moritz C, Mable BK (1996) *Molecular Systematics* (2nd ed.). Sinauer Associates, Sunderland, 655 pp. <https://doi.org/10.2307/1447682>
- Hulme PE (2009) Trade, transport and trouble: Managing invasive species pathways in an era of globalization. *Journal of Applied Ecology* 46: 10–18. <https://doi.org/10.1111/j.1365-2664.2008.01600.x>
- Jurajda P, Vassilev M, Polačik M, Trichkova T (2006) A first record of *Percottus glenii* (Perciformes: Odontobutidae) in the Danube River in Bulgaria. *Acta Zoologica Bulgarica* 58: 279–282.
- Kearse M, Moir R, Wilson A, Stones-Havas S, Cheung M, Sturrock S, Buxton S, Cooper A, Markowitz S, Duran C, Thierer T, Ashton B, Meintjes P (2012) Geneious basic: an integrated and extendable desktop software platform for the organization and analysis of sequence data. *Bioinformatics* 28: 1647–1649. <https://doi.org/10.1093/bioinformatics/bts199>
- Korte E, Lesnik V, Lelek A, Sondermann W (1999) Impact and overexploitation on fish community structure in the upper River Dniester (Ukraine). *Folia Zoologica* 48(2): 137–142.

- Kostrzewa J, Grabowski M, Zięba G (2004) Nowe inwazyjne gatunki ryb w wodach Polski. Archives of Polish Fisheries 12: 21–34. [in Polish]
- Koščo J, Košuth P, Hrtan E (1999) Býčkovec hlavatý (*Perccottus glehni*), ďalší nový prvok ichtyofauny Slovenska. Poľovníctvo a Rybárstvo 51(6): 1–33. [in Slovakian]
- Koščo J, Lusk S, Halačka K, Lusková V (2003) The expansion and occurrence of the Amur sleeper (*Perccottus glenii*) in eastern Slovakia. Folia Zoologica 52: 329–336.
- Koščo J, Manko P, Miklisová D, Košuthová L (2008) Feeding ecology of invasive *Perccottus glenii* (Perciformes, Odontobutidae) in Slovakia. Czech Journal of Animal Science 53: 479–486. <https://doi.org/10.17221/340-CJAS>
- Kottelat M, Freyhof J (2007) Handbook of European Freshwater Fishes. Publications Kottelat, Cornol and Freyhof, Berlin, 646 pp.
- Kuderskiy LA (1980) Rotan v prudakh Gorkovskoy oblasti. In: Rybokhoziaystvennoye izucheniye vnutrennikh vodoyemov. Sbornik Nauchnykh Trudov GosNIORKh 25: 28–33 [in Russian]
- Kuderskiy LA (1982) Rotan v prudakh Leningradskoy oblasti. Sbornik Nauchnykh Trudov GosNIORKh 191: 70–75. [in Russian]
- Kumar S, Stecher G, Li M, Knyaz C, Tamura K (2018) MEGA X: Molecular evolutionary genetics analysis across computing platforms. Molecular Biology and Evolution 35: 1547–1549. <https://doi.org/10.1093/molbev/msy096>
- Kutsokan I (2017) The Chinese sleeper (*Perccottus glenii* Dybowski, 1877) in Ukraine: new data on distribution. Journal of Applied Ichthyology 33(6): 1100–1107. <https://doi.org/10.1111/jai.13454>
- Kutsokan Y, Tsyba A, Kvach Y (2014) The occurrence of the Chinese sleeper *Perccottus glenii* Dybowski, 1877 in the Southern Bug River basin, Ukraine. BioInvasions Records 3(1): 45–48. <https://doi.org/10.3391/bir.2014.3.1.08>
- Kvach Y, Dykyi I, Janko K (2016a) First record of the Chinese sleeper, *Perccottus glenii* Dybowski, 1877 (Actinopterygii: Odontobutidae) in the Dnieper Estuary, southern Ukraine (Black Sea drainage). BioInvasions Records 5(4): 285–290. <https://doi.org/10.3391/bir.2016.5.4.14>
- Kvach Y, Kutsokan Y, Stepien CA, Markovych M (2016b) Role of the invasive Chinese sleeper *Perccottus glenii* Dybowski 1877 (Actinopterygii: Odontobutidae) in the distribution of fish parasites in Europe: new data and a review. Biologia 71(8): 941–951. <https://doi.org/10.1515/biolog-2016-0112>
- Leunda PM (2010) Impacts of non-native fishes on Iberian freshwater ichthyofauna: current knowledge and gaps. Aquatic Invasions 5: 239–262. <https://doi.org/10.3391/ai.2010.5.3.03>
- Librado P, Rozas J (2009) DnaSP v5: a software for comprehensive analysis of DNA polymorphism data. Bioinformatics 25: 1451–1452. <https://doi.org/10.1093/bioinformatics/btp187>
- Liesnik VV (2008) Rybni uhrupovannia malykh vodoyem Shatskoho natsionalnoho pryrodnoho parku. In: Stan i bioriznomanittia ekosystem Shatskoho natsionalnoho pryrodnoho parku: Materialy naukovoyi konferensii, Shatsk, 11–14 veresnia 2008 r. Spolom (Lviv): 85–86. [in Ukrainian]
- Luca M, Ureche D, Nicuță D, Ghiorghiță G, Druică RC, Gorgan LD (2014) The genetic variability of the invasive *Perccottus glenii* from Siret River, using the cytochrome b gene. Annals of the Romanian Society for Cell Biology 19(1): 11–20.

- Lukina II (2011) Distribution of the Amur sleeper (*Perccottus glenii* Dybowski, 1877) in Belarus. Russian Journal of Biological Invasions 2(2–3): 209–212. <https://doi.org/10.1134/S2075111711030088>
- Miller PJ, Vasil'eva ED (2003) *Perccottus glenii* Dybowski 1877. In: Miller PJ (Ed.) The Freshwater Fishes of Europe (Vol. 8/1). Aula-Verlag, Weibelsheim, 135–156.
- Mori T (1936) Studies on the Geographical Distribution of Freshwater Fishes in Eastern Asia. Toppan Print, Tokio, 88 pp.
- Moshu A, Kiriak D (2011) Rasprostranenie rotana-goloveshki – *Perccottus glenii* Dybowski, 1877 (Perciformes: Odontobutidae) v vodoemakh Prut-Dnestrovskogo mezhdurechya. Academician Leo Berg – 135 years: Collection of Scientific Articles. EcoTyras, Bendery, 415–420. [in Russian]
- Movchan YV (1989) Pervaya nakhodka goloveshki (rotana) – *Percottus glehni* Dybowski (Pisces, Eleotridae) v vodoyemakh Ukrainy. Vestnik Zoologii 5: 1–87. [in Russian]
- Nabatov AA (1914) Komnatnyi Presnovodnyi Akvarium. Akvarium, Petrograd, 532 pp. [in Russian]
- Nehring S, Steinhof J (2015) First records of the invasive Amur sleeper, *Perccottus glenii* Dybowski, 1877 in German freshwaters: a need for realization of effective management measures to stop the invasion. BioInvasions Records 4(3): 223–232. <https://doi.org/10.3391/bir.2015.4.3.12>
- Nei M (1987) Molecular Evolutionary Genetics. Columbia University Press, New York, 522 pp. <https://doi.org/10.7312/nei-92038>
- Nijman V (2010) An overview of international wildlife trade from Southeast Asia. Biodiversity Conservation 19: 1101–1114. <https://doi.org/10.1007/s10531-009-9758-4>
- Plikšs M, Aleksejevs E (1998) Zivis. Gandrs, Riga, 304 pp. [in Latvian]
- Popa LO, Popa OP, Pisciă EI, Iftime A, Matacă S, Diaconu F, Murariu D (2006) The first record of *Perccottus glenii* Dybowski, 1877 (Pisces: Odontobutidae) and *Ameiurus melas* Rafinesque, 1820 (Pisces: Ictaluridae) from the Romanian sector of the Danube. Travaux du Muséum National d'Histoire Naturelle “Grigore Antipa” 49: 323–329.
- Pupina A, Pupins M, Skute A, Pupina Ag, Karklins A (2015) The distribution of the invasive fish Amur sleeper, rotan *Perccottus glenii* Dybowski, 1877 (Osteichthyes, Odontobutidae), in Latvia. Acta Biologica Universitatis Daugavpiliensis 15(2): 329–341.
- Pupins M, Pupina A (2012) Invasive fish *Perccottus glenii* in biotopes of *Bombina bombina* in Latvia on the north edge of the fire-bellied toad's distribution. Acta Biologica Universitatis Daugavpiliensis (Supplement 3): 82–90
- Pupins M, Pupina A (2018) Reciprocal predation between preserved and invasive species: adult *Bombina bombina* predate young white baits of alien fish *Perccottus glenii*. Acta Biologica Universitatis Daugavpiliensis 18(2): 217–223.
- Rakauskas V, Masiulytė R, Pikūnienė A (2016a) Predator-prey interactions between a recent invader, the Chinese sleeper (*Perccottus glenii*) and the European pond turtle (*Emys orbicularis*): a case study from Lithuania. Acta Herpetologica 11: 101–109. https://doi.org/10.13128/Acta_Herpetol-18261
- Rakauskas V, Stakėnas S, Virbickas T, Bukelskis E (2016b) Non-indigenous fish in the northern branch of the central European invasion corridor. Reviews in Fish Biology and Fisheries 26(3): 491–508. <https://doi.org/10.1007/s11160-016-9438-x>

- Ratnasingham S, Hebert PD (2007) BOLD: The barcode of life data system (<http://www.barcodinglife.org>). *Molecular Ecology Resources* 7: 355–364. <https://doi.org/10.1111/j.1471-8286.2007.01678.x>
- Rechulicz J, Płaska W, Nawrot D (2015) Occurrence, dispersion and habitat preferences of Amur sleeper (*Percottus glenii*) in oxbow lakes of a large river and its tributary. *Aquatic Ecology* 49: 389–399. <https://doi.org/10.1007/s10452-015-9532-5>
- Reshetnikov AN (2004) The fish *Percottus glenii*: history of introduction to western regions of Eurasia. *Hydrobiologia* 522: 349–350. <https://doi.org/10.1023/B:HYDR.0000030060.29433.34>
- Reshetnikov AN (2010) The current range of Amur sleeper *Percottus glenii* Dybowski, 1877 (Odontobutidae, Pisces) in Eurasia. *Russian Journal of Biological Invasions* 1(2): 119–126. <https://doi.org/10.1134/S2075111710020116>
- Reshetnikov AN (2013) Spatio-temporal dynamics of the expansion of rotan *Percottus glenii* from West-Ukrainian center of distribution and consequences for European freshwater ecosystems. *Aquatic Invasions* 8(2): 193–206. <https://doi.org/10.3391/ai.2013.8.2.07>
- Reshetnikov AN, Ficetola GF (2011) Potential range of the invasive fish rotan (*Percottus glenii*) in the Holarctic. *Biological Invasions* 13: 2967–2980. <https://doi.org/10.1007/s10530-011-9982-1>
- Reshetnikov AN, Schliwen UK (2013) First record of the invasive alien fish rotan *Percottus glenii* Dybowski, 1877 (Odontobutidae) in the Upper Danube drainage (Bavaria, Germany). *Journal of Applied Ichthyology* 29: 1367–1369. <https://doi.org/10.1111/jai.12256>
- Rizevski VK, Pliuta MV, Ermolaev VV (1999) Morfologicheskaja kharakteristika rotanogoloveshki (*Percottus glenii* Dybowski) iz vodoemov vodnoy sistemy Minska. *Vesti Natsiyanalnay akademii navuk Belarusi (Seria Biological Sciences)* 3: 119–121. [in Russian]
- Sabodash VM, Tkachenko VA, Tsyba AA (2002) Finding of a population of rotan *Percottus glenii* (Pisces, Odontobutidae) in water bodies of the Kiev Oblast. *Vestnik Zoologii* 36(2): 1–90. [in Russian]
- Saitou N, Nei M (1987) The neighbor-joining method: A new method for reconstructing phylogenetic trees. *Molecular Biology and Evolution* 4: 406–425. <https://doi.org/10.1093/oxfordjournals.molbev.a040454>
- Seleznev VV (1974) Malotsennyye i sornyye vidy ryb kitayskogo kompleksa v Kapchagayskom vodokhranilishche. In: *Rybnyye resursy vodoemov Kazakhstana i ikh ispolzovanie*, Issue 8. Kainar (Alma-Ata): 143–148. [in Russian]
- Semenchenko VP, Rizevsky VK, Mastitsky SE, Vezhnovets VV, Pluta MV, Razlutsky VI, Laenko T (2009) Checklist of aquatic alien species established in large river basins of Belarus. *Aquatic Invasions* 4(2): 337–347. <https://doi.org/10.3391/ai.2009.4.2.5>
- Syvokhop YM (1998) Pershi znakhidky rotana (*Percottus glenii* Dybowski) na Zakarpatti. *Tezy Studentskoyi Konferentsii, Seria Biologia, Patent No 3. Vydavnytsvo UDU, Uzhgorod*, 44–45. [in Ukrainian]
- Tajima F (1989) Statistical method for testing the neutral mutation hypothesis by DNA polymorphism. *Genetics* 123(3): 585–595.
- Weir BS, Hill WG (2002) Estimating F-statistics. *Annual review of genetics* 36: 721–750. <https://doi.org/10.1146/annurev.genet.36.050802.093940>

- Virbickas J (2000) Lietuvos žuvis. Ekologijos institutas, Vilnius, 192 pp. [in Lithuanian]
- Vitule JRS, Freire CA, Simberloff D (2009) Introduction of nonnative freshwater fish can certainly be bad. *Fish and Fisheries* 10: 98–108. <https://doi.org/10.1111/j.1467-2979.2008.00312.x>
- Xu W, Hou GY, Li CY, Kong XF, Zheng XH, Li JT, Sun XW (2013) Complete mitochondrial genome of Chinese sleeper, *Percottus glenii*. *Mitochondrial DNA* 24(4): 339–341. <https://doi.org/10.3109/19401736.2012.760081>
- Xu W, Yin W, Chen A, Li J, Lei G, Fu C (2014) Phylogeographical analysis of a cold-temperate freshwater fish, the Chinese sleeper (*Percottus glenii*) in the Amur and Liaohe river basins of Northeast Asia. *Zoological Science* 31(10): 671–679. <https://doi.org/10.2108/zs130046>

Supplementary material 1

Table S1. Table presents Chinese sleeper haplotypes frequency (belonging to three distinguished groups) found in studies sites.

Authors: Tomasz Rewicz, Michał Grabowski, Joanna Grabowska

Data type: distribution

Copyright notice: This dataset is made available under the Open Database License (<http://opendatacommons.org/licenses/odbl/1.0/>). The Open Database License (ODbL) is a license agreement intended to allow users to freely share, modify, and use this Dataset while maintaining this same freedom for others, provided that the original source and author(s) are credited.

Link: <https://doi.org/10.3897/neobiota.57.48958.suppl1>

Supplementary material 2

Table S2. Values of F_{ST} population pairwise.

Authors: Tomasz Rewicz

Data type: statistical data

Explanation note: Statistically significant values are shown in bold ($P \leq 0.05$).

Copyright notice: This dataset is made available under the Open Database License (<http://opendatacommons.org/licenses/odbl/1.0/>). The Open Database License (ODbL) is a license agreement intended to allow users to freely share, modify, and use this Dataset while maintaining this same freedom for others, provided that the original source and author(s) are credited.

Link: <https://doi.org/10.3897/neobiota.57.48958.suppl2>

Micro-habitat and season dependent impact of the invasive *Impatiens glandulifera* on native vegetation

Judith Bieberich^{1,2}, Heike Feldhaar², Marianne Lauerer¹

1 University of Bayreuth, Ecological Botanical Gardens, Bayreuth Center for Ecology and Environmental Research (BayCEER), Universitätsstraße 30, 95447 Bayreuth, Germany **2** University of Bayreuth, Animal Ecology I, Bayreuth Center for Ecology and Environmental Research (BayCEER), Universitätsstraße 30, 95447 Bayreuth, Germany

Corresponding author: Judith Bieberich (judith.bieberich@uni-bayreuth.de)

Academic editor: José Hierro | Received 20 February 2020 | Accepted 14 April 2020 | Published 17 June 2020

Citation: Bieberich J, Feldhaar H, Lauerer M (2020) Micro-habitat and season dependent impact of the invasive *Impatiens glandulifera* on native vegetation. NeoBiota 57: 109–131. <https://doi.org/10.3897/neobiota.57.51131>

Abstract

The impact of invasive species is often difficult to assess due to species × ecosystem interactions. *Impatiens glandulifera* heavily invaded several habitat types in Central Europe but its impact on native plant communities is rated ambiguously. One reason could be that the impact differs between habitat types or even between environmentally heterogeneous patches (micro-habitats) within one habitat type. In the present study a vegetation survey was performed within heterogeneous riverside habitats in Germany investigating the impact of *I. glandulifera* on native vegetation in dependence of environmental conditions. The vegetation was recorded in summer and spring because of seasonal species turnover and thus potentially different impact of the invasive plant. We found that the cover of *I. glandulifera* depended on environmental conditions resulting in a patchy occurrence. *I. glandulifera* did not have any impact on plant alpha-diversity but reduced the cover of the native vegetation, especially of the dominant species. This effect depended on micro-habitat and season. The native vegetation was most affected in bright micro-habitats, especially those with a high soil moisture. Not distinguishing between micro-habitats, plant species composition was not affected in summer but in spring. However, environmental conditions had a higher impact on the native vegetation than *I. glandulifera*. We conclude that within riparian habitats the threat of *I. glandulifera* to the native vegetation can be rated low since native species were reduced in cover but not excluded from the communities. This might be due to patchy occurrence and year-to-year changes in cover of *I. glandulifera*. The context-dependency in terms of micro-habitat and season requires specific risk assessments which is also an opportunity for nature conservation to develop management plans specific to the different habitats. Particular attention should be given to habitats that are bright and very wet since the effect of *I. glandulifera* was strongest in these habitats.

Keywords

context-dependency, early-flowering spring vegetation, environment, plant community, plant invasion, riverside vegetation

Introduction

Biological invasions are one aspect of anthropogenic global change. Invasive species can alter ecosystems processes, change native community structure and reduce diversity (Ehrenfeld 2010, Vilà et al. 2011). The success of an invader depends, among other things, on its ability to occupy various habitats. A broad tolerance to abiotic site factors can thus facilitate the establishment in different communities. Alternatively, superior fitness within a particular niche can lead to success in particular communities (MacDougall et al. 2009). Ecosystems in turn affect invasion processes (Kueffer et al. 2013) as site specific conditions can modify the performance of the invader and its interaction with other organisms. Since such species \times ecosystem interactions (Kueffer et al. 2013) make it difficult to generalize the impact of an invasive species on native ecosystems it is important to understand such context-dependencies. Knowledge of species \times ecosystem interactions helps to understand species invasions and allows nature conservation authorities to develop more targeted management plans, prioritizing those habitats where an invasive species should have highest impact.

A good model system to study plant species \times ecosystem interactions is *Impatiens glandulifera*. Originating from the Himalayan Mountain ranges, it now occurs all over Europe over a broad range of elevation, geographical latitude, and ecosystem types (Pyšek and Prach 1995, Larsson and Martinsson 1998, Kollmann and Bañuelos 2004, Pacanoski and Saliji 2014, Laube et al. 2015). After introduction to Europe in the 19th century it spread mainly along riverbanks and into wet habitats such as fens, mesotrophic grasslands, and woodland, but also forests out of the riparian zone, and into ruderal vegetation (Beerling and Perrins 1993, Pyšek and Prach 1993, 1995, Čuda et al. 2017). The invasion success of *I. glandulifera* is, among other factors, favored by a strong competitive and allelopathic effect, reducing the growth of native plants as seen in experimental studies (Vrchotová et al. 2011, Gruntman et al. 2014, Ruckli et al. 2014a, Loydi et al. 2015, Bieberich et al. 2018). However, field studies showed ambiguous results. In riparian habitats Cockel et al. (2014) and Hulme and Bremner (2006) found a strong negative impact of *I. glandulifera* on the native vegetation, while others found a weak impact in riparian habitats (Hejda and Pyšek 2006, Hejda et al. 2009, Diekmann et al. 2016) and in forests (Čuda et al. 2017). Sometimes the weak effect of *I. glandulifera* is thought to be due to high fluctuations in its population size (Kasperek 2004, Diekmann et al. 2016).

The impact of an invasive species can also depend on environmental conditions because its competitive ability depends on environmental conditions (Amarasekare 2003). Previous studies indicate that high soil nutrient availability and medium light is

beneficial for *I. glandulifera* growth (Andrews et al. 2005, Čuda et al. 2014). In a heterogeneous habitat the competitive environment for *I. glandulifera* and the residents can change from patch to patch determining which of the species becomes dominant and leading to a mosaic of the different species (Amarasekare 2003). Such a patchy occurrence of invasive and native species could facilitate spatial co-existence (Amarasekare 2003) and could be a reason for the overall low impact of the invader as found in some studies (Hejda and Pyšek 2006, Hejda et al. 2009, Diekmann et al. 2016, Čuda et al. 2017). Another possibility for species co-existence is temporal niche partitioning. In riparian habitats, especially forests, in the temperate region the plant community in spring often differs compared to summer due to seasonal species turnover with spring communities often being characterized by early flowering geophytes (Ellenberg and Leuschner 2010, Czapiewska et al. 2019).

We hypothesize that within heterogeneous riparian habitats, the impact of *I. glandulifera* on the resident vegetation depends on the environmental conditions at a particular patch (subsequently named micro-habitat) because the growth of *I. glandulifera* also depends on this. Regarding seasonal effects we hypothesize a lower impact of *I. glandulifera* in spring compared to summer because of species turnover, and in particular differences in *I. glandulifera* plant size and cover, thus competition for resources (Grime 1977, Goldberg 1990). In order to test our hypotheses we conducted a field study in Germany within riparian habitats in spring and summer. This is the first study on the impact on spring vegetation and on seasonal differences in the impact of *I. glandulifera* on native vegetation. Here we especially directly link the impact of *I. glandulifera* with environmental conditions.

Materials and methods

Study sites and plot design

Within five riparian field sites ranging from alder woods to abandoned meadows we systematically sampled (Table 1, Fig. 1) the environmental conditions and the vegetation. Each site comprises patches of *Impatiens glandulifera* and heterogeneous micro-habitats regarding tree cover and soil moisture. All sites are located in the region around Bayreuth, Germany at an elevation between 345 m a.s.l. and 426 m a.s.l.. Within each site, plots were arranged on a grid of 20 m × 20 m. Every grid intersection point was used as position for a plot of 2 m × 2 m, independently of environmental condition, *I. glandulifera* or native vegetation cover (Fig. 1). This systematic design allowed us a representative sampling over the whole gradient of environmental conditions and *I. glandulifera* cover and regression analysis instead of comparison between invaded and uninvaded plots only. Across the five sites 114 plots of 2 m × 2 m were established in total (Table 1). In spring two plots were not accessible because of a very high soil water content and one plot was hit by a fallen tree, decreasing the number of replicates to 111 in spring.

Table 1. Field sites used for this study. For each site the main habitat type, the name of the next locality and the adjacent river is given as well as the GPS-location, approximate area and number of established plots.

Main habitat	alder forest	alder swamp forest	abandoned meadow	abandoned meadow	abandoned meadow
Next town	Ludwigschorgast	Neunkirchen	Weidenberg	Pegnitz	Waischenfeld
GPS-location	50°6.66'N	49°55.20'N	49°56.95'N	49°46.84'N	49°49.98'N
	11°35.20'E	11°38.05'E	11°42.15'E	11°32.80'E	11°20.17'E
Area	20000 m ²	7000 m ²	16000 m ²	4000 m ²	9000 m ²
n plots summer	44	17	27	11	15
n plots spring	44	15	27	11	14

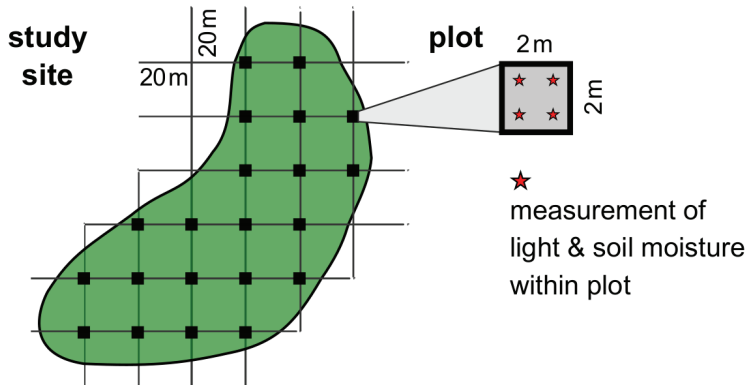


Figure 1. Plot design used for this study. Plots were arranged on a grid laid over the study site. Positions for light and soil moisture measurements within each plot are marked.

Data collection

The herb layer vegetation was surveyed in summer while *I. glandulifera* was flowering (2016-07-12/08-17), and in spring while the spring geophytes were flowering (2017-04-20/05-04). All vascular plant species were determined using standard literature (Schmeil et al. 2011, Eggenberg and Möhl 2013, Jäger et al. 2013, Aas 2017, Jäger 2017), and their cover was estimated according to extended Braun-Blanquet scale (Braun-Blanquet 1964, Reichelt and Wilmanns 1973). Additionally the maximum height of the vegetation, and in summer 2017 the cover of *I. glandulifera* was measured as described in Suppl. materials 1, 2. The environmental variables volumetric soil water content, light (relative photosynthetically active radiation), tree layer species composition and cover, and Ellenberg indicator values were gathered once in each plot in summer. The volumetric soil water content (named soil water content hereafter) was measured on 2017-05-23/05-28 in the uppermost soil layer with a SM-150 sensor (Delta-T Devices). Recordings were taken at four positions per plot and their median was calculated (Fig. 1). Relative photosynthetically active radiation (PAR, Parent and Messier 1996, Gendron et al. 1998) was measured with Quantum sensors (LICOR) when trees were fully foliate (2016-08-03/10-03). In the plot four single point records were taken just above the herb layer (Fig. 1). Simultaneously a reference value was taken at a totally unshaded site nearby

using a second Quantum sensor. This sensor was connected to a BayEOS logger (Bay-CEER, University of Bayreuth) taking records every 30 s and saving them as means over 5 minutes. Relative PAR was calculated with the median of the point records within the plots divided by the particular logged reference matching in time. All light measurements were taken under a homogeneous overcast sky with the sun invisible and no rain, and always between 11:00 and 17:00. The tree layer was characterized estimating the cover of each tree species separately (2017-08-17/09-07) according to extended Braun-Blanquet scale (Braun-Blanquet 1964, Reichelt and Wilmanns 1973). Mean Ellenberg indicator values for light L, soil moisture F, soil nutrients N, and soil reaction R were calculated per plot based on the summer vegetation. Based on additional information included in the F-value, the percentage of plants preferring either periodically wet soils or constantly wet soils was calculated. Hereafter, these parameters are named index of periodically wet soil and index of constantly wet soil.

Statistical analysis

All statistical analyses were done with the software package R 3.5.2 (R Core Team 2018). To find the polynomial model best describing the dependence of cover of *I. glandulifera* on light and soil water content a multiple regression analysis was performed. To identify environmental variables affecting the cover of *I. glandulifera*, we performed an automated model selection (Bartoń 2018) separately for summer and spring vegetation. First of all a global model was built with the cover of *I. glandulifera* as response variable and 13 predictor variables that were expected to affect the cover of *I. glandulifera*: relative PAR (squared because of hump-shaped relationship), soil water content (squared), number of tree species, cover of these tree species occurring at least in 20 plots (*Alnus glutinosa*, *Salix fragilis*, *Acer pseudoplatanus*, *Fraxinus excelsior*, *Betula pendula*), Ellenberg values N, R, and indices for periodically or constantly wet soils. Ellenberg values L, and F were excluded because they correlated with relative PAR and soil water content, (Pearson correlation coefficient 0.549 and 0.544 respectively). All variables were standardized to zero mean and unit variance (VEGAN, (Oksanen et al. 2018)). For analysis of spring vegetation, the cover of *I. glandulifera* was log-transformed to counter heteroscedasticity of the model. The study site was considered as a random factor (NLME, (Pinheiro et al. 2018)). Next a set of models with combinations of all parameters was generated from the global model and the models were weighted by their AICc (MuMIn, (Bartoń 2018)). Models with $\Delta AICc > 2$ were used to calculate the relative importance of each variable as the sum of AICc weights of all models including the variable.

Using the variables resulting from the model selection, we performed a piecewise structural equation model (piecewiseSEM, (Lefcheck 2016)) to test the effects of the environmental variables on *I. glandulifera*, and how in turn *I. glandulifera* affects the resident vegetation (all species except *I. glandulifera*). This also allowed us to infer whether the resident vegetation is more affected by *I. glandulifera* or by the environment based on the regression coefficients of the SEM. The resident vegetation was represented by species number, total

cover (sum of the cover of all resident species in a plot) and the cover of those herbaceous species occurring in more than 20 plots. The construction of the initial models is visualized in Suppl. material 3, Fig. 1. The SEMs were fitted separately for summer and spring vegetation, and within the models the study site was considered as a random factor. For each path in the piecewise structural equation model, a standardized regression coefficient (β) and its significance were calculated as well as conditional R^2 -values for all response variables.

To analyze plant community composition in summer, or respectively spring, we performed a Detrended Correspondence Analysis of the cover of the resident plant species with downweighting of rare species (DCA, package VEGAN (Oksanen et al. 2018)). DCA was confirmed to be appropriate because the DCA-axis gradient length was more than four times the standard deviation. Cover of *I. glandulifera*, as well as environmental parameters, were post-hoc fitted into the DCA result. Additionally, a Constrained Correspondence Analysis (CCA, VEGAN) was performed with the same data constraining the resident community with *I. glandulifera* cover. With an ANOVA-like permutation test (VEGAN) significance of the constraints was tested.

With the summer dataset of the year 2016, we analyzed whether the impact of *I. glandulifera* on the resident vegetation differed between micro-habitat groups. The groups were created by dividing the dataset according to the median of light (23.9 % PAR) and soil water content (51.5 %). Subsequently, they are named moist–bright ($n = 30$), wet–bright ($n = 28$), moist–dark ($n = 27$) and wet–dark ($n = 29$). For each of this groups separately and for the complete dataset impact of *I. glandulifera* on various variables representing the resident vegetation was analyzed: Impact on species number, Shannon-index and total plant cover was tested with linear models. Some parameters in the wet–dark group were log-transformed to counter heteroscedasticity of the models. Impact on cover of *Filipendula ulmaria*, *Phalaris arundinacea* and *Urtica dioica* was tested with a quantile regression (R package QUANTREG (Koenker 2018)) because data were not homogenous in variance hence linear regression was not the appropriate test (Cade and Noon 2003). We took the 0.50, 0.75, 0.85 and 0.95 quantiles emphasizing the upper quantiles because after visual inspection of the data we expected *I. glandulifera* to especially restrict maximum cover of other plants. For each quantile regression, standard errors and p -values were calculated by bootstrap analysis. Impact of *I. glandulifera* on community composition was tested with a DCA (with downweighting of rare species) and with CCA (VEGAN).

Results

Vegetation characteristics

I. glandulifera occurred in about 80 % of all plots in summer (87 of 114) and in spring (91 of 111, Fig. 2). Especially in spring the cover of *I. glandulifera* was often very low and rarely above 25 %. In summer *I. glandulifera* reached more than 50 % cover in 28 plots. By summer 2017 the cover of *I. glandulifera* changed largely in few plots (Suppl.

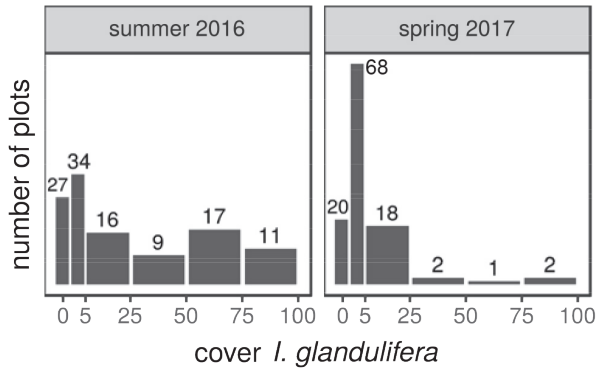


Figure 2. Distribution of cover of *Impatiens glandulifera* in summer 2016 and spring 2017. Shown categories correspond to the Braun-Blanquet scale.

material 1). In summer, *I. glandulifera* plants were higher than the resident vegetation if they reached more than 20 % cover, while in spring *I. glandulifera* was always lower than the resident vegetation (Suppl. material 2). The resident vegetation consisted of in total 128 plant species in summer 2016 and 109 in spring 2017 ranging from 2 to 20 species per plot. None of these plant species was an endangered one. Besides *I. glandulifera* further alien species were recorded: *Lamium argentatum* occurred in 14 plots, sometimes reaching more than 75 % cover. *Fallopia japonica*, *Lysimachia punctata*, *Bidens frondosa* and *Epilobium ciliatum* each occurred in only one plot with always less than 5 % cover. Most frequent native species were typical ones of tall herbaceous vegetation at riparian sites (Fig. 4A, B). Especially *Urtica dioica*, *Filipendula ulmaria*, and *Phalaris arundinacea* in summer, and additionally the geophytes *Ranunculus ficaria* and *Anemone nemorosa* in spring could reach cover of more than 50 %. In spring further early flowering species such as *Corydalis cava*, *Caltha palustris*, *Polygonum bistorta*, *Cardamine amara* and *Alliaria petiolata* occurred.

Relationship between environmental variables, cover of *Impatiens glandulifera* and the resident vegetation

Light (relative PAR) and soil water content spanned nearly the whole gradient from 0–100 %. However, Ellenberg values that correlated with light and soil moisture showed rather smaller gradients (L-value for light 4–7.5, F-value for soil moisture 5.5–9.3) indicating that there were medium light conditions and no sites with dry soils. *I. glandulifera* occurred over the whole range of light and soil water content measured in this study, but in summer it reached high cover mainly at 50–70 % light and 30–40 % soil water content (Fig. 3). The relationship between *I. glandulifera* and light and soil water content was hump-shaped being a typical species reaction on a long environmental gradient (light: linear model: $f(x) = x + x^2 + x^3$, $F_{(3,110)} = 7.221$, $R^2 = 0.142$, $p < 0.001$).

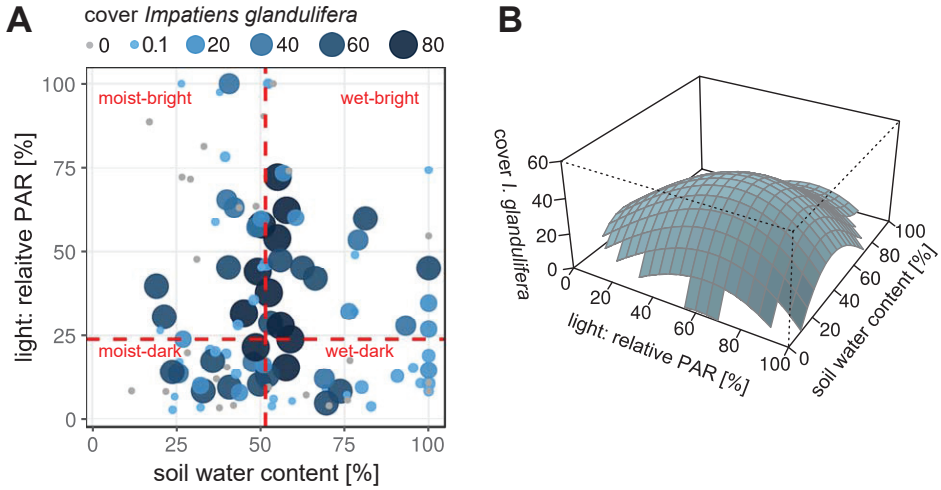


Figure 3. Cover of *Impatiens glandulifera* in summer 2016 in dependence of light and volumetric soil water content. **A** Cover of *I. glandulifera* is represented by point size and color as given in the legend. Grouping the plots into the micro-habitats moist–bright, wet–bright, moist–dark and wet–dark is based on the medians of light and soil water content. **B** Fitted function of the same data shown in 3d-space. $f(\text{cover}) = \text{light} + \text{light}^2 + \text{light}^3 + \text{water content} + \text{water content}^3$. Linear model, $R^2 = 0.208$, $F_{(5,108)} = 6.928$, $p < 0.001$, $n = 114$.

Notably soil water content on its own had only low explanatory power (linear model, $f(x) = x + x^3$, $F_{(2,111)} = 4.88$, $R^2 = 0.064$, $p = 0.009$) but in combination with light the R^2 increased to 0.208 (Fig. 3A, B).

The piecewise SEM revealed that in summer 39 % of the variation in the cover of *I. glandulifera* was explained by the environmental variables identified as important by the model selection ($R^2 = 0.39$, Fig. 4A, Suppl. material 4: Table S1). The reaction of *I. glandulifera* to light was unimodal hence the cover was highest at moderate light ($\beta = -0.294$). The cover of *I. glandulifera* was enhanced by a high Ellenberg value N for nutrients and by periodically wet soils (Fig. 4A). In contrast it was reduced by constantly wet soil and cover of the specific tree species *Acer pseudoplatanus*, *Fraxinus excelsior*, and *Alnus glutinosa*. In turn, *I. glandulifera* had no impact on the number of plant species but on plant cover. It strongly reduced the cover of *U. dioica* ($\beta = -0.387$), slightly that of *F. ulmaria* (not significant, $p = 0.073$) and the total cover of the resident vegetation. Besides the effect of *I. glandulifera* the parameters representing the resident vegetation were mainly directly affected by the environmental variables. For example, the number of plant species increased with the number of tree species and strongly decreased with increasing Ellenberg value N. Cover of *U. dioica* was determined by Ellenberg value N, index of constant wet soil and by cover of *A. glutinosa* similarly to *I. glandulifera*.

The piecewise SEM on spring vegetation showed that 30 % of the variation of the *I. glandulifera* cover was explained by the environmental variables identified as important by the model selection (Fig. 4B, Suppl. material 4: Table S1). As in sum-

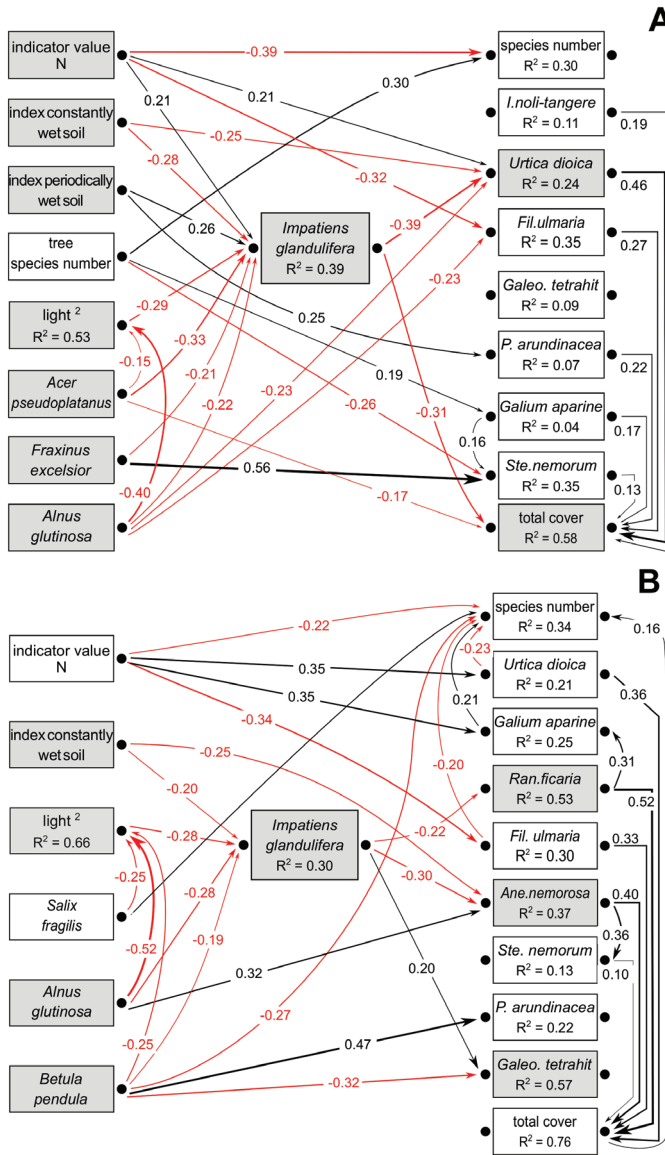


Figure 4. Results of the piecewise structural equation modeling for summer (A) and spring (B). Arrows show significant correlations between the environmental variables shown to be important by the model selection (Suppl. material 4, Table 1), cover of *Impatiens glandulifera* and resident vegetation parameters. Included resident species are the most frequent ones: *Ranunculus ficaria* (*Ran.ficaria*), *Urtica dioica*, *Filipendula ulmaria* (*Fil.ulmaria*), *Galium aparine*, *Anemone nemorosa* (*Ane.nemorosa*), *Phalaris arundinacea* (*Parundinacea*), *Galeopsis tetrahit* (*Galeo.tetrahit*), *Stellaria nemorum* (*Ste.nemorum*) and *Impatiens noli-tangere* (*I.noli-tangere*). Arrows show significant correlations, red arrows negative ones, black arrows positive ones. The thicker the arrows, the higher are the standardized regression coefficients (β), which are stated next to the arrows. R^2 values for the component models are given within the boxes of all response variables. Variables that are directly connected to *I. glandulifera* are highlighted by gray colored boxes. For the spring model cover of *I. glandulifera* was log-transformed. n = 114 plots for summer, n = 111 for spring.

mer, constantly wet soils and cover of the tree species *A. glutinosa* and *Betula pendula* reduced the cover of *I. glandulifera*, and reaction to light was unimodal (Fig. 4B). In contrast to summer, periodically wet soils were not found to be important (model selection, Suppl. material 4: Table S1), and the increase of *I. glandulifera* cover with increasing Ellenberg value N was not significant (SEM, Fig. 4B). Also *I. glandulifera* did not affect *U. dioica* and total plant cover, and the cover of *Galeopsis tetrahit* was even slightly increased. However, the cover of *R. ficaria* and *A. nemorosa* were reduced by *I. glandulifera*. The resident vegetation was mainly directly affected by the environmental variables and by interactions between the resident species. For example, the cover of *R. ficaria* and *G. aparine* were positively correlated and the cover of *U. dioica* and *R. ficaria* reduced the species number.

In summer *I. glandulifera* had no impact on plant community composition: The cover of *I. glandulifera* did not correlate with the axes of a DCA of the resident community ($p = 0.222$, Fig. 5) and was not able to constrain resident community in a CCA ($p = 0.116$, without figure). In contrast the resident plant community in spring was strongly affected by the cover of *I. glandulifera* of the previous summer 2016 ($p < 0.001$, DCA; $p = 0.052$, CCA; Fig. 5), and slightly by current cover in spring 2017 ($p = 0.048$, DCA; $p = 0.551$, CCA). In summer and in spring the resident plant community was also shaped by most of those environmental variables important for the cover of *I. glandulifera* (Fig. 5).

Micro-habitat specific impact of *Impatiens glandulifera* on the resident vegetation in summer

With the summer dataset four micro-habitat groups were created reflecting different conditions of light and soil water content (Fig. 3). These groups differed in their plant community composition (DCA $p = 0.008$, CCA $p = 0.001$). In each group the cover of *I. glandulifera* ranged from 0 to at least 80 % but its mean differed between groups, being highest in the wet–bright group (Table 2). The impact of *I. glandulifera* on plant cover was different between micro-habitat groups (Table 2, Suppl. material 6: Fig. S2). The cover of *I. glandulifera* reduced the total plant cover in all micro-habitat except for the wet–dark group. The cover of *U. dioica* was reduced in the moist–bright and wet–dark groups, as well as the cover of *F. ulmaria* in the two bright micro-habitats. These were exactly those micro-habitats where the highest average cover of these species was observed (Table 2, Suppl. material 6: Fig. S2). In contrast, the cover of *Phalaris arundinacea* was not negatively affected at all, but its cover slightly increased with the cover of *I. glandulifera* under low light conditions. *I. glandulifera* had no impact on plant species number and Shannon-index in any micro-habitat group. In contrast plant species composition was changed under bright conditions especially with high soil water content. Within the wet–bright micro-habitat for example *Calystegia*

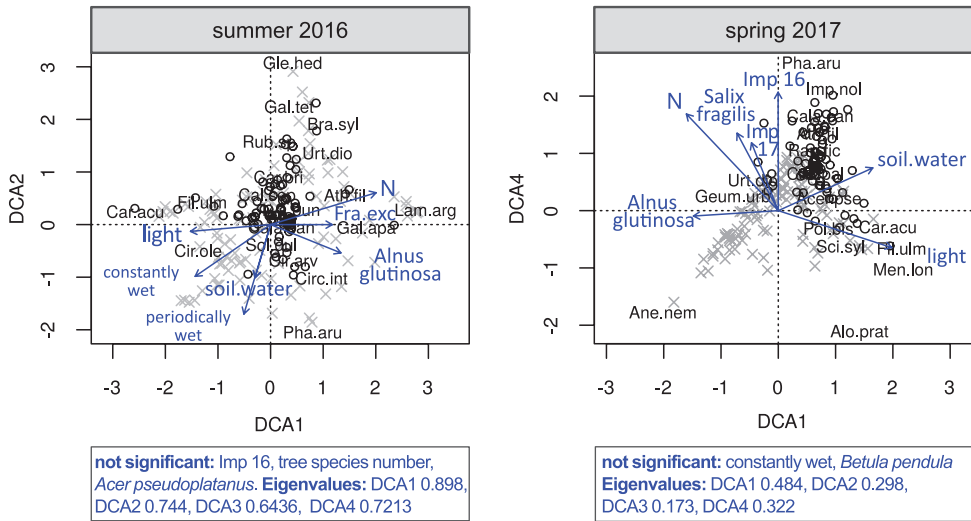


Figure 5. Ordination (DCA) of the resident plant community in summer 2016 and spring 2017. Cover of *I. glandulifera* in summer 2016 (Imp 16) and in spring 2017 (Imp 17) and important environmental variables (Suppl. material 4, Table 1) as well as volumetric soil water content (soil.water) were post-hoc fitted onto the DCA. Significant variables are shown as arrows. Plots are indicated as crosses, species as open circles. Most abundant species are labeled. Not significant environmental variables and Eigenvalues of DCA axes are given in boxes below the plots. $n = 114$ plots for summer, $n = 111$ for spring. For abbreviations of the species names see Suppl. material 5: Table S2.

sepium, *Glechoma hederacea*, and *Polygonum bistorta* tended to occur at high cover of *I. glandulifera* (CCA). In contrast *Carex acutiformis*, *Geranium palustre* and also some species of very wet plots as *Galium elongatum* and *Equisetum fluviatile* occurred at low cover of *I. glandulifera* (Suppl. material 7: Fig. S3). Considering all parameters representing the native vegetation *I. glandulifera* had the lowest impact in the wet–dark micro-habitat where also the cover of *I. glandulifera* was lowest.

Discussion

In this field study, we examined the impact of *Impatiens glandulifera* on native vegetation in riparian habitats depending on micro-site conditions and season. We found that the cover of *I. glandulifera* depended on environmental conditions. *I. glandulifera* did not affect resident plant species alpha-diversity at all. Plant cover in contrast was reduced and species composition changed depending on micro-habitat and season. However, the resident vegetation was more strongly shaped by environmental conditions than by the cover of *I. glandulifera*.

Table 2. Micro-habitat specific impact of *I. glandulifera* on the resident vegetation. With the complete dataset and four subsets representing different micro-habitats regarding light (relative PAR) and soil water content (see also Fig. 3) it was tested whether vegetation parameters depend on cover of *I. glandulifera*. Resulting *p*-values from linear models (total cover, species number, Shannon index), DCA and CCA (species composition) are given. Log-transformations of data are indicated: (log-log) means predictor and response variable transformed, (log) means response variable transformed. For quantile regression (cover of *Filipendula ulmaria*, *Phalaris arundinacea* and *Urtica dioica*) 0.50, 0.75, 0.85 and 0.95 quantiles were used (τ). Quantile regressions with ($p < 0.1$) are reported including their regression equation. Bold letters indicate $R^2 > 0.1$ and $p < 0.001$. Number of plots and mean cover of *I. glandulifera* (\bar{x}_{Imp}) are given per group. Different letters indicate whether there are differences in the \bar{x}_{Imp} between groups (Kruskal-Wallis Anova, $\chi^2 = 10.6$, $df = 3$, $p = 0.014$). See Suppl. material 6, 7: Fig. S2 and S3 for plots of the raw data.

parameter	quantile	complete dataset n = 114 $\bar{x}_{\text{Imp}} = 23\%$	moist-bright n = 30 $\bar{x}_{\text{Imp}} = 22\%$ (ab)	wet-bright n = 28 $\bar{x}_{\text{Imp}} = 39\%$ (a)	moist-dark n = 27 $\bar{x}_{\text{Imp}} = 20\%$ (ab)	wet-dark n = 29 $\bar{x}_{\text{Imp}} = 13\%$ (b)
total cover		$F_{(1,112)} = 27.3$, $p < \mathbf{0.001}$, $R^2 = \mathbf{0.189}$	$F_{(1,28)} = 28.44$, $p < \mathbf{0.001}$, $R^2 = \mathbf{0.486}$	$F_{(1,26)} = 9.59$, $p = \mathbf{0.005}$, $R^2 = \mathbf{0.241}$	$F_{(1,25)} = 8.12$, $p = \mathbf{0.009}$, $R^2 = \mathbf{0.215}$ (log)	$F_{(1,27)} = 3.62$, $p = 0.068$, $R^2 = 0.086$ (log)
cover <i>Urtica dioica</i>	τ 0.50					
	τ 0.75		$p = \mathbf{0.023}$, $f(x) = 63 - 0.67x$			
	τ 0.85	$p = \mathbf{0.003}$, $f(x) = 63 - 0.61x$	$p < \mathbf{0.001}$, $f(x) = 87.5 - 0.90x$			
	τ 0.95	$p = 0.052$, $f(x) = 87.5 - 0.67x$	$p < \mathbf{0.001}$, $f(x) = 87.8 - 0.68x$			$p = \mathbf{0.022}$, $f(x) = 63 - 0.69x$
cover <i>Filipendula ulmaria</i>	τ 0.50			$p = 0.056$, $f(x) = 21 - 0.21x$		
	τ 0.75	$p = 0.057$, $f(x) = 21 - 0.14x$	$p = 0.094$, $f(x) = 36 - 0.41x$			
	τ 0.85		$p = \mathbf{0.046}$, $f(x) = 49 - 0.56x$	$p = \mathbf{0.050}$, $f(x) = 63 - 0.62x$		
	τ 0.95	$p = \mathbf{0.030}$, $f(x) = 63 - 0.6x$	$p < \mathbf{0.001}$, $f(x) = 88 - 1.0x$	$p = \mathbf{0.032}$, $f(x) = 88 - 0.81x$		
cover <i>Phalaris arundinacea</i>	τ 0.50	$p = \mathbf{0.039}$, $f(x) = 0 + 0.03x$			$p = 0.053$, $f(x) = 0 + 0.03x$	
	τ 0.75					$p = \mathbf{0.013}$, $f(x) = 2 + 0.57x$
	τ 0.85					$p = 0.052$, $f(x) = 3 + 0.56x$
	τ 0.95	$p = 0.093$, $f(x) = 37.5 + 0.8x$				
species number		$F_{(1,112)} = 2.16$, $p = 0.145$, $R^2 = 0.010$	$F_{(1,28)} = 2.54$, $p = 0.122$, $R^2 = 0.051$	$F_{(1,26)} = 2.76$, $p = 0.109$, $R^2 = 0.061$	$F_{(1,25)} = 1.80$, $p = 0.191$, $R^2 = 0.030$	$F_{(1,27)} = 0.04$, $p = 0.846$, $R^2 = -0.036$ (log-log)
Shannon index		$F_{(1,112)} = 0.52$, $p = 0.472$, $R^2 = -0.004$	$F_{(1,28)} = 0.12$, $p = 0.728$, $R^2 = -0.031$	$F_{(1,26)} = 0.05$, $p = 0.833$, $R^2 = -0.037$	$F_{(1,25)} = 2.86$, $p = 0.103$, $R^2 = 0.067$	$F_{(1,27)} = 0.37$, $p = 0.547$, $R^2 = 0.023$ (log-log)
species composition: DCA		$p = 0.222$	$p = 0.099$	$p = \mathbf{0.032}$	$p = 0.715$	$p = 0.401$
CCA		$p = 0.116$	$p = \mathbf{0.016}$	$p = \mathbf{0.001}$	$p = 0.891$	$p = 0.823$

Patchiness of *Impatiens glandulifera* is associated with environmental conditions

Within our study sites, *I. glandulifera* occurred over a broad range of environmental conditions but it was unevenly distributed within the sites forming invaded and uninvaded patches. Its cover correlated with environmental variables. A positive effect of nutrients and moderate light as well as low importance of soil water content (measured at one point in time), is consistent with literature (Andrews et al. 2005, Čuda et al. 2014). However, we showed that soil water content in combination with light was a good predictor for the cover of *I. glandulifera*, with the cover being highest at moderate light and moderate soil water content. Ellenberg values indicated moreover that constantly high soil moisture had a negative effect on the cover but in summer periodically wet soils were favorable. A high N-supply is also more important in summer than for early establishment in spring. Considering a larger spatial scale, such a patchy occurrence can enable the co-existence of species that would outcompete each other within one patch (Amarasekare 2003). For example, in our study *I. glandulifera* and *U. dioica* coexisted within one study site forming a patchy mosaic.

***Impatiens glandulifera* had no impact on plant diversity but on plant cover**

We found that *I. glandulifera* reduced the cover of the resident vegetation but it had no impact on species composition in summer or on plant species alpha-diversity at all. Thus the resident plant species seem to be able to coexist within *I. glandulifera* stands, albeit reaching only lower cover. Changes in *I. glandulifera* cover from year-to-year as they are reported in literature (Kasperek 2004) and which were also observed in our study, should then enable the resident plants to recover when *I. glandulifera* declines leading to co-existence at a larger time-scale (Stouffer et al. 2018).

I. glandulifera especially reduced the cover of the most dominant native species. Species were most affected in those micro-habitats where their average cover was highest and in each season those species with the highest cover were the most affected ones. These were *Urtica dioica* and *Filipendula ulmaria* in summer, and *Ranunculus ficaria* and *Anemone nemorosa* in spring. We suggest that this is due to competition for space and resources strengthening at high cover. Still, it cannot be ruled out that also less frequent species with lower cover are affected by *I. glandulifera*. Rare occurrence and thus small sample size of a species as well as huge variability result in low statistical power and may lead to an underestimation of the effect of the invader (Davidson and Hewitt 2014).

Similar to other studies comparing plots with and plots without *I. glandulifera*, we are not able to show a causal impact of *I. glandulifera* on native vegetation but only correlations (Hejda and Pyšek 2006). However, in our study the link to environmental conditions can help to disentangle negative correlation because of different spatial niches from negative correlation because of suppression within one spatial niche.

A. nemorosa and *I. glandulifera* could be an example for different spatial niches, because *A. nemorosa* was enhanced by a high cover of *Alnus glutinosa* which in contrast reduced the cover of *I. glandulifera*. *U. dioica* however, seems causally suppressed by *I. glandulifera*. The cover of both species correlated negatively, and according to the SEM they were favored by the same environmental conditions. Experimental studies confirm that *U. dioica* is negatively affected by *I. glandulifera* and that this effect is larger than vice versa (Tickner et al. 2001, Gruntman et al. 2014, Bieberich et al. 2018).

The impact of *Impatiens glandulifera* depended on the micro-habitat

The habitat depending impact of *I. glandulifera* indicates that the impact gets stronger with increasing cover of *I. glandulifera*. This is also indicated by Cockel et al. (2014). In our study the wet–dark micro-habitat with the lowest cover of *I. glandulifera*, was the least affected. The plant species composition was most affected in the wet–bright micro-habitat which had also a strong gradient and highest average cover of *I. glandulifera*. Species that tended to occur only in plots without *I. glandulifera* generally occurred less frequently (for example *Equisetum fluviatile*) while those that tended to occur at high cover of *I. glandulifera* (for example *Glechoma hederacea*) were very common ones.

Micro-habitat specific interactions between native species and an invader can also be due to micro-habitat specific performance of the plant species. If two C-strategists compete for resources, which should be the case with our dominant species, the magnitude of competition is highest under most favorable as well as under most unfavorable environmental conditions (stress-gradient hypothesis, Maestre et al. 2009). In the strongly competitive situation inferiority of the natives in fitness leads to suppression by the invader (MacDougall et al. 2009). We suggest that this can explain the micro-habitat depending impact of *I. glandulifera* on *U. dioica* and *F. ulmaria*. Both natives were most reduced by *I. glandulifera* when they grew under environmental conditions that were, according to the SEM, most favorable for them (*U. dioica* in the moist–bright group and *F. ulmaria* in bright micro-habitats). *U. dioica* was additionally negatively affected by *I. glandulifera* in the wet–dark micro-habitat which was shown by the SEM to be unfavorable for *U. dioica*.

Plant communities in summer and spring were affected differently

Plant species composition in summer was not affected by *I. glandulifera* but in spring it was, despite the fact that *I. glandulifera* plants were smaller than the resident vegetation in spring. The reason could be a seasonally varying allelopathic effect of *I. glandulifera* because it is known, that in spring *I. glandulifera* has a higher content of the allelopathic compound 2-MNQ compared to summer (Ruckli et al. 2014a). In a previous experimental study we showed that *I. glandulifera* has a species-specific allelopathic and competitive impact on native plants especially in the seedlings- and juvenile-stage (Bieberich et al. 2018). Furthermore, cover of *I. glandulifera* from the previous sum-

mer 2016 affected species composition in spring while it did not affect the resident community in summer 2016 itself. Allelopathic legacy effects (Grove et al. 2012) may explain this: 2-MNQ could persist in the soil (Ruckli et al. 2014b) and affect early growing plants even before *I. glandulifera* germinates.

Assessment of the invasiveness of *Impatiens glandulifera*

Negative impact on biodiversity and ecosystem functions, processes and services are the criteria to grade an alien species as invasive (Ehrenfeld 2010, Hulme et al. 2013, Barney et al. 2013). German and European Union nature conservation authorities emphasize the impact on diversity and threat to other species (European Union 2014, Nehring et al. 2015). Taking this study and all available ones into account, the impact of *I. glandulifera* on plant species diversity can be rated to be relatively low (Hejda and Pyšek 2006, Hejda et al. 2009, Diekmann et al. 2016, Čuda et al. 2017) even if some studies showed stronger effects (Hulme and Bremner 2006, Cockel et al. 2014, Kiełtyk and Delimat 2019). Indeed, we found a negative impact on the dominant natives, *U. dioica* and *F. ulmaria*, but they are in general very common and widespread in Central Europe and thus not expected to be threatened (Schreiber 1958, Weber 1995). However, suppression of abundant dominant plant species could lead to changes in ecosystem processes as they account for functions such as primary production and nutrient cycles (Grime 1998).

The micro-habitat and season dependent impact of *I. glandulifera* requires that its invasion risk has to be assessed separately for different habitats. We found the lowest impact in the wet–dark micro-habitat which corresponds to alder swamp-forests. The impact was highest at bright conditions, as abandoned meadows, but especially under high soil moisture as found in marshes or open patches of swamp-forests. Special attention should be given to habitats with rare or specialized communities or with distinct spring communities. For nature conservation this is a great opportunity to develop more targeted management strategies of *I. glandulifera* and invasive species in general with vigorous efforts only in selected habitats.

Conclusion

I. glandulifera can reduce the cover of native plants and especially dominant species depending on micro-habitat and season. Against our expectations, we did not find that the vegetation in spring was less affected than in summer. A threat to the native vegetation is unlikely since the impact on plant alpha-diversity was low, which may be due to the patchy occurrence and year-to-year changes in the cover of *I. glandulifera*. However it has to be kept in mind that a reduction of dominant and frequent native plant species could change ecosystem processes. We suggest that the documented small-scale habitat-dependency is also relevant on larger spatial scales. Wet–dark habitats like swamp-forests should be generally least affected by *I. glandulifera* while wet–bright ones like marshes are most affected.

Acknowledgments

We would like to thank the Bavarian state water authority (Wasserwirtschaftsamt) Hof, especially Ludwig Schmidt, for providing the study sites, Alfred Bolze for support in the plant species determination, and Lionel S. Vailshery for proofreading the manuscript.

Judith Bieberich was funded by the Cusanuswerk (Bischöfliche Studienförderung), the Bayreuth Center for Ecology and Environmental Science (BayCEER), and the Bayreuth University Graduate School. This publication was funded by the German Research Foundation (DFG) and the University of Bayreuth in the funding program Open Access Publishing.

The authors have declared that no competing interests exist.

References

- Aas G (2017) Bäume und Sträucher – Bestimmung wild wachsender Gehölze Mitteleuropas vorrangig nach vegetativen Merkmalen. (Bayreuth): 1–243.
- Amarasekare P (2003) Competitive coexistence in spatially structured environments: a synthesis. *Ecology Letters* 6: 1109–1122. <https://doi.org/10.1046/j.1461-0248.2003.00530.x>
- Andrews M, Maule HG, Raven JA, Mistry A (2005) Extension growth of *Impatiens glandulifera* at low irradiance: importance of nitrate and potassium accumulation. *Annals of Botany* 95: 641–648. <https://doi.org/10.1093/aob/mci059>
- Barney JN, Tekiel DR, Dollete ES, Tomasek BJ (2013) What is the “real” impact of invasive plant species? *Frontiers in Ecology and the Environment* 11: 322–329. <https://doi.org/10.1890/120120>
- Bartoń K (2018) MuMIn: Multi-Model Inference. <https://cran.r-project.org/package=MuMIn>
- Berling DJ, Perrins J (1993) *Impatiens glandulifera* Royle (*Impatiens roylei* Walp.). *Journal of Ecology* 81: 367–382. <https://doi.org/10.2307/2261507>
- Bieberich J, Lauerer M, Drachler M, Heinrichs J, Müller S, Feldhaar H (2018) Species- and developmental stage-specific effects of allelopathy and competition of invasive *Impatiens glandulifera* on co-occurring plants. *PLoS ONE* 13: e0205843. <https://doi.org/10.1371/journal.pone.0205843>
- Braun-Blanquet J (1964) *Pflanzensoziologie: Grundzüge der Vegetationskunde*. Springer (Wien): 1–865. https://doi.org/10.1007/978-3-7091-8110-2_1
- Cade BS, Noon BR (2003) A gentle introduction to quantile regression for ecologists. *Frontiers in Ecology and the Environment* 1: 412–420. [https://doi.org/10.1890/1540-9295\(2003\)001\[0412:AGITQR\]2.0.CO;2](https://doi.org/10.1890/1540-9295(2003)001[0412:AGITQR]2.0.CO;2)
- Cipollini KA, Schradin KD (2011) Guilty in the court of public opinion: testing presumptive impacts and allelopathic potential of *Ranunculus ficaria*. *The American Midland Naturalist* 166: 63–74. <https://doi.org/10.1674/0003-0031-166.1.63>
- Cockel CP, Gurnell AM, Gurnell J (2014) Consequences of the physical management of an invasive alien plant for riparian plant species richness and diversity. *River Research and Applications* 30: 217–229. <https://doi.org/10.1002/rra.2633>

- Čuda J, Skálová H, Janovský Z, Pyšek P (2014) Habitat requirements, short-term population dynamics and coexistence of native and invasive *Impatiens* species: a field study. *Biological Invasions* 16: 177–190. <https://doi.org/10.1007/s10530-013-0512-1>
- Čuda J, Vítková M, Albrechtová M, Guo WY, Barney JN, Pyšek P (2017) Invasive herb *Impatiens glandulifera* has minimal impact on multiple components of temperate forest ecosystem function. *Biological Invasions* 19: 3051–3066. <https://doi.org/10.1007/s10530-017-1508-z>
- Czapiewska N, Dyderski MK, Jagodziński AM (2019) Seasonal dynamics of floodplain forest understory – impacts of degradation, light availability and temperature on biomass and species composition. *Forests* 10: <https://doi.org/10.3390/f10010022>
- Davidson AD, Hewitt CL (2014) How often are invasion-induced ecological impacts missed? *Biological Invasions* 16: 1165–1173. <https://doi.org/10.1007/s10530-013-0570-4>
- Diekmann M, Effertz H, Baranowski M, Dupré C (2016) Weak effects on plant diversity of two invasive *Impatiens* species. *Plant Ecology* 217: 1503–1514. <https://doi.org/10.1007/s11258-016-0663-0>
- Eggenberg S, Möhl A (2013) *Flora Vegetativa: ein Bestimmungsbuch für Pflanzen der Schweiz im blütenlosen Zustand*. Haupt (Bern): 1–733.
- Ehrenfeld JG (2010) Ecosystem consequences of biological invasions. *Annual Review of Ecology, Evolution, and Systematics* 41: 59–80. <https://doi.org/10.1146/annurev-ecolsys-102209-144650>
- Ellenberg H, Leuschner C (2010) *Vegetation Mitteleuropas mit den Alpen*. Ulmer (Stuttgart): 1–1334.
- European Union (2014) Regulation (EU) No 1143/2014 of the European Parliament and of the Council of 22 October 2014 on the prevention and management of the introduction and spread of invasive alien species. *Official Journal of the European Union* L317: 35–55. <http://data.europa.eu/eli/reg/2014/1143/oj>
- Gendron F, Messier C, Comeau PG (1998) Comparison of various methods for estimating the mean growing season percent photosynthetic photon flux density in forests. *Agricultural and Forest Meteorology* 92: 55–70. [https://doi.org/10.1016/S0168-1923\(98\)00082-3](https://doi.org/10.1016/S0168-1923(98)00082-3)
- Goldberg D (1990) Components of resource competition in plant communities. In: Grace JB, Tilman D (Eds) *Perspectives on plant competition*. Academic Press (San Diego): 27–49. <https://doi.org/10.1016/B978-0-12-294452-9.50007-2>
- Grime JP (1977) Evidence for the existence of three primary strategies in plants and its relevance to ecological and evolutionary theory. *The American Naturalist* 111: 1169–1194. <https://doi.org/10.1086/283244>
- Grime JP (1998) Benefits of plant diversity to ecosystems: immediate, filter and founder effects. *Journal of Ecology* 86: 902–910. <https://doi.org/10.1046/j.1365-2745.1998.00306.x>
- Grove S, Haubensak KA, Parker IM (2012) Direct and indirect effects of allelopathy in the soil legacy of an exotic plant invasion. *Plant Ecology* 213: 1869–1882. <https://doi.org/10.1007/s11258-012-0079-4>
- Gruntman M, Pehl AK, Joshi S, Tielbörger K (2014) Competitive dominance of the invasive plant *Impatiens glandulifera*: using competitive effect and response with a vigorous neighbour. *Biological Invasions* 16: 141–151. <https://doi.org/10.1007/s10530-013-0509-9>

- Hejda M, Pyšek P (2006) What is the impact of *Impatiens glandulifera* on species diversity of invaded riparian vegetation? *Biological Conservation* 132: 143–152. <https://doi.org/10.1016/j.biocon.2006.03.025>
- Hejda M, Pyšek P, Jarošík V (2009) Impact of invasive plants on the species richness, diversity and composition of invaded communities. *Journal of Ecology* 97: 393–403. <https://doi.org/10.1111/j.1365-2745.2009.01480.x>
- Hulme PE, Bremner ET (2006) Assessing the impact of *Impatiens glandulifera* on riparian habitats: partitioning diversity components following species removal. *Journal of Applied Ecology* 43: 43–50. <https://doi.org/10.1111/j.1365-2664.2005.01102.x>
- Hulme PE, Pyšek P, Jarošík V, Pergl J, Schaffner U, Vilà M (2013) Bias and error in understanding plant invasion impacts. *Trends in Ecology and Evolution* 28: 212–218. <https://doi.org/10.1016/j.tree.2012.10.010>
- Jäger EJ (2017) Rothmaler – Exkursionsflora von Deutschland. Gefäßpflanzen: Grundband. Springer Spektrum (Berlin): 1–930. <https://doi.org/10.1007/978-3-662-49708-1>
- Jäger EJ, Ritz CM, Müller F, Welk E, Wesche K (2013) Rothmaler – Exkursionsflora von Deutschland Teil: Gefäßpflanzen: Atlasband. Springer Spektrum (Heidelberg): 1–822. <https://doi.org/10.1007/978-3-8274-2723-6>
- Kasperek G (2004) Fluctuations in numbers of neophytes, especially *Impatiens glandulifera*, in permanent plots in a west German floodplain during 13 years. In: Kühn I, Klotz S (Eds) *Biological invasions. Challenges for science*. *Neobiota* 3: 27–37.
- Kieltyk P, Delimat A (2019) Impact of the alien plant *Impatiens glandulifera* on species diversity of invaded vegetation in the northern foothills of the Tatra Mountains, Central Europe. *Plant Ecology* 220: 1–12. <https://doi.org/10.1007/s11258-018-0898-z>
- Koenker R (2018) `quantreg`: Quantile Regression. <https://cran.r-project.org/package=quantreg>
- Kollmann J, Bañuelos MJ (2004) Latitudinal trends in growth and phenology of the invasive alien plant *Impatiens glandulifera* (Balsaminaceae). *Diversity and Distributions* 10: 377–385. <https://doi.org/10.1111/j.1366-9516.2004.00126.x>
- Kueffer C, Pyšek P, Richardson DM (2013) Integrative invasion science: model systems, multi-site studies, focused meta-analysis and invasion syndromes. *New Phytologist* 200: 615–633. <https://doi.org/10.1111/nph.12415>
- Larsson C, Martinsson K (1998) *Impatiens glandulifera* in Sweden – an invasive species or a harmless garden escape? *Svensk Botanisk Tidskrift* 92: 329–345.
- Laube J, Sparks TH, Bässler C, Menzel A (2015) Small differences in seasonal and thermal niches influence elevational limits of native and invasive Balsams. *Biological Conservation* 191: 682–691. <https://doi.org/10.1016/j.biocon.2015.08.019>
- Lefcheck JS (2016) `piecewiseSEM`: Piecewise structural equation modeling in R for ecology, evolution, and systematics. *Methods in Ecology and Evolution* 7: 573–579. <https://doi.org/10.1111/2041-210X.12512>
- Loydi A, Donath TW, Eckstein RL, Otte A (2015) Non-native species litter reduces germination and growth of resident forbs and grasses: allelopathic, osmotic or mechanical effects? *Biological Invasions* 17: 581–595. <https://doi.org/10.1007/s10530-014-0750-x>
- MacDougall AS, Gilbert B, Levine JM (2009) Plant invasions and the niche. *Journal of Ecology* 97: 609–615. <https://doi.org/10.1111/j.1365-2745.2009.01514.x>

- Maestre FT, Callaway RM, Valladares F, Lortie CJ (2009) Refining the stress-gradient hypothesis for competition and facilitation in plant communities. *Journal of Ecology* 97: 199–205. <https://doi.org/10.1111/j.1365-2745.2008.01476.x>
- Nehring S, Essl F, Rabitsch W (2015) Methodik der naturschutzfachlichen Invasivitätsbewertung für gebietsfremde Arten, Version 1.3 – BfN-Skripten 401. Bundesamt für Naturschutz (Bonn): 1–48.
- Oksanen J, Blanchet FG, Friendly M, Kindt R, Legendre P, McGlenn D, Minchin PR, O'Hara RB, Simpson GL, Solymos P, Stevens MHH, Szoecs E, Wagner H (2018) vegan: community ecology package. <https://cran.r-project.org/package=vegan>
- Pacanoski Z, Saliji A (2014) The invasive *Impatiens glandulifera* Royle (Himalayan balsam) in the Republic of Macedonia: First record and forecast. *EPPO Bulletin* 44: 87–93. <https://doi.org/10.1111/epp.12102>
- Parent S, Messier C (1996) A simple and efficient method to estimate microsite light availability under a forest canopy. *Canadian Journal of Forest Research* 26: 151–154. <https://doi.org/10.1139/x26-017>
- Pinheiro J, Bates D, DebRoy S, Sarkar D, RCoreTeam (2018) nlme: linear and nonlinear mixed effects models. <https://cran.r-project.org/package=nlme>
- Pyšek P, Prach K (1993) Plant invasions and the role of riparian habitats: a comparison of four species alien to Central Europe. *Journal of Biogeography* 20: 413–420. <https://doi.org/10.2307/2845589>
- Pyšek P, Prach K (1995) Invasion dynamics of *Impatiens glandulifera* – a century of spreading reconstructed. *Biological Conservation* 74: 41–48. [https://doi.org/10.1016/0006-3207\(95\)00013-T](https://doi.org/10.1016/0006-3207(95)00013-T)
- RCoreTeam (2018) R: A language and environment for statistical computing. <https://www.r-project.org/>
- Reichelt G, Wilmanns O (1973) Vegetationsgeographie. Westermann (Braunschweig): 1–210.
- Ruckli R, Hesse K, Glauser G, Rusterholz H-P, Baur B (2014a) Inhibitory potential of naphthoquinones leached from leaves and exuded from roots of the invasive plant *Impatiens glandulifera*. *Journal of Chemical Ecology* 40: 371–8. <https://doi.org/10.1007/s10886-014-0421-5>
- Ruckli R, Rusterholz H-P, Baur B (2014b) Invasion of an annual exotic plant into deciduous forests suppresses arbuscular mycorrhiza symbiosis and reduces performance of sycamore maple saplings. *Forest Ecology and Management* 318: 285–293. <https://doi.org/10.1016/j.foreco.2014.01.015>
- Schmeil O, Fitschen J, Seybold S (2011) Die Flora Deutschlands und der angrenzenden Länder: ein Buch zum Bestimmen aller wildwachsenden und häufig kultivierten Gefäßpflanzen / Schmeil – Fitschen. Von Siegmund Seybold. Quelle und Meyer (Wiebelsheim): 1–919.
- Schreiber A (1958) *Urtica dioica* L. In: Rechinger K-H (Ed.) *Gustav Hegi – Illustrierte Flora von Mitteleuropa*. Band III, Teil 1. Carl Hanser Verlag (München): 299–303.
- Stouffer DB, Wainwright CE, Flanagan T, Mayfield MM (2018) Cyclic population dynamics and density-dependent intransitivity as pathways to coexistence between co-occurring annual plants. *Journal of Ecology* 106: 838–851. <https://doi.org/10.1111/1365-2745.12960>

- Tickner DP, Angold PG, Gurnell AM, Mountford JO, Sparks T (2001) Hydrology as an influence on invasion: experimental investigations into competition between the alien *Impatiens glandulifera* and the native *Urtica dioica* in the UK. In: Brundu G, Brock J, Camarda I, Child L, Wade M (Eds) Plant invasions: species ecology and ecosystem management. Blackhuys Publishers (Leiden): 159–168.
- Vilà M, Espinar JL, Hejda M, Hulme PE, Jarošík V, Maron JL, Pergl J, Schaffner U, Sun Y, Pyšek P (2011) Ecological impacts of invasive alien plants: a meta-analysis of their effects on species, communities and ecosystems. *Ecology Letters* 14: 702–708. <https://doi.org/10.1111/j.1461-0248.2011.01628.x>
- Vrchotová N, Šerá B, Krejčová J (2011) Allelopathic activity of extracts from *Impatiens* species. *Plant, Soil and Environment* 57: 57–60. <http://www.agriculturejournals.cz/publishedArticles/PSE/2011-57-2-57> <https://doi.org/10.17221/156/2010-PSE>
- Weber HE (1995) *Filipendula ulmaria*. In: Conert H, Jäger E, Kadereit J, Schultze-Motel W, Wagenitz G, Weber H (Eds) *Gustav Hegi – Illustrierte Flora von Mitteleuropa*. Band IV, Teil 2A. Blackwell Wissenschafts-Verlag (Berlin): 277–280.

Supplementary material 1

Year-to-year changes in cover of *Impatiens glandulifera*

Authors: Judith Bieberich, Heike Feldhaar, Marianne Lauerer

Data type: pdf-file describing additional data collection, analysis and results

Copyright notice: This dataset is made available under the Open Database License (<http://opendatacommons.org/licenses/odbl/1.0/>). The Open Database License (ODbL) is a license agreement intended to allow users to freely share, modify, and use this Dataset while maintaining this same freedom for others, provided that the original source and author(s) are credited.

Link: <https://doi.org/10.3897/neobiota.57.51331.suppl1>

Supplementary material 2

Maximum vegetation height in summer and spring

Authors: Judith Bieberich, Heike Feldhaar, Marianne Lauerer

Data type: pdf-file describing additional data collection, analysis and results

Copyright notice: This dataset is made available under the Open Database License (<http://opendatacommons.org/licenses/odbl/1.0/>). The Open Database License (ODbL) is a license agreement intended to allow users to freely share, modify, and use this Dataset while maintaining this same freedom for others, provided that the original source and author(s) are credited.

Link: <https://doi.org/10.3897/neobiota.57.51331.suppl2>

Supplementary material 3

Figure S1. Initial model of the piecewise structural equation modeling (SEM) for summer (A) and spring (B)

Authors: Judith Bieberich, Heike Feldhaar, Marianne Lauerer

Data type: pdf-file

Explanation note: Arrows show the hypothesized connections between variables the SEM was started with. Within the SEM all additional significant correlations between variables were then identified and the significance of each path was calculated. The results are shown in Figure 4A, B.

Copyright notice: This dataset is made available under the Open Database License (<http://opendatacommons.org/licenses/odbl/1.0/>). The Open Database License (ODbL) is a license agreement intended to allow users to freely share, modify, and use this Dataset while maintaining this same freedom for others, provided that the original source and author(s) are credited.

Link: <https://doi.org/10.3897/neobiota.57.51331.suppl3>

Supplementary material 4

Table S1. Result of the automated model selection approach identifying environmental variables that affected the cover of *Impatiens glandulifera* in summer 2016 and spring 2017

Authors: Judith Bieberich, Heike Feldhaar, Marianne Lauerer

Data type: pdf-file containing a table with results

Copyright notice: This dataset is made available under the Open Database License (<http://opendatacommons.org/licenses/odbl/1.0/>). The Open Database License (ODbL) is a license agreement intended to allow users to freely share, modify, and use this Dataset while maintaining this same freedom for others, provided that the original source and author(s) are credited.

Link: <https://doi.org/10.3897/neobiota.57.51331.suppl4>

Supplementary material 5

Table S2. Abbreviations of species names as shown in Figure 5

Authors: Judith Bieberich, Heike Feldhaar, Marianne Lauerer

Data type: xls-table

Copyright notice: This dataset is made available under the Open Database License (<http://opendatacommons.org/licenses/odbl/1.0/>). The Open Database License (ODbL) is a license agreement intended to allow users to freely share, modify, and use this Dataset while maintaining this same freedom for others, provided that the original source and author(s) are credited.

Link: <https://doi.org/10.3897/neobiota.57.51331.suppl5>

Supplementary material 6

Figure S2. Micro-habitat specific impact of *I. glandulifera* on the resident vegetation

Authors: Judith Bieberich, Heike Feldhaar, Marianne Lauerer

Data type: pdf-file

Explanation note: With the complete dataset and four subsets representing different micro-habitats regarding light (relative PAR) and soil water content (see also Fig. 3) it was tested whether vegetation parameters depend on cover of *I. glandulifera*. Results of all statistical tests are given in Table 2. For total cover, species number, and Shannon index linear models were used. Resulting regression lines are shown if $p < 0.001$. For cover of *Filipendula ulmaria*, *Phalaris arundinacea* and *Urtica dioica* quantile regressions were applied using the 0.50, 0.75, 0.85 and 0.95 quantiles. Quantile regression lines are shown in blue color when $R^2 > 0.1$ and $p < 0.001$ or in grey color when $R^2 < 0.1$ and $p > 0.001$.

Copyright notice: This dataset is made available under the Open Database License (<http://opendatacommons.org/licenses/odbl/1.0/>). The Open Database License (ODbL) is a license agreement intended to allow users to freely share, modify, and use this Dataset while maintaining this same freedom for others, provided that the original source and author(s) are credited.

Link: <https://doi.org/10.3897/neobiota.57.51331.suppl6>

Supplementary material 7

Figure S3. Micro-habitat specific impact of *I. glandulifera* on the resident plant species composition

Authors: Judith Bieberich, Heike Feldhaar, Marianne Lauerer

Data type: pdf-file

Explanation note: With four data subsets representing different micro-habitats regarding light (relative PAR) and volumetric soil water content (see also Fig. 3) it was tested with DCA and CCA analyses whether the resident species composition changed depending on cover of *I. glandulifera*. In the case of significance cover of *I. glandulifera* is shown as arrow. All statistical results are given in Table 2.

Copyright notice: This dataset is made available under the Open Database License (<http://opendatacommons.org/licenses/odbl/1.0/>). The Open Database License (ODbL) is a license agreement intended to allow users to freely share, modify, and use this Dataset while maintaining this same freedom for others, provided that the original source and author(s) are credited.

Link: <https://doi.org/10.3897/neobiota.57.51331.suppl7>

Supplementary material 8

Additional information: information on the published datasets

Authors: Judith Bieberich, Heike Feldhaar, Marianne Lauerer

Data type: table

Copyright notice: This dataset is made available under the Open Database License (<http://opendatacommons.org/licenses/odbl/1.0/>). The Open Database License (ODbL) is a license agreement intended to allow users to freely share, modify, and use this Dataset while maintaining this same freedom for others, provided that the original source and author(s) are credited.

Link: <https://doi.org/10.3897/neobiota.57.51331.suppl8>

Supplementary material 9

Dataset plant cover

Authors: Judith Bieberich, Heike Feldhaar, Marianne Lauerer

Data type: table

Copyright notice: This dataset is made available under the Open Database License (<http://opendatacommons.org/licenses/odbl/1.0/>). The Open Database License (ODbL) is a license agreement intended to allow users to freely share, modify, and use this Dataset while maintaining this same freedom for others, provided that the original source and author(s) are credited.

Link: <https://doi.org/10.3897/neobiota.57.51331.suppl9>

Supplementary material 10

Dataset environment and vegetation characteristics

Authors: Judith Bieberich, Heike Feldhaar, Marianne Lauerer

Data type: table

Copyright notice: This dataset is made available under the Open Database License (<http://opendatacommons.org/licenses/odbl/1.0/>). The Open Database License (ODbL) is a license agreement intended to allow users to freely share, modify, and use this Dataset while maintaining this same freedom for others, provided that the original source and author(s) are credited.

Link: <https://doi.org/10.3897/neobiota.57.51331.suppl10>

Spatiotemporal patterns of non-native terrestrial gastropods in the contiguous United States

Nicholas S. Gladstone¹, Trystan A. Bordeau²,
Christy Leppanen³, Michael L. McKinney²

1 School of Fisheries, Aquaculture and Aquatic Sciences, Auburn University, Auburn, AL 36849, USA **2** Department of Earth and Planetary Sciences, University of Tennessee, Knoxville, TN 37996, USA **3** Department of Ecology and Evolutionary Biology, University of Tennessee, Knoxville, TN 37996, USA

Corresponding author: Nicholas S. Gladstone (nscottgladstone@gmail.com)

Academic editor: Sven Jelaska | Received 18 March 2020 | Accepted 14 May 2020 | Published 17 June 2020

Citation: Gladstone NS, Bordeau TA, Leppanen C, McKinney ML (2020) Spatiotemporal patterns of non-native terrestrial gastropods in the contiguous United States. *NeoBiota* 57: 133–152. <https://doi.org/10.3897/neobiota.57.52195>

Abstract

The contiguous United States (CONUS) harbor a significant non-native species diversity. However, spatiotemporal trends of some groups such as terrestrial gastropods (i.e., land snails and slugs) have not been comprehensively considered, and therefore management has been hindered. Here, our aims were to 1.) compile a dataset of all non-native terrestrial gastropod species with CONUS occurrence records, 2.) assess overarching spatiotemporal patterns associated with these records, 3.) describe the continental origin of each species, and 4.) compare climatic associations of each species in their indigenous and introduced CONUS ranges. We compiled a georeferenced dataset of 10,097 records for 22 families, 48 genera, and 69 species, with > 70% of records sourced from the citizen science database iNaturalist. The species *Cornu aspersum* Müller, 1774 was most prevalent with 3,672 records. The majority (> 92%) of records exhibit an indigenous Western European and Mediterranean distribution, with overlap in broad-scale climatic associations between indigenous and CONUS ranges. Records are most dense in urban metropolitan areas, with the highest proportion of records and species richness in the state of California. We show increased prevalence of non-native species through time, largely associated with urbanized areas with high human population density. Moreover, we show strong evidence for a role for analogous climates in dictating geographic fate and pervasiveness between indigenous and CONUS ranges for non-native species.

Keywords

Non-native, land snails, slugs, citizen science, invasive species, data aggregation

Introduction

The accidental and deliberate introduction of non-native species is a notable worldwide phenomenon, which has been identified as one of the leading causes of global biodiversity decline (McKinney and Lockwood 1999; Clavero and Garcia-Berthou 2005; Butchart et al. 2010). Moreover, many introduced non-native species are harmful to local and regional economic activities as well as human health (Pimentel et al. 2005; Simberloff 2013; Hulme 2014). The contiguous United States (CONUS; the lower 48 states excluding Alaska and Hawaii) is one of the largest geopolitical areas in the world and contain a diverse array of ecosystems and associated native fauna and flora. Along with many intentional non-native species introductions over several centuries, CONUS has many global transport hubs, facilitating many accidental introductions, and consequently harbors an estimated 50,000 documented non-native species (Pimentel et al. 2005).

Despite much attention devoted to the study of introduced non-native species and their potential impacts in general, some taxonomic groups have received comparatively little study (Pyšek et al. 2008; Jeschke et al. 2012; Lowry et al. 2013). Invertebrate species – primarily insects – comprise a significant proportion of non-native species in the U.S. (US Congress Office of Technology Assessment 1993) and are associated with a myriad of negative impacts on native ecosystems, biodiversity, and economic production (Simberloff et al. 2013; Liebhold et al. 2016). However, the pervasiveness of non-native non-insect invertebrates, such as mollusks, has not been thoroughly studied (Keller et al. 2007; Cowie et al. 2009). Though not all introduced non-native species are directly harmful or later become invasive, monitoring spatiotemporal trends of their presence and spread is useful for management efforts and informs effective policy (Baker and Bode 2016; Mangiante et al. 2018).

Terrestrial gastropods (i.e., land snails and slugs) are generally characterized by low vagility, and they are commonly introduced to new areas from human activities such as the horticultural trade (Cowie et al. 2008; Bergey et al. 2014), non-native pet trade (Cowie and Robinson 2003), use as biocontrol agents (Civeyrel and Simberloff 1996; Cowie 2001), and other cargo shipments (Robinson 1999). Introduced terrestrial gastropods are pests to agriculture and human health and cause significant biodiversity declines in some areas of the world (Cowie et al. 2009; Mazza et al. 2014; Chiba and Cowie 2016; Yeung and Hayes 2018). Broad-scale study of introduced terrestrial gastropods has been primarily limited to dispersal vectors, individual species impacts in specific sites, and risk assessment based on life history traits and invasion history (Robinson 1999; Cowie and Robinson 2003; Cowie et al. 2009). Little study has been given to the geographic fate of these animals when introduced, overarching patterns of presence in their introduced environments, and geographic density through time, all necessary to inform effective policy and management.

Monitoring and study of non-native species can benefit from increasing access to species occurrence data. The Global Biodiversity Information Facility (GBIF; www.gbif.org) and its U.S. Node, Biodiversity Information Serving Our Nation (BISON;

www.bison.usgs.gov), provide open access databases collectively containing hundreds of millions of occurrence records for species across the tree of life. Other recent efforts focus on digitization of molluscan collections (Shea, Sierwald et al. 2018; Sierwald et al. 2018) and the creation of invertebrate-specific data portals (e.g., InvertEBase, MolluscaBase). There have been criticisms about data quality associated with such large-scale data aggregates (e.g., GBIF) and similar digital resources (Yesson et al. 2007; Troia and McManamay 2016; Bayraktarov et al. 2019) and as such broad-scale analyses of ecology and biogeography may not always be biologically accurate with the data available (Nekola et al. 2019). These limitations considered, these eclectic data resources still allow for numerous evaluations, such as cataloging and estimating the potential pervasiveness of non-native species (e.g., Darrigran et al. 2020). Moreover, compiling all available data for terrestrial gastropods may generate support for additional study and overall improvement of data quality.

Here we describe spatiotemporal patterns of non-native terrestrial gastropods in CONUS. Our aims are to: 1.) compile a dataset of all non-native terrestrial gastropod species with CONUS occurrence records, 2.) assess overarching patterns associated with those records, i.e., spatial and temporal distribution 3.) describe the continental origin of each species, and 4.) compare climatic associations of each species in their indigenous and introduced CONUS ranges.

Methods

Species selection, data collection and contributing sources

To generate our dataset, we first formalized a working definition of the term ‘non-native’ in the context of our research objectives. We defined non-native terrestrial gastropods as any species that has been either intentionally or accidentally introduced into CONUS and that is indigenous to areas outside of North America. As the geographic distributions of terrestrial gastropod species are generally understudied, native ranges of species documented only outside of CONUS but within North America might indeed include CONUS. Therefore, species that are native to Canada and Mexico are not considered in this study, nor are extralimital species that are native to portions of the U.S. but have been translocated to other regions within the country (e.g., *Euglandina rosea* Férussac, 1821). To identify non-native species’ records, we compiled all available information from state and federal governmental technical reports, scientific literature (e.g., Robinson 1999, Cowie et al. 2009), online data aggregators (GBIF, BISON), citizen science databases (iNaturalist), online collection portals specific to museum collections (InvertEBase), online data repositories specific to invasive or pest species (e.g., USDA APHIS, found at www.aphis.usda.gov/aphis/home/), and direct conversation with several malacologists (Robert Cowie, Daniel Dourson, Gerald Dinkins personal communication). Though we are confident in the overall breadth of our search efforts, we also acknowledge that this may represent an incomplete dataset.

Importantly, we also recognize the body of analytical and statistical quandaries associated with data sourced from citizen science networks and other large data aggregators (Bird et al. 2014; Kosmala et al. 2016; Bayraktarov et al. 2019). Our goal was to catalog and outline the potential pervasiveness of these non-native species by synthesizing all available data. Therefore, we note that we did not correct for spatial biases (e.g., spatial autocorrelation), nor did we adjust our data based on possible pseudo-replication, detection rates, or other common sources of geospatial data error. Thus, we encourage readers to treat our results as a synthesized dataset from which they can then begin to adjust for spatial biases for future geospatial modeling (e.g., species distribution modeling).

We utilized the online portal MolluscaBase (available at www.molluscabase.org) to verify the taxonomic identity of all species and to avoid double counting synonymous records. In cases of species being known by several taxonomic identities, searches for each identity were subsequently searched for, placed under the most updated synonym, and records were thoroughly searched by all authors to avoid overlap. When records were identified as erroneous, questionable, or of limited utility (e.g., falling outside CONUS or directly within the centroid of a county), they were removed from the dataset. If a detailed location description was provided for a record that did not contain a georeference, we georeferenced these records using the web application GEOLocate (available at www.geo-locate.org/).

Data were separated into three different sets for reporting: 1.) all records with or without georeferences, 2.) all records with georeferences, and 3.) all records with georeferences and temporal data. The second dataset with all georeferenced records was used for all downstream summaries beyond explicit analyses of spatiotemporal trends, for which the third dataset was used. Lastly, records were categorized by source: 1.) museum and natural history collections, 2.) state or federal governmental agency, 3.) scientific literature that did not already have records associated with a museum collection, and 4.) citizen science database.

Continental origin and climatic associations

Literature and geospatial data pertaining to each species identified as non-native in CONUS were reviewed and used to assign a continental origin with respect to the species' indigenous range. Several species (e.g., *Cornu aspersum* Müller, 1774) were assigned multiple continental origins, as they exhibit intercontinental geographic distributions in their indigenous ranges. In scenarios where continental origin was obscure or unknown, the species was removed from this analysis (i.e., all species in the genus *Allopeas* Baker, 1935, *Gulella* Pfeiffer, 1856, *Laevicaulis* Férussac, 1822, *Opeas* Alber, 1850, and *Subulina* Beck, 1837). To assess climatic associations of each species in its native and CONUS environments, we categorized species by the Köppen-Geiger climate classification system (Rubel et al. 2017). Georeferenced records collected via GBIF and historical literature designating indigenous range were separately gathered

and projected in ArcMap v.10.7 by ESRI. These records were spatially joined with a high resolution Köppen-Geiger climate zone projection (Rubel et al. 2017; available at koeppen-geiger.vu-wien.ac.at/present.htm) and the climate classification was extracted to each individual record. Similarly, we repeated this process for our curated database of comprehensive CONUS records to classify introduced climate association. Many species occupy multiple climate zones and are therefore included in all such occupied zones respective to each species. To visualize these data, the *circlize* package (Gu et al. 2014) was used in R v.3.6.1 (R Core Team). To enhance the interpretability of these visualizations, all classifications that yielded lower than ten observations were removed.

Spatiotemporal trends in the contiguous United States

To assess spatial distribution through time of all non-native species, we projected records on a map of the contiguous U.S. at five time intervals starting from the first georeferenced record: 1862–1940, 1941–1960, 1961–1980, 1981–2000, and 2001–2019. The initial, large interval was used due to sparsity of records from the first georeferenced record until the mid-20th century, followed by a standard two-decade delimitation. To identify areas with many non-native species records, the Point Density tool in ArcMap v.10.7 was used with a circular neighborhood of 75 km at each respective time interval. All time intervals were standardized to a single density scale.

Species richness and number of records in CONUS were quantified by political state boundaries by spatially joining record location data to a polygon layer of the contiguous U.S. Additionally, records were assessed in association to contemporary land cover type and human population density. We used the 2016 National Land Cover Database (NLCD; available at <https://www.mrlc.gov/data/nlcd-2016-land-cover-conus>) through the U.S. Geological Survey (Yang et al. 2018). Human population density data were obtained through the 2018 U.S. Census from the U.S. Census Bureau (TIGER/Line shapefiles; available at <https://www.census.gov/cgi-bin/geo/shapefiles/index.php>). The raster files were converted to point data and spatially joined to a polygon layer of 0.5 km buffers created around each record location. Land cover type was consolidated into seven categories: agricultural, barren, developed, forest, herbaceous, shrub/scrub, and wetlands.

Results

Data collection, species occurrences and data sources

From all sources, we assembled a dataset comprising 13,311 records for 25 families, 59 genera and 93 species. Of these records, 10,097 records included georeferences (with 134 records georeferenced by the authors), and 9,297 records included temporal information and georeferences. The full georeferenced dataset was used to generate the

final taxonomic list, containing 22 families, 48 genera and 69 species (see Table 1). The majority of non-native species records are in California (5,735 of 10,097), with 26 of the total 69 species documented represented within the state (Fig. 1). Non-native species richness is more evenly distributed across various states, with all but two states (Nebraska and South Dakota) with at least one non-native species record.

The most prevalent and widespread species documented is *Cornu aspersum*, with nearly three times as many CONUS records (3,672) as the next most prevalent species *Otala lactea*. *Cornu aspersum* records are densely clustered in metropolitan areas along the west coast (incl. California, Oregon and Washington) with many records in south-central Texas, the southern Midwest, and along the eastern seaboard (Fig. 2).

The second most prevalent species, *O. lactea* (1,297 records) exhibits a similarly broad introduced distribution to *C. aspersum*, most commonly associated with coastal areas in the west (California, Oregon) and in the east (Florida). Additional records are clustered within the northeast (Michigan, New York, Vermont). Records of the third and fourth most prevalent species, *Rumina decollata* (998 records) and *Limax maximus* (756), are primarily within metropolitan areas along the west coast (e.g., Los Angeles and San Francisco, CA, Seattle, WA) and in the central U.S. (e.g., Dallas, TX). These major urban hubs appear to be hot spots for introduction of these terrestrial gastropods. The most geographically widespread non-native species was *L. maximus*, being found from coast to coast in 37 of the 48 states.

Of the four contributing source categories to all records, a large majority (7,917 of 10,097 records) are from the citizen science database iNaturalist. Museum and natural history collections contribute 2,131 records, state and federal governmental agencies contribute 24 records, and 25 records come from scientific literature not associated with museum collections.

Continental origins and climatic associations

Europe is the continental origin for the majority of non-native CONUS species identified, with 25 genera and 45 species with a strictly European origin. An additional ten genera and eight species have a broad Mediterranean distribution that encompasses Western Europe and Northern Africa (see Table 1). Proportionally, species indigenous to the aforementioned continental regions collectively make up 92.2% of CONUS records, and the remainder of species with certain origins come from Asia (2.8%), the Caribbean (0.06%), and Central and South America (0.01%) (see Fig. 3). Of the species documented, *Cornu aspersum* records are the most widespread and numerous. This species has a Mediterranean distribution (and was accordingly categorized with both an African and European origin in Fig. 3) but given that the majority of species are being translocated from Europe, we infer that this species may be disproportionately transported from the northern extent of its native range. Thus, the frequency of introduction from northern Africa is likely to be proportionally smaller.

Table 1. Non-native species list curated from the full georeferenced dataset. The ‘x’ designates genera or species with obscure or unknown continental origins.

Species Name	Number of records	Origin	State Records
<i>Cornu aspersum</i>	3,672	Europe, Africa	AL, AR, AZ, CA, CO, FL, GA, ID, KS, LA, MA, NH, NM, NV, NY, OH, OR, PA, SC, TN, TX, UT, VA, WA
<i>Otala lactea</i>	1,288	Europe, Africa	CA, FL, GA, KY, MO, MS, NM, NY, PA, TX, VA, WV
<i>Rumina decollata</i>	989	Europe, Africa	AL, AZ, CA, FL, GA, LA, MS, NC, NM, OR, PA, SC, TX, WV
<i>Limax maximus</i>	745	Europe	AL, AR, AZ, CA, CO, CT, DC, DE, GA, ID, IL, IN, KS, KY, MA, MD, ME, MI, MO, MT, NC, NJ, NV, NY, OH, OK, OR, PA, SC, TN, TX, UT, VA, VT, WA, WI, WV
<i>Limacus flavus</i>	371	Europe	AL, AR, AZ, CA, DC, FL, IN, KS, LA, MD, MO, MS, NC, NJ, NY, OK, OR, PA, TN, TX, WA, WI
<i>Cepaea nemoralis</i>	317	Europe	CA, CT, ID, IL, KY, MA, ME, MI, MN, MT, NJ, NY, OH, PA, RI, TN, UT, VA, WA, WV
<i>Oxychilus draparnaudi</i>	294	Europe	AL, CA, DE, GA, ID, IL, IN, MA, MI, NC, NJ, NY, OH, OR, PA, SC, TN, TX, VA, VT, WA
<i>Bradybaena similaris</i>	277	Asia	AL, FL, GA, LA, MS, NC, OK, SC, TX, WI, WV
<i>Arion subfuscus</i>	224	Europe	AL, CT, DC, DE, IL, IN, KY, MA, MD, ME, MI, MN, NC, ND, NH, NJ, NY, OH, OR, PA, TX, VA, VT, WA, WI, WV, WY
<i>Milax gagates</i>	185	Europe	AR, CA, DC, OK, OR, TX, VA
<i>Arion rufus</i>	126	Europe	AR, CA, FL, ME, MT, NY, OK, OR, PA, WA
<i>Allopeas gracile</i>	115	x	AL, FL, GA, IL, LA, MO, NC, NJ, OK, PA, SC, TX, VA
<i>Subulina octona</i>	112	x	FL, IL, OK, PA, TN, TX, VA
<i>Theba pisana</i>	105	Europe, Africa	CA, NY, TX
<i>Oxychilus cellarius</i>	95	Europe	CA, IA, IL, IN, MA, MD, ME, MI, NJ, NY, OH, OK, OR, PA, RI, SC, VA, WA
<i>Arion hortensis</i>	85	Europe	CA, CT, DC, DE, IL, KY, MA, ME, NC, NJ, NY, OH, PA, VA, WA, WV
<i>Arion</i> sp.	74	Europe	CT, DE, IA, IL, KY, ME, MI, MN, NC, NH, NY, OR, PA, TN, TX, VA, VT, WA
<i>Opeas pyrgula</i>	72	x	AL, FL, GA, IL, LA, MD, MS, NC, SC, TN, TX, VA, WV
<i>Allopeas micra</i>	71	x	FL, MO, TX
<i>Ambigolimax valentianus</i>	66	Europe	AL, AR, CA, DC, DE, GA, MD, MS, NC, NY, OK, SC, TN, TX, WA
<i>Limax</i> sp.	63	Europe	AL, AZ, CA, CO, IL, KS, KY, LA, MA, MD, MT, NC, NJ, NM, NY, OH, OR, PA, WA, WV
<i>Arion circumscriptus</i>	58	Europe	CA, GA, ID, IN, MA, MD, ME, MI, NC, ND, NY, OK, PA, WI
<i>Xerotricha conspurcata</i>	56	Europe, Africa	CA, WA
<i>Bulimulus guadalupensis</i>	49	Caribbean	FL
<i>Succinea putris</i>	46	Europe	MA, ME, MI, NY, OH, PA, VT
<i>Myosotella myosotis</i>	45	Europe, Africa	CA, FL, NY, OR
<i>Arion fasciatus</i>	41	Europe	CT, IA, IL, IN, MA, MD, ME, MI, MN, NC, NY, PA, TN, WI, WV
<i>Arion intermedius</i>	33	Europe	CA, DC, IL, IN, MA, MD, NJ, NY, OH, OR, VA, WA
<i>Arion ater</i>	26	Europe	MD, MT, NC, NJ, NY, WA
<i>Ceriuella cisalpina</i>	25	Europe	MD, NC, NJ, OH, VA
<i>Deroceras agreste</i>	25	Europe	CA, CT, DC, IN, MA, MI, NJ, NM, NY, OR, PA, WA
<i>Gulella bicolor</i>	25	x	FL, SC, TX
<i>Oxychilus</i> sp.	25	Europe	CA, FL, NJ, NY, PA, WA
<i>Massylaea vermiculata</i>	23	Europe, Africa	LA, NJ, NY, OH, PA, TX, WV
<i>Cepaea hortensis</i>	22	Europe	CA, MA, NY, OH, RI, TX
<i>Allopeas clavulinum</i>	21	x	FL, IL, LA, MS, NC, OK, PA, TX
<i>Helix pomatia</i>	18	Europe	CA, FL, MA, MI, NY, PA, WI
<i>Opeas hannense</i>	18	x	FL, GA, IL, LA, MO, NC
<i>Hygromia</i> sp.	17	Europe, Africa	MA, ME
<i>Cochlicella barbara</i>	16	Europe	CA, SC
<i>Oxychilus alliaris</i>	15	Europe	CA, ID, IN, NJ, NY, PA, RI, WA
<i>Lissachatina fulica</i>	12	Africa	FL
<i>Otala punctata</i>	12	Europe, Africa	GA
<i>Ceciloides acicula</i>	9	Europe	CA, IL, PA, TX
<i>Ovachlamys fulgens</i>	9	Asia	FL, IL
<i>Helicella</i> sp.	8	Europe	NC, SC, VA
<i>Lehmannia marginata</i>	8	Europe	CA, IL, MA, ME, MO, OR, TX

Species Name	Number of records	Origin	State Records
<i>Leptinaria</i> sp.	7	South America, Central America, Caribbean	TX
<i>Trochulus hispidus</i>	7	Europe	AL, IL, NJ, NY, VT
<i>Lauria cylindracea</i>	6	Europe	CA
<i>Monacha cartusiana</i>	5	Europe	AL, DE, OH
<i>Veronicella</i> sp.	5	Central America, Caribbean	FL, TX
<i>Cepaea</i> sp.	4	Europe	NC, NY
<i>Cernuella virgata</i>	4	Europe	KY, MI, NJ
<i>Milax</i> sp.	4	Europe	OR, TX
<i>Tandonia kusceri</i>	4	Europe	IL
<i>Arion distinctus</i>	3	Europe	OH, WV
<i>Laevicaulis alte</i>	3	x	FL, TX
<i>Tandonia budapestensis</i>	3	Europe	DC, PA
<i>Arion vulgaris</i>	2	Europe	OR
<i>Bradybaena</i> sp.	2	Asia	NC
<i>Helicella elegans</i>	2	Europe	NC, SC
<i>Helicella caperata</i>	2	Europe	NC, VA
<i>Helicella variabilis</i>	2	Europe	NC
<i>Lehmanna</i> sp.	2	Europe	WA, WV
<i>Xerolenta obvia</i>	2	Europe	MT
<i>Xeroplexa intersecta</i>	2	Europe	NC
<i>Allopeas</i> sp.	1	x	FL
<i>Arianta arbustorum</i>	1	Europe	MA
<i>Arion silvaticus</i>	1	Europe	IL
<i>Cochlicella ventricosa</i>	1	Europe	SC
<i>Cochlicella acuta</i>	1	Europe	MI
<i>Cochlodina bidens</i>	1	Europe	NY
<i>Ena obscura</i>	1	Europe	IN
<i>Helicarion</i> sp.	1	Africa	NC
<i>Helicella intersecta</i>	1	Europe	VA
<i>Leptinaria lamellata</i>	1	South America, Central America, Caribbean	FL
<i>Lissachatina immaculata</i>	1	Africa	NM
<i>Megalobulimus oblongus</i>	1	South America, Central America, Caribbean	NY
<i>Neocyclotus</i> sp.	1	Central America, South America	OR
<i>Oxychilus helveticus</i>	1	Europe	CA
<i>Papillifera</i> sp.	1	Europe, Africa	NY
<i>Subulina</i> sp.	1	Europe, Africa	GA
<i>Veronicella cubensis</i>	1	Central America, Caribbean	FL
<i>Xeropicta krynickii</i>	1	Europe, Africa	KY

Climate zone associations in indigenous and CONUS ranges of most species were similar. Of the seven species reported from tropical climate zones in the Caribbean, Central America, or South America, all CONUS records were also associated with tropical or humid subtropical climates (largely found in southern Florida). Likewise, > 97% of CONUS records for the two introduced Asian species come from the same zone as their indigenous environment. All but two species (*Lissachatina fulica* Bowdich, 1822, and *L. immaculata* Lamarck, 1822) with indigenous ranges including Africa are associated with Mediterranean-influenced climates, although most of these species'

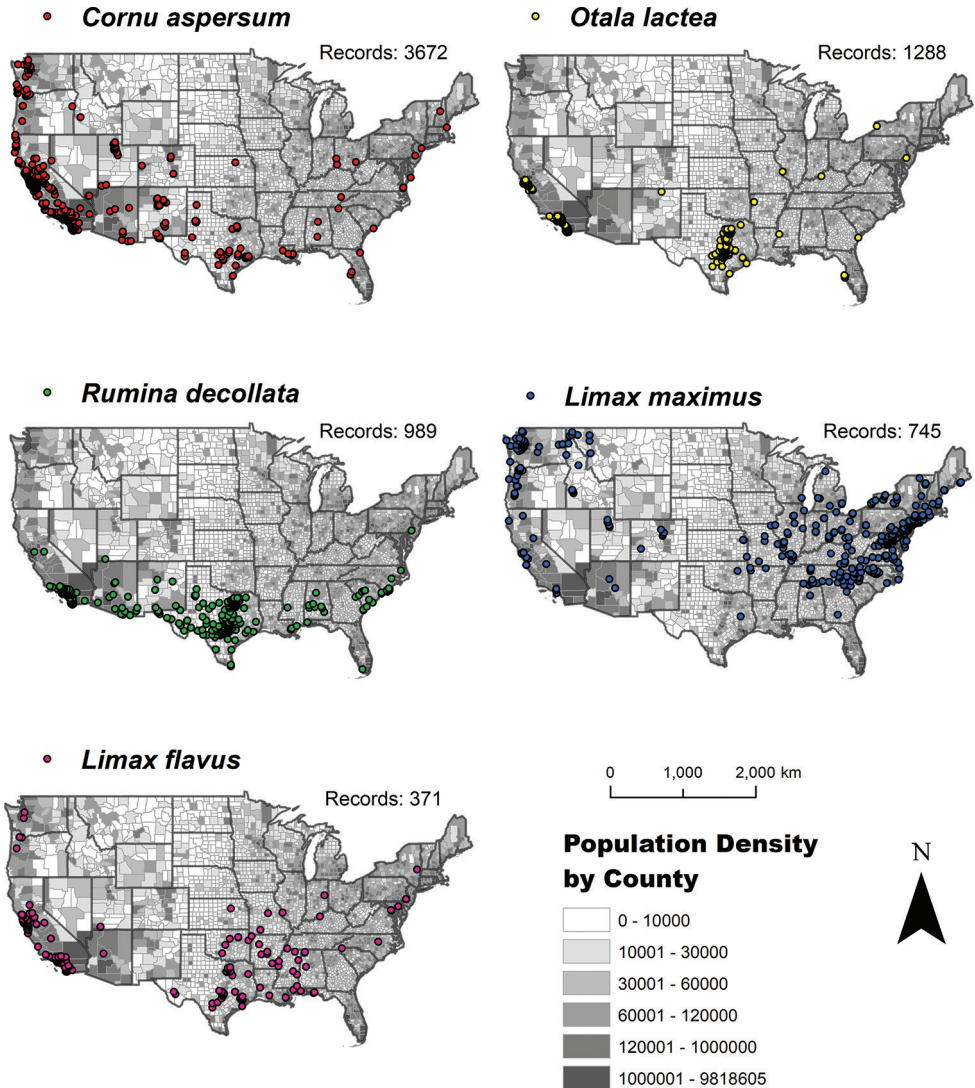


Figure 2. CONUS distribution of the five most prevalent non-native species in relation to county-based U.S. population density.

Discussion

Spatial and climatic mechanisms for species introduction

Our results indicate that hot spots of gastropod introductions occur in highly urbanized areas. This generally conforms to previous findings showing a significant correlation, at several spatial scales, between introduced species diversity and human population size. Examples of this correlation include invasive plants (Campos et al. 2016; Vinogradova

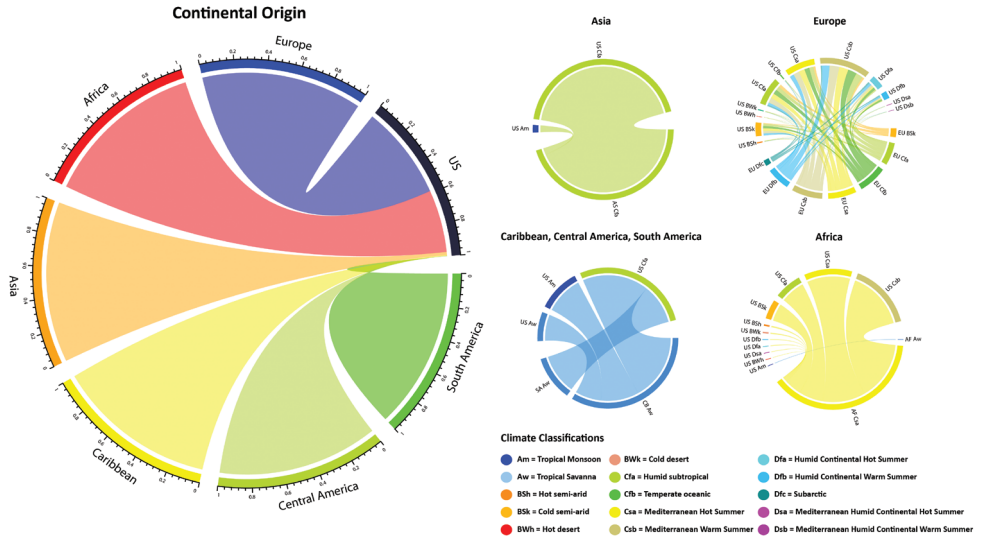


Figure 3. **Left:** Relative contribution of each continental indigenous origin for non-native CONUS terrestrial gastropod species records. **Right:** Climatic associations of each non-native species in the indigenous range and its CONUS records utilizing the Köppen-Geiger climate classification scheme. Illustrations are subdivided by continent or a grouping of continents in relative proximity. Color codes are defined for each classification, and the two-letter code preceding each climate code identifies the respective region (AF = Africa, AS = Asia, CA = Central America, CB = Caribbean, EU = Europe, SA = South America, US = United States).

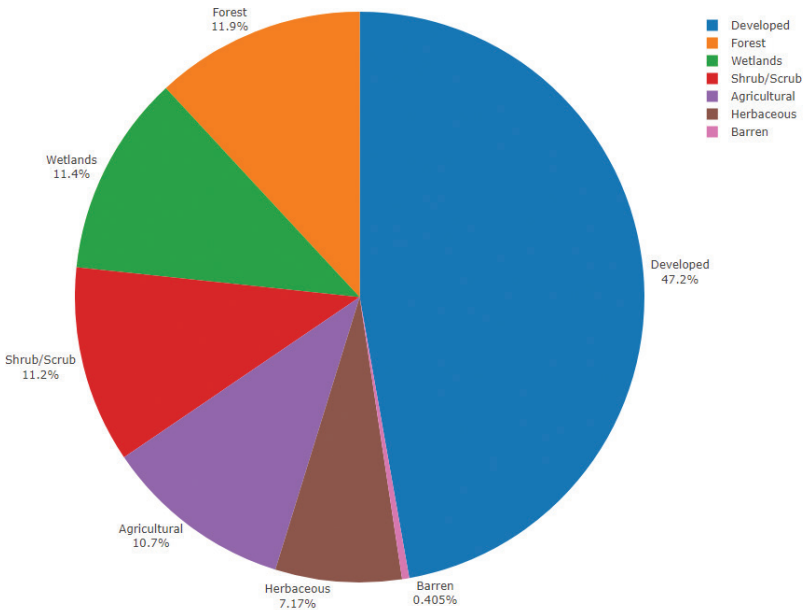


Figure 4. Proportions of 2016 NLCD land cover type in relation to 0.5 km buffer surrounding each record.

et al. 2018) and invasive animals (Spear et al. 2013). One driver of this association is that increasing human population density leads to increased importation (dispersal) of non-native species into an area via intentional and unintentional introductions. More people in an area inevitably leads to more opportunities for introduction of ornamental plants, weeds, pets and many other well-documented pathways of non-native species importation (Pimentel et al. 2005; Simberloff 2013). Another driver of this correlation is that more people in an area produce increased anthropogenic disturbances, altering native habitat which eliminates many native species and creates habitat for non-native species (McKinney 2001). There is also a likely artifactual contribution to this correlation: increasing human population densities create a sampling bias by increasing the likelihood that more species (including introduced and invasive species) will be observed and recorded (Barbosa et al. 2013). This is especially true given the rapid rise of citizen science programs and social media platforms, especially iNaturalist.

The geospatial analyses also show that introduction hot spots tend to occur in highly populated areas concentrated along coastal regions at several latitudes (Fig. 5). Comparable areas of human population density located away from coastal areas tend to have much lower non-native species diversity. This pattern conforms to findings that ports of entry are gateways to many introduced species, especially non-native horticultural plants (Jehlik et al. 2019) and animals such as invasive insects (Langor et al. 2009) and invasive terrestrial gastropods (Bergey et al. 2014) that are hitchhikers on such plants. A key implication is that these organisms might gradually disperse into the interior of the continent, as seen in Fig. 5. This could be accelerated by punctuated dispersal events, e.g., following applicable aforementioned mechanisms, that might also occur.

Our results also suggest that native to introduced range climate analogs are positive factors in non-native terrestrial gastropod diversity and pervasiveness. Most non-native terrestrial gastropod species found in our study are located in climate zones similar to their native ranges, e.g., species primarily of Mediterranean origin recorded in Pacific coastal states in the introduced range. Previous studies have documented evidence of such climate matching in other groups, including invasive fishes (Howeth et al. 2016) and reptiles and amphibians (van Wilgen et al. 2009). A study of European non-native land snails also found evidence of climate matching but with several important exceptions that demonstrated the importance of including (where possible) species traits as an explanatory variable in understanding non-native snail distributions (Capinha et al. 2014).

Non-native species diversity and prevalence

The contiguous U.S. (CONUS) harbors a greater non-native terrestrial gastropod diversity than other New World nations (Naranjo-García and Castillo-Rodríguez 2017; Darrigran et al. 2020). This may be the product of greater interest in malacology within the U.S., as well as the popularity and accessibility of citizen science media. However, there are still notable sampling gaps within the country, and therefore this representation probably underestimates the full taxonomic scope of non-native terrestrial gas-

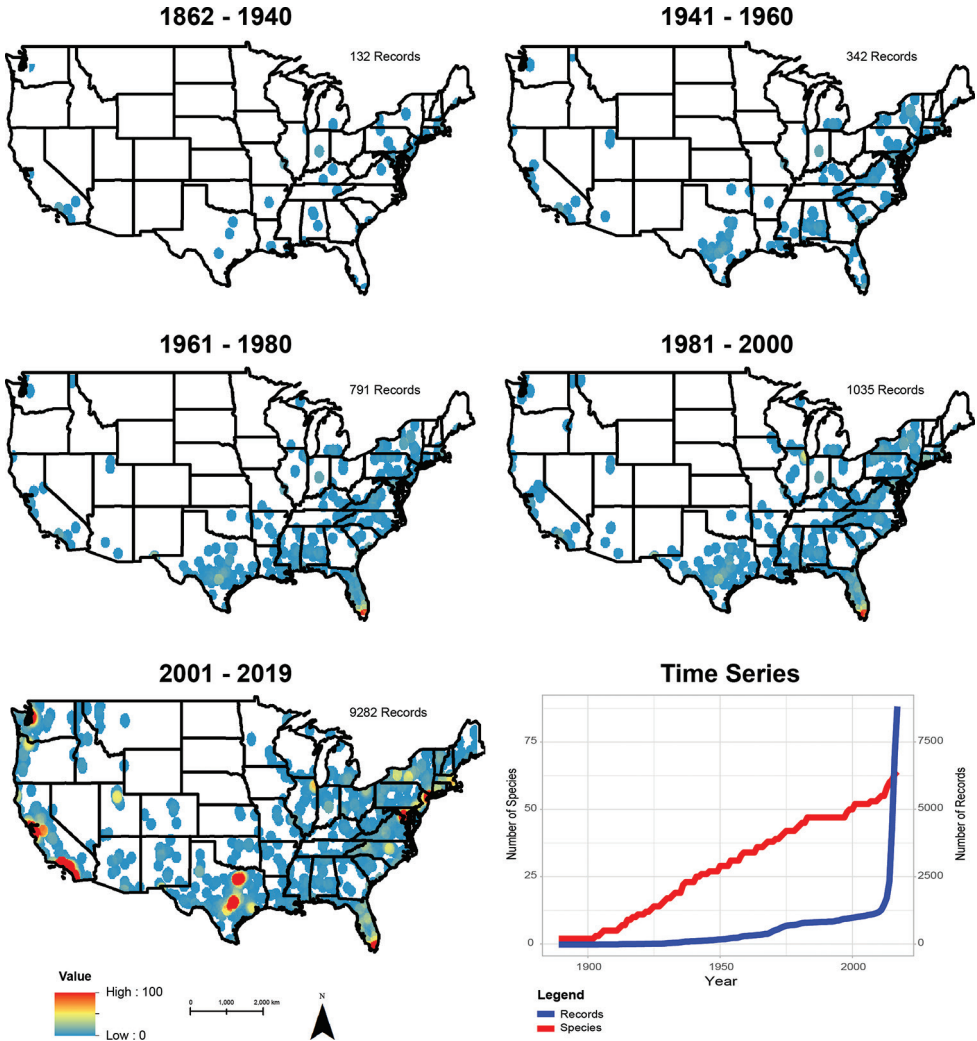


Figure 5. Point density map of non-native species records at five different time intervals. High-density values were associated with 100 or more records within a 75 km circular neighborhood around each individual record. Records were cumulative for each respective interval and tallied on the right side of each map. Time series data associated with new species and records shown in bottom right.

tropods. Our results corroborate findings of Dawson et al. (2017), that the majority of species richness and abundance records were found in predominantly coastal areas. This is also supported by a recent study of non-native mollusks in South America (Darrigran et al. 2020).

Although most non-native terrestrial gastropod species exhibit climate matching to their indigenous ranges (discussed above), there is notable variation in the extent of occurrence and abundance of records between species. While analogous climate conditions might thus promote successful introductions of terrestrial gastropods in CONUS

or other areas, there are clearly other factors driving the success of some non-native species relative to others. Generalist characteristics and broad thermal tolerances might contribute to survivability in a new habitat (McKinney and Lockwood 1999). Also, other life history traits and reproductive strategies in terrestrial gastropods might facilitate establishment from small populations (i.e., hermaphroditism, large clutch sizes; Robinson 1999). For example, there is a substantial literature attributing such traits to *Cornu aspersum*, the most widely recorded species in our dataset (Guiller et al. 2012; Gaitán-Espitia et al. 2013; Nicolai et al. 2013; Nespolo et al. 2014).

The pet and aquarium trade, increasing trade in ornamental and agricultural plants, as well as human food preferences have contributed to the importation and spread of invasive terrestrial gastropods within the contiguous U.S. Though our findings cannot directly quantify the relative importance of each of these dispersal vectors, there are apparent correlations between the geographical abundance of records for particular species and likely mechanisms. For example, *C. aspersum* and *Otala lactea* are among the most common land snail species used in human food consumption (escargot) owing to their fast reproductive rates and high nutritional content (Dragičević and Baltić 2005). These species are found in high densities in major U.S. cities such as San Francisco and Los Angeles, CA, Portland, OR, and Dallas, TX. Increased demand for exotic dishes in such communities, some with high socioeconomic areas, might provide greater opportunity for escape and persistence (i.e., via high propagules pressure) compared with less cosmopolitan areas. Other idiosyncratic drivers of success may be at play when considering the pervasiveness of these non-native species.

Potential impacts in light of spatial patterns

We did not consider impacts of any non-native species in this study, and therefore cannot directly infer potential economic or ecological harm associated with our results. The invasiveness and deleterious impacts of many of these species have been comprehensively reviewed in other literature (e.g., Robinson 1999; Cowie and Robinson 2003; Cowie et al. 2009), and we encourage those interested to seek additional information about these topics elsewhere. Using our data, however, we can provide further utility to previous projections of select non-native species and their negative impacts (if any), specifically those of Cowie et al. (2009). This previous research sought to quantify the potential ‘pest significance’ of a variety of non-native gastropod species based on life history traits, propagule associations, invasion history, general ecology, and other biological and historical factors. Species considered (both aquatic and terrestrial in this case) were then scored individually and proportionally to all others within their dataset using these factors, with those scoring highest being projected as most ecologically harmful.

Of the non-native terrestrial species considered of high potential risk included in Cowie et al. (2009), we surprisingly note that few have a substantial number of records in our dataset. For example, the genus *Cerņuella* was scored individually and propor-

tionally highest among terrestrial groups in Cowie et al. (2009), yet our data collection yields only 29 records of this genus in CONUS associated with two species (Table 1). The most prevalent species in our dataset, *C. aspersum*, was ranked in the lower extent of the top one third of the nearly 50 species considered in Cowie et al. (2009), along with another fairly prevalent species in our dataset (*Theba pisana*). All other species in this top one third of their dataset have fewer than 20 records. We do note, however, that the majority of our records do not have associated estimates of abundance (and thus this was not considered in our study), so few records of any one species should not infer a lack of future ecological harm. Instead, it can be used to inform management efforts in areas with species considered potential pests.

Source contribution

While the spatiotemporal trends exhibited in our dataset are consistent with other studies of non-native taxonomic groups within the U.S. (e.g., Mangiante et al. 2018), it is important to acknowledge limitations in this study and provide caution about its interpretability. Citizen science has become an increasingly popular tool both in terms of scientific analysis and to connect the general populous with the scientific community (Follett and Strezov 2015). So much so, in fact, that it here represents a impressively significant portion of our final dataset. For example, the Los Angeles County Museum of Natural History has initiated a new mollusk-specific citizen science program called *Snails and Slugs Living in Metropolitan Environments* (SLIME; <https://nhm.org/community-science-nhm/slime>). There have been a number of published products associated with this program (e.g., Ballard et al. 2017; Vendetti et al. 2018), and the vast majority of records in Los Angeles County (and by extension many in our dataset) are a product of participants of this program via iNaturalist. Thus, while these efforts have been successful and prolific, we advise caution when using all data provided for geospatial modeling without first accounting for common sources of geospatial error (e.g., spatial autocorrelation, pseudo-replication).

Conclusion

Our study seems to support a growing interest in the distribution of non-native terrestrial gastropods through time, with rapidly increasing amounts of records being contributed to museum collections and other digital repositories. We believe this trend will grow as citizens grow steadily aware of what non-native species might be in their vicinity, which can be greatly informed by localized science outreach and BioBlitz programs (e.g., Ballard et al. 2017). In conclusion, our results represent the first synthesized geospatial dataset of non-native terrestrial gastropods in CONUS, with over 10,000 individual records spanning over 150 years of collection efforts. A significant biodiversity is represented in our dataset, though the number of records disproportion-

ally indicates the increased prevalence of just a handful of species. We show increased prevalence of non-native species through time, largely associated with urbanized areas with high human population density. Moreover, we show strong evidence for a role for analogous climates in dictating geographic fate and pervasiveness between indigenous and CONUS ranges for non-native species. We believe this study serves as a first step toward a more driven effort to outline future research of these non-native species, including more geospatially-robust predictive distribution modeling, risk assessment, and overall management.

Acknowledgements

We thank I Killius and E Pieper for additional logistical efforts, R Cowie for helpful comments early in the manuscript's conception, and A Simpson for information regarding the use of BISON data.

References

- Baker CM, Bode M (2016) Placing invasive species management in a spatiotemporal context. *Ecological Applications* 26(3): 712–725. <https://doi.org/10.1890/15-0095>
- Ballard HL, Robinson LD, Young AN, Pauly GB, Higgins LM, Johnson RF, Tweddle JC (2017) Contributions to conservation outcomes by natural history museum-led citizen science: examining evidence and next steps. *Biological Conservation* 208: 87–97. <https://doi.org/10.1016/j.biocon.2016.08.040>
- Barbosa M, Pautasso M, Figueiredo D (2013) Species-people correlations and the need to account for survey effort in biodiversity analyses. *Diversity and Distributions* 19(9): 1188–1197. <https://doi.org/10.1111/ddi.12106>
- Bayraktarov E, Ehmke G, O'Connor J, Burns EL, Nguyen HA, McRae L, Possingham HP, Lindenmayer FB (2019) Do big unstructured biodiversity data mean more knowledge? *Frontiers in Ecology and the Environment* 6: 1–239. <https://doi.org/10.3389/fevo.2018.00239>
- Bergey EA, Figueroa LL, Mather CM, Martin RJ, Ray EJ, Kurien JT, Westrop DR, Suriyawong P (2014) Trading in snails: plant nurseries as transport hubs for non-native species. *Biological Invasions* 16(7): 1441–1451. <https://doi.org/10.1007/s10530-013-0581-1>
- Bird TJ, Bates AE, Lefcheck JS, Hill NA, Thomson RJ, Edgar GJ, Stuart-Smith RD, Wotherspoon S, Krkosek M, Stuart-Smith JF, Pecl GT (2014) Statistical solutions for error and bias in global citizen science datasets. *Biological Conservation* 173: 144–154. <https://doi.org/10.1016/j.biocon.2013.07.037>
- Butchart SHM, Walpole M, Collen B, Van Strien A, Scharlemann JPW, Almond REA, Baillie JE, Bomhard B, Brown C, Bruno J, Carpenter KE (2010) Global biodiversity: indicators of recent declines. *Science* 328(5982): 1164–1168. <https://doi.org/10.1126/science.1187512>
- Campos JA, Baquero GG, Cano L, Loidi J, Herrera M (2016) Climate and Human Pressure Constraints Co-Explain Regional Plant Invasion at Different Spatial Scales. *PLoS ONE* 11(10): e0164629. <https://doi.org/10.1371/journal.pone.0164629>

- Capinha C, Roedder D, Pereira HM, Kappes H (2014) Response of non-native European terrestrial gastropods to novel climates correlates with biogeographical and biological traits. *Global Ecology and Biogeography* 23(8): 857–866. <https://doi.org/10.1111/geb.12176>
- Chiba S, Cowie RH (2016) Evolution and extinction of land snails on oceanic islands. *Annual Review of Ecology, Evolution, and Systematics* 47: 123–141. <https://doi.org/10.1146/annurev-ecolsys-112414-054331>
- Civeyrel L, Simberloff D (1996) A tale of two snails: is the cure worse than the disease? *Biodiversity & Conservation* 5(10): 1231–1252. <https://doi.org/10.1007/BF00051574>
- Cowie RH, Robinson DG (2003) Pathways of introduction of nonindigenous land and freshwater snails and slugs. In: Ruiz G, Carlton JT (Eds) *Invasive Species: Vectors and Management Strategies*. Island Press, Washington, 93–122.
- Cowie RH (2001) Can snails ever be effective and safe biocontrol agents? *International Journal of Pest Management* 47(1): 23–40. <https://doi.org/10.1080/09670870150215577>
- Cowie RH, Hayes KA, Tran CT, Meyer III WM (2008) The horticultural industry as a vector of alien snails and slugs: widespread invasions in Hawaii. *International Journal of Pest Management* 54(4): 267–276. <https://doi.org/10.1080/09670870802403986>
- Cowie RH, Dillon RT, Robinson DG, Smith JW (2009) Alien non-marine snails and slugs of priority quarantine importance in the United States: A preliminary risk assessment. *American Malacological Bulletin* 27(1/2): 113–133. <https://doi.org/10.4003/006.027.0210>
- Clavero M, García-Berthou E (2005) Invasive species are a leading cause of animal extinctions. *Trends in Ecology & Evolution* 20(3): 1–110. <https://doi.org/10.1016/j.tree.2005.01.003>
- Darrigran G, Agudo-Padrón I, Baez P, Belz C, Cardoso F, Carranza A, Collado G, Correoso M, Cuezco MG, Fabres A, Gutiérrez Gregoric DE, Letelier S, Ludwig S, Mansur MC, Pastorino G, Penchaszadeh P, Peralta C, Rebolledo A, Rumi A, Santos S, Thiengo S, Vidigal T, Damborenea C (2020) Non-native mollusks throughout South America: emergent patterns in an understudied continent. *Biological Invasions* 22(3): 853–871. <https://doi.org/10.1007/s10530-019-02178-4>
- Dawson W, Moser D, Van Kleunen M, Kreft H, Pergl J, Pyšek P, Weigelt P, Winter M, Lenzner B, Blackburn TM, Dyer EE (2017) Global hotspots and correlates of alien species richness across taxonomic groups. *Nature Ecology & Evolution* 1(7): p.0186. <https://doi.org/10.1038/s41559-017-0186>
- Dragičević O, Baltić MŽ (2005) Snail meat: significance and consumption. *Veterinarski Glasnik*, 59(3–4): 463–474. <https://doi.org/10.2298/VETGL0504463D>
- Follett R, Strezov V (2015) An analysis of citizen science based research: usage and publication patterns. *PloS ONE* 10(11): e0143687. <https://doi.org/10.1371/journal.pone.0143687>
- Gaitán-Espitia JD, Arias MB, Lardies MA, Nespolo RF (2013) Variation in thermal sensitivity and thermal tolerances in an invasive species across a climatic gradient: lessons from the land snail *Cornu aspersum*. *PLoS ONE* 8(8): e70662. <https://doi.org/10.1371/journal.pone.0070662>
- Gu Z, Gu L, Eils R, Schlesner M, Brors B (2014) *circlize* implements and enhances circular visualization in R. *Bioinformatics* 30(19): 2811–2812. <https://doi.org/10.1093/bioinformatics/btu393>
- Guiller A, Martin M, Hiraux C, Madec L (2012) Tracing the invasion of the Mediterranean land snail *Cornu aspersum aspersum* becoming an agricultural and garden pest in areas recently introduced. *PLoS ONE* 7(12): e49674. <https://doi.org/10.1371/journal.pone.0049674>

- Howeth JG, Gantz CA, Angermeier PL, Marchetti MP, Olden J (2016) Predicting invasiveness of species in trade: climate match, trophic guild and fecundity influence establishment and impact of non-native freshwater fishes. *Diversity and Distributions* 22(2): 148–160. <https://doi.org/10.1111/ddi.12391>
- Hulme PE (2014) Invasive species challenge the global response to emerging diseases. *Trends in Parasitology* 30(6): 267–270. <https://doi.org/10.1016/j.pt.2014.03.005>
- Jehlik V, Dostalek J, Frantik T (2019) Alien plants in central European river ports. *Neobiota*, 45: 93–115. <https://doi.org/10.3897/neobiota.45.33866>
- Jeschke JM, Aparicio LG, Haider S, Heger T, Lortie CJ, Pyšek P, Strayer DL (2012) Taxonomic bias and lack of cross-taxonomic studies in invasion biology. *Frontiers in Ecology and the Environment* 10(7): 349–350. <https://doi.org/10.1890/12.WB.016>
- Keller RP, Drake JM, Lodge DM (2007) Fecundity as a basis for risk assessment of nonindigenous freshwater molluscs. *Conservation Biology* 21(1): 191–200. <https://doi.org/10.1111/j.1523-1739.2006.00563.x>
- Kosmala M, Wiggins A, Swanson A, Simmons B (2016) Assessing data quality in citizen science. *Frontiers in Ecology and the Environment* 14(10): 551–560. <https://doi.org/10.1002/fee.1436>
- Langor DW, DeHaas LJ, Footitt RG (2009) Diversity of non-native terrestrial arthropods on woody plants in Canada. *Biological Invasions* 11(1): 5–19. https://doi.org/10.1007/978-1-4020-9680-8_2
- Liebhald AM, Berec L, Brockerhoff EG, Epanchin-Niell RS, Hastings A, Herms DA, Kean JM, McCullough DG, Suckling DM, Tobin PC, Yamanaka T (2016) Eradication of invading insect populations: from concepts to applications. *Annual Review of Entomology* 61: 335–352. <https://doi.org/10.1146/annurev-ento-010715-023809>
- Lowry E, Rollinson EJ, Laybourn AJ, Scott TE, Aiello-Lammens ME, Gray SM, Mickley J, Gurevitch J (2013) Biological invasions: a field synopsis, systematic review, and database of the literature. *Ecology and Evolution* 3(1): 182–196. <https://doi.org/10.1002/ece3.431>
- Mangiante MJ, Davis AJS, Panlasigui S, Neilson ME, Pfingsten I, Fuller PL, Darling JA (2018) Trends in nonindigenous aquatic species richness in the United States reveal shifting spatial and temporal patterns of species introductions. *Aquatic Invasions* 13(3): 323–338. <https://doi.org/10.3391/ai.2018.13.3.02>
- Mazza G, Tricarico E, Genovesi P, Gherardi F (2014) Biological invaders are threats to human health: an overview. *Ethology Ecology & Evolution* 26(2–3): 112–129. <https://doi.org/10.1080/03949370.2013.863225>
- McKinney ML (2001) Effects of human population, area, and time on non-native plant and fish diversity in the United States. *Biological Conservation* 100: 243–252. [https://doi.org/10.1016/S0006-3207\(01\)00027-1](https://doi.org/10.1016/S0006-3207(01)00027-1)
- McKinney ML, Lockwood JL (1999) Biotic homogenization: a few winners replacing many losers in the next mass extinction. *Trends in Ecology & Evolution* 14(11): 450–453. [https://doi.org/10.1016/S0169-5347\(99\)01679-1](https://doi.org/10.1016/S0169-5347(99)01679-1)
- Naranjo-García E, Castillo-Rodríguez ZG (2017) First inventory of the introduced and invasive mollusks in Mexico. *Nautilus* 131(2): 107–126. <https://www.biodiversitylibrary.org/item/276658#page/5/mode/1up>

- Nekola JC, Hutchins BT, Schofield A, Najev B, Perez KE (2019) Caveat consumptor notitia museo: Let the museum data user beware. *Global Ecology and Biogeography* 28: 1722–1734. <https://doi.org/10.1111/geb.12995>
- Nespolo RF, Bartheld JL, Gonzalez A, Bruning A, Roff DA, Bacigalupe LD, Gaitán-Espitia, JD (2014) The quantitative genetics of physiological and morphological traits in an invasive terrestrial snail: additive vs. non-additive genetic variation. *Functional Ecology* 28(3): 682–692. <https://doi.org/10.1111/1365-2435.12203>
- Nicolai A, Vernon P, Lenz R, Le Lannic J, Briand V, Charrier M (2013) Well wrapped eggs: effects of egg shell structure on heat resistance and hatchling mass in the invasive land snail *Cornu aspersum*. *Journal of Experimental Zoology Part A: Ecological Genetics and Physiology* 319(2): 63–73. <https://doi.org/10.1002/jez.1767>
- Pimentel D, Zuniga R, Morrison D (2005) Update on the environmental and economic costs associated with alien-invasive species in the United States. *Ecological Economics* 52(3): 273–288. <https://doi.org/10.1016/j.ecolecon.2004.10.002>
- Pyšek P, Richardson DM, Pergl J, Jarošík V, Sixtova Z, Weber E (2008) Geographical and taxonomic biases in invasion ecology. *Trends in Ecology & Evolution* 23(5): 237–244. <https://doi.org/10.1016/j.tree.2008.02.002>
- Robinson DG (1999) Alien invasions: the effects of the global economy on non-marine gastropod introductions into the United States. *Malacologia-Philadelphia* 41(2): 413–438. <https://www.cabdirect.org/cabdirect/abstract/20000806106>
- R Core Team (2013) R: A language and environment for statistical computing. R Foundation for Statistical Computing, Vienna. <http://www.R-project.org/>
- Rubel F, Brugger K, Haslinger K, Auer I (2017) The climate of the European Alps: Shift of very high resolution Köppen-Geiger climate zones 1800–2100. *Meteorologische Zeitschrift* 26(2): 115–125. <https://doi.org/10.1127/metz/2016/0816>
- Shea EK, Sierwald P, Bieler R, Rosenberg G (2018) Priorities and opportunities for digitizing mollusk collections. *American Malacological Bulletin* 36(2): 171–177. <https://doi.org/10.4003/006.036.0202>
- Sierwald P, Bieler R, Shea EK, Rosenberg R (2018) Mobilizing mollusks: Status update on mollusk collections in the USA and Canada. *American Malacological Bulletin* 36(2): 177–215. <https://doi.org/10.4003/006.036.0202>
- Simberloff D (2013) *Invasive species: what everyone needs to know*. Oxford University Press, Oxford.
- Simberloff D, Martin J, Genovesi P, Maris V, Wardle DA, Aronson J, Courchamp F, Galil B, García-Berthou E, Pascal M, Pyšek P (2013) Impacts of biological invasions: what's what and the way forward. *Trends in Ecology & Evolution* 28(1): 58–66. <https://doi.org/10.1016/j.tree.2012.07.013>
- Spear D, Foxcroft LC, Bezuidenhout H, McGeoch MA (2013) Human population density explains alien species richness in protected areas. *Biological Conservation* 159: 137–147. <https://doi.org/10.1016/j.biocon.2012.11.022>
- Troia MJ, McManamay RA (2016) Filling in the GAPS: evaluating completeness and coverage of open-access biodiversity databases in the United States. *Ecology and Evolution* 6(14): 4654–4669. <https://doi.org/10.1002/ece3.2225>

- U.S. Congress, Office of Technology Assessment (1993) Harmful Non-Indigenous Species in the United States, OTA-F-565, U.S. Government Printing Office, Washington, 391 pp. https://www.anstaskforce.gov/Documents/OTA_Report_1993.pdf
- van Wilgen NJ, Roura-Pascal N, Richardson DM (2009) A quantitative climate-match score for risk-assessment screening of reptile & amphibian introductions. *Environmental Management* 44: 590–607. <https://doi.org/10.1007/s00267-009-9311-y>
- Vendetti JE, Lee C, LaFollette P (2018) Five new records of introduced terrestrial gastropods in Southern California discovered by citizen science. *American Malacological Bulletin* 36(2): 232–247. <https://doi.org/10.4003/006.036.0204>
- Vinogradova Y, Pergl J, Essl F, Hejda M, van Kleunen M, Pyšek P (2018) Invasive alien plants of Russia: insights from regional inventories. *Biological Invasions* 20(8): 1931–1943. <https://doi.org/10.1007/s10530-019-02162-y>
- Yang L, Jin S, Danielson P, Homer C, Gass L, Case A, Costello C, Dewitz J, Fry J, Funk M (2018) A New Generation of the United States National Land Cover Database: Requirements, Research Priorities, Design, and Implementation Strategies. *ISPRS Journal of Photogrammetry and Remote Sensing* 146: 108–123. <https://doi.org/10.1016/j.isprsjprs.2018.09.006>
- Yeung NW, Hayes KA (2018) Biodiversity and Extinction of Hawaiian Land Snails: How Many Are Left Now and What Must We Do To Conserve Them—A Reply to Solem (1990). *Integrative and Comparative Biology* 58(6): 1157–1169. <https://doi.org/10.1093/icb/icy043>
- Yesson C, Brewer PW, Sutton T, Caithness N, Pahwa JS, Burgess MW, Gray WA, White RJ, Jones AC, Bisby FA, Culham A (2007) How global is the global biodiversity information facility? *PloS ONE* 2(11): e1124. <https://doi.org/10.1371/journal.pone.0001124>

Supplementary material I

All records with associated georeferences used in analyses

Authors: Nicholas S. Gladstone, Trystan A. Bordeau, Christy Leppanen, Michael L. McKinney

Data type: Geospatial

Copyright notice: This dataset is made available under the Open Database License (<http://opendatacommons.org/licenses/odbl/1.0/>). The Open Database License (ODbL) is a license agreement intended to allow users to freely share, modify, and use this Dataset while maintaining this same freedom for others, provided that the original source and author(s) are credited.

Link: <https://doi.org/10.3897/neobiota.57.52195.suppl1>